ELUCIDATING THE RESPONSE OF ACTIVATED SLUDGE CULTURES TO TOXIC CHEMICALS AT THE PROCESS, FLOC AND METABOLIC SCALES

Inês Domingues da Silva Henriques

Dissertation submitted to the faculty of the Virginia Polytechnic Institute and State University in partial fulfillment of the requirements for the degree of

Doctor of Philosophy
In
Civil Engineering

Dr. Nancy G. Love, Chair
Dr. Patricia M. Dove
Dr. John T. Novak
Dr. Ann M. Stevens
Dr. Peter J. Vikesland

11th of May, 2006
Blacksburg, VA

Keywords: activated sludge, toxic chemicals, floc structure, extracellular polymeric substances, metabolic footprinting, liquid chromatography-mass spectrometry, discriminant function analysis

ELUCIDATING THE RESPONSE OF ACTIVATED SLUDGE CULTURES TO TOXIC CHEMICALS AT THE PROCESS, FLOC AND METABOLIC SCALES

Inês Domingues da Silva Henriques

ABSTRACT

Activated sludge treatment systems rely on a microbial consortium structurally organized in bioflocs to treat pollutants present in wastewater. The treatment process efficiency in these systems can be severely affected by toxic chemicals present in the influent wastewater. The effects of chemical toxins at the treatment process level are determined by the mechanisms that occur at the biofloc and cellular levels, which can be physical, chemical and physiological in nature. We believe that the overall process effects of chemical toxins on activated sludge systems likely result from a combination of all three types of mechanisms and that they are interdependent, in the sense that specific bacterial stress response mechanisms (physiological mechanisms that protect the cell from toxic conditions) may lead to physical/chemical alterations at the floc level, and vice-versa. Ultimately, understanding the mechanisms that occur at the floc and metabolic scales will help to design more robust and efficient treatment systems, and to develop tools to prevent and mitigate the effects of toxic chemicals on activated sludge systems. In this research, we set out to establish the link between the effects of chemical toxins on activated sludge cultures at the process, floc and metabolic scales.

First, the effects of shock loads of different toxic sources (1-chloro-2,4-dinitrobenzene (CDNB), cadmium, 1-octanol, 2,4-dinitrophenol (DNP), weakly complexed cyanide, pH 5, 9 and 11, and high ammonia levels) on activated sludge process parameters (biomass growth, respiration rate, flocculation, chemical oxygen demand (COD) removal, dewaterability and settleability) were studied. For all chemical shocks except ammonia and pH, concentrations that caused 15, 25 and 50% respiration inhibition were used to provide a single pulse chemical shock to sequencing batch reactor (SBR) systems containing a nitrifying (10 day solids retention time – SRT) and a non-nitrifying (2 day SRT) biomass. We found that cadmium and pH 11 shocks were the conditions that most detrimentally affected all the processes, followed by CDNB. DNP and cyanide primarily led to effects on respiration, while pH 5, 9, octanol and various ammonia concentrations did not impact the treatment process to a significant extent. Additionally, there was a clear correlation between biomass deflocculation and increases in the effluent soluble COD of the shocked reactors for different chemical sources. With this study, we were able to establish a source-effect matrix linking classes of chemical toxins to their potential inhibitory effects on activated sludge processes, thereby contributing to a better understanding of the potential effects of toxic industrial discharges into biological treatment systems.

The findings of the first phase of the research, specifically the correlation between chemical-induced deflocculation and increases in soluble COD, served as a motivation to explore the role of floc structure in the response of activated sludge cultures to toxic compounds, and to conduct a more in-depth analysis of the supernatant (soluble phase) of toxin-exposed activated sludge. In one study, we evaluated the respiration inhibition induced by octanol, cadmium, N-ethylmaleimide (NEM), cyanide and DNP on activated sludge biomasses with different floc structures but similar physiological characteristics, with the objective of assessing the role of the

extracellular polymeric substances (EPS) in flocs as a protection barrier against chemical toxins. Mechanical shearing was applied to fresh mixed liquor to produce biomasses with different floc structure properties and specific oxygen uptake rate assays were conducted on the sheared and unsheared mixed liquors. The results showed that the respiration inhibition by octanol and cadmium was more intense in sheared mixed liquor (which had less EPS material available in the flocs and smaller floc sizes) than in the unsheared biomass. Conversely, the respiration inhibition induced by NEM and cyanide was similar for the different mixed liquors tested. These results allowed us to conclude that the EPS matrix functions as a protective barrier for the bacteria inside activated sludge flocs to chemicals that it has the potential to interact with, such as hydrophobic (octanol) and positively-charged (cadmium) compounds, but that the toxicity response for soluble, hydrophilic toxins (NEM and cyanide) is not significantly influenced by the presence of the polymer matrix.

In the final study that was conducted, we used the metabolomics-based technique metabolic footprinting to assess if the soluble phase of mixed liquor exposed to different chemical toxins exhibited a toxin-specific biochemical composition. We hypothesized that toxin-specific effects could be distinguished through footprint patterns of those soluble samples. The impact of cadmium, DNP and NEM shock loads on the composition of the soluble fraction of activated sludge mixed liquor was analyzed by liquid chromatography-mass spectrometry (LC-MS). The results from this study indicated that there was a significant release of biomolecules (proteins, carbohydrates and humic acids) from the floc structure into the bulk liquid due to chemical stress. More importantly, using a multivariate statistical method called discriminant function analysis with genetic algorithm variable selection (GA-DFA), we were able to show that the soluble phase samples from the different reactors could be differentiated, thereby indicating that the footprints generated by LC-MS were different for the four conditions tested and, therefore, toxin-specific. These footprints, thus, contain information about specific biomolecular differences between the samples, and we found that only a limited number of m/z (mass to charge) ratios from the mass spectra data was needed to differentiate between the control and each chemical toxin-derived samples. In addition, since the experiments were conducted with mixed liquor from four distinct wastewater treatment plants, the discriminating m/z ratios may potentially be used as universal stress biomarkers. These results are promising and indicate that LC-MS may be used for the discovery of activated sludge stress biomarkers, to allow the development of new toxin detection technologies for prevention of upset events in activated sludge systems.

ACKOWLEDGMENTS

I would like to acknowledge the following funding sources, which provided research and fellowship support during my Ph.D.:

- Water Environment Research Foundation
- Fundação para a Ciência e a Tecnologia, Portugal
- Fundação Luso-Americana para o Desenvolvimento, Portugal
- The Charles E. Via, Jr. Department of Civil and Environmental Engineering, Virginia Tech
- National Institute of Standards and Technology

I am grateful to the members of my committee, Dr. Patricia Dove, Dr. John Novak, Dr. Ann Stevens and Dr. Peter Vikesland for their advice and assistance. I am especially grateful to Dr. Diana Aga and Dr. Pedro Mendes for their help, support and valuable insights. A special thanks to Dr. Charles Bott who helped me during the last phase of my research. It has been a real pleasure and an honor to work with them all and I truly hope that we will continue to collaborate in the future.

I want to thank Dr. Nancy Love, my research advisor, for the tremendous support she has given me over the past six years. She is truly an amazing advisor and woman, and has pushed me beyond limits I could never dream of achieving. I thank her especially for always being available, always being sincere and honest, for deeply respecting me as an individual, and teaching me the most fundamental principles of professional ethics as a teacher, a mentor and a researcher. She will always be my role-model.

I also want to thank Dr. António Câmara, who almost a decade ago was the first to encourage me to study abroad, and is now giving me the possibility to go back home. He cannot imagine the enormous impact he has had in my life and for that I will always be grateful.

I wish to thank my fellow graduate students Rick Kelly, Giacomo Sonzini, Jennifer Dauphinais, David Holbrook, Mert Muftugil, Joy and Chris Muller, for making me laugh and enjoy lab work even during the most intense periods. And all the great undergraduate assistants that helped me so much with my research: Kelly Mattson, Katherine Linares, Susanne Ayres, Michael Hare, Amanda Romine, Mark Garland, Kevin Grove and Maeva Tureau. Also, to my good friends that in the last six years helped Blacksburg feel like home: Ângela, Pedro, Paulo, Renate, Andrea, Giacomo, Diogo and Ana.

A last but important word of appreciation goes to my family.

To my mother, who has taught me the principles of honesty, courage, perseverance, humbleness and respect for others. And with whom I learned to always, always put my best effort into everything I do. To my father, for teaching me to enjoy the small accomplishments in life and showing me that happiness is closer and simpler than we tend to think. To Rui and Mané, for loving me as their own children and teaching me what a family is all about.

To my beautiful daughter Beatriz, who helped me put things in perspective throughout the Ph.D. process and for really have turned me into a better and happier person.

Above all, to the love of my life and my best friend, João, who has helped me tremendously by believing in me and making me believe in myself, telling me I'm the best at least fifty times a day, and yes, for having spent so much time and energy taking care of Beatriz in the last year of my Ph.D. He was able to always guide our life and provide the stability and orientation that we needed to accomplish our personal and professional goals. He tells me I'm the best, but really, nothing of what I have accomplished would be possible without his incredible emotional support, love, and friendship.

DEDICATION

Para o João, esta dissertação é quase mais tua do que minha.

Para os meus pais, por terem criado as oportunidades que me permitiram chegar aqui.

TABLE OF CONTENTS

LIST OF FIGURES

Chapter 3. Activated Sludge Inhibition by Chemical Stressors – A Comprehensive Study

Chapter 4. Floc Structure and Floc Size Play a Role in the Toxicity Response of Activated Sludge Bacteria to Chemical Toxins

LIST OF TABLES

LIST OF ABBREVIATIONS

AA	Amino Acid
AP	Alkaline Phosphatase
APCI	Atmospheric Pressure Chemical Ionization
APCI-MS	Atmospheric Pressure Chemical Ionization – Mass Spectrometry
BOD	Biochemical Oxygen Demand
Cd	Cadmium
CDNB	1-Chloro-2,4-Dinitrobenzene
CE	Capillary Electrophoresis
CE-ESI-MS	Capillary Electrophoresis – Electrospray Ionization – Mass Spectrometry
CER	Cation Exchange Resin
CLM	Confocal Laser Microscopy
COD	Chemical Oxygen Demand
CST	Capillary Suction Time
CSTR	Continuous Stirred Tank Reactor
DA	Discriminant Analysis
DAPI	4',6-Diamidino-2-phenylindole
DCB	Divalent Cation Bridging
DF	Discriminant Function
DFA	Discriminant Function Analysis
DGGE	Denaturing Gradient Gel Electrophoresis
DLVO	Double Layer Theory
DNA	Deoxyribonucleic Acid
DNP	2,4-Dinitrophenol
DO	Dissolved Oxygen
EPS	Extracellular Polymeric Substances
ESI	Electrospray Ionization
ESI-TOF-MS	Electrospray Ionization – Time of Flight – Mass Spectrometry
FISH	Fluorescence In-Situ Hybridization
FT	Fourier Transform
FT-IC-MS	Fourier Transform – Ion Cyclotron – Mass Spectrometry

FT-IR	Fourier Transform Infrared Spectroscopy
G	Velocity Gradient
G6PDH	Glucose 6-Phosphate Dehydrogenase
GA	Genetic Algorithm
GA-DFA	Discriminant Function Analysis with Genetic Algorithm Variable Selection
GC	Gas Chromatography
GC-MS	Gas Chromatography – Mass Spectrometry
GGKE	Glutathione-Gated Potassium Efflux
HRT	Hydraulic Retention Time
IC	Ion Cyclotron
IC_{15}	Inhibitory Concentration 15% - concentration that inhibits respiration by 15%
IC_{25}	Inhibitory Concentration 25% - concentration that inhibits respiration by 25%
IC_{50}	Inhibitory Concentration 50% - concentration that inhibits respiration by 50%
IC_{xx}	Inhibitory Concentration xx% - concentration that inhibits respiration by xx%
IR	Infrared Spectroscopy
K_{ow}	Octanol/Water Partition Coefficient
LC	Liquid Chromatography
LC-ESI-MS	Liquid Chromatography – Electrospray Ionization – Mass Spectrometry
LC-MS	Liquid Chromatography – Mass Spectrometry
m/z ratio	Mass to Charge Ratio
MLSS	Mixed Liquor Suspended Solids
MLTS	Mixed Liquor Total Solids
MLTVS	Mixed Liquor Total Volatile Solids
MLVSS	Mixed Liquor Volatile Suspended Solids
MS	Mass Spectrometry
NEM	N-Ethyl-Maleimide
NMR	Nuclear Magnetic Resonance
OUR	Oxygen Uptake Rate
PCA	Principal Component Analysis
PLS	Partial Least Squares
PLS-DA	Partial Least Squares Discriminant Analysis
PMF	Proton Motive Force

PSD	Particle Size Distribution
RNA	Ribonucleic Acid
S/N ratio	Signal-to-Noise Ratio
SBR	Sequencing Batch Reactor
SOUR	Specific Oxygen Uptake Rate
SRB	Sulfate Reducing Bacteria
SRT	Solids Retention Time
SVI	Sludge Volume Index
TEM	Transmission Electron Microscopy
TOF	Time of Flight
TSS	Total Suspended Solids
Zn-Cn	Zinc-Cyanide complex ($Zn_x(CN)_y^{+z}$)

Chapter 1. Executive Summary

Introduction

Activated sludge is the most widely used biological wastewater treatment process. It is based on the biological degradation of both soluble organic and inorganic components and particulate matter carried out by microbial flocs. Activated sludge treatment plants are often exposed to toxic upset events, which originate mostly from industrial waste streams and can adversely impact all the fundamental processes within the treatment system. As a result of toxic shock load inputs, activated sludge plant operators commonly observe loss of nitrification, decrease in biochemical oxygen demand (BOD) removal efficiency and disruption of bioflocculation (deflocculation) (Love and Bott, 2000).

Substantial research has been conducted to assess the effects of toxins on the activated sludge process. Yet, these studies typically focus on only one aspect of the process (e.g., BOD or chemical oxygen demand (COD) removal, nitrification or settleability of the biomass), failing to make a comprehensive analysis of all the potential effects of that toxin. Additionally, the use of laboratory-scale reactors fed with synthetic wastewater in most of these studies may change the characteristics of the biomass to a great extent and provide limited information about real world systems. Moreover, the criteria to select the toxin concentrations are not consistent across the literature, which doesn't allow a systematic comparison between the effects of different toxins. Therefore, there is a need for comprehensive studies that can adequately mimic the conditions at a treatment plant, both in terms of biomass, influent and toxic shock characteristics. The goal of the first phase of this research was, thus, to establish source-effect relationships for activated sludge exposed to different industrially-relevant chemical toxins.

Establishing source-effect relationships for activated sludge systems exposed to toxic chemicals is important, since it will allow operators to better predict the effects of toxic shock loads on the treatment process and, therefore, to better manage and operate their systems by minimizing the effects of such shock loads. However, given the biological nature of activated sludge systems, effects observed at the process level are ultimately determined by mechanisms that occur at the floc and metabolic/physiological levels. Therefore, there is also a strong need for studies that

specifically look into the mechanistic causes of the process effects observed macroscopically and that can establish a link between the effects and mechanisms that occur at the different scales.

Many studies in the literature have focused on the composition and structure of activated sludge flocs, contributing to a better understanding of the interactions between different floc components and to the formulation of a conceptual model for floc structure and architecture. However, with a few exceptions, the mechanisms that occur at the floc and metabolic levels within activated sludge biomass during a toxic shock event are largely unknown. The results from the source-effect studies conducted during the first phase of this research motivated us to pursue more in-depth studies with the objective of understanding (1) the role of floc structure in the toxicity response of activated sludge bacteria to chemical stress, and (2) the metabolic mechanisms behind the release of biofloc materials into the soluble phase of mixed liquor as a response to chemical stress.

Overall, we believe that this work will allow a better understanding of: (1) the factors that control the toxicity response of activated sludge to a wide range of chemical toxins and (2) the relationship between process effects, floc structure and bacterial physiology during exposure of activated sludge flocs to toxic conditions. Consequently, this research may also contribute to the development of more efficient operational practices to both create robust wastewater treatment systems that can better sustain the impacts of shock loads of chemical toxins, and provide operators with tools to minimize and prevent the effects of such shock loads on the treatment process. Ultimately, this research could also promote the development of new sensing technologies for wastewater treatment upset early warning and, more broadly, for environmental monitoring.

Phase 1: Activated Sludge Inhibition by Chemical Stressors – A Comprehensive Study (Chapter 3)

The specific objective of the studies conducted during the first phase of this research was to establish source-effect relationships for activated sludge exposed to shock loads of chemical toxins. Six different classes of industrially-relevant chemicals were selected as sources and the effects of varying shock concentrations of those toxins on activated sludge COD removal ability,

flocculation ability, biomass growth, respiration rates, settleability and dewaterability were assessed. These studies were conducted on both nitrifying (10 day solids retention time, SRT) and non-nitrifying (2 day SRT) activated sludge mixed liquors. The chemical classes (and model compound within each class) chosen as toxic shock sources included heavy metals (cadmium), uncouplers of oxidative phosphorylation (2,4-dinitrophenol, DNP), organic electrophilic chemicals (1-chloro-2,4-dinitrobenzene, CDNB), hydrophobic chemicals (1-octanol), respiration inhibitors (weakly complexed cyanide), high ammonia loadings, and alkaline and acidic pH conditions.

Among the process effects studied, inhibition of respiratory functions and COD removal were the most affected. All the toxins tested detrimentally affected COD removal and respiration rates to some extent in at least one of the biomasses used in this study. The next most prevalent process effect was loss of flocculation ability (increase in effluent total suspended solids, TSS), followed by reduced biomass growth (decrease in mixed liquor volatile suspended solids, MLVSS). Both mixed liquor settleability and dewaterability were not affected to a great extent by the toxins evaluated in this study.

The toxic sources that most detrimentally impacted all the analyzed processes were cadmium and pH 11 shocks, followed by CDNB. Cyanide and DNP shock loads showed significant effects primarily at the level of respiration inhibition, while pH 5, pH 9, octanol and ammonia did not impact the treatment process as greatly. Differences were found between the effects of the toxic sources on the 2 day and 10 day SRT mixed liquors. However, these differences were not consistent among the different sources and effects studied, revealing that it was not possible to identify a general trend of increased sensitivity for either biomass, under the conditions of the study.

One of the interesting facts that we concluded from these studies was that when significant effects were observed to occur at the level of COD removal, there was a clear tendency for that effect to take place together with biomass deflocculation in the shocked reactors. An increase in soluble COD in the effluent of the SBR reactors can originate from different mechanisms, such as: (1) inhibition of catabolic functions, which results in a decrease of the biomass substrate

uptake ability, (2) passive release of intracellular soluble materials due to cell lysis, (3) active excretion of intracellular substances from specific bacterial stress responses, and (4) release of materials from the extracellular polymeric substances (EPS) matrix that embeds the bacterial cells in activated sludge flocs. For different toxins, it is likely that these different mechanisms contribute to varying extents to the observed effluent soluble COD increases.

This work showed that COD removal, bioflocculation, biomass growth and biomass respiration were inhibited to different extents by distinct classes of industrial chemical toxins. Interestingly, the process that was most severely impacted by the different toxins varied with chemical class and seemed to be intrinsically related to the nature of the chemical and its predominant mode of action on bacterial cells. Therefore, it becomes important to understand the floc and metabolic scales-causal mechanisms behind the source-effect relationships for each chemical class, as this information may help develop smart biosensors that can differentiate between different chemical shock loads and prevent major process upset.

Phase 2: Role of Floc Structure and Release of Biomolecules from Activated Sludge Flocs During Exposure to Chemical Toxins

Floc Structure and Floc Size Play a Role in the Toxicity Response of Activated Sludge Bacteria to Chemical Toxins (Chapter 4)

In the first phase of this research, we found significant differences in the treatment process effects of shock loads for a wide range of chemical toxins when applied to activated sludge cultures with different SRTs. Although we recognize that the dissimilar responses may have been due to physiological differences between the mixed liquors tested, we also hypothesized that floc structure, which varies significantly with SRT, also played a role in the observed results.

Specifically, we focused on the role of EPS. EPS forms a gel-like matrix in which bacterial cells are embedded within activated sludge flocs. We hypothesized that the EPS matrix functions as a protective barrier against toxic compounds that it has the potential to interact with, such as hydrophobic and positively-charged toxins. For example, negatively charged residues in bound EPS protein can bind heavy metals, leading to reduced toxicity because the metal is less

bioavailable in comparison to systems without significant quantities of EPS. In the case of soluble uncharged hydrophilic toxins that more easily diffuse through the EPS matrix, the toxicity response is probably a function of other mechanisms.

The specific objective of this study was to compare the inhibition induced by a wide range of chemical toxins (octanol, cadmium, DNP, cyanide and N-ethylmaleimide - NEM) on mixed liquors with different floc structures. Mechanical shear stress was used to test the hypothetical protective effect of EPS to the bacteria within activated sludge flocs. Shearing mixed liquor breaks up the flocs and simultaneously releases EPS from the floc matrix into the bulk liquid, thereby permitting the production of biomasses at a single physiological growth state with different floc structures. Inhibition of respiratory activity through specific oxygen uptake rate (SOUR) assays was used as the indicator of biomass toxicity.

The main conclusions from this research work corroborated our hypothesis. EPS in activated sludge flocs protects the bacterial community against chemicals that establish interactions with the polymer matrix, presumably by impeding access of the chemical to the bacterial cells. This effect was seen with both cadmium and octanol, through a decrease in the respiration rate of sheared biomass versus unsheared biomass. In addition, floc size is an important parameter when evaluating the toxicity of specific chemicals to activated sludge bacteria, but does not explain *per se* the toxicity responses observed for sheared and unsheared mixed liquors to cadmium, octanol, cyanide, NEM and DNP. Specifically, floc structure and size do not play a role in the toxicity response of activated sludge to hydrophilic, soluble toxins, such as cyanide and NEM. The results reported in this study contribute to a better understanding of the mechanisms that occur at the floc level, which contribute to the process effects observed in response to a wide range of chemical toxins in activated sludge systems.

Metabolic Footprinting: A New Approach to Identify Physiological Changes in Complex Microbial Communities upon Exposure to Toxic Chemicals (Chapter 5)

In the final study that was conducted, we explored the connection between two process effects (deflocculation and increases in soluble COD) that were observed during the source-effect experiments in phase 1, and their potential relationship to mechanisms that occur at the floc and

metabolic scales. Specifically, we hypothesized that activated sludge flocs release soluble materials upon exposure to chemical stress and that the composition of these materials is toxin-specific. The release of these materials can take place through different mechanisms that occur at the floc and metabolic scales, but ultimately results in a clear process effect of increased COD in the effluent of the treatment system. The mechanisms through which the release effect may occur include: 1) release of intracellular materials into the bulk liquid due to major cell lysis caused by intense toxicity, 2) release of intracellular compounds actively secreted due to specific bacterial stress response mechanisms, 3) solubilization of EPS components due to physical-chemical interactions that take place between the chemical and the EPS matrix, that lead to a rearrangement of the EPS molecular network, and 4) release of EPS components as a secondary consequence of bacterial stress response mechanisms. These mechanisms, particularly 3) and 4), can also result in floc disintegration, leading to deflocculation of activated sludge biomass and consequent increases in effluent TSS; floc cohesion is intimately connected to the EPS matrix and the different types of interactions established between different components within that matrix, and mechanisms that contribute to destabilize those interactions ultimately result in a weakening of floc structure. Hence the connection between increases in soluble COD and effluent TSS observed during the source-effect studies. Therefore, the analysis of the soluble materials in the supernatant of chemically stressed mixed liquor could reveal important physiological and structural changes induced by the stress condition. To test our hypothesis, we used the metabolomics-based technique metabolic footprinting to assess if the supernatant (soluble phase) of mixed liquor exposed to different chemical toxins exhibited a toxin-specific biochemical composition.

The impact of cadmium, DNP and NEM shock loads on the composition of the soluble fraction of activated sludge mixed liquor was analyzed by liquid chromatography-mass spectrometry (LC-MS). The results from this study indicated that there was a significant release of biomolecules (proteins, carbohydrates and humic acids) from the floc structure into the bulk liquid due to chemical stress. More importantly, using a multivariate statistical method called discriminant function analysis with genetic algorithm variable selection (GA-DFA), we were able to show that the soluble phase samples from the different reactors could be differentiated, thereby indicating that the footprints generated by LC-MS were different for the four conditions

tested and, therefore, toxin-specific. These footprints, thus, contain information about specific biomolecular differences between the samples, and we found that only a limited number of m/z (mass to charge) ratios from the mass spectra data was needed to differentiate between the control and each chemical toxin-derived samples. In addition, since the experiments were conducted with mixed liquor from four distinct wastewater treatment plants, the discriminating m/z ratios may potentially be used as universal stress biomarkers. Alkaline phosphatase (AP) assays indicated that the source of the soluble substances found in the shocked reactor samples was not cell lysis, but rather an extracellular source, such as the floc polymer matrix, active secretion of intracellular substances due to specific bacterial stress response mechanisms, or a combination of both mechanisms, which we believe may be interdependent.

In this study, we have shown that the activation of specific responses by activated sludge cultures due to exposure to toxic chemicals results in detectable changes in the chemical composition of the mixed liquor's soluble phase, and that these changes are common to different activated sludge populations. Furthermore, we have shown that it is possible to "measure" and "expose" those changes through the utilization of mass spectrometry analytical techniques combined with multivariate statistical methods. To our knowledge, this study reflects the first attempt to use metabolomics-derived techniques to a complex and environmentally-relevant microbial population. These results are promising and indicate that LC-MS may be used for (1) the elucidation of the mechanisms behind the responses of bacterial populations to chemical stress and (2) the discovery of bacterial stress biomarkers, to allow the development of new toxin detection technologies for environmental monitoring of both engineered and natural systems.

References

Love, N. G. and Bott, C. B. (2000) *A Review and Needs Survey of Upset Early Warning Devices*. Project 99-WWF-2. Water Environment Research Foundation. Alexandria, VA.

Chapter 2. Literature Review

Biofilms and Activated Sludge Flocs – Structure, Composition and Physiology

Parallelism between biofilms and biological flocs

In the environment, bacteria predominantly exist as biofilms, either attached to a surface or as non-attached aggregates, and are usually composed of complex communities of microorganisms embedded in a polymer matrix (Costerton et al., 1995). The basic structural and functional unit of a biofilm is a microcolony, which is composed of a group of cells embedded in an extracellular polymer matrix that maintains the cells together and defines the boundaries of the microcolony (Costerton, 1995). A mature biofilm is, therefore, composed of many microcolonies, which assume different sizes and shapes, interspersed with a complex network of pores and channels that allow water to flow within the biofilm. The composition of the polymer matrix varies with the bacteria that form the biofilm, as well as with the environmental conditions surrounding biofilm development.

Activated sludge flocs have been found to possess a similar structure to that of surface-attached biofilms. The main components of activated sludge are microorganisms, extracellular polymeric substances (EPS) and particles from wastewater that get entrapped in the flocs (Jorand et al., 1995). Microcolonies have been described and identified as the basic unit of activated sludge flocs. Flocs have a highly porous structure, determined both through surface area measurements (Andreadakis, 1993) and microscopy (Jorand et al., 1995), and the matrix is composed of EPS, which plays a key structural role in the overall arrangement of the different components and cohesiveness of the structure. Moreover, the similarities as far as the multilevel character of both biofilm and floc structures are also noteworthy. It is clear that biofilms and biological flocs have many features in common and, in fact, the characteristics of flocs fit within the classical definition of a biofilm (Costerton et al., 1995):

"Biofilms are defined as matrix-enclosed bacterial populations adherent to each other and/or to surfaces or interfaces. This definition includes microbial aggregates and floccules (…)"

Therefore, it becomes legitimate to consider the current knowledge on biofilms, since so much scientific effort has been undertaken on these systems in the last decade, and extrapolate that knowledge to biological flocs, because the physical, chemical and physiological mechanisms occurring within biofilm systems will likely have important similarities to those that occur within biological flocs.

Composition of the EPS matrix and interaction between different components

This section will concentrate on studies carried out with activated sludge samples, since activated sludge is the primary focus of this work and the EPS matrix in activated sludge flocs has been the focus of many studies. Proteins and carbohydrates are usually the predominant constituents, but other components such as multivalent cations, DNA, RNA, and lipids have also been related to specific characteristics of EPS. EPS studies are difficult because there is not a universal extraction method that can ensure all EPS is recovered without damaging cell components. It is, therefore, necessary to interpret the results of these studies with caution.

Proteins and Polysaccharides. Proteins are usually the predominant component of activated sludge EPS, both in laboratory-scale and full-scale industrial and municipal systems (Dignac et al., 1998; Higgins and Novak, 1997b; Urbain et al., 1993; Bura et al., 1998; Frølund et al., 1996; Wilen et al., 2003), as opposed to what is usually found in pure cultures, where polysaccharides seem to be the main component and the matrix is often reported as an exopolysaccharide matrix (for example, see Costerton et al., 1995 and Mah and O'Toole, 2001). In nitrifying granules, carbohydrates also predominate over proteins in the EPS fraction (Tay et al., 2002). Dignac et al. (1998) proposed three main sources for the proteins present in EPS samples extracted from activated sludge: excreted proteins/enzymes, proteins from cell lysis and proteins from wastewater that get entrapped in the floc. An important outcome of this work was obtained from amino acid (AA) analysis and found that ~ 25% of the AAs were aspartic and glutamic acid (negatively charged AAs) and ~ 45-50% were hydrophobic residues such as alanine, leucine, glycine and valine. Accordingly, the authors proposed that proteins within the floc play an important structural role. Hydrophobic AAs are hypothesized to be involved in hydrophobic interactions within the floc (see below) and negatively charged AAs could be important in electrostatic interactions of proteins with multivalent cations (see below). Urbain et al. (1993)

carried out an extensive study to try to understand the variables related to floc structure that most impacted settleability, measured as the sludge volume index (SVI). Mixed liquor samples from seven different full-scale units taken at different times (total of 16 samples) were analyzed and the Pearson's correlation coefficient was used to estimate relationships between the different variables measured. The total amount of protein in EPS correlated well with the amount of other EPS components, such as polysaccharides and DNA, i.e. flocs with higher amounts of protein also had higher amounts of polysaccharides and DNA.

Higgins and Novak (1997c) carried out a protein characterization study on EPS samples obtained from laboratory-scale reactors and both industrial and domestic full-scale plants, and collected evidence that the bound protein found in all tested activated sludge EPS samples is primarily composed of a lectin-like protein with a 15,000 Da size and an AA composition consistent with that found by Dignac et al. (1998) and characteristic of lectins. Lectins are proteins that bind sugar molecules and are highly specific to the type of carbohydrate that they interact with (reviewed by Weiner et al., 1995). Lectins are also called agglutinins because they agglutinate cells together (reviewed by Weiner et al., 1995). Therefore, if the proteins present in the EPS matrix are primarily lectins, the carbohydrate fraction that is also found within that matrix could be directly associated with the protein fraction. In fact, Higgins and Novak (1997c) observed that when the bound protein was removed from the floc through the utilization of a proteolytic enzyme, a release of up to 75% of polysaccharide also occurred, which is consistent with that idea. Dignac et al. (1998) found that carbohydrate release from the floc was effective through sonication alone, while protein extraction required additional steps (see below); this could indicate that, if carbohydrates establish interactions with the protein fraction, these interactions are weaker than those that occur between proteins and other floc components, such as bacterial cells. Once again, this is consistent with the theory of lectin-like proteins being an important portion of EPS protein, since lectins are usually located on bacterial appendages like pili and fimbriae (Mirelman, 1986).

The association between the protein and carbohydrate fractions of EPS has also been shown by the application of size-exclusion chromatography and Fourier transform infrared micro-spectroscopy to EPS samples (Garnier et al., 2005; Gorner et al., 2003). The results indicated

that proteins varying in size between 10 and 600 kDa were found in EPS, while carbohydrate molecules were much smaller averaging 0.5 to 1 kDa. There was no clear tendency for the association of smaller or larger proteins with the carbohydrate fraction.

Overall, these results are extremely important because they demonstrate the interactions that may occur between the two most important EPS components, proteins and polysaccharides. In addition, they indicate that the majority of the protein fraction in activated sludge EPS is only composed of one type of protein, suggesting that lectins are excreted with specific structural purposes and that, most likely, different members of the complex community contribute to the common goal of production and maintenance of that structure/matrix. Contrary to what occurs with pure culture biofilms, where the polymer matrix is often composed of polysaccharides, proteins in activated sludge seem to play the most important role in floc aggregation and cohesion.

Nucleic Acids. Besides protein and polysaccharides, other components are found in activated sludge EPS, such as nucleic acids. Although the percentages of nucleic acids is normally quite low relative to the protein and polysaccharide fractions (Bura et al., 1998; Frølund et al., 1996; Liao et al., 2001), their role in bioflocculation may be more important than generally accepted. Watanabe et al. (1998) isolated a marine bacterium belonging to the genus *Rhodovulum*, which could flocculate under specific growth conditions; it was found that the cells deflocculated completely when subject to RNase and DNase treatments but not with enzymes that target polysaccharides or proteins. EPS from this bacterium was found to be mainly composed or RNA and protein, and RNA is apparently secreted for structural purposes by the bacterium to enhance flocculation; cell lysis was shown to be minimal during the experiments, which is consistent with this hypothesis. Recently, it was found that DNA may also play a structural role in *Pseudomonas aeruginosa* biofilm architecture (Whitchurch et al., 2002), since DNase I strongly inhibited biofilm development. It is suggested that the source of DNA is not cell lysis, but an active excretion mechanism through membrane vesicles that are released during growth of the bacteria (Whitchurch et al., 2002). This phenomenon has been previously observed in two distinct *P. aeruginosa* strains, and it was established that the vesicles contained DNA (Kadurugamuwa and Beveridge, 1995). The role of DNA as a structural element in biofilm

formation is in accordance with the structural role of RNA found in *Rhodovulum* flocs. To date, no such role has been shown in activated sludge flocs and the presence of nucleic acids in EPS is usually attributed to the release of these molecules into the floc matrix through cell lysis (Dignac et al., 1998). Nevertheless, Urbain et al. (1993) found that the amount of DNA in activated sludge EPS did not have a strong correlation to either the mixed liquor volatile suspended solids (MLVSS) or cell numbers in the floc. In addition, Palmgren and Nielsen (1996) reported that the amount of DNA present in the EPS matrix was much higher than estimates of total intracellular DNA based on cell numbers, which seems to suggest that lysis is not the only process contributing to DNA accumulation in the floc matrix of activated sludge. The authors hypothesize that nucleic acids may play a role in maintaining the stability of activated sludge flocs, but definite evidence is yet to be reported regarding this topic.

Lipids. Lipids have also been found in activated sludge EPS, although usually in lower amounts than those found for proteins or polysaccharides (Conrad et al., 2003). Regarding the composition of the lipids in the EPS matrix, glycolipids were found to be the most abundant type (more than 50%), while phospholipids and neutral lipids were present in smaller amounts (Conrad et al., 2003). A comparison between two wastewater treatment plants showed that the fatty acid profiles were similar, although differences in microbial community structure were also seen (Conrad et al., 2003). Microscopic observations indicated that higher solids retention time (SRT) mixed liquors accumulate more of this material (Liss et al., 2002).

Cations. Cations have been shown to play a major role in floc architecture and floc settling and dewatering (Higgins and Novak, 1997b; Sobeck and Higgins, 2002; Higgins and Novak, 1997a; Biggs et al., 2001; Sanin and Vesilind, 2000; Li, 2005). The addition of divalent cations to the feed of laboratory continuous stirred tank reactors (CSTRs) maintained at steady-state improved the solids settleability and dewaterability, as well as the cake solids, floc density and effluent total suspended solids (TSS); flocs were also more resistant to shear and polymer demand for sludge conditioning decreased (Higgins and Novak, 1997b). The addition of sodium, on the other hand, resulted in deterioration of the same parameters, which was attributed to displacement of the divalent cations by sodium (Higgins and Novak, 1997b). Moreover, the addition of increasing concentrations of calcium to sonicated mixed liquor samples resulted in

increasing median floc size after reflocculation, which was shown to be due to uptake of calcium ions into the floc matrix and concurrent release of sodium and magnesium ions (Biggs et al., 2001).

These studies show that the activated sludge floc matrix has ion exchange properties and that divalent cations likely act as bridging agents between negatively charged sites within the floc. These sites could be primarily located in the protein fraction, which would be consistent with the large fraction of negatively charged AAs found in EPS protein (see above). Evidence for this has been presented by several authors (Dignac et al., 1998; Higgins and Novak, 1997b). The utilization of light sonication and/or cation exchange resins (CERs) for EPS extraction has been widely used. Dignac et al. (1998) observed that a higher recovery of proteins from the flocs was achieved when CER was used in combination with sonication than with sonication alone and that the same did not occur with carbohydrates; this indicates that cations may be preferably linked to proteins. Likewise, Higgins and Novak (1997b) observed that in reactors with increased calcium and magnesium in the feed, the bound protein content increased in comparison to a control, but the polysaccharide content remained relatively stable, indicating that cations interact preferably with proteins in EPS. The concentration of protein in EPS was also shown to correlate with the concentration of calcium ($r = 0.93$) (Urbain et al., 1993).

Most studies have focused on the role of divalent cations, such as calcium and magnesium, in floc structure and cohesion. However, work by others has shown that iron also plays an important role in floc structure. Iron (III) reduction has been shown to be an important process occurring under anaerobic conditions in activated sludge and because of its significant concentrations in activated sludge flocs, especially in plants that use Fe (III) to carry out phosphorus removal, this cation needs to be taken into account when considering the role of cations on activated sludge floc structure (Rasmussen and Nielsen, 1996; Nielsen, 1996).
It has been demonstrated that microbial-mediated reduction of floc-associated Fe (III) to Fe (II) causes deflocculation or deterioration of floc properties in activated sludge (Caccavo et al., 1996; Wilen et al., 2000b). Likewise, the addition of sulfide to activated sludge under anaerobic conditions results in strong deflocculation, which is allegedly motivated by the removal of iron from the floc matrix through chemical precipitation (Nielsen and Keiding, 1998; Wilen et al.,

2000b). Therefore, it seems that independent of the mechanism of iron reduction in the floc matrix, the process is always followed by a deterioration of floc structure and strength, and the reduction of the cation charge from +3 to +2 alone is sufficient for deflocculation to be observed (like Fe (III), Fe (II) is mainly associated with the floc matrix (Rasmussen and Nielsen, 1996)) which is indicative of a potentially important function within the floc matrix. Nielsen and Keiding (1998) have suggested that Fe (III) has a greater flocculation potential than calcium. In a recent study, Li (2005) showed that Fe (III) has a great impact on floc structure and morphology. Increasing amounts of Fe (III) in the influent of sequencing batch reactors (SBRs) fed with real wastewater caused decreasing TSS, chemical oxygen demand (COD), protein and polysaccharide concentrations in the effluent, as well as decreasing mixed liquor SVIs, therefore supporting the notion that Fe (III) has a flocculation/sequestering potential in activated sludge systems. The floc sizes, however, decreased with increasing Fe (III) dosages, which was associated with a decrease in filamentous organisms' abundance in the mixed liquor due to the presence of the cation. Similar to iron, aluminum is another trivalent cation that is currently being studied regarding its potential role in floc structure (Park *et al*., 2003).

Hydrophobicity. The internal hydrophobicity of a floc is another important parameter, given that hydrophobic interactions within flocs may be structurally important. EPS contains both hydrophilic and hydrophobic compounds, but polysaccharides are mainly hydrophilic and proteins form the majority of the hydrophobic fraction (Jorand et al., 1998). This is in agreement with EPS protein composition and the predominance of hydrophobic AAs. Moreover, lipids are also found in EPS and could partially account for the internal hydrophobicity of the EPS matrix (Conrad et al., 2003; Liss et al., 2002). Correlations between different floc structure parameters and the settleability of activated sludge were determined and indicate that as the total amount of EPS in a floc increases, the settleability decreases and, inversely, as the internal hydrophobicity increases, the settleability of the sludge improves (Urbain et al., 1993; Liao et al., 2001; Wilen et al., 2003) and the flocculation ability of the mixed liquor (measured as effluent TSS) also improves (Liao et al., 2001). Moreover, flocs with higher EPS concentrations have a worse flocculation ability and, concurrently, lower hydrophobicity (Wilen et al., 2003).

Bacterial strains with different cell surface hydrophobicity/hydrophilicity properties have been isolated from activated sludge (Jorand et al., 1994; Zita and Hermansson, 1997) and some strains were shown to modify their cell surface hydrophobicity characteristics depending on the growth phase. Nevertheless, it seems that strains with hydrophobic surfaces flocculate better than strains with hydrophilic surfaces (Jorand et al., 1994) and adhesion to preexisting flocs is enhanced by hydrophobic cell surfaces (Zita and Hermansson, 1997; Olofsson et al., 1998). Environmental factors, such as oxygen availability and the presence of toxic substances, can also impact cell surface hydrophobicity. Oxygen limitation seems to lower cell surface hydrophobicity, and this effect is most pronounced during stationary phase (Palmgren et al., 1998). Farrell and Quilty (2002) studied a *P. putida* strain capable of degrading phenol and mono-chlorophenols and observed that the culture formed large clumps of bacteria during growth on high concentrations of the mono-chlorophenols. This response was attributed to an increased cell surface hydrophobicity. The fact that bacterial cells can adapt their surface characteristics according to growth phase, toxicity and oxygen and nutrients availability, indicates that physiology may impact floc structure. This factor is discussed further below.

Conceptual models of activated sludge flocs

The growing scientific knowledge on the composition of activated sludge and interactions between the different components of the activated sludge floc has led to the proposition of conceptual models for floc structure/architecture. A model for floc structure was proposed by Jorand et al. (1995) based on transmission electron microscopy (TEM) of activated sludge flocs and particle size distribution (PSD) analysis of sonicated samples. TEM of floc sections showed that it was mainly a heterogeneous structure composed of bacteria, voids, waste particles and biopolymers. Bacteria were both present as single cells and organized in aggregates with defined boundaries and within which cells were unmeshed in a polymer gel-like matrix. Within each aggregate, bacteria had the same morphology and some dividing cells were observed. Using a polysaccharide stain, they detected carbohydrate linkages between individual cells, but other polymers could also be present that were not detected by that particular staining technique. PSD analysis through deconvolution of distribution curves revealed that the activated sludge samples were characterized by four main floc sizes: 2.5, 13, 51 and 125 μm. These researchers suggest a model of floc structure based on these observations and previous work conducted by others that

consists of a multilevel structure formed by 2.5 μm primary particles (bacterial cells) that group and form 13 μm secondary particles (microcolonies), which are linked together to form the third structural level of larger 50 - 125 μm flocs. Work by Klausen et al. (2004) found that, for a specific wastewater treatment plant, the average size of the microcolonies within a floc (with a diameter above 6 μm) was 12 μm and a floc was composed of approximately 15 microcolonies. Jorand et al. (1995) suggest the existence of two types of biopolymers holding particles together; one that is responsible for cell-cell linkage within the microcolonies and another type that brings together microcolony particles to form the larger flocs. Physical evidence of these different types of polymers has not been gathered.

Zartarian et al. (1994) conducted TEM and confocal laser microscopy (CLM) studies with activated sludge flocs and detected a very similar structure to that found by Jorand et al. (1995). They reported that flocs have irregular shape boundaries, observed that isolated bacteria were present, and observed both different cell morphologies and microcolonies within the flocs. They also reported that dividing cells could be observed inside microcolonies.

Sobeck and Higgins (2002) conducted a study with laboratory scale Eckenfelder reactors and synthetic feed with the objective of testing three different models for bioflocculation, and specifically the role of cations in floc structure. They considered three theories in evaluating their data, including the double layer or DLVO theory, the divalent cation bridging (DCB) theory and the alginate theory, which could be considered a subset of the DCB theory. The main results of the study supported the DCB theory more strongly than the other two theories, reinforcing the idea that cation bridging between adjacent polymer molecules is key to floc cohesion.

Higgins and Novak (1997c) also proposed a new model for floc structure based on their results that puts an emphasis on the role of lectin-like proteins in particle aggregation. Lectins are directly linked to bacteria and interact with sugar residues, which may bridge cells to one another. Divalent cations may be important not only as bridging agents but also to ensure protein activity, as lectin-like proteins have been shown to need calcium, magnesium and/or manganese for activity. It is not clear at what organizational level this model should be associated with, since different levels are not discussed. However, it is possible that these types

of interactions occur only within microcolonies, since lectins are primarily associated with bacterial cell surfaces, and that at higher organizational levels within the floc other types of interactions occur, including cation bridging, for example. This would be consistent with the suggestion of Jorand et al. (1995).

An interesting finding by Urbain et al. (1993) indicates that no statistically significant correlation was found between the concentration of EPS components like proteins or polysaccharides and the concentration of biomass (either measured through volatile matter after centrifugation or total number of cells), which the authors suggest may support the theory that flocs are not composed of repetitions of an elementary unit, i.e., floc $\neq$ [(cells + proteins + cations + polysaccharides) x n]. This is interesting because it indicates that, although microcolonies seem to be the basic structural unit of flocs, their size and composition may differ from case to case, such that the concentration of EPS and bacterial cell numbers are not the same in all microcolonies and flocs. In other words, flocs have a heterogeneous composition. Recent work by Klausen et al. (2004) corroborates this finding. Using fluorescence in-situ hybridization (FISH) to identify the bacterial groups represented in activated sludge flocs microcolonies, they concluded that different bacterial groups can affect floc structure in completely different manners. For example, hydrophobic interactions seemed to be important for the strength of *Delta-proteobacteria* and *Firmicutes* microcolonies, while calcium and magnesium EPS cross-linkages were important to maintain the strength of *Delta-* and *Gamma-proteobacteria* and *Bacteroidetes* microcolonies. Heterogeneity of activated sludge flocs can, therefore, be directly linked to the microbial community present in the flocs.

The concept of fractal geometry has been applied to activated sludge flocs. Snidaro et al. (1997) used CLM to determine the fractal dimension of the 13 μm and the 125 μm particles; the fractal dimension of the 13 μm particles or microcolonies was ~ 3 (i.e. 13 μm particles tended to be tridimensional), which represents a compact structure to which growth through cell division can be associated. TEM observations and additional fractal dimension measurements by other authors corroborate this finding (Zartarian et al., 1994). On the other hand, the 125 μm particles were found to have a fractal dimension of ~ 2.5, which indicates that the aggregation mechanism follows the “diffusion limited particle-cluster aggregation model” (Snidaro et al., 1997). Similar

results were obtained by Wu et al. (2002) which determined the fractal dimension of activated sludge flocs through both free settling tests and small angle light scattering. They concluded that the fractal dimension determined through light scattering was higher (2.12) than the one determined through settling tests (1.55) and explained the results as the outcome of the 2 different techniques, which target different levels of organization within the floc: light scattering gives information on the small scale particles (microcolonies), while the settling technique gives insight into the larger scale floc structure. The different fractal dimensions determined for the activated sludge flocs indicate that flocs are multifractal objects with different level structures that are formed through distinct dominant mechanisms. These results are consistent with Snidaro et al. (1997).

A clear model of activated sludge flocs is not yet defined. Although much of the floc composition, interaction between the different components and overall structure is known, the mechanisms of flocculation and maintenance of the floc cohesiveness, such as the forces that contribute to keep microcolonies together, are not yet understood. However, it seems clear that the EPS matrix plays a key structural role in floc architecture and that microcolonies are the basic functional and structural unit in activated sludge flocs.

Biofilm development and bioflocculation dynamics

Biofilm formation has recently been analyzed in detail in terms of the developmental stages and phenotypes that biofilm cells assume (Sauer et al., 2002). Five stages were identified in the development of *P. aeruginosa* biofilms: reversible attachment (up to 2 hours), irreversible attachment (2 hours to 3 days), maturation 1 (3 to 6 days), maturation 2 (6 to 9 days) and dispersion (9 to 12 days). These developmental stages and in particular the cycling nature of biofilm formation and dispersion suggests that a similar mechanism may occur with bacterial flocs, through which a dynamic equilibrium is established between flocculation and deflocculation forces/mechanisms.

The flocculation dynamics of activated sludge have been studied using an on-line instrument to assess the variation of the PSD with time (Biggs and Lant, 2000; Biggs et al., 2003; Chaignon et al., 2002). The reflocculation of activated sludge after sonication, which was conducted to break

up the flocs into their basic microcolony building blocks, was observed to occur in three phases: first, the aggregation forces control the process and the floc mean diameter increases rapidly; then, the magnitude of the aggregation mechanism decreases gradually relative to the breakup forces; and finally, the rates of floc aggregation and breakup reach the same level and a dynamic equilibrium between the two mechanisms is established, which translates into a steady-state median floc size that is maintained until a perturbation occurs (Biggs and Lant, 2000). This reflocculation behavior has also been observed after mixed liquor shearing by velocity gradient (G) values of 370 s^{-1} (Chaignon et al., 2002) and 113 s^{-1} (Biggs et al., 2003). However, the first study concluded that flocculation dynamics exhibited a reversible behavior, i.e. the floc mean diameter returned to its initial value, while the second study found that the process was irreversible and that the floc mean diameter decreased after shear and was dependent both on the number and intensity of the shear events previously imparted onto the activated sludge. The differences could be due to the shear intensity applied in each case; nonetheless, these studies show that after shearing events, reflocculation occurs rapidly (less than 2 hours), which is important from a practical standpoint. Similarly, biofilm structure is also impacted by hydrodynamics (Liu and Tay, 2001), with cells grown under high shear forming thinner and denser biofilms than cells grown under low shear conditions, which could be compared to the variations of floc diameter under shear/reflocculation conditions.

A more important conclusion of the work conducted by Chaignon et al. (2002) is that in addition to the dynamic equilibrium between floc formation and destruction, the exchange of materials between different flocs involves equilibrium, as demonstrated through transfer of talc mineral particles between different activated sludge flocs. This mechanism can be extremely important and have repercussions at the level of polymers, signal molecules or nutrient exchange among different flocs of the activated sludge community, and at a more global level can be interpreted as a mechanism that allows the different players in the community to sense their environment and interact with the other bacteria. Clearly, this topic deserves further attention.

Although the above flocculation/reflocculation studies are valuable and provide insight into the flocculation processes in activated sludge, the emphasis was placed on the physical and chemical characteristics and interactions that may occur between particles and physiology-dependent

mechanisms were not accounted for. This is especially important to consider because these studies were carried out with diluted activated sludge samples that were not aerated or fed during the experiments, so it is particularly difficult to extrapolate these results to real-world applications.

Link between physiology of biofilms and biological flocs and biofilm/floc structure

The physiology of biofilm cells has been compared to that of planktonic cells for various bacterial strains. Through proteome analysis it was possible to see that *P. aeruginosa* planktonic and early attached cells appear to have similar physiologies, and as biofilm development progresses the difference between biofilm and planktonic cells increases dramatically; this difference is most noticeable during maturation 2 stage, with 50% of the protein 2D gel spots upregulated when compared to planktonic cells; during dispersion the biofilm cells regain a planktonic-like physiology (Sauer et al., 2002). Among the proteins that showed significant changes in activity with biofilm stage are proteins involved in EPS production, resistance to oxidative damage and aerobic and anaerobic metabolism (Sauer et al., 2002). Similar results were found for *Escherichia coli* regarding specific proteins that are preferentially expressed in biofilms (Prigent-Combaret et al., 1999). These studies show a tremendous difference in physiology between planktonic and biofilm cells. However, a microarray study with *P. aeruginosa* planktonic and 5 days-old biofilms indicated that only 1% of the genes are differentially expressed in the two growth modes (Whiteley et al., 2001). The differences between the studies are not clear and may be related to experimental methods and growth conditions.

In activated sludge systems, an attempt has been made to correlate physiological characteristics with floc structure parameters. Andreadakis (1993) tested activated sludges with different SRTs but similar biomass concentrations and found that, although lower SRT biomasses had a much higher viability (measured as dehydrogenase activity), no significant trends in surface area, floc size, carbohydrate content or floc density were found, showing that different physiologies did not translate into clear differences in the quality or quantity of floc components. This study was conducted with laboratory-scale reactors, which were fed with synthetic feed and the size of the flocs was particularly small (median of ~ 40 μm) compared to most reported sizes of full-scale

systems. In a similar study, Liao et al. (2001) studied the effects of SRT on the surface properties of activated sludge and EPS production. They used laboratory-scale SBRs fed with synthetic wastewater and also chose to maintain the biomass concentration by varying the feed concentration in order to eliminate the possible influence of the solids concentration variable from the analysis. They used effluent TSS as an indicator for bioflocculation within the system and observed that higher SRTs led to lower effluent TSS concentrations. The EPS was mainly composed of proteins (predominant) and carbohydrates and DNA in small and variable amounts and the ratio of protein/polysaccharides increased with SRT, due to both an increase in protein and a decrease in polysaccharides. The total amount of EPS in the sludge, though, was not SRT-dependent and is important to note, since other studies have shown a tendency for longer SRTs to have lower concentrations of EPS in the floc matrix (Wilen et al., 2003). They also found that hydrophobicity was higher at higher SRTs, which can account for the better flocculation characteristics of higher SRT sludges (see above), and that the surface charge of flocs correlated well with hydrophobicity, with more hydrophobic flocs corresponding to less negatively-charged flocs. Increased hydrophobicity at higher SRTs could be due to the presence of lipids (Liss et al., 2002). Moreover, microscopic observations of the EPS matrix showed that low SRT flocs have a more hydrated surface, while higher SRT flocs possess less hydrated material on the surface (Liss et al., 2002), which is consistent with the hydrophobicity measurements by Liao et al. (2001). The interpretation and extrapolation of these results to full-scale systems is difficult because many different variables may play a role in the outcome of the studies, such as the existence of an active nitrifying population at higher SRTs or the fact that, in order to get the same biomass concentrations, the lower SRT reactors had to receive a much higher feed concentration.

Although physiological characteristics can influence mixed liquor floc structure properties, the type of bacterial species present in the community can also impact floc structure properties and, therefore, floc size and settleability. The proliferation of filamentous bacteria, for example, can greatly impact the floc structure and settleability of activated sludge (Govoreanu et al., 2003; Wilen et al., 2003) resulting in a common problem in wastewater treatment plants called filamentous bulking. Wilen et al. (2003) suggested that the impact of filaments can be so significant, that common relationships determined for non-filamentous sludges, such as

increasing SVI with increasing EPS in the floc matrix, cannot be applied to activated sludges with large numbers of filaments. Distinct non-filamentous bacterial species present in activated sludge flocs also have different floc-forming properties (Klausen et al., 2004). Microcolonies consisting of bacteria from the *Beta-*, *Gamma-* and *Delta-proteobacteria* and *Actinobacteria* groups are more resistant to shear than those from the *Alpha-proteobacteria*, *Firmicutes* and *Bacteroidetes*, suggesting that the bacteria within the later microcolonies are kept together by weaker forces. In addition, the cohesiveness of the microcolonies belonging to the different bacterial groups is maintained by distinct forces. For example, the strength of the *Beta-proteobacteria* microcolonies is apparently maintained by EPS entanglements, while bacteria within *Delta-proteobacteria* microcolonies are kept together by both divalent cation bridging and hydrophobic interactions.

The nutrient content of the feed has also been reported to influence the composition of the EPS matrix and structural parameters of the activated sludge flocs, as shown in laboratory-scale reactors fed with synthetic wastewater with different COD:N:P ratios (Bura et al., 1998). Sponza (2002) also reported different EPS compositions from mixed liquors fed with different industrial wastewaters adjusted for different COD:N:P ratios and, although the variations relative to the control reactor (without nutrient limitation) were distinct from those found by Bura et al. (1998), the main point remains that the characteristics of the feed impact the composition of the floc matrix. The differences between the two studies could be due to differences in the experimental setup and methods for EPS extraction. Moreover, when activated sludge is subjected to starvation conditions (aerobic digestion), the active cell numbers and specific oxygen uptake rate (SOUR) decrease rapidly and after a few days the flocculation ability of the remaining biomass deteriorates markedly (Oviedo et al., 2003), showing that starvation-induced stress interferes with flocculation processes.

Wilen et al. (2000b) specifically studied the impact of short-term changes of microbial activity on the stability of activated sludge flocs, which was measured over time as the turbidity of lightly centrifuged samples for a given experimental condition. This work was carried out with samples from a full-scale activated sludge system. They observed that the addition of the readily biodegradable substrates glucose and ethanol improved floc strength compared to a starved

control. In addition, anaerobic conditions had a negative impact on floc aggregation and the addition of nitrate under anaerobic conditions improved floc structure relative to strictly anaerobic conditions. Likewise, azide and a temperature reduction to 4^{o}C also had a negative impact on the floc structure. These results strongly indicate that flocculation is intimately coupled with microbial activity within activated sludge flocs and that environmental changes can have a great impact on floc properties on the short-term.

Finally, the operating conditions of the treatment system can greatly affect flocculation. For example, a simple parameter such as the SBR cycle time has been shown to have a major impact on granulation of a nitrifying enrichment culture, showing that contrary to common belief that nitrifiers have poor flocculation ability and EPS production (Tsuneda et al., 2001), these organisms can be "forced" to aggregate under specific operating conditions (Tay et al., 2002). Nitrifier granulation was shown to occur mainly due to increased cell surface hydrophobicity at cycle times of 6 and 12 hours, relative to 24 hours (Tay et al., 2002).

Overall these results seem to indicate that the feed composition, operational characteristics, physiological state and type of bacterial species present in the floc greatly impact the physical-chemical characteristics of the flocs that are formed. These different factors are interrelated and, therefore, this is not an unexpected conclusion.

Effects of Toxins on Biofilms and Activated Sludge Systems, Resistance Mechanisms and Stress Responses

Known mechanisms for resistance of biofilms to antimicrobial agents

The main hypotheses regarding the mechanisms through which biofilm cells have increased resistance to antimicrobial agents are described next (reviewed by Costerton et al., 1999; Mah and O'Toole, 2001; Stewart, 2002):

- Failure of the toxin to penetrate the biofilm. Extracellular polymeric substances function as a barrier between the toxins and the bacterial cells. This barrier could function either

through sorption or reaction of EPS components with the antimicrobial agent, as well as through retardation of toxin penetration, giving biofilm cells a better opportunity to express a specific stress response (see below).

- Slow growth and stress responses. It is known that at least some bacteria within a biofilm live in a starved or slow growing state, which has been shown to confer greater resistance to stress conditions and antibiotics in particular, since many of these agents target actively growing cells. This is linked to the expression of RpoS during stationary phase, a regulator that controls the general stress response in many Gram-negative bacteria. More recently, evidence that RpoS levels may increase in response to factors other than a starved physiological state, such as quorum sensing, has led to the hypothesis that the general stress response controlled by RpoS may be turned on in biofilms regardless of the growth phase of the cells within that biofilm, thereby functioning as a protection mechanism of biofilms against exogenous insults.
- Heterogeneity. Biofilms are heterogeneous structures where gradients of nutrients, waste products and signaling factors can be observed. This heterogeneity results in different physiologies of the cells within a biofilm and, therefore, to different capabilities of withstanding stress by different elements of the community. For example, cells that are close to the interface with the liquid medium may be more susceptible than those totally embedded in the EPS matrix.
- Quorum sensing. Although some evidence exists that quorum sensing may be related to increased resistance to antimicrobial agents in biofilms, for example through its connection to RpoS, more research is needed to fully understand the role of quorum sensing as a contributing factor to resistance mechanisms.
- Induction of a specific protection phenotype. A relatively recent idea is that some cells forming a subpopulation of the biofilm may assume a specific biofilm protection phenotype, functionally different from the other bacteria in the biofilm, and that results in the expression of different mechanisms to fight antimicrobial agents, such as increasing expression of multiple drug efflux pumps or altering the composition of outer membrane proteins. This phenotype may be activated by biofilm-specific environmental or physiological signals. This idea would signify a specialization of cells inside a biofilm, much like occurs in eukaryotic tissues and organs.

The mechanisms described above are likely to work under different conditions and be specific for particular toxins or stresses. Depending on the antimicrobial agent, the biofilm community structure and the environmental conditions under which biofilm growth occurs, different mechanisms will likely be responsible for the resistance behavior (Mah and O'Toole, 2001).

Given the similarities between biofilms and biological flocs, the mechanisms presented may influence the resistance/sensitivity to stress of activated sludge flocs. The activated sludge response to different toxins is also likely dependent on the different factors mentioned above. For example, toxins that interact with EPS, either through sorption or reaction mechanisms, may be impeded from reaching the cells within a floc, but others that readily diffuse through the floc matrix may elicit other resistance mechanisms. The role of EPS as a protection barrier is discussed below.

Regulation of EPS synthesis and functions of the polymer matrix

The regulation of EPS synthesis and, therefore, the understanding of EPS functions has been primarily studied in pure culture systems, especially with *E. coli* and *P. aeruginosa*, but may also be applicable to activated sludge communities. One of the best-studied exopolysaccharides from biofilms is alginate, which is produced by many bacterial strains and in particular by *P. aeruginosa* strains. Alginate and more generally EPS substances are synthesized by bacteria in response to stressful environmental conditions, such as nutrient starvation, slow growth rates, ethanol dehydration, increased oxygen, dessication, low temperature and high osmotic pressure and ionic strength (reviewed by Boyd and Chakrabarty, 1995; Weiner et al., 1995). Alginate production by *P. aeruginosa* is upregulated under increased oxygen conditions (Bayer et al., 1990; Sabra et al., 2002). This bacterium grows best under microaerophilic conditions and, therefore, utilizes specific mechanisms to decrease the amount of oxygen reaching the cells, such as producing an alginate capsule, reducing the oxygen transfer rate from the gas into the liquid phase, presumably through the secretion of rhamnolipids, and secreting proteins into the medium (Sabra et al., 2002). It has been hypothesized that these mechanisms protect the cells from oxidative stress and that the sensitivity to oxygen may be one of the reasons for its preferred mode of growth as a biofilm (Sabra et al., 2002). Other species, such as *Vibrio cholerae*, also

produce exopolysaccharides, which confer extra resistance to osmotic and oxidative stress (Wai et al., 1998). In the case of marine sulfate-reducing bacteria (SRB), biofilms of a mixed community formed cell clusters and increased the production of extracellular polymeric substances when the feed contained toxic metals (cadmium, zinc, chromium, lead, copper or aluminum), phenol or glutaraldehyde, as opposed to sea water only (Fang et al., 2002). The EPS produced by the SRB community was mainly composed of proteins (84-92%), with polysaccharides being about 8-16% of the total mass/cm^2 of biofilm. Again, this is evidence that stress conditions favor the production of EPS. This is not only seen in pure cultures, but also in mixed community biofilms.

In a paper relating binding of heavy metals by activated sludge EPS, Guibaud et al. (2005) indicated that EPS extracted from activated sludge had a higher binding capacity than EPS extracted from pure cultures of organisms isolated from the same activated sludge. They suggest that this behavior might be related to the fact that the pure cultures of bacteria were grown without exposure to the metals and, therefore, did not have an opportunity to activate EPS synthesis/modification mechanisms, which could afford them better protection from the metals by increasing the ability of EPS to bind the metal ions. In another study with activated sludge from full-scale facilities, Garnier et al. (2005) observed that the EPS composition (characterized by size exclusion chromatography and fourier transform infrared spectroscopy) changed dramatically (shifted to smaller molecules) during deflocculation events, showing that modifications in the composition of activated sludge EPS occur under stress conditions.

EPS also functions as a protective barrier against chemical toxins. The protection mechanisms occur either through sorption or reaction with the chemical (reviewed by Costerton et al., 1999; Mah and O'Toole, 2001; Stewart, 2002), as shown in a mixed species biofilm where reaction of proteins in EPS with chlorine served as a protection factor to the community (Leriche et al., 2003). Activated sludge EPS has been shown to have a great affinity for heavy metals (Guibaud et al., 2005; Jang et al., 2001; Liu et al., 2001). Carboxylic and phosphate groups have been shown to play a major role in the binding of heavy metals to activated sludge EPS molecules (Guibaud et al., 2005). Therefore, reduced bacterial exposure to the toxins is expected due to the interactions between EPS and the metal ions. In a recent study with both wild type and a mutant

P. aeruginosa strain that isogenically overproduces alginate, it was observed that the latter formed highly structured and heterogeneous biofilms that were much more resistant to the antibiotic tobramycin than the former, which formed more homogeneous biofilms (Hentzer et al., 2001). Farrell and Quilty (2002) showed that a *P. putida* strain capable of degrading mono-chlorophenols formed clumps when subjected to high concentrations of the compounds, and this autoaggregation was proposed as a response to chemical stress induced by the high concentrations of the mono-chlorophenols and as a protective mechanism allowing toxin utilization as substrate. In addition, alginate and more generally the EPS matrix has been shown to retard the diffusion of certain antibiotics through the biofilm matrix, which in some cases was attributed to the presence of antibiotic-inactivating or modifying enzymes in the EPS matrix, such as beta-lactamases (reviewed by Stewart, 2002). Retardation of toxin penetration may also afford a better opportunity for biofilm cells to express specific stress responses, which would not be possible in planktonic cells that become quickly overwhelmed by the toxin (reviewed by Stewart, 2002).

Besides functioning as a protective barrier against unfavorable environmental conditions and antimicrobial agents, other functions have been proposed for bacterial EPS (reviewed by Weiner et al., 1995), such as its structural role in biofilm/floc formation and maintenance and as an agent in cell-cell interactions. Activation of alginate biosynthesis is observed following attachment of *P. aeruginosa* cells to a solid surface (Davies et al., 1993; Davies and Geesey, 1995; Hoyle et al., 1993) and is, therefore, one of the important steps in biofilm formation.

Alginate production appears to be also connected to RpoS, as a mutation in the *rpoS* gene led to a dramatic decrease in alginate production by a *P. aeruginosa* strain (Suh et al., 1999). Although *rpoS* and quorum sensing signals may be interlinked (Whiteley et al., 2000; Latifi et al., 1996; You et al., 1998; Van Delden et al., 2001; Aguilar et al., 2003; Baca-Delancey et al., 1999; Liu et al., 2000; Schuster et al., 2004), EPS production does not appear to be linked to quorum sensing, as a biofilm formed by a *P. aeruginosa lasI* mutant produced similar EPS amounts as the wild type biofilm, despite the fact that it did not differentiate into complex structures (Davies et al., 1998). In a dual species biofilm formed by a *Pseudomonas sp.* strain and a *P. putida* strain, EPS was found to be produced preferentially in tower-like and mushroom-like structures, unlike the

more uniform production on single species biofilms (Cowan et al., 2000). The reason for this is unknown.

Lectins are another class of molecules that may be present in EPS and have been found in activated sludge (see above). In *P. aeruginosa*, the cytoplasmic lectins PA-IL and PA-IIL have been implicated in cell adhesion (Wentworth et al., 1991) and lectin synthesis was found to be initiated only in stationary phase and regulated both by quorum sensing (*rhl* locus) and RpoS, as demonstrated by disruption of lectin synthesis in *rhlI*, *rhlR* and *rpoS* mutants (Winzer et al., 2000). One relevant aspect of lectins that has been recently studied in *P. aeruginosa* is that these proteins contain hydrophobic sites that can potentially serve as binding sites for hydrophobic substances (Stoitsova et al., 2003). These sites can eventually function as binding sites for hydrophobic toxins, which would reduce their accessibility to the bacterial cells and afford better protection to the cells in the event of a shock load of hydrophobic substances. Activated sludge biomass has been found to interact with organic hydrophobic substances, such as PAHs and halogenated hydrocarbons; furthermore, sorption of these compounds can be significant (up to 75% with PAHs) (Finlayson et al., 1998). It is possible that these interactions protect the activated sludge bacteria from the toxic effects of these compounds. These observations are also consistent with the composition of activated sludge EPS-associated protein, which has approximately 50% hydrophobic AAs (see above).

Together, these observations suggest that, in addition to its important structural function, EPS has a crucial role in protecting bacteria from external insults. The EPS matrix in activated sludge flocs may function in a similar fashion and assume the same protective role that has been identified in biofilms. Protection may occur mainly through physical-chemical interactions, such as those that occur through sorption and/or chemical reaction with EPS components, or from a physiological response that induces EPS synthesis in response to stress.

Given the characteristics of activated sludge EPS, it is therefore legitimate to hypothesize that EPS protects the bacteria in the activated sludge flocs from toxic compounds that it has the potential to interact with, such as hydrophobic and positively-charged toxins. For example, negatively charged residues in bound EPS protein can bind heavy metals, leading to reduced

toxicity because the metal is less bioavailable in comparison to systems without significant quantities of EPS. The binding of heavy metals to EPS has been shown in the literature (Guibaud et al., 2005; Jang et al., 2001; Liu et al., 2001). In the case of soluble uncharged hydrophilic toxins that more easily diffuse through the EPS matrix, the toxicity response is probably a function of other mechanisms (see above).

Causes and mechanisms for disruption of biological flocs

One of the most common problems encountered by wastewater treatment plants is a deterioration in the flocculation ability of the activated sludge mixed liquor, which translates into an increase in the effluent soluble organic materials (given by biochemical oxygen demand -BOD- and/or COD) and TSS. Sudden deflocculation events caused by shock loads of chemical toxins are one of the main upset events reported by wastewater treatment plant operators (Love and Bott, 2000). In addition, xenobiotic-induced deflocculation can be caused by chemicals with distinct structures and properties, such as organic hydrophobic chemicals, chlorinated phenols, uncouplers of oxidative phosphorylation, heavy metals, electrophilic chemicals, high pH and azide (Henriques et al., in review; Schwartz-Mittelmann and Galil, 2000; Neufeld, 1976; Wilen et al., 2000b; Bott and Love, 2002; Bott et al., 2001). Deflocculation can also result from anaerobic conditions (Wilen and Balmer, 1999; Wilen et al., 2000a), shear stress (Chaignon et al., 2002; Biggs et al., 2003; Mikkelsen and Keiding, 1999), cation imbalance (Higgins and Novak, 1997b) and reduction of floc-associated iron (Caccavo et al., 1996; Wilen et al., 2000b), and sudden temperature increases (Morgan-Sagastume and Allen, 2005).

The fact that toxins with such different structures and chemical and biological properties, as well as other environmental conditions, cause a similar macroscopic effect, suggests that different mechanisms for activated sludge floc disruption exist. The mechanism for electrophile-mediated deflocculation has been studied/described (Bott and Love, 2002) but a lot of questions remain regarding the remaining mechanisms. Additionally, in biofilms the focus has been on physiological changes that trigger biofilm dispersion under normal development conditions and few studies are available on biofilm dispersion by chemicals and the mechanisms behind it.

Bott and Love (2002) studied the mechanism for electrophile-induced deflocculation. Their work showed that electrophilic shocks invoke a rapid potassium efflux response in activated sludge systems. This stress response has been identified in pure cultures of Gram-negative, heterotrophic bacteria and has been found to occur through the glutathione-gated potassium efflux (GGKE) mechanism, by which the reaction of cytoplasmic glutathione with the electrophilic agent increases the oxidized fraction of glutathione in the cell, which then results in the activation of potassium efflux channels (Elmore et al., 1990; reviewed by Ferguson, 1999). This mechanism is thought to afford extra protection to the cell against the electrophilic agent since, simultaneous to potassium efflux, there is an acidification of the cytoplasm, which in turn activates important genes such as *dps*, a gene that codes for a DNA protection protein (Ferguson et al., 1998; Ferguson et al., 2000; reviewed by Ferguson, 1999). The connection between an increase in the extracellular potassium and the deflocculation event comes from the ion exchange capacities of activated sludge flocs (see above) and the potential replacement of divalent cations within the floc matrix with high potassium fluxes, which weakens the floc cohesiveness and results in break-up of the floc into smaller particles that do not settle well (Bott and Love, 2002).

Another deflocculation mechanism has been proposed for the deflocculation caused by phenol shocks. Schwartz-Mittelmann and Galil (2000) noticed a significant increase in non-settleable solids after a phenol shock event to activated sludge, relative to a control reactor fed with glucose and relative to a reactor containing non-growing cells shocked with the same amount of phenol (non-growth was defined as nitrogen-limiting conditions). Therefore, it appears that the deflocculation mechanism associated with the phenol shock was only elicited in active cells and is, therefore, dependent on bacterial activity. They also noticed an increase in soluble polysaccharides in the growing biomass shocked reactor relative to the non-growing shocked reactor, which was accompanied by an increase in particles smaller than 25 μm (shift in PSD to smaller flocs indicates floc breakup). Furthermore, the biomass flocs became less hydrophobic due to phenol shock. This could in part explain the breakup of the flocs, since hydrophobicity has been shown to be an important factor in floc aggregation (see above). The mechanism through which cells changed the hydrophobicity of their surfaces was not investigated; however, it could be associated with a known microbial stress response to hydrophobic substances whereby the composition of the cytoplasmic membrane is transformed through cis/trans

isomeration and other adaptation mechanisms, and changes on the outer membrane also occur, which reduce the hydrophobicity of the outer membrane (reviewed by Weber and de Bont, 1996). This reduction in hydrophobicity is motivated by alterations in lipopolysaccharide (LPS) content and protein secretion (Aono and Kobayashi, 1997; reviewed by Weber and de Bont, 1996).

Few studies have focused on the nature and origin of the soluble materials and particles released after a stress event, and the relationship of those materials to mechanisms that occur at the floc level, which lead to floc disruption. Wilen and Balmer (1999) found that more than 80% of the turbidity found in the effluent of a pilot plant activated sludge system (fed with wastewater after primary settling) was mainly composed of particles smaller than 2 μm; in addition, when the reactor was subjected to alternating aerobic and anaerobic conditions, the turbidity of the supernatant increased during the anaerobic period and decreased during the aerobic periods, and the total number of particles in the supernatant was directly related to the turbidity. In a follow-up study, the nature of the increased turbidity caused by anaerobic conditions was investigated (Wilen et al., 2000a). Deflocculation during anaerobic conditions was found to be directly related to the number of bacteria in the supernatant. Accordingly, the evolution of protein, carbohydrate and humic substances concentration in the supernatant during alternating aerobic and anaerobic conditions was similar to that of turbidity, showing that these materials were also released during the deflocculation event and contributed to the increase in supernatant turbidity. These results suggest that a reaction to oxygen limitations by bacteria that prefer aerobic conditions can be their release from the floc as a way to search for availability of oxygen. Release of proteins, carbohydrates, humic substances and DNA has also been observed during activated sludge deflocculation caused by temperature upshifts from 30 to 45^{o}C (Morgan-Sagastume and Allen, 2005). The release of these materials was attributed to EPS solubilisation and floc fragmentation, as a significant increase in effluent TSS was also observed. Cell lysis was measured to have occurred, but only to a small extent, with an estimate of 1-2% of cells lysing due to the increase in temperature.

The fact that different environmental conditions induce the release of biopolymers into the bulk liquid of bacterial cultures suggests that different mechanisms for floc disruption and biopolymer

release exist. This implies that the nature of the released materials may be different for each mechanism. It is, therefore, possible to conjecture and hypothesize about the nature of those materials and relate their characteristics to the mechanism that most likely is responsible for the observed effect. For example, deflocculation events caused by cation imbalance (through an increase in monovalent cation concentrations) may result in a partial displacement of calcium and magnesium from negatively charged sites, which are replaced with monovalent cations. This creates repulsion between microaggregates and breaks up the floc, leading to non-settling floc fragments and smaller flocs in the settling fraction. EPS components may or may not be released to the bulk phase, depending on their primary interactions. In chemical-induced deflocculation, several hypotheses concerning the nature of the released materials can be drawn, because different mechanisms for deflocculation likely exist. For the case of thiol reactive chemicals, it is the GGKE physiological stress response that causes a cation imbalance and induces floc breakup, resulting in smaller flocs and fragments that do not settle. In this case, however, in addition to release of materials from the EPS matrix, release of intracellular materials is also expected, as a result of cell lysis and/or active secretion mechanisms provoked by the stress response.

It is clear that activated sludge floc disruption can be induced by different chemicals and distinct environmental conditions. The mechanisms through which deflocculation occurs are likely specific for each deflocculation agent, as is the nature of the materials (both soluble and particulate) that are released from the floc matrix. The characterization of these materials and comparison to the floc composition before and after chemical addition may help to understand the mechanisms that occur at the floc/molecular level and potentially contribute to the development of better and new operation parameters and practices.

Metabolic footprinting as a technique to identify changes in microbial physiology induced by stress conditions

The analysis of the soluble materials in the supernatant and the EPS of stressed mixed liquor may reveal important physiological changes induced by the stress condition, such as changes in the amount and/or composition of EPS substances and release of intracellular components into the bulk liquid derived from specific stress responses and/or cell lysis. Analyzing aggregate

biomolecules, such as total protein and total carbohydrates that are released upon exposure to stress, can yield important information. However, a more detailed analysis of these biomolecules can provide a footprint of the different compounds within the biomolecule classes that are released under stress conditions. This has the potential to provide much more information, both quantitative and qualitative. For example, distinct footprint patterns can relate to the nature of the chemical or chemicals causing the stress. The extent to which selected bands in the footprint are expressed may reveal dose:response relationships. Furthermore, using an aggregate footprinting method allows one to use the method on indigenous activated sludge cultures, and does not rely upon knowing specifics about the composition of the community.

Within the field of metabolomics, there is a technique called metabolic footprinting, which consists in analyzing and comparing the "exome", "exometabolome" or extracellular matrix (spent culture medium in the case of bacterial cultures) produced under different conditions (Kell et al., 2005; Dunn and Ellis, 2005; Villas-Boas et al., 2005). Metabolic fingerprinting, on the other hand, refers to the analysis of the intracellular metabolome (Dunn and Ellis, 2005; Villas-Boas et al., 2005). Metabolic footprinting is particularly interesting as an application to activated sludge systems, as it does not require complex extraction and quenching/preservation methods and allows analysis and comparison of mixed liquor supernatant under different environmental conditions. The first time this technique was described, it was used to show that it was possible to differentiate between different physiological states of wild type yeast and different yeast single-gene deletion mutants (Allen et al., 2003). Metabolic footprinting has also been used to distinguish between different *E. coli* tryptophan mutants (Kaderbhai et al., 2003) and between modes of action of several antifungal substances on yeast cells (Allen et al., 2004). For example, the footprints of yeast cells exposed to sublethal concentration of respiratory inhibitors could be differentiated from those of yeast cells exposed to an uncoupler of oxidative phosphorylation (Allen et al., 2004). The application of metabolic footprinting to compare changes in extracellular metabolite patterns in response to toxin exposure may, therefore, be a powerful technique to detect physiological changes that lead to a deterioration of process performance in activated sludge systems.

The main techniques currently used to generate metabolic fingerprints/footprints are based on nuclear magnetic resonance (NMR) and mass spectrometry (MS) coupled to chromatography (Grivet et al., 2003; Dunn and Ellis, 2005; Villas-Boas et al., 2005). Some examples of the application of these techniques to detect changes in physiology of bacterial pure cultures or eukaryotic organisms can be found in the literature. NMR techniques have been successfully used to compare metabolic profiles of *Crotalaria cobalticola* plant cells following exposure to cobalt chloride (Bailey et al., 2004) and to distinguish between healthy and diseased red abalone individuals (Viant et al., 2003). Metabolic fingerprinting using direct atmospheric pressure chemical ionization-MS (APCI-MS) was used to detect the differences between control and transgenic "staygreen" harvested lettuce heads (Garratt et al., 2005). The analysis permitted the identification of higher levels of three volatile organic compounds (acetaldehyde, ethanol and dimethyl sulfide) in the transgenic plants relative to the control. Kaderbhai et al. (2003) produced metabolic footprinting of different *E. coli* tryptophan mutants to demonstrate that different strains could be differentiated through analysis of the growth medium; both liquid chromatography-electrospray ionization-MS (LC-ESI-MS) and Fourier transform infrared spectroscopy (FT-IR) were used as techniques; the authors concluded that both techniques produced profiles that could be used to distinguish between the different strains. Allen and coworkers (2003, 2004) used direct injection ESI-Time of Flight-MS (ESI-TOF-MS) for their studies with yeast cells, to show that metabolic footprinting could be used to distinguish between different physiological states, different yeast mutant strains and yeast cultures exposed to different antifungal agents (see above). Fourier transform ion cyclotron-MS (FT-IC-MS) has been used to investigate the cold acclimation of *Arabidospis thaliana* leaves and compare the metabolomes of leaves shifted to cold conditions versus leaves developed under low temperatures (Gray and Heath, 2005). Other mass spectrometry-based tools have been used, including tandem MS (MS/MS) coupled with LC-ESI (Mashego et al., 2004), gas chromatography (GC) coupled to MS (Jonsson et al., 2004) and capillary electrophoresis-ESI-MS (CE-ESI-MS) (Soo et al., 2004). Finally, Weckwerth et al. (2004) developed an extraction method to separate metabolites, proteins and RNA and were able to determine the existence of 652 metabolites, 297 proteins and clear RNA bands from a single *A. thaliana* leaf sample using GC-TOF-MS for metabolites, LC-MS/MS for proteins and northern blot analysis for RNA.

Comparison of the metabolic fingerprints/footprints generated by the analytical techniques described above is conducted using multivariate statistical analysis methods. There are basically two types of statistical methods that are used for comparison purposes: supervised and unsupervised methods (Goodacre et al., 2004). The most commonly used unsupervised methods are principal component analysis and hierarchical cluster analysis (Dettmer and Hammock, 2004). The idea of unsupervised methods is that the method itself groups the different samples based on the similarities of their profiles, but without any *a priori* information regarding the different treatments used experimentally (Goodacre et al., 2004). In contrast, supervised methods, are powerful statistical methods that use a "teacher" signal to extract information from the input profiles. In other words, when using supervised methods, the group to which a specific sample belongs to is known *a priori* and the method uses that information to generate a model that tries to pair the pattern information with the target group that the sample belongs to, thus providing better clustering of the data (Goodacre et al., 2004). Partial least squares (PLS) and discriminant function analysis (DFA) are two examples of supervised methods (Goodacre et al., 2004). Other data analysis techniques have recently been developed, to deal with multilevel, multidimensional data sets, in which variations may occur due to different factors/variables simultaneously (Jansen et al., 2005; Smilde et al., 2005). Some examples of these statistical methods are multilevel simultaneous component analysis (Jansen et al., 2005), ANOVA-simultaneous component analysis (Smilde et al., 2005), partial least squares discriminant analysis (PLS-DA) (Jonsson et al., 2004) and the application of genetic algorithms for variable selection prior to applying a supervised method to the data (Jarvis and Goodacre, 2005).

Few studies have applied the concept of metabolic fingerprinting/footprinting to complex environmental samples and/or microbial communities. In fact, the only examples found in the literature refer to studies that use a broader definition of the term metabolic fingerprinting, which includes carbon utilization profiles by bacteria as metabolic fingerprints. For example, metabolic fingerprinting was recently applied to track the source of fecal contamination in surface waters (Ahmed et al., 2005). First, a database was developed by collecting fecal samples from septic tanks (human) and different animal species. A biochemical fingerprinting method called the PhPlate system (kinetic measurement of the utilization of 46 different substrates) was used to create metabolic fingerprints for enterococci and *E. coli* strains isolated from the samples.

Analysis of water samples from a specific creek within the area of study and comparison with the database, allowed identification of the source for more than 65% of the bacteria present in the water samples. The developed method could distinguish between human and animal contamination, as well as differentiate between different animal species. In this study, metabolic fingerprint proved to be a reliable method to trace the source of fecal contamination in a watershed, a very specific and important environmental application. Other studies applied metabolic fingerprinting to study differences in microbial communities under different environmental conditions. For example, metabolic fingerprinting based on carbon utilization profiles (Biolog system, utilization of 95 different carbon sources) was used to show that different heterotrophic microbial communities develop in different maize rizhosphere compartments (Baudoin et al., 2001). The PhPlate system was utilized to generate metabolic fingerprints of the microbial communities from rat gastrointestinal tracks (Smith and Mackie, 2004). In conjunction with denaturing gradient gel electrophoresis (DGGE), the metabolic fingerprinting data generated through the PhPlate system showed that different fecal bacteria populations developed when condensed tannins were or were not included in the rats' diet and that a shift to tannin-resistant bacteria occurred when these compounds were included in the diet. The application of metabolic fingerprinting/footprinting to activated sludge samples has not been found in the literature. There is, however, one study of activated sludge EPS that uses size exclusion chromatography and FT-IR to characterize and compare EPS from different wastewater treatment plants and different operational conditions (Gorner et al., 2003; Garnier et al., 2005). An important piece of evidence from this study is that EPS fingerprints seem to be fairly stable for each plant, but differ from plant to plant, suggesting that the composition of the EPS matrix is plant-specific (Garnier et al., 2005). This is not surprising, as the EPS matrix depends on the activated sludge bacterial community (Klausen et al., 2004) and this is specific for each plant. In addition, EPS fingerprints were fairly stable with time when normal operation occurred, but changed dramatically when upset events causing deflocculation of the biomass took place (Garnier et al., 2005). The EPS composition shifted to smaller molecules when upset events occurred and this was observed both in a municipal plant in which a deflocculation event was attributed to high sodium input, and in a paper mill plant in which the deflocculation event did not have an identified cause. This study shows that alterations at the level of EPS composition occur in response to stress events in activated sludge communities, and that those

alterations may be identified through fingerprints generated through a spectroscopic technique, which is extremely relevant for this work.

The characterization of both the soluble, EPS and insoluble materials that are released from activated sludge flocs during an upset event may lead to the development of methods that allow fast and reliable identification of the toxin causing the upset event, and the development of early warning tools to prevent those upsets from happening.

References

Aguilar, C., Bertani, I., and Venturi, V. (2003) Quorum sensing system and stationary phase sigma factor (*rpoS*) of the onion pathogen *Burkholderia cepacia* genomovar I type strain ATCC 25416. *Appl. Environ. Microbiol.* **69:** 1739-1747.

Ahmed, W., Neller, R., and Katouli, M. (2005) Host species-specific metabolic fingerprint database for enterococci and *Escherichia coli* and its application to identify sources of fecal contamination in surface waters. *Appl. Environ. Microbiol.* **71:** 4461-4468.

Allen, J., Davey, H.M., Broadhurst, D., Heald, J.K., Rowland, J.J., Oliver, S.G., and Kell, D.B. (2003) High-throughput classification of yeast mutants for functional genomics using metabolic footprinting. *Nat. Biotechnol.* **21:** 692-696.

Allen, J., Davey, H.M., Broadhurst, D., Rowland, J.J., Oliver, S.G., and Kell, D.B. (2004) Discrimination of modes of action of antifungal substances by use of metabolic footprinting. *Appl. Environ. Microbiol.* **70:** 6157-6165.

Andreadakis, A.D. (1993) Physical and chemical properties of activated sludge floc. *Water Res.* **27:** 1707-1714.

Aono, R. and Kobayashi, H. (1997) Cell surface properties of organic solvent-tolerant mutants of *Escherichia coli* K-12. *Appl. Environ. Microbiol.* **63:** 3637-3642.

Baca-Delancey, R.R., South, M.M.T., Ding, X.D., and Rather, P.N. (1999) *Escherichia coli* genes regulated by cell-to-cell signaling. *P. Natl. Acad. Sci. USA* **96:** 4610-4614.

Bailey, N.J.C., Oven, M., Holmes, E., Zenk, M.H., and Nicholson, J.K. (2004) An NMR-based metabolomic approach to the analysis of the effects of xenobiotics on endogenous metabolite levels in plants. *Spectrosc.-Int. J.* **18:** 279-287.

Baudoin, E., Benizri, E., and Guckert, A. (2001) Metabolic fingerprint of microbial communities from distinct maize rhizosphere compartments. *Eur. J. Soil Biol.* **37:** 85-93.

Bayer, A.S., Eftekhar, F., Tu, J., Nast, C.C., and Speert, D.P. (1990) Oxygen-dependent up-regulation of mucoid exopolysaccharide (alginate) production in *Pseudomonas aeruginosa*. *Infect. Immun.* **58:** 1344-1349.

Biggs, C., Lant, P., and Hounslow, M. (2003) Modelling the effect of shear history on activated sludge flocculation. *Water Sci. Technol.* **47:** 251-257.

Biggs, C.A., Ford, A.M., and Lant, P.A. (2001) Activated sludge flocculation: direct determination of the effect of calcium ions. *Water Sci. Technol.* **43:** 75-82.

Biggs, C.A. and Lant, P.A. (2000) Activated sludge flocculation: on-line determination of floc size and the effect of shear. *Water Res.* **34:** 2542-2550.

Bott, C.B., Duncan, A.J., and Love, N.G. (2001) Stress protein expression in domestic activated sludge in response to xenobiotic shock loading. *Water Sci. Technol.* **43:** 123-30.

Bott, C.B. and Love, N.G. (2002) Investigating a mechanistic cause for activated sludge deflocculation in response to shock loads of toxic electrophilic chemicals. *Water Environ. Res.* **74:** 306-315.

Boyd, A. and Chakrabarty, A.M. (1995) *Pseudomonas aeruginosa* biofilms - role of the alginate exopolysaccharide. *J. Ind. Microbiol.* **15:** 162-168.

Bura, R., Cheung, M., Liao, B., Finlayson, J., Lee, B.C., Droppo, I.G., Leppard, G. G., and Liss, S. N. (1998) Composition of extracellular polymeric substances in the activated sludge floc matrix. *Water Sci. Technol.* **37:** 325-333.

Caccavo, F.J., Frølund, B., Van Ommen Kloeke, F., and Nielsen, P. (1996) Deflocculation of activated sludge by the dissimilatory Fe (III)-reducing bacterium *Shewanella alga* BrY. *Appl. Environ. Microbiol.* **62:** 1487-1490.

Chaignon, V., Lartiges, B.S., El Samrani, A., and Mustin, C. (2002) Evolution of size distribution and transfer of mineral particles between flocs in activated sludges: an insight into floc exchange dynamics. *Water Res.* **36:** 676-684.

Conrad, A., Kontro, M., Keinanen, M.M., Cadoret, A., Faure, P., Mansuy-Huault, L., and Block, J.C. (2003) Fatty acids of lipid fractions in extracellular polymeric substances of activated sludge flocs. *Lipids* **38:** 1093-1105.

Costerton, J.W. (1995) Overview of microbial biofilms. *J. Ind. Microbiol.* **15:** 137-140.

Costerton, J.W., Lewandowski, Z., Caldwell, D.E., Korber, D.R., and Lappinscott, H.M. (1995) Microbial biofilms. *Annu. Rev. Microbiol.* **49:** 711-745.

Costerton, J.W., Stewart, P.S., and Greenberg, E.P. (1999) Bacterial biofilms: a common cause of persistent infections. *Science* **284:** 1318-1322.

Cowan, S.E., Gilbert, E., Liepmann, D., and Keasling, J.D. (2000) Commensal interactions in a dual-species biofilm exposed to mixed organic compounds. *Appl. Environ. Microbiol.* **66:** 4481-4485.

Davies, D.G., Chakrabarty, A.M., and Geesey, G.G. (1993) Exopolysaccharide production in biofilms - substratum activation of alginate gene expression by *Pseudomonas aeruginosa*. *Appl. Environ. Microbiol.* **59:** 1181-1186.

Davies, D.G. and Geesey, G.G. (1995) Regulation of the alginate biosynthesis gene *algC* in *Pseudomonas aeruginosa* during biofilm development in continuous culture. *Appl. Environ. Microbiol.* **61:** 860-867.

Davies, D.G. , Parsek, M.R., Pearson, J.P., Iglewski, B.H., Costerton, J.W., and Greenberg, E.P. (1998) The involvement of cell-to-cell signals in the development of a bacterial biofilm. *Science* **280:** 295-298.

Dettmer, K. and Hammock, B.D. (2004) Metabolomics – a new exciting field within the "omics" sciences. *Environ. Health Persp.* **112:** A396-A397.

Dignac, M.F., Urbain, V., Rybacki, D., Bruchet, A., Snidaro, D., and Scribe, P. (1998) Chemical description of extracellular polymers: implication on activated sludge floc structure. *Water Sci. Technol.* **38:** 45-53.

Dunn, W.B. and Ellis, D.I. (2005) Metabolomics: current analytical platforms and methodologies. *Trac-Trend. Anal. Chem.* **24:** 285-294.

Elmore, M.J., Lamb, A.J., Ritchie, G.Y., Douglas, R.M., Munro, A., Gajewska, A., and Booth, I.R. (1990) Activation of potassium efflux from *Escherichia coli* by glutathione metabolites. *Mol. Microbiol.* **4:** 405-412.

Fang, H.H.P., Xu, L.C., and Chan, K.Y. (2002) Effects of toxic metals and chemicals on biofilm and biocorrosion. *Water Res.* **36:** 4709-4716.

Farrell, A. and Quilty, B. (2002) Substrate-dependent autoaggregation of *Pseudomonas putida* CP1 during the degradation of mono-chlorophenols and phenol. *J. Ind. Microbiol. Biot.* **28:** 316-324.

Ferguson, G.P. (1999) Protective mechanisms against toxic electrophiles in *Escherichia coli*. *Trends Microbiol.* **7:** 242-247.

Ferguson, G.P., Battista, J.R., Lee, A.T., and Booth, I.R. (2000) Protection of the DNA during the exposure of *Escherichia coli* cells to a toxic metabolite: the role of the KefB and KefC potassium channels. *Mol. Microbiol.* **35:** 113-122.

Ferguson, G.P., Creighton, R.I., Nikolaev, Y., and Booth, I.R. (1998) Importance of RpoS and Dps in survival of exposure of both exponential- and stationary-phase *Escherichia coli* cells to the electrophile N-ethylmaleimide. *J. Bacteriol.* **180:** 1030-1036.

Finlayson, J.C., Liao, B., Droppo, I.G., Leppard, G.G., and Liss, S.N. (1998) The relationship between the structure of activated sludge flocs and the sorption of hydrophobic pollutants. *Water Sci. Technol.* **37:** 353-357.

Frølund, B., Palmgren, R., Keiding, K., and Nielsen, P.H. (1996) Extraction of extracellular polymers from activated sludge using a cation exchange resin. *Water Res.* **30:** 1749-1758.

Garnier, C., Gorner, T., Lartiges, B.S., Abdelouhab, S., and de Donato, P. (2005) Characterization of activated sludge exopolymers from various origins: a combined size-exclusion chromatography and infrared microscopy study. *Water Res.* **39:** 3044-3054.

Garratt, L.C., Linforth, R., Taylor, A.J., Lowe, K.C., Power, J.B., and Davey, M.R. (2005) Metabolite fingerprinting in transgenic lettuce. *Plant Biotechnol. J.* **3:** 165-174.

Goodacre, R. , Vaidyanathan, S., Dunn, W.B., Harrigan, G.G. , and Kell, D.B. (2004) Metabolomics by numbers: acquiring and understanding global metabolite data. *Trends Biotechnol.* **22:** 245-252.

Gorner, T., de Donato, P., Ameil, M.H., Montarges-Pelletier, E., and Lartiges, B.S. (2003) Activated sludge exopolymers: separation and identification using size exclusion chromatography and infrared micro-spectroscopy. *Water Res.* **37:** 2388-2393.

Govoreanu, R., Seghers, D., Nopens, I., De Clercq, B., Saveyn, H., Capalozza, C. et al. (2003) Linking floc structure and settling properties to activated sludge population dynamics in an SBR. *Water Sci. Technol.* **47:** 9-18.

Gray, G.R. and Heath, D. (2005) A global reorganization of the metabolome in *Arabidopsis* during cold acclimation is revealed by metabolic fingerprinting. *Physiol. Plantarum* **124:** 236-248.

Grivet, J.P., Delort, A.M., and Portais, J.C. (2003) NMR and microbiology: from physiology to metabolomics. *Biochimie* **85:** 823-840.

Guibaud, G., Comte, S., Bordas, F., Dupuy, S., and Baudu, M. (2005) Comparison of the complexation potential of extracellular polymeric substances (EPS) extracted from activated sludges and produced by pure bacteria strains, for cadmium, lead and nickel. *Chemosphere* **59:** 629-638.

Henriques, I. D. S., Kelly, R.T., Dauphinais, J.L., and Love, N. G. (in review) Activated sludge inhibition by chemical stressors – a comprehensive study. *Water Environ. Res.*

Hentzer, M., Teitzel, G.M., Balzer, G.J., Heydorn, A., Molin, S., Givskov, M., and Parsek, M.R. (2001) Alginate overproduction affects *Pseudomonas aeruginosa* biofilm structure and function. *J. Bacteriol.* **183:** 5395-5401.

Higgins, M.J. and Novak, J.T. (1997a) Dewatering and settling of activated sludges: the case for using cation analysis. *Water Environ. Res.* **69:** 225-232.

Higgins, M.J. and Novak, J.T. (1997b) The effect of cations on the settling and dewatering of activated sludges: laboratory results. *Water Environ. Res.* **69:** 215-224.

Higgins, M.J. and Novak, J.T. (1997c) Characterization of exocellular protein and its role in bioflocculation. *J. Environ. Eng.-ASCE* **123:** 479-485.

Hoyle, B., Williams, L., and Costerton, J. (1993) Production of mucoid exopolysaccharide during development of *Pseudomonas aeruginosa* biofilms. *Infect. Immun.* **61:** 777-780.

Jang, A., Kim, S.M., Kim, S.Y., Lee, S.G., and Kim, I.S. (2001) Effect of heavy metals (Cu, Pb, and Ni) on the compositions of EPS in biofilms. *Water Sci. Technol.* **43:** 41-48.

Jansen, J.J., Hoefsloot, H.C.J., van der Greef, J., Timmerman, M.E., and Smilde, A.K. (2005) Multilevel component analysis of time-resolved metabolic fingerprinting data. *Anal. Chim. Acta* **530:** 173-183.

Jarvis, R.M. and Goodacre, R. (2005) Genetic algorithm optimization for pre-processing and variable selection of spectroscopic data. *Bioinformatics* **21:** 860-868.

Jonsson, P., Gullberg, J., Nordstrom, A., Kusano, M., Kowalczyk, M., Sjostrom, M., and Moritz, T. (2004) A strategy for identifying differences in large series of metabolomic samples analyzed by GC/MS. *Anal. Chem.* **76:** 1738-1745.

Jorand, F., Boue-Bigne, F., Block, J.C., and Urbain, V. (1998) Hydrophobic/hydrophilic properties of activated sludge exopolymeric substances. *Water Sci. Technol.* **37:** 307-315.

Jorand, F., Guicherd, P., Urbain, V., Manem, J., and Block, J.C. (1994) Hydrophobicity of activated sludge flocs and laboratory-grown bacteria. *Water Sci. Technol.* **30:** 211-218.

Jorand, F., Zartarian, F., Thomas, F., Block, J.C., Bottero, J.Y., Villemin, G., Urbain, V., and Manem, J. (1995) Chemical and structural (2D) linkage between bacteria within activated sludge flocs. *Water Res.* **29:** 1639-1647.

Kaderbhai, N.N., Broadhurst, D.I., Ellis, D.I., Goodacre, R., and Kell, D.B. (2003) Functional genomics via metabolic footprinting: monitoring metabolite secretion by *Escherichia coli* tryptophan metabolism mutants using FT-IR and direct injection electrospray mass spectrometry. *Compar. Funct. Genom.* **4:** 376-391.

Kadurugamuwa, J.L. and Beveridge, T.J. (1995) Virulence factors are released from *Pseudomonas aeruginosa* in association with membrane vesicles during normal growth and exposure to gentamicin - a novel mechanism of enzyme secretion. *J. Bacteriol.* **177:** 3998-4008.

Kell, D.B., Brown, M., Davey, H.M., Dunn, W.B., Spasic, I., and Oliver, S.G. (2005) Metabolic footprinting and systems biology: the medium is the message. *Nat. Rev. Microbiol.* **3:** 557-565.

Klausen, M.M., Thomsen, T.R., Nielsen, J.L., Mikkelsen, L.H., and Nielsen, P.H. (2004) Variations in microcolony strength of probe-defined bacteria in activated sludge flocs. *FEMS Microbiol. Ecol.* **50:** 123-132.

Latifi, A., Foglino, M., Tanaka, K., Williams, P., and Lazdunski, A. (1996) A hierarchical quorum sensing cascade in *Pseudomonas aeruginosa* links the transcriptional activators LasR and RhiR (VsmR) to expression of the stationary phase sigma factor RpoS. *Mol. Microbiol.* **21:** 1137-1146.

Leriche, V., Briandet, R., and Carpentier, B. (2003) Ecology of mixed biofilms subjected daily to a chlorinated alkaline solution: spatial distribution of bacterial species suggests a protective effect of one species to another. *Environ. Microbiol.* **5:** 64-71.

Li, J.Y. (2005) Effects of Fe (III) on floc characteristics of activated sludge. *J. Chem. Technol. Biot.* **80:** 313-319.

Liao, B.Q., Allen, D.G., Droppo, I.G., Leppard, G.G., and Liss, S.N. (2001) Surface properties of sludge and their role in bioflocculation and settleability. *Water Res.* **35:** 339-350.

Liss, S.N., Liao, B.Q., Droppo, I.G., Allen, D.G., and Leppard, G.G. (2002) Effect of solids retention time on floc structure. *Water Sci. Technol.* **46:** 431-438.

Liu, X., Ng, C., and Ferenci, T. (2000) Global adaptations resulting from high population densities in *Escherichia coli* cultures. *J. Bacteriol.* **182:** 4158-4164.

Liu, Y., Lam, M.C., and Fang, H.H.P. (2001) Adsorption of heavy metals by EPS of activated sludge. *Water Sci. Technol.* **43:** 59-66.

Liu, Y. and Tay, J.H. (2001) Metabolic response of biofilm to shear stress in fixed-film culture. *J. Appl. Microbiol.* **90:** 337-342.

Love, N. G. and Bott, C. B. (2000) *A Review and Needs Survey of Upset Early Warning Devices*. Project 99-WWF-2. Water Environment Research Foundation. Alexandria, VA.

Mah, T.F.C. and O'Toole, G.A. (2001) Mechanisms of biofilm resistance to antimicrobial agents. *Trends Microbiol.* **9:** 34-39.

Mashego, M.R., Wu, L., Van Dam, J.C., Ras, C., Vinke, J.L., Van Winden, W.A., Van Gulik, W.M., and Heijnen, J.J. (2004) MIRACLE: mass isotopomer ratio analysis of U-C-13-labeled extracts. A new method for accurate quantification of changes in concentrations of intracellular metabolites. *Biotechnol. Bioeng.* **85:** 620-628.

Mikkelsen, L.H. and Keiding, K. (1999) Equilibrium aspects of the effects of shear and solids content on aggregate deflocculation. *Adv. Colloid Interfac.* **80:** 151-182.

Mirelman, D. (1986) *Microbial Lectins and Agglutinins*. John Wiley & Sons, Inc. New York, NY.

Morgan-Sagastume, F. and Allen, D.G. (2005) Activated sludge deflocculation under temperature upshifts from 30 to 45 degrees C. *Water Res.* **39:** 1061-1074.

Neufeld, R.D. (1976) Heavy metals-induced deflocculation of activated sludge. *J. Water Pollut. Control Fed.* **48:** 1940-1947.

Nielsen, P.H. (1996) The significance of microbial Fe (III) reduction in the activated sludge process. *Water Sci. Technol.* **34:** 129-136.

Nielsen, P.H. and Keiding, K. (1998) Disintegration of activated sludge flocs in presence of sulfide. *Water Res.* **32:** 313-320.

Olofsson, A.C., Zita, A., and Hermansson, M. (1998) Floc stability and adhesion of green-fluorescent protein-marked bacteria to flocs in activated sludge. *Microbiol.-UK* **144:** 519-528.

Oviedo, M.D.C., Lopez-Ramirez, J.A., Marquez, D.S., and Alonso, J.M.Q. (2003) Evolution of an activated sludge system under starvation conditions. *Chem. Eng. J.* **94:** 139-146.

Palmgren, R., Jorand, F., Nielsen, P.H., and Block, J.C. (1998) Influence of oxygen limitation on the cell surface properties of bacteria from activated sludge. *Water Sci. Technol.* **37:** 349-352.

Palmgren, R. and Nielsen, P.H. (1996) Accumulation of DNA in the exopolymeric matrix of activated sludge and bacterial cultures. *Water Sci. Technol.* **34:** 233-240.

Park, C., Abu-Orf, M.M., and Novak, J.T. (2003) Predicting the digestibility of waste activated sludges using cation analysis. *Water Environment Federation 76th Annual Technical Exhibition and Conference,* Los Angeles, CA.

Prigent-Combaret, C., Vidal, O., Dorel, C., and Lejeune, P. (1999) Abiotic surface sensing and biofilm-dependent regulation of gene expression in *Escherichia coli*. *J. Bacteriol.* **181:** 5993-6002.

Rasmussen, H. and Nielsen, P.H. (1996) Iron reduction in activated sludge measured with different extraction techniques. *Water Res.* **30:** 551-558.

Sabra, W., Kim, E.J., and Zeng, A.P. (2002) Physiological responses of *Pseudomonas aeruginosa* PAO1 to oxidative stress in controlled microaerobic and aerobic cultures. *Microbiol.-SGM* **148:** 3195-3202.

Sanin, D. and Vesilind, P.A. (2000) Bioflocculation of activated sludge: the role of calcium ions and extracellular polymers. *Environ. Technol.* **21:** 1405-1412.

Sauer, K., Camper, A.K., Ehrlich, G.D., Costerton, J.W., and Davies, D.G. (2002) *Pseudomonas aeruginosa* displays multiple phenotypes during development as a biofilm. *J. Bacteriol.* **184:** 1140-1154.

Schuster, M. , Hawkins, A.C., Harwood, C.S., and Greenberg, E.P. (2004) The *Pseudomonas aeruginosa* RpoS regulon and its relationship to quorum sensing. *Mol. Microbiol.* **51:** 973-985.

Schwartz-Mittelmann, A. and Galil, N.I. (2000) Biological mechanisms involved in bioflocculation disturbances caused by phenol. *Water Sci. Technol.* **42:** 105-110.

Smilde, A.K. , Jansen, J.J., Hoefsloot, H.C.J., Lamers, R., van der Greef, J., and Timmerman, M.E. (2005) ANOVA-simultaneous component analysis (ASCA): a new tool for analyzing designed metabolomics data. *Bioinformatics* **21:** 3043-3048.

Smith, A.H. and Mackie, R.I. (2004) Effect of condensed tannins on bacterial diversity and metabolic activity in the rat gastrointestinal tract. *Appl. Environ. Microbiol.* **70:** 1104-1115.

Snidaro, D., Zartarian, F., Jorand, F., Bottero, J.Y., Block, J.C., and Manem, J. (1997) Characterization of activated sludge flocs structure. *Water Sci. Technol.* **36:** 313-320.

Sobeck, D.C. and Higgins, M.J. (2002) Examination of three theories for mechanisms of cation-induced bioflocculation. *Water Res.* **36:** 527-538.

Soo, E.C., Aubry, A.J., Logan, S.M., Guerry, P., Kelly, J.F., Young, N.M., and Thibault, P. (2004) Selective detection and identification of sugar nucleotides by CE-electrospray-MS and its application to bacterial metabolomics. *Anal. Chem.* **76:** 619-626.

Sponza, D.T. (2002) Extracellular polymer substances and physicochemical properties of flocs in steady- and unsteady-state activated sludge systems. *Process Biochem.* **37:** 983-998.

Stewart, P.S. (2002) Mechanisms of antibiotic resistance in bacterial biofilms. *Int. J. Med. Microbiol.* **292:** 107-113.

Stoitsova, S.R., Boteva, R.N., and Doyle, R.J. (2003) Binding of hydrophobic ligands by *Pseudomonas aeruginosa* PA-I lectin. *BBA-Gen. Subjects* **1619:** 213-219.

Suh, S.J., Silo-Suh, L., Woods, D.E., Hassett, D.J., West, S.E.H., and Ohman, D.E. (1999) Effect of RpoS mutation on the stress response and expression of virulence factors in *Pseudomonas aeruginosa*. *J. Bacteriol.* **181:** 3890-3897.

Tay, J.H., Yang, S.F., and Liu, Y. (2002) Hydraulic selection pressure-induced nitrifying granulation in sequencing batch reactors. *Appl. Microbiol. Biot.* **59:** 332-337.

Tsuneda, S., Park, S., Hayashi, H., Jung, J., and Hirata, A. (2001) Enhancement of nitrifying biofilm formation using selected EPS produced by heterotrophic bacteria. *Water Sci. Technol.* **43:** 197-204.

Urbain, V., Block, J.C., and Manem, J. (1993) Bioflocculation in activated sludge – an analytic approach. *Water Res.* **27:** 829-838.

Van Delden, C., Comte, R., and Bally, M. (2001) Stringent response activates quorum sensing and modulates cell density-dependent gene expression in *Pseudomonas aeruginosa*. *J. Bacteriol.* **183:** 5376-5384.

Viant, M.R. , Rosenblum, E.S., and Tjeerdema, R.S. (2003) NMR-based metabolomics: a powerful approach for characterizing the effects of environmental stressors on organism health. *Environ. Sci. Technol.* **37:** 4982-4989.

Villas-Boas, S.G., Mas, S., Akesson, M., Smedsgaard, J., and Nielsen, J. (2005) Mass spectrometry in metabolome analysis. *Mass Spectrom. Rev.* **24:** 613-646.

Wai, S.N., Mizunoe, Y., Takade, A., Kawabata, S., and Yoshida, S. (1998) *Vibrio cholerae* O1 strain TSI-4 produces the exopolysaccharide materials that determine colony morphology, stress resistance, and biofilm formation. *Appl. Environ. Microbiol.* **64:** 3648-3655.

Watanabe, M., Sasaki, K., Nakashimada, Y., Kakizono, T., Noparatnaraporn, N., and Nishio, N. (1998) Growth and flocculation of a marine photosynthetic bacterium *Rhodovulum* Sp. *Appl. Microbiol. Biot.* **50:** 682-691.

Weber, F.J. and de Bont, J.A.M. (1996) Adaptation mechanisms of microorganisms to the toxic effects of organic solvents on membranes. *BBA-Rev. Biomembranes* **1286:** 225-245.

Weckwerth, W., Wenzel, K., and Fiehn, O. (2004) Process for the integrated extraction, identification, and quantification of metabolites, proteins and RNA to reveal their co-regulation in biochemical networks. *Proteomics* **4:** 78-83.

Weiner, R., Langille, S., and Quintero, E. (1995) Structure, function and immunochemistry of bacterial exopolysaccharides. *J. Ind. Microbiol.* **15:** 339-346.

Wentworth, J.S., Austin, F.E., Garber, N., Gilboa-Garber, N., Paterson, C.A., Doyle, R.J. (1991) Cytoplasmic lectins contribute to the adhesion of *Pseudomonas aeruginosa*. *Biofouling* **4:** 99-104.

Whitchurch, C.B., Tolker-Nielsen, T., Ragas, P.C., and Mattick, J.S. (2002) Extracellular DNA required for bacterial biofilm formation. *Science* **295:** 1487.

Whiteley, M., Bangera, M.G., Bumgarner, R.E., Parsek, M.R., Teitzel, G.M., Lory, S., and Greenberg, E.P. (2001) Gene expression in *Pseudomonas aeruginosa* biofilms. *Nature* **413:** 860-864.

Whiteley, M., Parsek, M.R., and Greenberg, E.P. (2000) Regulation of quorum sensing by RpoS in *Pseudomonas aeruginosa*. *J. Bacteriol.* **182:** 4356-4360.

Wilen, B.M. and Balmer, P. (1999) The effect of dissolved oxygen concentration on the structure, size and size distribution of activated sludge flocs. *Water Res.* **33:** 391-400.

Wilen, B.M., Jin, B., and Lant, P. (2003) Relationship between flocculation of activated sludge and composition of extracellular polymeric substances. *Water Sci. Technol.* **47:** 95-103.

Wilen, B.M., Keiding, K., and Nielsen, P.H. (2000a) Anaerobic deflocculation and aerobic reflocculation of activated sludge. *Water Res.* **34:** 3933-3942.

Wilen, B.M., Nielsen, J.L., Keiding, K., and Nielsen, P.H. (2000b) Influence of microbial activity on the stability of activated sludge flocs. *Colloid. Surface. B* **18:** 145-156.

Winzer, K., Falconer, C., Garber, N.C., Diggle, S.P., Camara, M., and Williams, P. (2000) The *Pseudomonas aeruginosa* lectins PA-IL and PA-IIL are controlled by quorum sensing and by RpoS. *J. Bacteriol.* **182:** 6401-6411.

Wu, R.M., Lee, D.J., Waite, T.D., and Guan, J. (2002) Multilevel structure of sludge flocs. *J. Colloid. Interf. Sci.* **252:** 383-392.

You, Z.Y., Fukushima, J., Tanaka, K., Kawamoto, S., and Okuda, K. (1998) Induction of entry into the stationary growth phase in *Pseudomonas aeruginosa* by N-acylhomoserine lactone. *FEMS Microbiol. Lett.* **164:** 99-106.

Zartarian, F., Mustin, C., Bottero, J.Y., Villemin, G., Thomas, F., Ailleres, L., Champenois, M., Grulois, P., and Manem, J. (1994) Spatial arrangement of the components of activated sludge flocs. *Water Sci. Technol.* **30:** 243-250.

Zita, A. and Hermansson, M. (1997) Effects of bacterial cell surface structures and hydrophobicity on attachment to activated sludge flocs. *Appl. Environ. Microbiol.* **63:** 1168-1170.

Chapter 3. Activated Sludge Inhibition by Chemical Stressors – A Comprehensive Study

Inês D. S. Henriques, Richard T. Kelly II, Jennifer L. Dauphinais and Nancy G. Love

ABSTRACT: The effects of shock loads of 1-chloro-2,4-dinitrobenzene (CDNB), cadmium, 1-octanol, 2,4-dinitrophenol (DNP), weakly complexed cyanide, pH 5, 9 and 11, and high ammonia levels on activated sludge biomass growth, respiration rate, flocculation, chemical oxygen demand (COD) removal, dewaterability and settleability were studied. For all chemical shocks except ammonia and pH, concentrations that caused 15, 25 and 50% respiration inhibition were used to provide a single pulse chemical shock to sequencing batch reactor (SBR) systems containing a nitrifying (10 day solids retention time – SRT) and a non-nitrifying (2 day SRT) biomass. Cadmium and pH 11 shocks were the conditions that most detrimentally affected all the processes, followed by CDNB. DNP and cyanide primarily led to effects on respiration, while pH 5, 9, octanol and various ammonia concentrations did not impact the treatment process to a significant extent. We believe that establishing source-effect relationships that link classes of chemical toxins to their potential inhibitory effects on activated sludge processes will help to develop methods that prevent and/or attenuate the impacts of toxic shock loads on activated sludge systems.

KEYWORDS: activated sludge, toxins, shock load, COD removal, flocculation, respiration, oxygen uptake rate (OUR), growth, settleability, dewaterability

Introduction

Biological wastewater treatment systems are susceptible to toxic shock loads of industrial chemicals, which can adversely impact the treatment process efficiency (Love and Bott, 2000). Many transient upset events are known to be caused by shock loads of toxic chemicals. Furthermore, studies have shown that chemical toxins can detrimentally impact all the essential processes within an activated sludge treatment system.

For example, deflocculation events, which involve the breakup of biomass flocs resulting in increased effluent total suspended solids (TSS), have been found to result from chemical insults to treatment systems. Phenol (Schwartz-Mittelmann and Galil, 2000), heavy metals (Neufeld, 1976; Bott and Love, 2001) and organic electrophilic chemicals (Bott and Love, 2002) are some of the sources that have been found to induce deflocculation of activated sludge mixed

liquor. Similarly, chemical oxygen demand (COD) removal has been found to be affected by heavy metals (Weber and Sherrard, 1980; Bott and Love, 2001), high ammonia loadings (Li and Zhao, 1999), and organic compounds such as 3-chloroaniline (Boon et al., 2003) or high concentrations of 2,4-dinitrophenol (DNP) (Rich and Yates, 1955).

Many studies have found that respiration inhibition occurs in response to the presence of toxic chemicals, such as heavy metals (Madoni et al., 1999; Bott et al., 2001; Lajoie et al., 2003) and different classes of organic compounds (Bott et al., 2001). Consequently, respiration inhibition is frequently used to detect incoming toxicity to wastewater treatment plants through the use of online respirometers (Vanrolleghem et al., 1994; Kong et al., 1996a; Kong et al., 1996b; Buitron et al., 2005).

Industrial chemical toxins have also been found to cause detrimental effects on settleability and dewaterability of activated sludges. In a study performed by Kjellerup et al. (2001), both settleability and dewaterability were found to decrease at a full-scale industrial wastewater treatment facility in response to an unknown chemical shock. A study done by Boon et al. (2003) also found decreased settleability to occur in activated sludge exposed to chloroaniline, and Novak (2001) has correlated poor settleability of mixed liquor with the presence of high ammonium concentrations.

Although some studies found in the literature have been conducted to assess the effects of toxins on the activated sludge process, these reports usually focus on only one aspect of the process such as COD removal, nitrification or settleability of the biomass and do not make a comprehensive analysis on all the potential effects of that toxin. Additionally, the laboratory-scale reactors used in these studies are usually fed synthetic wastewater, which may change the characteristics of the biomass to a great extent and provide limited information about real world systems. Moreover, continuous feed of a certain concentration of a toxin is usually preferred over providing shock loads of the same source and the criteria to select those concentrations is not consistent across the literature, which doesn't allow a systematic comparison between the effects of different toxins. Furthermore, some chemical classes have been studied more than others. For example, studies on the impact of organic electrophiles, hydrophobic chemicals or extreme pH levels on activated sludge are scarce or nonexistent in the literature. Therefore, there is a need for comprehensive studies that can adequately mimic the conditions at a treatment plant, both in terms of biomass, influent and toxic shock characteristics.

The objective of this research was to establish source-effect relationships for activated sludge exposed to shock loads of chemical toxins. Six different classes of industrially-relevant chemicals were selected as sources and the effects of varying shock concentrations of those toxins on activated sludge COD removal ability, flocculation ability, biomass growth, respiration rates, settleability and dewaterability were assessed. These studies were conducted on both nitrifying and non-nitrifying activated sludge mixed liquors. Results are reported for both activated sludges in terms of the magnitude of the effect and time of recovery of shocked laboratory-scale reactors relative to a control reactor, to which no toxin was added. The chemical classes (and model compound within each class) chosen as toxic shock sources included heavy metals (cadmium), uncouplers of oxidative phosphorylation (DNP), organic electrophilic chemicals (1-chloro-2,4-dinitrobenzene, CDNB), hydrophobic chemicals (1-octanol), respiration inhibitors (weakly complexed cyanide), high ammonia loadings, and alkaline and acidic pH conditions. This work is part of a broader project focused on developing comprehensive source-effect relationships for different chemical sources and identifying the causal mechanisms linking these sources and their effects. The effects of the chemical toxins used in this study on nitrification were also assessed and those results were reported elsewhere (Kelly et al., 2004). In addition, a critical comparison of respiration inhibition by the different chemicals tested on a short-term and long-term basis is discussed in Henriques et al. (in review).

Methodology

Pilot Plant Reactors. A pilot plant unit served as the source of mixed liquor for sequencing batch reactor (SBR) laboratory experiments. It consisted of two SBRs maintained at two different solids retention times (SRTs), 10 days (nitrifying system) and 2 days (non-nitrifying biomass). Both reactors had a working volume of 180 L, a hydraulic retention time (HRT) of one day and were maintained at approximately 20^{o}C. The SBRs were operated using four cycles per day, with a cycle consisting of a five hour reaction/aeration time and a one hour settling/decant period. The 10 day SRT reactor was fed over a period of less than ten minutes at the beginning of each cycle and the 2 day SRT reactor was step-fed one third of the influent at the beginning of each cycle, and at 1 hour and 45 minutes and 3 hours and 30 minutes into the cycle. This was done to prevent nitrification from occurring in the 2 day SRT system. Feed consisted of raw domestic wastewater supplemented with a carbon source containing equal COD quantities of acetate and glucose, as well as KGRO All-Purpose Plant Food fertilizer (KMart,

Troy, MI) with a total nitrogen (N):available phosphate (P_2O_5):soluble potash (K_2O) content of 15:30:15 on a mass basis. For the nitrifying reactor, approximately 400 mg/L as COD supplement was added, while approximately 800 mg/L as COD was added to the non-nitrifying system to achieve realistic biomass concentrations. The feed was settled for 30 minutes prior to the fill period to mimic primary clarification. Details regarding the operation and treatment performance of the pilot plant unit can be found in Love et al. (2005).

Laboratory Reactor Configuration and Operation. The laboratory-scale reactors were designed to mimic the pilot plant SBRs regarding the number of cycles and reaction/settling periods, as well as the SRTs and feed characteristics (influent was refrigerated in the laboratory). Both nitrifying and non-nitrifying laboratory reactors consisted of 3.5 L working volume beakers and were fed at the beginning of each cycle for a period of less than 10 minutes. No supplement was added to the 10 day SRT cadmium experiment, and no fertilizer was added with the COD supplement for the 10 day SRT octanol experiment. The 10 day SRT laboratory-scale reactor system was maintained at room temperature (approximately 23°C), while the 2 day SRT system was kept at 18°C to prevent nitrification from occurring throughout the experiment. For the 2 day SRT laboratory reactors, temperature control was used as a nitrification prevention strategy instead of the step-feeding approach used in the pilot plant, to simplify reactor operation. One reactor was used as a control reactor, to which no contaminant was added, and three other reactors were shocked at the beginning of cycle one (single pulse event) with set amounts of each contaminant and monitored over time. Biomass wastage was conducted manually daily during the reaction/aeration period of a cycle and did not account for the solids lost in the effluent. For all the toxins tested except ammonia and pH shock, the concentrations of each contaminant added to the reactors were defined as the concentrations that inhibited short-term (less than 30 minutes) oxygen uptake by the biomass by 15, 25 and 50% (termed inhibitory concentration IC_{15}, IC_{25} and IC_{50}, respectively; discussed below).

Experiments with the nitrifying biomass (10 day SRT) were monitored for 30 days (3x SRT) or less if recovery to control levels was observed to occur earlier, while the 2 day SRT system was monitored for 6 days (3x SRT). Parameters monitored included effluent soluble COD, effluent TSS, mixed liquor total and volatile suspended solids (MLSS and MLVSS), mixed liquor specific oxygen uptake rate (SOUR), mixed liquor capillary suction time (CST) and mixed liquor sludge volume index (SVI). The characteristics of the influent wastewater were

also monitored throughout each of the shock experiments and detailed results are reported in Love et al. (2005). The concentrations of the contaminants in the effluent and mixed liquor of the shocked reactors were also determined whenever possible and are reported in the same publication (Love et al., 2005).

Toxins. The contaminants selected for the source-effect experiments included cadmium (added as $CdCl_2$), CDNB, DNP, 1-octanol, cyanide (added as a zinc-cyanide complex – $Zn_x(CN)_y^{+z}$ – solution to mimic electroplating waste), ammonia (added as NH_4HCO_3) and pH shock. Zinc sulfate ($ZnSO_4$) was added to the control reactor of the complexed cyanide shock experiments to offset any potential toxicity from the metal in the shocked reactors. Cadmium, cyanide and DNP were added as concentrated stock solutions. Due to low water solubility of octanol and CDNB, extra steps were required for addition of these toxins to the activated sludge. To shock the SBR reactors, octanol was either dissolved overnight or through sonication in autoclaved or raw influent, respectively. CDNB was melted (at about 100ºC) and dissolved using sonication into pre-heated raw influent prior to introducing the shock load to the SBR reactors. In both cases the mixture was cooled to room temperature before addition to the mixed liquor. For pH shock, H_2SO_4 or Na/Ca hydroxides were added to adjust the mixed liquor pH to 5, 9, and 11. A solution with equal normality of sodium and calcium hydroxides was used to maintain a similar monovalent to divalent cation ratio in the mixed liquor. For ammonia shock, use of the bicarbonate form of ammonium prevented low pH effects due to increased nitrification from interfering with the interpretation of effects by ammonium.

Inhibitory Concentration (IC_{xx}) Determination. SOUR-based IC_{xx} assays were conducted one day prior to initiating each shock experiment to ensure that mixed liquor composition was representative of the biomass that would be used to inoculate the laboratory-scale SBRs. A detailed description of how these assays were performed and the IC_{15}, IC_{25} and IC_{50} concentrations of cadmium, DNP, CDNB, octanol and complexed cyanide used to shock the reactors are included in Henriques et al. (in review). The reactors exposed to ammonia upset were shocked with 40, 130 and 280 mg/L N (approximately 3x, 9x and 18x the average ammonia in the influent, respectively) for the 2 day SRT system and 70, 190 and 390 mg/L N (approximately 2x, 5x and 10x the average ammonia in the influent, respectively) for the 10 day SRT system.

Analytical Procedures. SOUR assays were used to monitor respiration inhibition in the stressed reactors. A mixed liquor sample was aerated for at least three to five minutes and placed in a 300 ml biochemical oxygen demand (BOD) bottle to which 100-120 mg/L of soluble COD was previously added to ensure that respiration was not substrate-limited during the test. Soluble COD was composed of 34% protein (beef extract, bacto-casitone, yeast extract), 18% carbohydrate (fructose, galactose, glucose) and 48% organic acids/alcohols (glacial acetic acid and glycerol) on a COD basis. SOUR tests were performed in duplicate using a dual channel Accumet Research AR25 pH/mV/°C/ISE Meter (Fisher Scientific International, Hampton, NH) and two Orion 97-08 oxygen electrodes coupled with localized mixers (Thermo Electron Corporation, Waltham, MA). Dissolved oxygen readings were recorded every six seconds using an automated data acquisition system (Labview 6i, National Instruments, Austin, TX). The OUR was determined through the slope of the linear portion of the dissolved oxygen versus time curve. The SOUR was calculated by dividing the OUR by the MLVSS concentration.

Effluent soluble COD, effluent TSS, MLSS, MLVSS, CST and SVI were conducted according to Standard Methods (APHA et al.,1998). The CST test was conducted with mixed liquor taken directly from the SBR reactors during the reaction period. The SVI test was performed using 250 mL graduated cylinders. Samples for effluent soluble COD were filtered through a 0.45 μm nitrocellulose filter immediately after effluent collection.

Data Presentation and Statistical Analysis. To assess the significance of an effect in a shocked reactor in comparison to the control reactor, and the recovery of the shocked reactors to control reactor levels, statistics were performed using Dunnett's method for multiple comparisons with a control (Berthouex and Brown, 1994). The significance level (α) used was 0.05, while the criterion to determine recovery to control levels was defined as three consecutive data points not significantly different from the control. Data included in the figures represents the average of triplicate (COD, MLVSS, effluent TSS) or duplicate (SOUR) measurements. For easier visualization of the data, error bars were not included. Due to the large amount of data generated during these studies, only the most significant results are shown in the figures.

Results

Severe Inhibition of COD Removal by Cadmium and pH 11 Shocks. Effluent soluble COD data show that cadmium had a strong impact on COD removal ability for both the 2 day and 10 day SRT reactors (Figures 1A and 1B). In the 10 day SRT system, the effluent soluble COD remained significantly elevated in the IC_{15}, IC_{25} and IC_{50} cadmium-stressed reactors relative to the control until cycle 15 (0.37x SRT), 23 (0.57x SRT) and 51 (1.3x SRT), respectively, after which the performance of all reactors was similar. Although partial statistical recovery was seen, complete recovery to control levels was not achieved in any of the 2 day SRT reactors. In this system, the maximum effluent COD level observed in the IC_{50} reactor was 13x higher than the control, while in the 10 day SRT IC_{50} reactor the maximum effluent COD level observed was 3x higher than the control. In both cases, the degree to which COD removal decreased corresponded with increasing cadmium concentrations.

COD removal efficiency was also impacted by CDNB in both the 10 day and 2 day SRT systems, but despite being statistically significant, the effects from the lower concentrations tested (IC_{15} and IC_{25} reactors) were modest (Figures 1C and 1D show the results from the IC_{50}-shocked reactors only). The effluent soluble COD in the 10 day SRT system remained elevated in the IC_{15}, IC_{25} and IC_{50}-stressed reactors relative to the control until cycle 20 (0.50x SRT), 24 (0.60x SRT), and 36 (0.90x SRT), respectively. Inhibition of COD removal efficiency was highest for the IC_{50}-shocked reactor, which had its maximum COD level (2.5x higher than the control) during cycle 2, but the inhibition in the IC_{15} and IC_{25} reactors did not significantly differ from each other and was much less severe (data not shown). For the 2 day SRT a similar response was observed. The IC_{50} reactor showed elevated effluent soluble COD with respect to the control reactor for the first 8 cycles (1.0x SRT) and had the highest inhibition of all reactors, with COD levels reaching as much as 4x those of the control reactor.

pH 11 shock had a significant detrimental effect on COD removal. The shock condition caused a maximum increase in effluent soluble COD relative to the control of 8x and 15x for the 10 day and 2 day SRT systems, respectively, and was the most severe COD removal response of all toxins tested (Figure 1E). Similar to cadmium, the 10 day SRT reactor recovered to control levels by cycle 52 (1.3x SRT), while the 2 day SRT reactor never recovered to control levels over a period of 3x SRTs. The other pH shock conditions did not cause significant effluent COD increases.

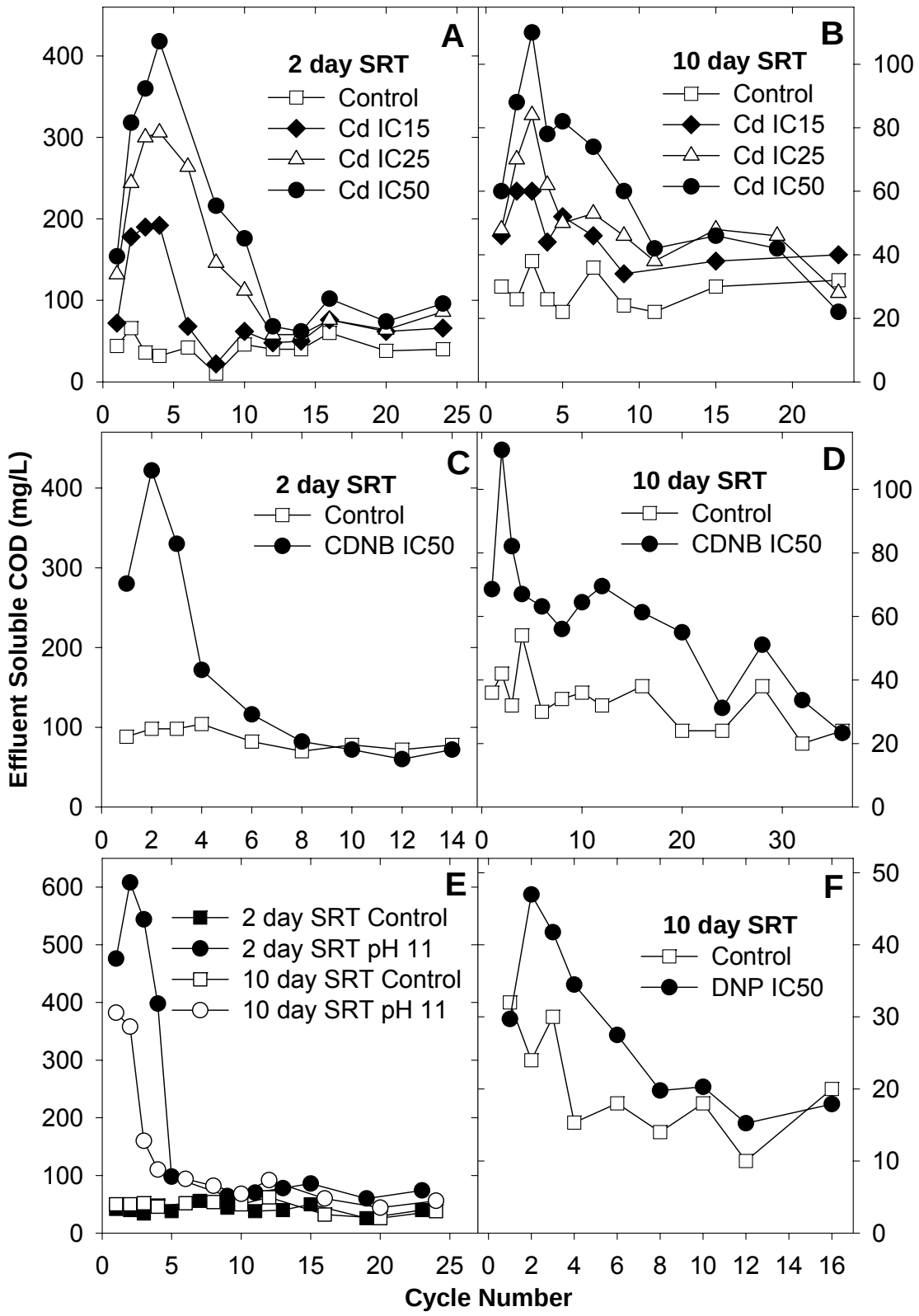

Figure 1 – Effluent soluble COD versus time for 2 day and/or 10 day SRT biomass exposed to shock loads of the indicated toxin (A and B – cadmium, Cd; C and D – CDNB; E – pH 11; F – DNP). Note different axis scales for figures A through F.

DNP, octanol, cyanide and ammonia shocks did not impact activated sludge COD removal ability or the effect was rather modest and/or short-lived (data not shown). Among these conditions, only DNP at the highest concentration tested showed a slight effect on the COD removal capacity of the 10 day SRT biomass, as shown in Figure 1F.

Deflocculation Effects Similar to COD Removal Effects. Deflocculation effects were observed for several of the toxic conditions tested on both the 10 day and 2 day SRT biomasses and were detected based on an increase in the effluent TSS of the stressed reactors.

Cadmium shock was found to have the strongest negative effect on the flocculation ability of both the 10 day and 2 day SRT biomasses, given that effluent TSS increased significantly in all shocked reactors upon exposure to the chemical and took a long time to recover or did not recover to control levels during the experiment (Figures 2A and 2B). However, contrary to what was observed with COD removal, the severity of the increase did not correspond with the cadmium dosage, as all tested concentrations yielded similar effluent TSS values. For the 10 day SRT system, maximum increases of 4-5x the control were observed, while for the 2 day SRT system a maximum increase of about 2.5x was noted for all reactors. Statistical recovery of the 10 day SRT reactors occurred after 83 cycles (2.1x SRT), while for the 2 day SRT system, the IC_{25} and IC_{50}–shocked biomasses did not recover their flocculation ability within the experimental period of 3x SRTs. The 2 day SRT IC_{15} reactor temporarily recovered to control levels after 8 cycles (1x SRT), but elevated effluent TSS levels were again noticed towards the end of the experimental period.

CDNB was also found to cause elevated TSS levels, with deflocculation patterns similar to cadmium, but not as severe (Figures 2C and 2D show the results for the IC_{50}-shocked reactors only). For the IC_{50} CDNB-shocked reactors, effluent TSS levels exceeded those in the control reactor by more than 1.5x and 3-4x, respectively for the 2 day and 10 day SRT systems, but the CDNB shock load did not affect the 10 day SRT IC_{15} reactor or the 2 day SRT IC_{15} and IC_{25} reactors. Statistical recovery in the reactors where significant effects were observed was also much faster than in the cadmium-shocked reactors, with the 10 day SRT IC_{25} and IC_{50} reactors recovering after 10 (0.25x SRT) and 28 (0.70x SRT) cycles respectively, and the 2 day SRT IC_{50} reactor recovering after 4 cycles (0.50x SRT).

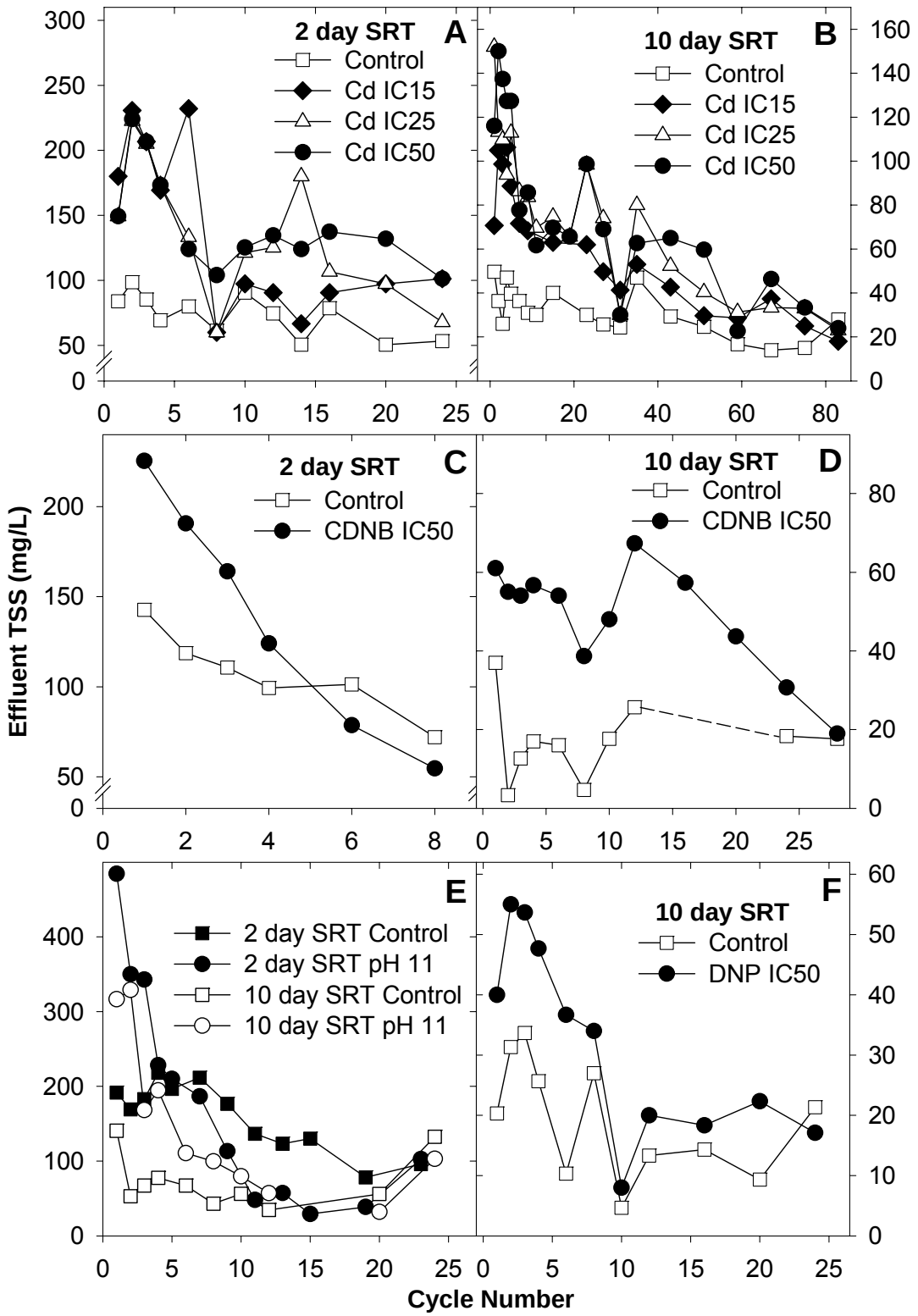

Figure 2 – Effluent TSS versus time for 2 day and/or 10 day SRT biomass exposed to shock loads of the indicated toxin (A and B – cadmium, Cd; C and D – CDNB; E – pH 11; F – DNP). The dashed line in Figure 2D represents a filamentous bulking event for which TSS levels are not shown in the graph. Note different axis scales for figures A through F.

The effluent TSS levels for both the 10 day and 2 day SRT pH 11 reactors showed immediate and substantial increases in effluent TSS, corresponding to 6x and 2.5x the control levels, respectively (Figure 2E). Despite the severity of the increase, recovery was more rapid than found for both cadmium and CDNB, with the 10 day SRT system recovering after 20 cycles (0.50x SRT) and the 2 day SRT reactor recovering after 4 cycles (0.50x SRT). The reactors receiving pH 5 and pH 9 shocks did not show significant increases in effluent TSS relative to the control reactors (data not shown) and, in fact, a slight but statistically significant improvement was observed in the effluent TSS of the 2 day SRT pH 5-shocked reactor relative to the control.

The remaining toxic conditions (octanol, DNP, cyanide and ammonia shock loads) did not produce strong deflocculation events or long recovery times from initial increases in effluent TSS. Of these, only octanol and DNP showed some deflocculation effects. For the first 20 cycles (0.50x SRT) of the 10 day SRT IC_{50} reactor shocked with DNP, moderate but statistically significant elevated effluent TSS levels were observed (Figure 2F). Effluent TSS increased in the 2 day and 10 day SRT IC_{50} reactors shocked with octanol to approximately 1.5-2x that of the respective control reactor, but in both cases the values returned to control levels within 8 cycles (data not shown). In addition to the brief deflocculation effects observed for octanol, a foaming event was observed immediately after octanol addition and increasing amounts of foam were observed with increasing concentrations of the contaminant.

Biomass Growth was Mostly Affected by Cadmium, pH 11 and DNP Shocks. Mixed liquor concentrations in the laboratory-scale reactors varied some during the experiments due, in part, to variations in sewage strength (see Love et al., 2005); nevertheless, a comparison of shocked reactors with the controls was still possible.

In the 10 day SRT systems (Figure 3B), cadmium shock resulted in a maximum decrease in MLVSS levels of 18% and 26%, respectively in the IC_{25} and IC_{50} reactors, after which the reactors returned to control levels at cycle 20 (IC_{25} reactor, 0.50x SRT) and cycle 35 (IC_{50} reactor, 0.88x SRT). No significant decrease in MLVSS was noted in the IC_{15} reactor. Although increased effluent TSS levels in the stressed reactors may partially account for the decrease in MLVSS, a mass balance on the reactors solids showed that the increase in effluent TSS alone could not explain the decrease in biomass concentration after cadmium shock (data not shown). Similar results were obtained for the 2 day SRT system (Figure 3A), which experienced a 25%

(IC_{15} reactor) and 40% (IC_{25} and IC_{50} reactors) decrease in MLVSS relative to the control. Recovery of MLVSS levels was not achieved in any of the shocked reactors.

pH 11 strongly affected biomass growth in both the 10 day and 2 day SRT systems, starting immediately after the shock event (Figure 3C). In the 2 day SRT reactor, decreased MLVSS levels relative to the control reactor were observed throughout the experiment. In the 10 day SRT system, a significant decrease in MLVSS was observed until cycle 29 (0.73**x** SRT), after which the pH 11-shocked reactor performed as the control. In both systems, strong

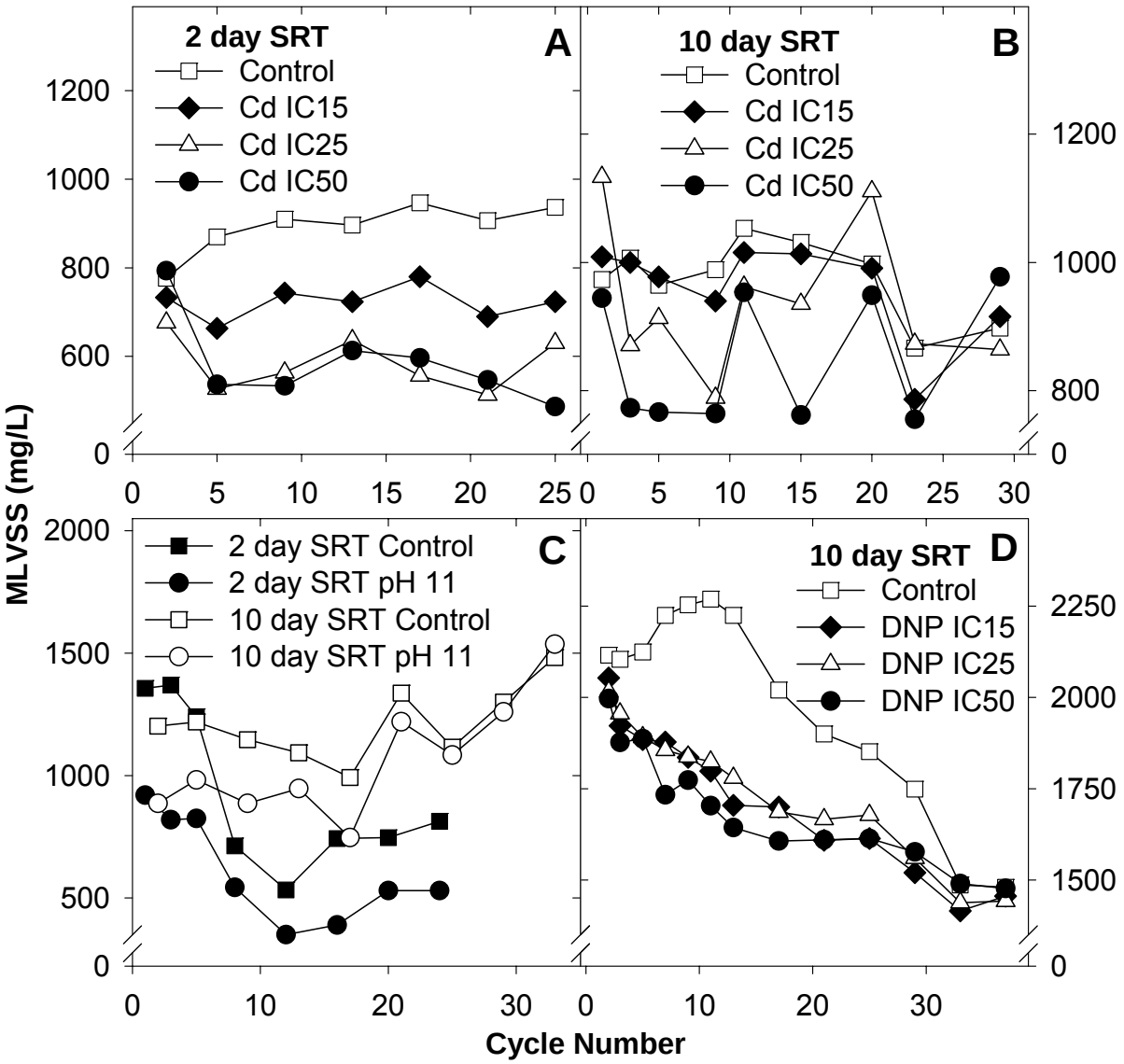

Figure 3 – MLVSS versus time for 2 day and/or 10 day SRT biomass exposed to shock loads of the indicated toxin (A and B – cadmium, Cd; C – pH 11; D – DNP). Note different axis scales for figures A through D.

deflocculation events were observed but, as with cadmium, the increased effluent TSS levels alone did not justify the decrease in MLVSS, indicating that biomass growth was impaired by pH 11 shock.

The results concerning biomass growth in the 10 day SRT DNP-shocked reactors (Figure 3D) indicate that strong growth inhibition occurred since the very first cycle of the experiment. In comparison to the control, the MLVSS concentrations in the DNP-treated reactors were statistically significantly lower since the beginning of the experiment and until cycle 33 (0.83x SRT). In addition, the difference between the IC_{15}, IC_{25} and IC_{50} MLVSS profiles was not significant, although the impact in the IC_{50} reactor seemed to have been slightly stronger. Combined with the COD removal data, the MLVSS results show the uncoupling effects associated with DNP, whereby biomass growth or anabolic processes were inhibited to a significant extent, but substrate removal or catabolic processes continued to occur near control levels during the same period. The 2 day SRT shocked reactors did not show a significant decrease in MLVSS relative to control levels (data not shown), which is also consistent with the results obtained for COD removal and oxygen uptake rate (see below). It is not clear why DNP shock did not yield typical results for an uncoupler of oxidative phosphorylation in the non-nitrifying, low SRT system.

pH 5, pH 9, cyanide, ammonia, octanol and CDNB shocks did not impact biomass growth to a great extent. The MLVSS concentration in the 10 day SRT IC_{50} reactor shocked with CDNB dropped a maximum of 25% relative to the control and recovered to control values after 29 cycles (0.72x SRT, data not shown). This reactor was the only one affected by CDNB shock regarding biomass growth.

Inhibition of Respiratory Functions Observed for All the Toxic Conditions Tested. Oxygen uptake by activated sludge biomass was severely affected by most of the shock conditions tested, which is not surprising since toxin doses were determined based on SOUR inhibition.

Cadmium detrimentally affected biomass oxygen uptake (Figures 4A and 4B). SOUR inhibition relative to the control reactor reached 74%, 84% and 92% in the IC_{15}, IC_{25} and IC_{50} 10 day SRT reactors and 93%, 96% and 98% in the 2 day SRT reactors 7 hours after the shock (cycle 2). In subsequent cycles, the degree of inhibition continued to correlate with increases in contaminant dose. SOUR levels started to increase immediately after cycle 2 and statistically

recovered to control levels by cycle 15 (0.37x SRT) in the 10 day SRT system. In the 2 day SRT system, the IC_{15} reactor recovered to control levels by cycle 17 (2.1x SRT), but both the IC_{25} and IC_{50} reactors did not recover during the experiment.

CDNB shock impacted biomass SOUR to a lesser extent than cadmium (Figures 4C and 4D). The maximum respiration rate decrease relative to the control was 37%, 64% and 89%, respectively for the IC_{15}, IC_{25} and IC_{50} 10 day SRT reactors and 14%, 20% and 83% in the 2 day SRT system. SOUR values in both systems returned to control levels in approximately 9 cycles (1.1x SRT for the 2 day SRT system and 0.23x SRT for the 10 day SRT system). As with cadmium, recovery of respiration rate was faster than recovery of COD removal.

As an uncoupler of oxidative phosphorylation, DNP was expected to cause an increase in oxygen uptake rate, since electron transfer across the electron transport chain tends to increase to compensate for the disruption of the proton motive force (PMF). The results obtained during this study indicate that at high concentrations, DNP did not stimulate oxygen uptake but instead had an inhibitory effect on respiration rates. In the 10 day SRT reactors (Figure 4F), the SOUR levels were 6%, 21% and 52% lower than the control 7 hours after the shock (cycle 2), which is close to the short-term SOUR inhibition levels. Starting with cycle 11, all the reactors showed a significantly higher SOUR than the control until the end of the experimental period (cycle 37), which indicated that at lower concentrations, 1.1, 2.2 and 7.2 mg/L DNP in the IC_{15}, IC_{25} and IC_{50} reactors in cycle 11, respectively (data not shown), the uncoupling effect was noticeable. This effect continued to be observed throughout the remaining cycles, even though DNP was not detected in the reactors after cycle 20 (data not shown). It is unclear why uncoupling continued to occur, even after DNP was no longer detected in the reactors.

The 2 day SRT reactors (Figure 4E) responded differently to DNP, with SOUR measurements throughout the experiment showing that moderate inhibition of oxygen uptake was caused by DNP shock. The initial concentrations clearly inhibited cellular respiration, and the respiration rates remained lower than the control throughout the entire experimental period. Although no stimulation of respiration rates was observed for the 2 day SRT biomass, the results are consistent with what was observed at the beginning of the 10 day SRT DNP stress experiment, as well as with the absence of biomass growth inhibition in the 2 day SRT system.

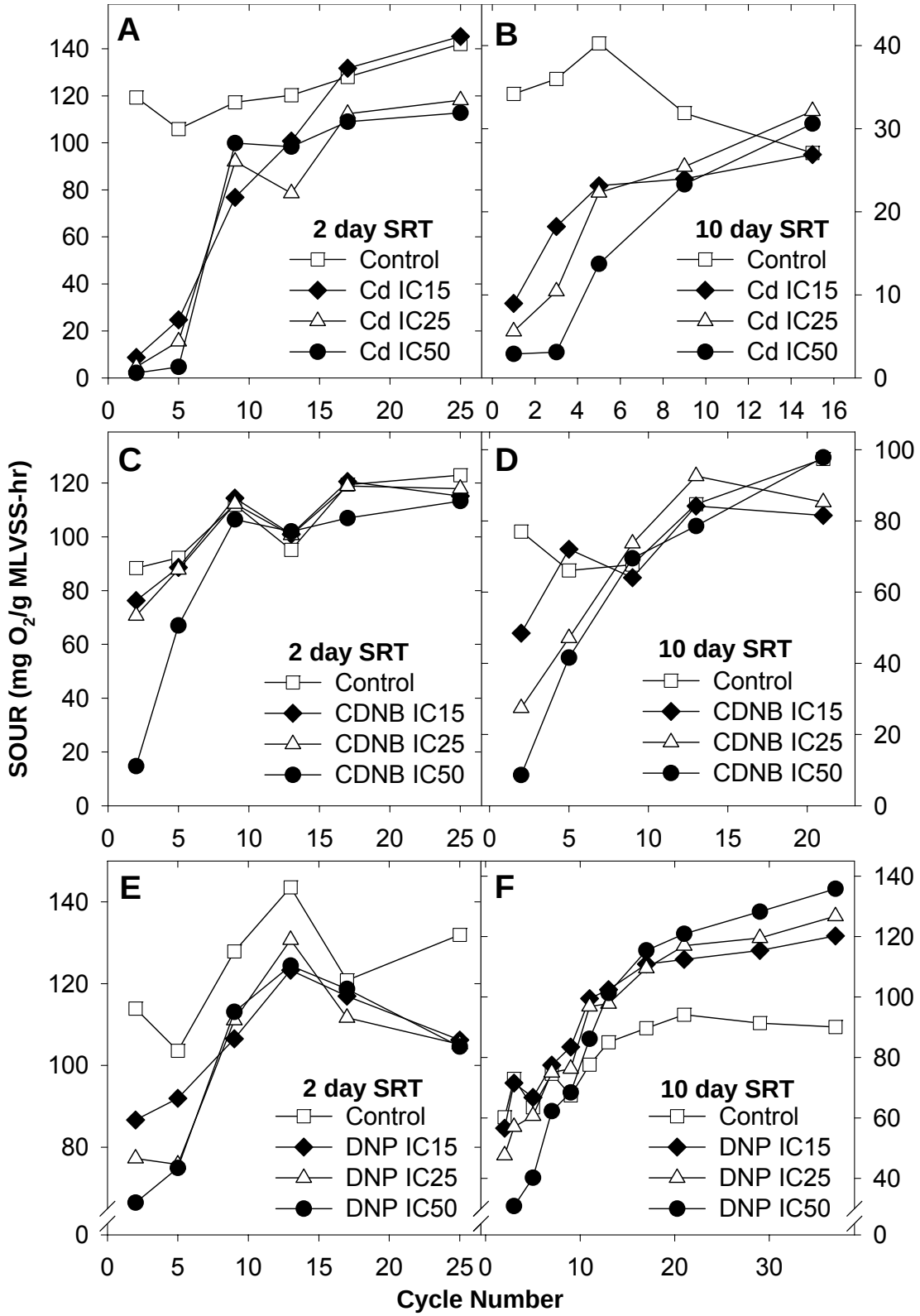

Figure 4 – SOUR versus time for 2 day and/or 10 day SRT biomass exposed to shock loads of the indicated toxin (A and B – cadmium, Cd; C and D – CDNB; E and F – DNP). Note different axis scales for figures A through F.

Contrary to cadmium, CDNB and pH 11, DNP affected respiration rates for longer periods and to a greater extent than it affected COD removal or biomass flocculation. This is interesting to note, as DNP directly impacts the respiratory chain of bacterial cells by disrupting the PMF.

Interestingly, like DNP, the greatest impact of cyanide shock was on the respiration rate of both biomasses tested (Figures 5A and 5B). Again, this is presumably related to the fact that the mode of action of this toxin directly affects the bacterial respiratory chain by inactivating key enzymes in that system. At the IC_{50} shock level, complexed cyanide resulted in long respiration inhibition effects in both systems, in comparison to most of the other toxic conditions. The increase in the SOUR of the control reactors with time during the complexed cyanide experiments was most likely due to an initial inhibitory effect by zinc, which has been observed to reduce the SOUR of activated sludge (Lajoie et al., 2003).

pH 11 shock had a severe but short-lived effect on biomass respiration (2 day SRT results in Figure 5C, 10 day SRT data not shown). In the 10 day SRT reactor, pH 11 shock caused an 86% inhibition of respiration 7 hours after the shock (cycle 2), while in the 2 day SRT system this value was 98%. Recovery to control levels was achieved in the 2 day SRT system in 8 cycles (1.0x SRT), while a very fast recovery of respiration rate (less than 5 cycles, 0.13x SRT) was observed in the 10 day SRT reactor. Relative to COD removal, SOUR recovery times were substantially faster. The results suggest that biomass respiration was severely inhibited by the initial pH values, but that cell death was not a major consequence of high pH shock since the biomass was able to recover its original respiration rate when the pH levels in the reactor dropped to 8.0 and 8.3 in cycle 5 for the 10 day and 2 day SRT systems, respectively (data not shown).

The other tested shock conditions, namely pH 5, pH 9, octanol and ammonia shocks, had some inhibitory effect on the biomass SOUR, but those effects were modest and/or short-lived. At the highest concentration tested, ammonia shock inhibited respiration in the 2 day SRT system to some extent, and this was one of the only process effects observed for ammonia stress (Figure 5D).

Impact of Toxins on Biomass Settleability were Mild. We observed a deterioration in biomass settleability due to shock events by DNP, pH 5 and cyanide (data not shown). However, the increase in SVI never resulted in values greater than 135 mL/g MLVSS and 150 mL/g MLVSS, for the 10 day and 2 day SRT reactors, respectively. The only exception to this

occurred in the 2 day SRT pH 5-shocked reactor, in which the SVI increased from 140 mL/g MLVSS in the control reactor to 190 mL/g MLVSS in the stressed reactor. Therefore, in most of the conditions tested and even in the reactors in which negative effects were observed, the biomass settling characteristics were not affected to an extent that would severely compromise its settleability in a final clarification step.

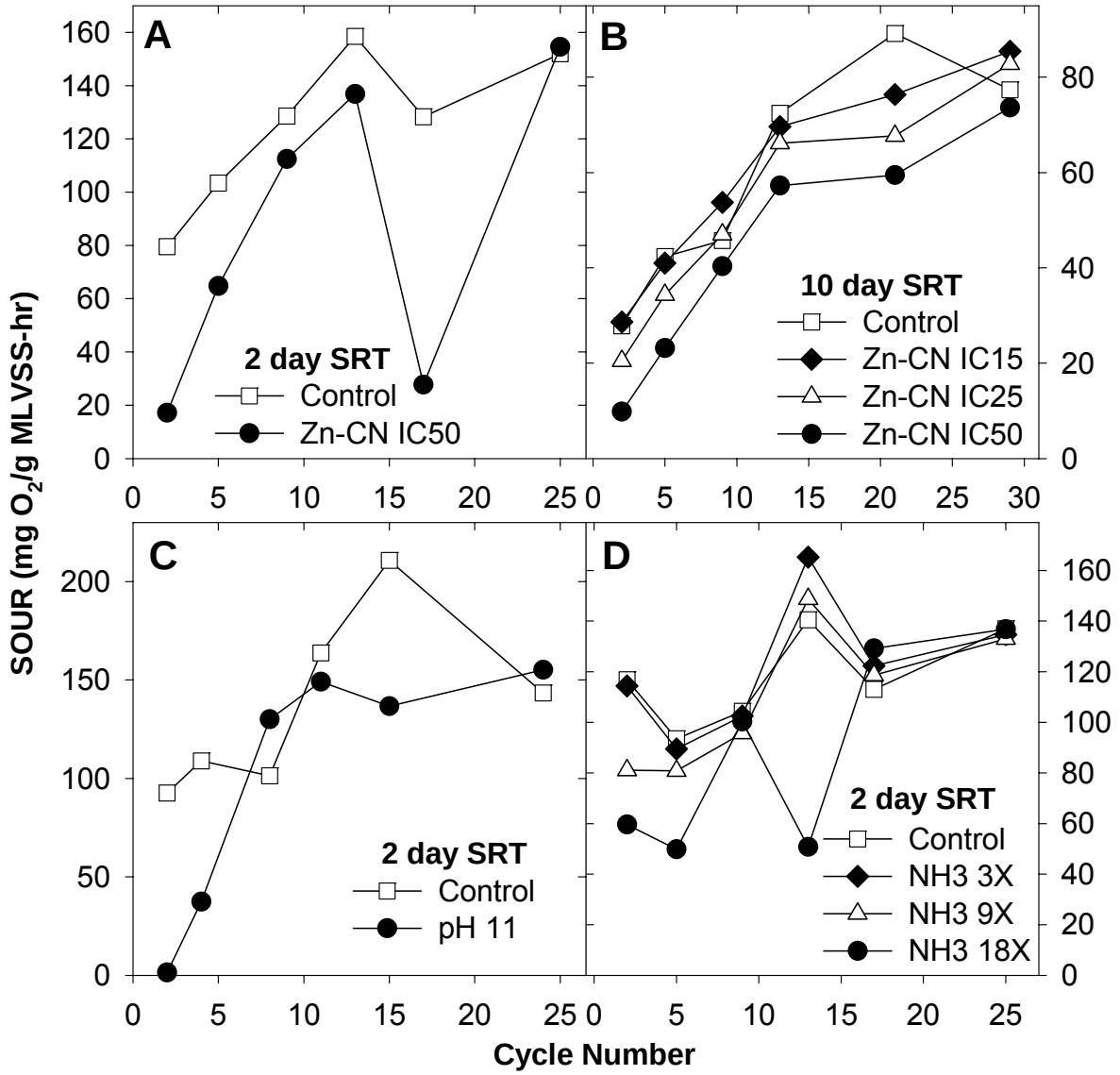

Figure 5 – SOUR versus time for 2 day and/or 10 day SRT biomass exposed to shock loads of the indicated toxin (A and B – zinc-cyanide complex, Zn-CN; C – pH 11; D – ammonia). Note different axis scales for figures A through D.

Biomass Dewaterability Significantly Affected by pH 11 Shock. For most of the toxic conditions tested, the effects on dewaterability were modest and short-lived. pH 11 shock was

the only condition that substantially decreased the dewaterability of the mixed liquor immediately after the shock, as CSTs increased about 7x (to 307 s) and 9x (to 135 s) in comparison to the control reactor (45 s and 14 s), for the 2 day and the 10 day SRT reactors, respectively (data not shown). In addition, the CST of mixed liquor from the 10 day SRT IC_{50} reactor shocked with cadmium remained elevated relative to the control levels for a period of almost 3x SRTs, although the magnitude of the effect was fairly small (data not shown).

Overall, as with settleability, effects on dewaterability tended to be mild and for most of the toxins tested except pH 11, it is not likely that the biosolids dewatering operations at a wastewater treatment facility would be severely impacted by any of these toxic conditions. As CST is usually conducted with thickened biosolids, the results from our studies most likely would have yielded greater differences between the CSTs of the control versus the shocked reactors if the CSTs had been determined with concentrated mixed liquor. Therefore, caution should be used when looking at these results.

Discussion

To our knowledge, this study is the first to systematically investigate the effects of toxins on the activated sludge process in order to establish comprehensive source-effect relationships. This work investigated a wide range of process effects caused by industrially-relevant classes of chemical compounds (sources) on activated sludge systems. The effects were related to biomass metabolism (COD removal, oxygen uptake rate, biomass growth) and to floc structure properties (flocculation ability, dewaterability and settleability). Table 1 summarizes the severity of each shock, both in terms of the intensity of the effect and recovery time to control levels, for both the 2 day and 10 day SRT activated sludges. A qualitative classification was used to allow an easier visualization of the main trends observed in the data.

Among the process effects studied, inhibition of respiratory functions and COD removal were the most affected processes. All the toxins tested detrimentally affected COD removal and respiration rates to some extent in both or just one of the biomasses used in this study. The next most prevalent process effect was loss of flocculation ability (increase in effluent TSS), followed by reduced biomass growth (decrease in MLVSS). In general, both mixed liquor settleability and dewaterability were not affected to a great extent by the toxins evaluated in this study. The only exception was the significant increase in CST caused by pH 11 stress.

Table 1 – Source-effect relationships for activated sludge exposed to toxic conditions.

		EFFECTS [d]											
	SOURCE	2 day SRT						10 day SRT					
		COD	TSS	MLVSS	SOUR	SVI	CST	COD	TSS	MLVSS	SOUR	SVI	CST
Maximum intensity of effect [a]	Cadmium	13	2.3	0.59	0.018	0.29	1.3	2.9	4.1	0.77	0.084	-	1.6
	DNP	-	-	-	0.58	1.1	-	2.0	1.8	0.75	0.48 - 1.5	1.3	1.3
	CDNB	4.3	1.6	-	0.17	0.45	**X**	2.6	4.3	0.80	0.11	0.24	-
	Octanol	1.4	1.5	0.86	0.86	-	1.2	2.5	2.0	-	0.72	-	1.2
	Cyanide	2.6	-	-	0.22	-	-	1.4	-	-	0.35	1.7	1.4
	pH 5	1.7	0.77	0.91	-	1.4	-	1.4	**X**	-	0.64	1.1	-
	pH 11	15	2.5	0.60	0.015	0.45	6.9	7.6	6.2	0.71	0.14	0.81	9.4
	Ammonia	1.3	-	-	0.51	1.1	1.4	-	-	-	1.1	-	-
Recovery time (SRTs) [b]	Cadmium	NR	NR	NR	NR	NR	0.63	1.1	2.7	0.88	0.38	-	2.7
	DNP	-	-	-	NR	0.63	-	0.40	0.60	1.1	> 1	> 1	0.33
	CDNB	1.3	0.75	-	1.1	NR	**X**	0.90	0.70	0.73	0.23	**X**	-
	Octanol	0.75	1.0	1.1	0.63	-	0.75	0.050	0.18	-	0.15	-	0.40
	Cyanide	0.38	-	-	1.6	-	-	0.15	-	-	0.73	0.13	0.43
	pH 5	NR	0.63	1.0	-	1.5	-	0.70	**X**	-	0.13	0.33	-
	pH 11	NR	0.50	NR	1.0	NR	1.0	1.3	0.50	0.73	0.13	0.53	**X**
	Ammonia	0.25	-	-	1.1	2.6	1.6	-	-	-	0.13	-	-
Source-effect summary [c]	Cadmium	↓↓↓↓	↓↓↓↓	↓↓↓↓	↓↓↓↓	+++	↓	↓↓↓↓	↓↓↓↓	↓↓	↓↓↓	0	↓↓↓
	DNP	0	0	0	↓↓↓	↓	0	↓↓	↓↓	↓↓↓	↓↓ / ++	↓	↓
	CDNB	↓↓↓	↓↓↓	0	↓↓↓	++	**X**	↓↓↓↓	↓↓↓↓	↓↓	↓↓↓	**X**	0
	Octanol	↓	↓↓	↓↓	↓	0	↓	↓	↓	0	↓	0	↓
	Cyanide	↓↓	0	0	↓↓↓	0	0	↓	0	0	↓↓↓	↓	↓
	pH 5	↓↓	+	↓	0	↓↓	0	↓	**X**	0	↓	↓	0
	pH 11	↓↓↓↓	↓↓↓↓	↓↓↓↓	↓↓↓↓	++	↓↓↓↓	↓↓↓↓	↓↓↓↓	↓↓↓	↓↓	+	↓↓↓↓
	Ammonia	↓	0	0	↓↓	↓	↓↓	0	0	0	+	0	0

[a] Maximum intensity of effect observed for the IC_{50} and the indicated pH and highest ammonia levels shocked reactors during the first 3 days of the experiment, relative to the control reactor (value in shocked reactor / value in control reactor). - means no significant effect.

[b] Time that took for the IC_{50} and the indicated pH and highest ammonia levels shocked reactors to return to control reactor performance (in SRTs). Recovery times were assessed through the Dunnett's test criteria and visual observation of the data in the cases where the application of the Dunnett's test criteria was not possible. NR means no recovery during the experiment. - means no significant effect.

[c] Source-effect summary. The qualitative scale reflects the intensity and recovery time (in [a] and [c], respectively) for the effects on the quality parameters indicated. The scale ranges from ↓↓↓↓ (most intense deterioration effect) to ++++ (most intense improvement effect). 0 represents no significant effect.

[d] Effects on effluent quality parameters (soluble COD and TSS) and mixed liquor quality parameters (MLVSS, SOUR, SVI and CST).

X Inconclusive results or data not available.

The fact that SOUR was inhibited by most of the toxic conditions tested was not unexpected, as the initial criterion for selection of the toxin concentrations for shock experiments was based on respiration inhibition. However, it is important to note that respiration inhibition was not always accompanied by significant deterioration of other process effects. For example

in the case of ammonia, octanol and cyanide shocks, although reduction in respiration rates was observed immediately after the shock for at least one of the mixed liquors used in this study, the effects on other process parameters, including those related to effluent quality, were very modest and recovered rapidly to control levels. This information is relevant for the optimization of upset early warning devices that rely on respiration rate measurements to trigger alarms in wastewater treatment plants. Cyanide, octanol or ammonia shock loads in the incoming influent could potentially result in false positive alarms in plants using online respirometers to detect influent toxicity. Similar conclusions can be drawn from the comparison of short-term and long-term SOUR inhibition curves (Henriques et al., in review).

Interestingly, when significant effects were observed to occur at the level of COD removal, there was a clear tendency for that effect to take place together with biomass deflocculation in the shocked reactors. An increase in soluble COD in the effluent of the SBR reactors can originate from different mechanisms, such as: (1) inhibition of catabolic functions, which results in a decrease of the biomass substrate uptake ability, (2) passive release of intracellular soluble materials due to cell lysis, (3) active excretion of intracellular substances from specific bacterial stress responses, and (4) release of materials from the extracellular polymeric substances (EPS) matrix that embeds the bacterial cells in activated sludge flocs. For different toxins, it is likely that these different mechanisms contribute to varying extents to the observed effluent soluble COD increases. Given the relatively fast recovery of SOUR values to control levels, which occurred in 1x SRT or less in most cases, cell lysis probably did not occur to a great extent in the shocked reactors. The link between deflocculation and increases in soluble COD may come from the contribution of EPS materials released into the bulk liquid due to the deflocculation process. It is plausible that floc breakup leads to rearrangement of the polymer matrix (or vice-versa), and that at least part of that matrix is lost into the bulk liquid, leading to increases in soluble COD.

COD removal efficiency and biomass flocculation ability were most severely affected by cadmium, pH 11 and CDNB shocks, in both the 2 day and the 10 day SRT system. This was observed both in terms of the intensity of the effect and the time it took for the stressed biomass to recover to control levels. Similarly, biomass growth was most severely affected by cadmium and pH 11 shocks, both in terms of the intensity of the effect and recovery time, but CDNB did not seem to inhibit growth to a significant extent, as only the 10 day SRT IC_{50} biomass growth

was affected by this chemical. DNP also considerably inhibited biomass growth in the 10 day SRT system. Therefore, in the case of COD removal, effluent TSS levels and inhibition of growth (MLVSS decrease), the intensity of an effect correlated well with the recovery time, as the strongest effects were also the ones that tended to take longer to recover. However, this was not observed for the effects on SOUR.

As mentioned above, SOUR values decreased after the shock for most of the conditions tested. Overall, decreases in SOUR tended to be short-lived and SOUR levels recovered to control levels much faster than COD removal efficiency or flocculation ability in the case of the compounds that caused the strongest inhibitory effects in those process parameters (cadmium, CDNB and pH 11). However, there was a clear difference between the toxins that produced the most dramatic reductions in respiration rates (cadmium, pH 11 and CDNB) and the toxins that induced the longest effects on SOUR inhibition (DNP and cyanide). This is interesting to note, as the modes of action of both DNP and cyanide directly target the respiratory functions and will most probably affect biomass respiration for as long as they persist in the system. For the case of cadmium, pH 11 and CDNB, the toxicity mechanisms at the cellular level are likely non-specific, and respiration is affected as a consequence of generalized damage to cellular structures. Therefore, respiration rates should recover as soon as the concentration of the contaminant decreases and basic cellular functions are operational. In fact, for these three chemicals, recovery of respiration rates was probably a priority for the bacterial community, as SOURs recovered much faster than COD removal or biomass growth. This priority may be linked to the need to generate energy to restore other cellular processes.

Ultimately, the data obtained from the source-effect studies suggest that the effects of a toxic shock load on specific processes, such as COD removal, flocculation ability, respiration or biomass growth, are intrinsically related to the toxicity mechanisms that each toxin elicits at the cellular level. A discussion of such toxicity mechanisms for each of the toxins used in this study is presented next.

Cadmium resulted in severe process upset both in the 2 day and 10 day SRT systems and affected all the processes analyzed in this paper to some extent. This is consistent with what is found in the literature regarding its effects on activated sludge systems and toxicity mechanisms induced at the molecular level. Both decreases in COD removal efficiency (Weber and Sherrard, 1980), and SOUR (Madoni et al., 1999) have been reported as effects of cadmium on activated

sludge. In addition, cadmium-induced deflocculation was also found in previous studies (Neufeld, 1976; Bott and Love, 2001). Activated sludge deflocculation by electrophilic chemicals, such as cadmium and CDNB, has been shown to be linked to a microbial stress response called the glutathione gated potassium efflux (GGKE) (Bott and Love, 2002; Bott and Love, 2004). For this reason, we have also measured soluble potassium levels in the effluent of the shocked reactors. An analysis and discussion of the effluent potassium levels in the stressed reactors and their correlation with effluent TSS concentrations is given in Henriques et al. (2004). In addition, cadmium was found to induce synthesis of GroEL, a heat shock protein, in activated sludge cultures stressed with concentrations as low as 5 mg/L (Bott and Love, 2001). Cadmium has also been reported to interfere with numerous cellular functions, promoting DNA mutagenesis (Hughes and Poole, 1989), enzyme inactivation and complex formation with phosphate groups in membrane phospholipids (Collins and Stotzky, 1989). Given its numerous effects at the cellular level, it is not possible to determine what specific mechanisms led to each of the observed effects, with the only exception being deflocculation. Nevertheless, the inhibition trends tended to correlate with the presence of measurable soluble cadmium in the stressed reactors (data not shown), corroborating previous reports that indicate the soluble form as the predominant stressor controlling cadmium toxicity (Collins and Stotzky, 1989; Hughes and Poole, 1989). Complete recovery was not achieved for the 2 day SRT SBRs but was reached in the 10 day SRT stressed bioreactors within 3x SRTs. Recovery in the 10 day SRT systems was linked to washout of soluble cadmium from the reactors. Soluble cadmium in the 2 day SRT reactors was much higher on a moles per cell basis than in the 10 day SRT reactors, and might explain why the 2 day SRT system did not recover as promptly.

From the three pH values selected to shock the SBR reactors, only pH 11 resulted in significant process upset. Extreme pH values such as pH 11 can directly damage external cell structures outside the cytoplasmic membrane, such as flagella, chemoreceptors and cell walls (Chong et al., 1997; Dilworth et al., 1999). The results presented here show that although severe inhibitory effects were noted for COD removal, flocculation ability and biomass growth that could be related to external cell structure damage, respiration inhibition recovered very rapidly, suggesting that cell lysis/death was not a major consequence of pH 11 shock. High pH is utilized as a technique to extract EPS from activated sludge flocs (Frølund et al., 1996; Higgins and Novak, 1997). Therefore, pH 11 shock most likely released polymer molecules from the flocs

into the bulk solution, which is consistent with its effects on effluent soluble COD, effluent TSS and CST. The case of pH 11 shock is probably the most obvious example of the connection between deflocculation and increases in soluble COD, as the solubilization of EPS molecules is the most likely mechanism behind such effects. The dramatic increase in CST values can be also linked to an increase in the concentration of biopolymers, which leads to an increase in the viscosity of the liquid.

CDNB affected mostly COD removal and biomass flocculation, but its influence on biomass respiration rate was short-lived. CDNB is an electrophilic chemical, and as such, it has the potential to inflict oxidative damage to cells. Although reports on the effects of CDNB in activated sludge systems are scarce, studies on the effects of organic electrophilic chemicals on pure cultures of Gram negative bacteria indicate that electrophiles such as CDNB can damage DNA and proteins (Apontoweil and Berends, 1975a; Apontoweil and Berends, 1975b; Ferguson et al., 1995), and in the latter case the mechanism usually involves reaction with thiol bonds (Ferguson et al., 1995; Ferguson et al., 1997; Mclaggan et al., 2000). As an electrophile, CDNB has been reported to elicit the GGKE stress response (Ferguson et al., 1995; Ferguson and Booth, 1998; Ferguson et al., 1998) and to form a conjugate with glutathione (Vuilleumier, 1997). The results from the CDNB source-effect experiments are consistent with these previous findings. Activated sludge deflocculation by CDNB has been previously connected to the GGKE mechanism (Bott and Love, 2002; Bott and Love, 2004). In addition, although statistical recovery of COD removal took approximately 1x SRT in both systems, the magnitude of COD removal inhibition in the 10 day SRT CDNB-stressed reactors was not severe. In association with the soluble CDNB (data not shown) and MLVSS data in these reactors, these results suggest that the GGKE protective mechanism might have a limited capacity in terms of the CDNB concentration/mass that it can take up, in order for the mechanism to be efficiently used by bacteria, i.e. the IC_{15} and IC_{25} did not seem to be greatly affected, while the effects on the IC_{50} reactor, where part of the dosed CDNB was found in its free soluble form during the cycles after the shock, were more dramatic.

In both the 10 day SRT and 2 day SRT systems, the process that was most severely affected by DNP shock was respiration. Biomass growth was also strongly inhibited in the 10 day SRT system. Given its known mode of action as an uncoupler of oxidative phosphorylation the results in the 10 day SRT are consistent with uncoupling between biomass growth and

substrate uptake. Most of the literature that analyzes the effects of DNP on activated sludge systems is related to the reduction of biomass yield in order to reduce biosolids production in activated sludge plants (Mayhew and Stephenson, 1998; Liu, 2000). However, there are few reports on the inhibitory effects of DNP on different process parameters, such as the ones presented here. It was interesting to note that, at the initial high DNP concentrations, there was an inhibitory effect on oxygen uptake rather than a stimulation, both in the nitrifying (10 day SRT) and non-nitrifying (2 day SRT) system, showing that at high concentrations other toxicity mechanisms rather than disruption of the PMF alone were probably occurring or that the energy content in the cells decreased to levels that did not allow the basic metabolic processes to proceed. Stimulation of oxygen uptake started to occur in the 10 day SRT system when the DNP levels in the reactors dropped to under 10 mg/L (data not shown) and elevated SOUR values remained even after the DNP concentrations decreased to below the detection limit. No stimulation of respiration was observed in the 2 day SRT system. The reason for such results are not clear.

Similar to DNP, cyanide shock affected respiration functions more severely than COD removal or biomass growth. Weak cyano-metal complexes, such as the zinc-cyanide complex used in this study, can dissociate extensively to the metal ion and CN^-/HCN, which creates a greater availability of the toxic form of cyanide and, therefore, a greater potential for biomass toxicity than strong cyanide complexes (Torrens, 2000). The results of the source-effect cyanide experiments are consistent with the primary toxicity mechanism identified for the toxin, which consists of chelation reactions with divalent and trivalent metals in metallic enzymes. Specifically, chelation of the iron center in the heme group of cytochrome oxidases, the terminal enzymes in the electron transport chain, prevents the reoxidation of the enzymes and leads to partial or complete inactivation of respiration (Solomonson, 1981; Knowles, 1988; Yoshikawa and Caughey, 1990; Arden et al., 1998).

Octanol shock had a very modest impact on both activated sludge systems. Given the weak effects that octanol induced on biomass respiration, COD removal, bioflocculation and biomass growth and its fast disappearance from the bulk liquid (data not shown), octanol was either consumed as a carbon source or became associated with the mixed liquor particles, which would reduce its bioavailability and toxicity. Data regarding effluent TSS and CST analysis in the shocked reactors showed that these parameters were moderately impacted by octanol, which

may suggest that sorption to activated sludge flocs was the predominant effect during the early stages of the experiment. Hydrophobic compounds such as octanol have been found to insert into biological membranes and to change the membrane structure (Ingram, 1977; Heipieper et al., 1994; Sikkema et al., 1995). Therefore, such mechanism could potentially result in a destruction and/or rearrangement of the interactions between different cells or between cells and EPS molecules within activated sludge flocs, thereby causing alterations at the level of floc structure. This could result in deflocculation and increased water retention, which would explain the mild effects observed in both activated sludge systems.

Ammonia shock was the condition that had less impact on both activated sludge systems. Since ammonium bicarbonate was used as the source of ammonia shock, the added alkalinity contributed to maintain a stable pH in the reactors (data not shown). Therefore, the results reported in this study pertain to the effects of ammonia (NH_3 and NH_4^+) alone. No significant effects were noted on any of the monitored process parameters in the 10 day SRT system, while only minor effects were noted on respiration, COD removal, CST and SVI on the 2 day SRT biomass. The brief effects on COD removal and respiration rates seem to suggest inhibition of metabolic activities occurred to some extent, and are consistent with previous studies, specifically in terms of a decrease in COD removal efficiency (Li and Zhao, 1999). We hypothesize that this inhibition may be related to free ammonia in the system, as free ammonia has been reported to inhibit some classes of bacteria, such as nitrifiers (Neufeld et al., 1980). The effects on SVI and CST could be related to an increase in the monovalent to divalent cation ratio in the mixed liquor (due to NH_4^+ addition), which has been linked to a deterioration of the settleability properties of activated sludge (Novak, 2001).

A comparison between the source-effect matrices generated for the non-nitrifying (2 day SRT) and the nitrifying mixed liquor (10 day SRT) reveals that it is not possible to identify a general trend of increased sensitivity for either biomass, under the conditions used in the present work. In terms of the intensity of an effect, the 2 day SRT biomass seemed to be more sensitive to increases in soluble COD. The effects on SOUR and SVI were comparable for both biomasses, but the effects on MLVSS reduction and CST increase were not consistent between the two systems. However, in terms of recovery time of the shocked reactors to control levels, in most cases the 2 day SRT biomass took longer to recover from the stress event than the 10 day SRT biomass, which indicates an increased susceptibility of the low SRT biomass to toxic shock

loads. For some of the most intense effects produced by cadmium and pH 11 shocks, the 2 day SRT biomass was not able to recover to control levels during the experimental period of 3x SRTs, while the 10 day SRT biomass always recovered within the same period. While physiological and community structure differences between the two systems may contribute to this observed trend, the differences in floc structure between the two activated sludges are also noteworthy. Floc structure differences have been previously suggested to impact the toxicity response of activated sludge, with smaller flocs leading to increased susceptibility to toxic conditions (Henriques et al., 2005; Henriques and Love, in preparation).

It is important to note that when a process effect did recover to control levels, for most cases the recovery occurred in less than 1-1.5x SRTs (2 day SRT system) or 1x SRT (10 day SRT system), which suggests that, in general, the biomass was able to react to the shock load and recover to a physiologically active state in a fairly short period. In other words, although this study shows that significant deterioration of treatment process efficiency can potentially occur as a result of upset events from many different sources, it also shows that activated sludge systems are likely to overcome the shock event within 1-2x SRTs. However, this trend does not hold if the effects of nitrification are considered, as nitrification was the process most detrimentally affected by chemical shock (Kelly et al., 2004).

Comprehensive assessments of the potential effects of a specific class of toxins on biological treatment processes are extremely important because they may contribute for the development of both mitigation and prevention measures and/or technology. This work showed that COD removal, bioflocculation, biomass growth and biomass respiration were inhibited to different extents by distinct classes of industrial chemical toxins. The process that was most severely impacted by the different toxins varied with chemical class and seemed to be intrinsically related to the nature of the chemical and its predominant mode of action on bacterial cells. Therefore, it becomes important to understand the causal mechanisms behind the source-effect relationships for each chemical class, as this information may help develop smart biosensors that can differentiate between different chemical shock loads and prevent major process upset.

Conclusions

Based on the results presented above, the following conclusions were made:

- Cadmium, pH 11 and CDNB shocks adversely impacted effluent soluble COD, effluent TSS, SOUR and MLVSS levels relative to the control reactor. Cyanide and DNP shocks resulted in significant decreases in biomass SOUR and respiration inhibition was the most affected process. Octanol, pH 5, pH 9 and ammonia shocks did not cause significant process upset.
- The processes that were most severely impacted by the toxic shock loads were respiration, COD removal and bioflocculation. Loss of COD removal and deflocculation tended to occur concurrently. Respiration inhibition did not necessarily translate into other process effects.
- The observed process effects were intrinsically related to the toxicity mechanisms elicited by the toxic source.
- In general, when recovery to control levels was observed after a shock event for respiration, COD removal, flocculation, biomass growth, settleability and dewaterability, the biomass was able to overcome the shock in less than 2x SRTs.

Acknowledgments

Credits. This work was funded by the Water Environment Research Foundation, project no. 01-CTS-2. Inês Henriques received a fellowship (SFRH/BD/4689/2001) from the Fundação para a Ciência e a Tecnologia, Portugal, and Richard Kelly received a Charles E. Via Fellowship. The authors would like to acknowledge the assistance of several undergraduate assistants and Julie Petruska and Jody Smiley during this work.

Authors. At the time of this research, Inês Henriques and Richard Kelly were Ph.D. students and Jennifer Dauphinais was a M.S. student in the Department of Civil and Environmental Engineering at Virginia Tech. Nancy Love is professor in the Department of Civil and Environmental Engineering at Virginia Tech. Correspondence should be addressed to Dr. Nancy G. Love, Department of Civil and Environmental Engineering, Virginia Tech, 418 Durham Hall, Mail Code 0246, Blacksburg, VA 24061; e-mail: nlove@vt.edu.

References

American Public Health Association; American Water Works Association; Water Environment Federation (1998) *Standard Methods for the Examination of Water and Wastewater*, 20th ed. Washington, DC.

Apontoweil, P.; Berends, W. (1975a) Glutathione Biosynthesis in *Escherichia coli* K-12 – Properties of Enzymes and Regulation. *Biochim. Biophys. Acta*, **399** (1), 1.

Apontoweil, P.; Berends, W. (1975b) Isolation and Initial Characterization of Glutathione-Deficient Mutants of *Escherichia coli* K-12. *Biochim. Biophys. Acta*, **399** (1), 10-22.

Arden, S. R.; Sinor, J. D.; Potthoff, W. K.; Aizenman, E. (1998) Subunit-Specific Interactions of Cyanide with the N-Methyl-D-Aspartate Receptor. *J. Biol. Chem.*, **273** (34), 21505.

Berthouex, P. M.; Brown, L. C. (1994) *Statistics for Environmental Engineers*. Lewis Publishers. Boca Raton, FL.

Boon, N.; Top, E. M.; Verstraete, W.; Siciliano, S. D. (2003) Bioaugmentation as a Tool to Protect the Structure and Function of an Activated Sludge Microbial Community Against a 3-Chloroaniline Shock Load. *Appl. Environ. Microbiol.*, **69** (3), 1511.

Bott, C. B.; Duncan, A. J.; Love, N. G. (2001) Stress Protein Expression in Domestic Activated Sludge in Response to Xenobiotic Shock Loading. *Water Sci. Technol.*, **43** (1), 123.

Bott, C. B.; Love, N. G. (2001) The Immunochemical Detection of Stress Proteins in Activated Sludge Exposed to Toxic Chemicals. *Water Res.*, **35** (1), 91.

Bott, C. B.; Love, N. G. (2002) Investigating a Mechanistic Cause for Activated Sludge Deflocculation in Response to Shock Loads of Toxic Electrophilic Chemicals. *Water Environ. Res.*, **74** (3), 306.

Bott, C. B.; Love, N. G. (2004) Implicating the Glutathione-Gated Potassium Efflux System as a Cause of Electrophile-Induced Activated Sludge Deflocculation. *Appl. Environ. Microbiol.*, **70** (9), 5569.

Buitron, G.; Schoeb, M. E.; Moreno-Andrade, L.; Moreno, J. A. (2005) Evaluation of Two Control Strategies for a Sequencing Batch Reactor Degrading High Concentration Peaks of 4-Chlorophenol. *Water Res.*, **39** (6), 1015.

Chong, N. M.; Pai, S. L.; Chen, C. H. (1997) Bioaugmentation of an Activated Sludge Receiving pH Shock Loadings. *Bioresour. Technol.*, **59** (2-3), 235.

Collins, Y. E.; Stotzky, G. (1989) *Factors Affecting the Toxicity of Heavy Metals to Microbes*. In: Metal Ions and Bacteria. Beveridge, T. J.; Doyle, R. J. (eds). John Wiley & Sons, Inc. New York, NY.

Dilworth, M. J.; Glenn, A. R.; Konings, W. N.; Booth, I. R.; Poole, R. K.; Krulwich, T. A.; Rowbury, R. J.; Stock, J. B.; Slonczewski, J. L.; Cook, G. M.; Padan, E.; Kobayashi, H.; Bennett, G. N.; Matin, A.; Skulachev, V. (1999) Problems of Adverse pH and Bacterial Strategies to Combat It. *Novartis Foundation Symposium*, **221**, 4. John Wiley & Sons, Ltd. West Sussex, England.

Ferguson, G. P.; Booth, I. R. (1998) Importance of Glutathione for Growth and Survival of *Escherichia coli* Cells: Detoxification of Methylglyoxal and Maintenance of Intracellular K^+. *J. Bacteriol*., **180** (16), 4314.

Ferguson, G. P.; Creighton, R. I.; Nikolaev, Y.; Booth, I. R. (1998) Importance of RpoS and Dps in Survival of Exposure of Both Exponential- and Stationary-Phase *Escherichia coli* Cells to the Electrophile N-Ethylmaleimide. *J. Bacteriol*., **180** (5), 1030.

Ferguson, G. P.; Mclaggan, D.; Booth, I. R. (1995) Potassium Channel Activation by Glutathione-S-Conjugates in *Escherichia coli* – Protection Against Methylglyoxal is Mediated by Cytoplasmic Acidification. *Mol. Microbiol*., **17** (6), 1025.

Ferguson, G. P.; Nikolaev, Y.; Mclaggan, D.; Maclean, M.; Booth, I. R. (1997) Survival During Exposure to the Electrophilic Reagent N-Ethylmaleimide in *Escherichia coli*: Role of KefB and KefC Potassium Channels. *J. Bacteriol*., **179** (4), 1007.

Frølund, B.; Palmgren, R.; Keiding, K.; Nielsen, P. H. (1996) Extraction of Extracellular Polymers From Activated Sludge Using a Cation Exchange Resin. *Water Res*., **30** (8), 1749.

Heipieper, H. J.; Weber, F. J.; Sikkema, J.; Keweloh, H.; Debont, J. A. M. (1994) Mechanisms of Resistance of Whole Cells to Toxic Organic Solvents. *Trends Biotechnol*., **12** (10), 409.

Henriques, I. D. S.; Holbrook, R. D.; Kelly, R. T.; Love, N. G. (2005) The Impact of Floc Size on Respiration Inhibition by Soluble Toxicants – A Comparative Investigation. *Water Res*., **39** (12), 2559.

Henriques, I. D. S.; Kelly, R.T.; Love, N. G. (2004) Deflocculation Effects Due to Chemical Perturbations in Sequencing Batch Reactors. *Water Sci. Technol*., **50** (10), 287.

Henriques, I. D. S.; Kelly, R. T.; Love, N.G. (in review) Short-Term versus Long-Term Respiration Inhibition in Nitrifying and Non-Nitrifying Activated Sludge Exposed to Chemical Toxins. *Water Environ. Res*.

Henriques, I. D. S.; Love, N.G. (in preparation) Floc Structure and Floc Size Play a Role in the Toxicity Response of Activated Sludge Bacteria to Chemical Toxins. *Water Res*.

Higgins, M. J.; Novak, J. T. (1997) The Effect of Cations on the Settling and Dewatering of Activated Sludges: Laboratory Results. *Water Environ. Res*., **69** (2), 215.

Hughes, M. N.; Poole, R. K. (1989) *Metals and Microorganisms*. Chapman and Hall. New York, NY.

Ingram, L. O. (1977) Changes in Lipid Composition of *Escherichia coli* Resulting From Growth with Organic Solvents and With Food Additives. *Appl. Environ. Microbiol.*, **33** (5), 1233.

Kelly, R. T.; Henriques, I. D. S.; Love, N. G. (2004) Chemical Inhibition of Nitrification in Activated Sludge. *Biotechnol. Bioeng.*, **85** (6), 683.

Kjellerup, B. V.; Keiding, K.; Nielsen, P. H. (2001) Monitoring and Troubleshooting of Non-Filamentous Settling and Dewatering Problems in an Industrial Activated Sludge Treatment Plant. *Water Sci. Technol.*, **44**, (2-3), 155.

Knowles, C. (1988) Cyanide Utilization and Degradation by Microorganisms. *Ciba Foundation Symposium*, **40**, 3.

Kong, Z.; Vaerewijck, M.; Verstraete, W. (1996a) On-Line StBOD Measurement and Toxicity Control of Wastewaters with a Respirographic Biosensor. *Environ. Technol.*, **17** (4), 399.

Kong, Z.; Vanrolleghem, P.; Willems, P.; Verstraete, W. (1996b) Simultaneous Determination of Inhibition Kinetics of Carbon Oxidation and Nitrification with a Respirometer. *Water Res.*, **30** (4), 825.

Lajoie, C. A.; Lin, S. C.; Kelly, C. J. (2003) Comparison of Bacterial Bioluminescence with Activated Sludge Oxygen Uptake Rates During Zinc Toxic Shock Loads in a Wastewater Treatment System. *J. Environ. Eng. – ASCE*, **129** (9), 879.

Li, X. Z.; Zhao, Q. L. (1999) Inhibition of Microbial Activity of Activated Sludge by Ammonia in Leachate. *Environ. Int.*, **25** (8), 961.

Liu, Y. (2000) Reduced Growth Yield of Activated Sludge in Organic Protonophore-Containing Batch Culture. *Microb. Ecol.*, **39** (2), 168.

Love, N. G.; Bott, C. B. (2000) *A Review and Needs Survey of Upset Early Warning Devices*. Project 99-WWF-2. Water Environment Research Foundation. Alexandria, VA.

Love, N. G.; Henriques, I. D. S.; Kelly, R. T. (2005) *Upset Early Warning Systems for Biological Treatment Processes – Source and Effect Relationships*. Report No. 01-CTS-2. Water Environment Research Foundation. Alexandria, VA.

Madoni, P.; Davoli, D.; Guglielmi, L. (1999) Response of SOUR and AUR to Heavy Metal Contamination in Activated Sludge. *Water Res.*, **33** (10), 2459.

Mayhew, M.; Stephenson, T. (1998) Biomass Yield Reduction: Is Biochemical Manipulation Possible Without Affecting Activated Sludge Process Efficiency? *Water Sci. Technol.*, **38** (8-9), 137.

Mclaggan, D.; Rufino, H.; Jaspars, M.; Booth, I. R. (2000) Glutathione-Dependent Conversion of N-Ethylmaleimide to the Maleamic Acid by *Escherichia coli*: An Intracellular Detoxification Process. *Appl. Environ. Microbiol.*, **66** (4), 1393.

Neufeld, R. D. (1976) Heavy Metals-Induced Deflocculation of Activated Sludge. *J. Water Pollut. Control Fed*., **48** (8), 1940.

Neufeld, R. D.; Hill, A. J.; Adekoya, D. O. (1980) Phenol and Free Ammonia Inhibition to *Nitrosomonas* Activity. *Water Res*., **14** (12), 1695.

Novak, J. T. (2001) The Effect of the Ammonium Ion on Activated Sludge Settling Properties. *Water Environ. Res*., **73** (4), 409.

Rich, L. G.; Yates, O. W. (1955) The Effect of 2,4-Dinitrophenol on Activated Sludge. *Appl. Microbiol*., **3**, 95.

Schwartz-Mittelmann, A.; Galil, N. I. (2000) Biological Mechanisms Involved in Bioflocculation Disturbances Caused by Phenol. *Water Sci. Technol*., **42** (1-2), 105.

Sikkema, J.; Debont, J. A. M.; Poolman, B. (1995) Mechanisms of Membrane Toxicity of Hydrocarbons. *Microbiol. Rev*., **59** (2), 201.

Solomonson, L. (1981) *Cyanide as a Metabolic Inhibitor*. In: Vennesland, B.; Conn, E.; Knowles, C.; Westley, J.; Wissing, F. (eds). Academic Press. New York, NY.

Torrens, K. D. (2000) Activated Sludge and Cyanide: a Deadly Combination? *Pollut. Eng*., **32** (3), 23.

Vanrolleghem, P. A.; Kong, Z.; Rombouts, G.; Verstraete, W. (1994) An Online Respirographic Biosensor for the Characterization of Load and Toxicity of Wastewaters. *J. Chem. Technol. Biotechnol*., **59** (4), 321.

Vuilleumier, S. (1997) Bacterial Glutathione S-Transferases: What are they Good for? *J. Bacteriol*., **179** (5), 1431.

Weber, A. S.; Sherrard, J. H. (1980) Effects of Cadmium on the Completely Mixed Activated Sludge Process. *J. Water Pollut. Control Fed*., **52** (9), 2378.

Yoshikawa, S.; Caughey, W. S. (1990) Infrared Evidence of Cyanide Binding to Iron and Copper Sites in Bovine Heart Cytochrome-C-Oxidase – Implications Regarding Oxygen Reduction. *J. Biol. Chem*., **265** (14), 7945.

Chapter 4. Floc Structure and Floc Size Play a Role in the Toxicity Response of Activated Sludge Bacteria to Chemical Toxins

Inês D. S. Henriques
Department of Civil and Environmental Engineering
Virginia Tech
418 Durham Hall (0246)
Blacksburg, VA 24061

Nancy G. Love*
Department of Civil and Environmental Engineering
Virginia Tech
418 Durham Hall (0246)
Blacksburg, VA 24061
TELEPHONE: 540 231 3980
FAX: 540 231 7916
E-MAIL: nlove@vt.edu

***** corresponding author

Abstract

The objective of this study was to evaluate the respiration inhibition induced by octanol, cadmium, N-ethylmaleimide (NEM), cyanide and 2,4-dinitrophenol (DNP) on activated sludge biomasses with different floc structures but similar physiological characteristics. Mechanical shearing was applied to fresh mixed liquor to produce biomasses with different floc structure properties. Specific oxygen uptake rate assays were conducted on the sheared and unsheared mixed liquors. The results showed that mechanical shearing resulted in release of biopolymers from the floc extracellular polymeric substances (EPS) matrix into the bulk liquid and a simultaneous reduction in floc size. Shearing did not impact biomass viability. The respiration inhibition by octanol and cadmium was more severe in sheared mixed liquor than in the unsheared biomass. Conversely, the respiration inhibition induced by NEM and cyanide was similar for the different mixed liquors tested. We conclude that the EPS matrix functions as a protective barrier for the bacteria inside activated sludge flocs to chemicals that it has the potential to interact with, such as hydrophobic (octanol) and positively-charged (cadmium) compounds, but that the toxicity response for soluble, hydrophilic toxins (NEM and cyanide) is not influenced by the presence of the polymer matrix. Additionally, floc size appears to be another important factor dictating the toxicity response of activated sludge to certain chemicals.

Key words

Activated sludge, floc structure, extracellular polymeric substances (EPS), toxins, specific oxygen uptake rate (SOUR), particle size distribution (PSD)

Introduction

Activated sludge is the most widely used biological wastewater treatment process. It is based on the biological degradation of both soluble organic and inorganic components and particulate matter carried out by microbial flocs, which are traditionally separated from the liquid stream through gravity sedimentation. Flocculation is, therefore, one of the most important mechanisms occurring in the activated sludge process.

Microscopic observations have shown that activated sludge flocs are multilevel porous structures in which macroflocs are formed by smaller aggregates or microcolonies, believed to result from the division of microorganisms (Jorand et al., 1995; Andreadakis, 1993; Snidaro et al., 1997; Zartarian et al., 1994). The cohesion of this multilevel structure is dictated by many factors, from which the internal hydrophobicity (Zita and Hermansson, 1997; Jorand et al., 1994; Jorand et al., 1998; Liao et al., 2001), the extracellular polymeric substances (EPS) composition (Dignac et al., 1998; Higgins and Novak, 1997b), and multivalent cation bridging (Higgins and Novak, 1997a) seem to be the most important. More specifically, it is believed that EPS, which is mainly composed of protein and polysaccharide polymers, forms a gel-like matrix in which microcolonies are embedded through both electrostatic and hydrophobic interactions (Snidaro et al., 1997; Dignac et al., 1998). Although much is known about the composition and structure of activated sludge flocs, the role played by the different floc components in the toxicity response of activated sludge to chemical toxins is largely unknown. We have found significant differences in the treatment process effects of shock loads for a wide range of chemical toxins when applied to activated sludge cultures with different solids retention times (SRTs) (Henriques et al., in review). Although we recognize that the dissimilar responses may be due to physiological differences between the mixed liquors tested, we also hypothesized that floc structure, which varies significantly with SRT (Liao et al., 2001; Liss et al., 2002; Wilen et al., 2003) also played a role in the observed results. Therefore, one of the questions that remains to be investigated is if floc morphology, composition and/or size are important factors that define the sensitivity of activated sludge cultures to chemical stress. We have previously suggested that the increased susceptibility of membrane bioreactor biomass to cadmium and 2,4-dinitrophenol

(DNP) in comparison with conventional activated sludge biomass was mainly due to differences in floc size (Henriques et al., 2005). However, we believe that other floc properties may contribute to the toxicity response of activated sludge to these and other chemicals.

The study of biofilms and the parallel of biofilms' structure and physiology with that of activated sludge flocs is inevitable, given the similarities between the two systems. Both activated sludge flocs and biofilms are biological aggregates containing several levels of organization and are porous structures in which cells are embedded in a polymer matrix (Costerton et al., 1995). Therefore, theories developed for biofilms may be valid for flocs as well (Scuras et al., 1998). One of the best studied properties of biofilms is their increased resistance to antimicrobial substances in comparison with free bacterial cells in suspension (reviewed by Costerton et al., 1999; Mah and O'Toole, 2001; Stewart, 2002) and several hypotheses exist regarding the mechanisms responsible for such behavior. Failure of the toxin to penetrate the biofilm due to the presence of EPS is one of the proposed mechanisms. The EPS barrier appears to function through sorption and/or reaction of matrix components with the antimicrobial agent, as well as through retardation of toxin penetration, giving biofilm cells a better opportunity to express specific stress responses. For example, in a mixed species biofilm, the reaction of proteins in EPS with chlorine served as a protection factor to the community (Leriche et al., 2003). Farrell and Quilty (2002) showed that a *Pseudomonas putida* strain capable of degrading mono-chlorophenols formed clumps when subjected to high concentrations of the compounds, and this autoaggregation was proposed to be a response to chemical stress induced by the high concentrations of the mono-chlorophenols and as a protective mechanism that allowed the toxin to be utilized as a substrate. In addition, the EPS matrix has been shown to retard the diffusion of certain antibiotics through the biofilm matrix, which in some cases was attributed to the presence of antibiotic-inactivating or modifying enzymes in the EPS matrix, such as beta-lactamases (Stewart, 2002).

Given the characteristics of activated sludge EPS, it is therefore legitimate to hypothesize that EPS protects the bacteria in activated sludge flocs from toxic compounds that it has the potential to interact with, such as hydrophobic and positively-charged toxins. For example, negatively charged residues in bound EPS protein can bind cationic species of heavy metals, leading to reduced toxicity because the metal is less bioavailable in comparison to systems without significant quantities of EPS. The binding of heavy metals to EPS has been shown in the

literature (Guibaud et al., 2005; Jang et al., 2001; Liu et al., 2001). In the case of soluble uncharged hydrophilic toxins that more easily diffuse through the EPS matrix, the toxicity response is probably a function of other mechanisms.

The objective of this work was to compare the inhibition induced by a wide range of chemical toxins (octanol, cadmium, DNP, cyanide and N-ethylmaleimide - NEM) on mixed liquors with different floc structures. Mechanical shear stress was used to test the hypothetical protective effect of EPS to the bacteria within activated sludge flocs. Shearing mixed liquor breaks up the flocs and simultaneously releases EPS from the floc matrix into the bulk liquid, thereby permitting the production of biomasses at a single physiological growth state with different floc structures. Inhibition of respiratory activity through specific oxygen uptake rate (SOUR) assays was used as the indicator of biomass toxicity.

Materials and Methods

Field sampling and sample preparation

Fresh activated sludge was obtained from the Blacksburg-Virginia Tech Sanitation Authority Wastewater Treatment Plant every morning before an experiment and immediately transported to the laboratory. In the laboratory, the mixed liquor was mixed, aerated and supplied with synthetic feed to stabilize the growth state of the biomass over the duration of the experiment. Two feed solutions were used in separate experiments: (1) a complex source of readily biodegradable compounds (RB feed) composed of 34% protein (beef extract, bacto-casitone, yeast extract), 18% carbohydrate (fructose, galactose, glucose) and 48% organic acids/alcohols (glacial acetic acid and glycerol) on a chemical oxygen demand (COD) basis and (2) acetate and glycerol as the only carbon and energy sources (84% acetate and 16% glycerol on a COD basis) (AG feed). The second feed solution was used in order to avoid interference of protein and carbohydrate components on the analysis of protein and polysaccharide during the experiments. Mixed liquor fed with RB solution received a load of approximately 80 mg COD/hr/L, while AG feed was dosed at 20 mg COD/hr/L, which is the average COD load received at the plant. From hereon, we will refer to the experiments in which RB feed was used as set A and to the experiments in which AG feed was used as set B. In both cases, the sludge was allowed to adapt to the new feed and laboratory conditions for a period of 1-2 hours before the start of an experiment, in order for biomass growth to stabilize. Feeding, aeration and mixing continued throughout the experimental period to maintain a stable biological activity of the

biomass. The volume of feed solution over the entire experimental period was negligible relative to the volume of mixed liquor.

Shearing was used to create different floc structures from the same mixed liquor source. After the stabilization period, aliquots of the source mixed liquor were subject to shearing (shearing times varied between 20 and 60 seconds) and the impact of selected toxic chemicals on the SOUR of sheared and unsheared mixed liquor was evaluated. A KADY Model-L laboratory high speed rotor-stator dispersion mill (Kady International, Scarborough, ME) was used to shear the mixed liquor. The shear process was conducted at a mean velocity gradient (G) of approximately 11,000 s^{-1} (Muller, 2001). Figure 1 shows the main aspects of the experimental design adopted for the experiments.

SOUR assays

SOUR experiments were used to assess the impact of selected toxins on mixed liquors with different floc structures. In most cases, experiments were performed such that different toxins were used on different days, meaning that the mixed liquor was different for each toxin tested. In addition, the SOUR runs were planned such that all the SOURs corresponding to a floc structure condition were run sequentially, but the concentrations of toxin within each run were randomized. SOUR assays were performed in duplicate using a dual channel Accumet Research AR25 pH/mV/°C/ISE Meter (Fisher Scientific International, Hampton, NH) and two Orion 97-08 oxygen electrodes coupled with localized mixers (Thermo Electron Corporation, Waltham, MA). Dissolved oxygen (DO) readings were recorded every six seconds using an automated data acquisition system (Labview 6i, National Instruments, Austin, TX). Two to five concentrations of each toxic chemical were used. Selection of the toxin concentrations was based on previous assays conducted in our laboratory (Henriques et al., in review). A mixed liquor sample was pre-aerated and placed in a biochemical oxygen demand (BOD) bottle to which the toxin and 100-120 mg/L of soluble COD (either added as RB or AG solution) was previously added, to ensure that respiration was not substrate-limited during the test. DO readings were started within 30 seconds of blending the toxin with the mixed liquor. Control SOURs, to which no toxin was added, were run for each condition both at the beginning and end of the experimental period in order to monitor changes in the physiological characteristics of the sludge with time. Each assay was run for a minimum of 20 minutes or until the DO concentration reached less than 1 mg/L.

The OUR was determined through the slope of the linear portion of the DO versus time curve. The SOUR was calculated by dividing the OUR by the mixed liquor volatile suspended solids (MLVSS) concentration, which was adjusted to account for the minor dilution effect occurring in the BOD bottle, due to addition of chemical and readily biodegradable COD. The first 1-2 minutes of data were eliminated to account for probe and mixing stabilization. All OUR best fit lines had regression coefficients (R^2) greater than 0.98. SOUR inhibition was calculated by the following equation:

$SOUR_{inhibition}$ (%) = [1 – ($SOUR_{toxin}$ / $SOUR_{control}$)] x 100

where $SOUR_{toxin}$ is the SOUR of the mixed liquor in the presence of a given toxin concentration and $SOUR_{control}$ is the average SOUR (assays conducted at the beginning and end of the experimental period) without any chemical.

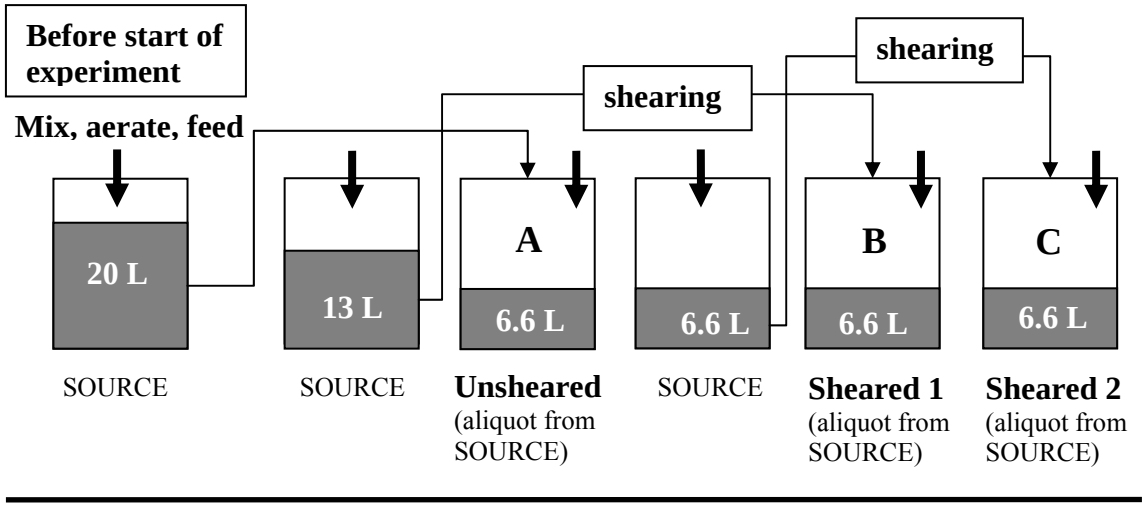

Sampling from containers **A**, **B**, and **C**, over time (sampling from containers occurred in a sequential manner, such that sampling from one container was completed before starting to sample from the next one):

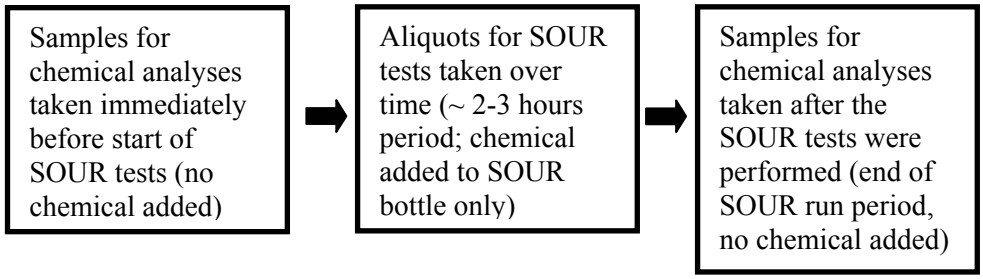

Figure 1 – Experimental design.

Selected chemical toxins

Five chemicals were selected for the experiments: NEM, a very soluble organic electrophilic chemical; cadmium (as cadmium chloride, $CdCl_2$), an electrophilic heavy metal that establishes strong sorption interactions with activated sludge; octanol, a hydrophobic organic chemical that strongly sorbs to biomass; cyanide (as sodium cyanide, NaCN), a very soluble toxin that blocks electron transport along the respiratory chain; and DNP, an uncoupler of oxidative phosphorylation that has a moderate solubility and may interact to some extent with the floc matrix. These toxins were selected because they represent a wide range of chemical structures, which leads to very different interactions with the activated sludge floc matrix, and to distinct physiological responses from activated sludge bacteria.

Standard solutions of the chemicals were used to measure specific volumes into 300 mL BOD bottles, which were used to run the SOUR tests. In the case of octanol, which is highly insoluble, mixed liquor supernatant was collected in advance and used as the matrix to solubilize octanol, both through sonication and continuous stirring during the experiment. This allowed the addition of much higher volumes of toxin solution into the BOD bottle, as mixed liquor was concentrated and added to the BOD bottle to achieve the same mixed liquor concentration as in the source activated sludge.

Chemical analyses

The impact of shear stress on the activated floc structure was evaluated through the measurement of multiple parameters on mixed liquor samples not exposed to any toxin. The particle size distribution (PSD) was measured in duplicate or triplicate using two independent samples taken before and after shearing and at the end of the SOUR runs for each condition, to evaluate the extent of initial floc disruption and eventual reflocculation during the SOUR run period. PSD was analyzed using a HORIBA LA-700 (HORIBA, Lda., Kyoto, Japan) laser scattering particle size distribution analyzer with a particle measurement range between 0.05 μm and 262.4 μm. Soluble protein, humic acids, polysaccharides and DNA in the bulk liquid were measured in triplicate to evaluate the extent of EPS release from the floc matrix due to shear, during the experiments when AG feed was used. Soluble was defined as anything passing through a 1.5 μm nitrocellulose filter. For protein and humic acid analysis a modification of the Lowry method (Lowry et al., 1951) by Frølund and coworkers (1995) was used, while for

carbohydrate analysis the Dubois method was used (Dubois et al., 1956). Protein and carbohydrate samples were collected, filtered and stored at –20^{o}C for later analysis. The nucleic acids in the bulk liquid were analyzed through a method using DAPI (4',6-Diamidino-2-phenylindole), a DNA stain, and fluorescence spectrophotometry, modified from the Brunk method (Brunk et al., 1979) by Frølund and coworkers (1996).

Mixed liquor total solids (MLTS), total volatile solids (MLTVS), suspended solids (MLSS) and MLVSS were used to monitor the biomass concentration during each experiment. Solids analysis was carried out in triplicate before and after shearing and at the end of the SOUR run periods, using the methods outlined in Standard Methods (APHA et al., 1998).

Statistical analysis was conducted using Student's t-Tests with two-tailed distributions. The significance level used to evaluate statistical significance was $\alpha = 0.05$.

Results and Discussion

Mixed liquor shearing led to release of EPS into the bulk liquid

Mechanical shearing of activated sludge mixed liquor resulted in release of biopolymers from the floc EPS matrix into the bulk liquid, as seen by an increase in the soluble fraction of proteins, carbohydrates, DNA and humic acids. Release of EPS from the floc matrix due to shearing was recorded through analysis of soluble protein, humic acids, polysaccharides and DNA in the bulk liquid of each mixed liquor during the set B experiments (Table 1). The data show similar trends regarding the release of the different biopolymers from the floc matrix due to shearing. Protein was the biopolymer fraction that was most intensely released from the floc structure due to shearing, with the concentration in the bulk liquid increasing to 11 – 48x and 5.4 – 22x that of the unsheared mixed liquor for the 60 second and 20 second-sheared biomasses, respectively. The release effect on the carbohydrate and DNA fractions was similar, with soluble polysaccharides concentration after shearing increasing to 2.7 – 5.2x and 1.6 – 4.0x and soluble DNA concentration increasing to 2.5 – 7.1x and 1.1 – 5.3x the concentration in the unsheared mixed liquor for the 60 second and 20 second-sheared biomasses, respectively. Mechanical shear stress resulted in the release of humic acids from the floc structure to a lesser extent than it induced release of other biopolymers, with the humic acid concentration after shearing varying between 0.9 – 2.3x for the 20 second-sheared mixed liquor and 1.1 – 3.8x for the 60 second-

sheared biomass relative to the unsheared sludge. Ultimately, this result indicates that the sheared biomass had less EPS in the flocs than the unsheared mixed liquor.

Table 1 – Concentration (mg/L) of DNA, carbohydrates, proteins and humic acids in the soluble phase of unsheared and sheared mixed liquor, at the beginning ("beg") and end of the SOUR run period for each condition. Shearing times are indicated. Data from set B. Standard deviations for multiple absorbance/fluorescence measurements for each analysis were less than 5% of the average value and are not shown.

Biopolymer	Shear condition	DNP		Cyanide		NEM		Cadmium		Octanol	
		beg	end	beg	end	beg	end	beg	end	beg	end
DNA	unsheared	0.7	0.7	0.7	0.7	0.8	0.7	0.7	0.7	1.1	1.1
	20 sec	3.7	1.3	1.2	0.9	0.9	1.0	1.2	0.9	2.1	1.6
	60 sec	5.0	1.5	3.1	1.1	2.3	1.1	2.4	1.1	2.8	2.0
Carbohydrates	unsheared	2.3	2.3	3.0	3.2	2.5	2.1	2.5	2.4	3.7	4.1
	20 sec	9.1	5.5	4.9	3.7	3.7	2.9	4.0	2.8	6.9	4.9
	60 sec	12.0	7.0	8.3	5.3	8.0	4.0	9.3	4.4	12.2	8.8
Proteins	unsheared	0.6	0.5	0.5	0.6	0.2	0.1	0.4	0.5	1.1	1.3
	20 sec	12.1	5.0	3.0	1.5	2.3	1.3	3.0	1.1	6.9	3.8
	60 sec	18.5	7.2	8.8	2.2	8.6	2.7	8.6	2.9	13.1	7.7
Humic acids	unsheared	5.2	5.6	6.4	6.5	6.8	7.8	6.8	6.7	8.0	7.7
	20 sec	12.5	5.6	7.1	6.4	6.6	6.4	6.8	6.5	8.0	8.4
	60 sec	20.6	5.9	11.0	7.1	9.0	6.9	11.0	7.3	8.4	7.5

Release of biopolymers from activated sludge flocs has been previously associated with deflocculation events and a reduction in floc size. For example, anaerobic conditions together with shear stress have been shown to decrease floc size, resulting in deflocculation and an increase in the soluble concentration of protein, humic substances and carbohydrates (Wilen et al., 2000b; Wilen et al., 2000a). Similarly, Morgan-Sagastume and Allen (2005) have shown that temperature upshifts, which also result in deflocculation of activated sludge mixed liquor, lead to release of proteins, carbohydrates, DNA and humic substances from the floc structure into the bulk liquid. These findings are consistent with the results presented here.

The concentration of soluble biopolymers in the supernatant of the unsheared mixed liquor was stable between the beginning and end of the SOUR testing period, showing that the floc structure was stable during the experimental period. However, during the SOUR testing period for each sheared biomass (2 – 3 hours), a considerable amount of the polymers released during the shear process was reintegrated in the floc structure, either through reflocculation or uptake by the biomass, as indicated by a decrease in the soluble concentrations of these compounds in both sheared mixed liquors (Table 1). On average, 63%, 61% and 69% of the

released proteins, carbohydrates and DNA were presumably reintegrated in the floc structure. However, the concentrations of these biopolymers in the bulk liquid of the sheared biomasses at the end of the SOUR run period was still significantly above those in the bulk liquid of unsheared mixed liquor. The concentrations in the soluble phase of the sheared mixed liquors were statistically higher than in the unsheared sludge by a factor of 2.5 – 15x (paired two-tailed distribution t-Test, $p = 0.0023$), 1.2 – 3.1x (paired two-tailed distribution t-Test, $p = 0.0032$) and 1.2 – 2.2x (paired two-tailed distribution t-Test, $p = 0.00051$) for the protein, carbohydrate and DNA fractions, respectively. This result indicates that a significant amount of the EPS released during mechanical shear remained in the supernatant during the entire experimental period and, therefore, that the EPS matrix was not fully reestablished during the SOUR testing period for the sheared biomasses. The small fraction of humic acids released after shearing was either almost completely reintegrated into the floc structure or degraded by other means, as there was no significant difference (paired two-tailed distribution t-Test, $p = 0.87$) between the soluble humic acid concentration of the unsheared and the sheared mixed liquors at the end of the SOUR test periods. Overall, we believe that the partial reintegration of biopolymers into the floc structure during the SOUR test periods had only a small effect on the toxicity data, as it most likely impacted just the SOURs that were conducted towards the end of that period and the reintegration was not complete.

Mixed liquor shearing led to a reduction in floc size

The PSD of all mixed liquors used during the experiments was strongly impacted by mechanical shear, with a significant reduction in floc size occurring as a result (Figures 2 and 3B). An example of this effect is shown in Figure 3B, which depicts the PSD of sheared and unsheared mixed liquor for the experiment carried out with cyanide as the chemical toxin (set B). The PSD results for set B were notably consistent among different experiments, with the mean floc diameter for unsheared mixed liquor varying between 66 and 69 μm, 20 seconds of shearing resulting in a mean diameter between 33 and 37 μm and 60 seconds resulting in a floc mean diameter between 25 and 30 μm (Figure 2).

A similar reduction in floc size due to mechanical shear was observed for the set A experiments (data not shown), but for these experiments the source, unsheared mixed liquor had a larger median floc diameter (81-86 μm and 114-120 μm) than the biomass utilized during the

set B experiments (Figure 3A). The potential impact of these differences on the toxicity data is discussed below.

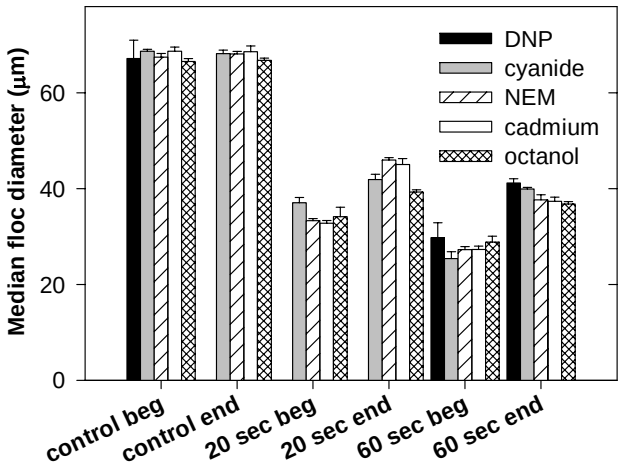

Figure 2 – Median floc diameters for unsheared (control) biomass and biomass sheared for 20 seconds and 60 seconds (data from set B). Error bars represent the standard deviation from six measurements, conducted on two independent samples. "beg" and "end" mean measurements conducted at the beginning and end of the SOUR run period, respectively, for each condition.

The PSD data also indicates to what extent reflocculation occurred after shearing, during the period that SOUR tests were being conducted (2 – 3 hours). The data show that some reflocculation occurred during this time period, which is consistent with the reintegration of biopolymers in the floc structure (set B, Figure 2 and 3B). In both the 20 second and 60 second-sheared biomasses, the reflocculation effect resulted in an increase of the floc mean diameter of 5 -15 μm, but both the PSD (example in Figure 3B) and the mean diameter (paired two-tailed distribution t-Test, $p = 3.9 \times 10^{-9}$) were still substantially different from that of the unsheared sludge. A reduction in floc size caused by mechanical shear followed by reflocculation under less turbulent conditions has been observed by others (Biggs and Lant, 2000; Biggs et al., 2003; Chaignon et al., 2002).

Mechanical shear did not impact biomass viability

The control SOURs (SOUR of mixed liquor with no added toxin) were also monitored in all the experiments, both at the beginning and end of each SOUR testing period, in order to test the viability and physiological stability of the biomass (data not shown). We concluded that, under the conditions of our study, the impact of mechanical shear on biomass viability was

negligible, and, consequently, the source of the released biopolymers during shearing was extracellular, confirming the EPS matrix as the origin of those materials.

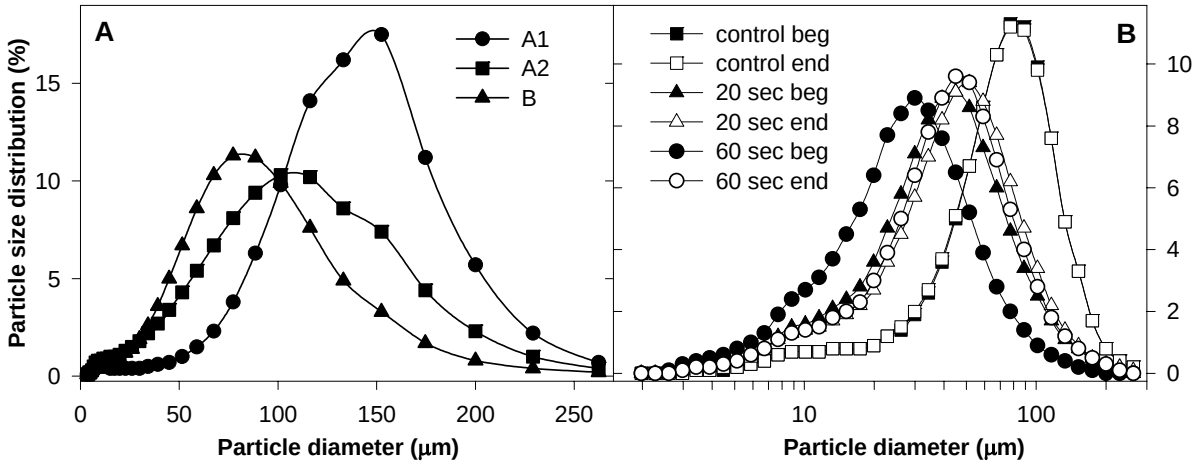

Figure 3 – PSD data obtained during the shear experiments. A – Example of PSD of unsheared mixed liquor from set A (A1 and A2) and set B (B). B – Example of PSD of unsheared (control) and sheared mixed liquor from the experiment conducted with cyanide as the chemical toxin (set B). "beg" and "end" mean measurements conducted at the beginning and end of the SOUR run period, respectively, for each condition.

A comparison between the control SOUR values measured at the beginning and end of each SOUR run period shows that the biomass was kept at a relatively stable physiological state within the entire experimental period, for all the experiments conducted (data not shown). This finding is corroborated by the solids analysis, which showed very little variation in the biomass concentration during each experiment (data not shown). In each experiment, the MLSS, MLVSS, MLTS and MLTVS concentrations had standard deviations that represented between 1.0% and 8.3% of the average of all the measurements taken during the experimental period. The MLVSS concentration of the biomasses used for the experiments varied between 1,350 and 1,800 mg/L. Although the control SOURs tended to remain stable during each experiment, the data show that between experiments the values varied, presumably due to daily changes in operational practices or wastewater loadings at the treatment plant from where the mixed liquor was retrieved.

More importantly, the control SOUR data obtained during the shear experiments indicate that the control SOURs for the unsheared mixed liquor was not different than the control SOURs of the sheared biomasses (data not shown, two-sample two-tailed distribution t-Test on set B data, $p = 0.57$), thereby indicating that biomass viability was not affected by shear stress.

Ultimately, this result implies that any differences in the toxicity data of sheared versus unsheared mixed liquor are not due to changes in biomass activity/viability. This finding is in accordance with previous observations (Henriques et al., 2005). In addition, using the same shear device and mixed liquor from the same facility, Muller (2001) also reported that the activity of glucose-6-phosphate dehydrogenase (G6PDH), an indicator of cell lysis, in sheared mixed liquor was not higher than that in unsheared mixed liquor. This is also consistent with the results of Biggs and Lant (2000), who did not observe G6PDH activity after sonicating mixed liquor samples for three minutes at an equivalent velocity gradient of approximately 18,000 s^{-1} (assuming a temperature of 4^{o}C).

SOUR inhibition was more pronounced in sheared mixed liquor than unsheared biomass for chemicals that have the potential to interact with EPS

The respiration inhibition data from the octanol (Figure 4) and cadmium (Figure 5) experiments suggest that floc structure plays a role in the susceptibility of activated sludge bacteria to these chemical toxins, as seen by an increase in inhibition for these chemicals when applied to the sheared relative to the unsheared mixed liquor, under at least one condition tested.

The shear experiment carried out with octanol (Figure 4) showed significant increased sensitivity of the sheared biomass to the toxin, relative to unsheared biomass, especially at the lower concentrations tested (difference as high as 20%). In addition, the biomass sheared for 60 seconds was slightly more inhibited (up to 8%) by octanol than the mixed liquor sheared for 20 seconds, showing a respiration inhibition pattern corresponding to the shear conditions applied. This result is important because octanol is a hydrophobic toxin that becomes easily associated with other hydrophobic substances. The utilization of octanol as the compound of reference to determine hydrophilic versus hydrophobic partition of other substances, which serves as an indicator of their hydrophobicity (the octanol/water partition coefficient, K_{ow}), shows that this is the case. Research by others has found that many hydrophobic substances are integrated in cell membranes, which have an hydrophobic lipid core (reviewed by Sikkema et al., 1995), and partitioning of 1-octanol into cell membranes have been suggested as the main mechanism of acclimation of *Tetrahymena pyriformis* to 1-octanol (Bearden et al., 1999). In addition, it has been shown that the internal hydrophobicity of a floc is one of the main forces that contributes to its strength and cohesiveness (Jorand et al., 1994; Jorand et al., 1998; Liao et al., 2001; Zita and Hermansson, 1997), hence it is reasonable to assume that octanol can easily establish

hydrophobic interactions within the floc matrix. Other hydrophobic compounds have been found to interact with activated sludge flocs (Finlayson et al., 1998). Therefore, if the EPS matrix is partially removed, for example through shear stress, bacterial cells and the cell membranes likely become more exposed and more susceptible to the toxic action of this type of toxin. Hence, the results from the octanol shear experiment support the hypothesis that floc structure plays a role in protecting bacterial cells from toxins that interact with the polymer matrix.

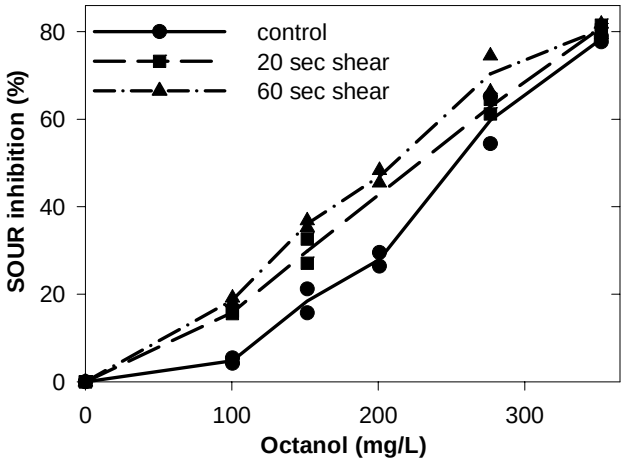

Figure 4 – Respiration inhibition of unsheared (control) and sheared mixed liquor by octanol (set B). Times of shearing are indicated. Data points represent actual SOUR values and lines represent the average of the SOUR duplicates (% inhibition relative to the control in both cases).

Heavy metals, such as cadmium, are known to establish strong interactions with activated sludge EPS (Guibaud et al., 2005; Jang et al., 2001; Liu et al., 2001). We have previously observed that in some cases more than 90% of the cadmium added to activated sludge cultures became associated with the solid fraction (Love et al., 2005). Therefore, we expected to see a similar result with cadmium to what we observed with octanol, since, by establishing interactions with the heavy metal, the presence of EPS in the floc might hinder access of the toxin to the bacterial cells. The SOUR of sheared mixed liquor was more strongly inhibited by cadmium than that of the unsheared sludge in two of the three experiments carried out with cadmium (Figure 5). While we observed an increased SOUR inhibition of as much as 20% between the unsheared and sheared biomasses, in the first two experiments (set A, Figures 5A and 5B), that difference was of only 6-7% in the later experiment (set B, Figure 5C), and was only seen for the highest concentrations tested.

The differences between the results obtained during the different experiments with cadmium could be explained by a number of factors. We believe that the factor that may have influenced the results more strongly was the particle size distribution of the source mixed liquor, which varied substantially between experiments. The median floc diameter of the source, unsheared mixed liquor used in the set B experiments (66-69 μm) was much smaller than in the previous set A experiments (81-86 μm for the experiment in Figure 5B and 114-120 μm for the experiment in Figure 5A), which implies that the differences, in terms of floc structure, between sheared and unsheared sludge, were not as significant in the set B experiment, making it more difficult to see any potential differences in toxicity between the different biomasses.

In summary, there was an increased toxicity response to octanol and cadmium by sheared mixed liquor when compared to unsheared biomass. Therefore, the results presented here agree with the idea that interactions between the floc EPS matrix and some chemical toxins provide the bacteria in the flocs with a protective mechanism, through which access of the toxin to the cells is more difficult. Such a protective mechanism has been previously observed in studies comparing cells embedded in biofilms in an EPS matrix with planktonic cells (free cells in suspension). Several studies indicate that the resistance of biofilms to antimicrobial agents, such as antibiotics and chlorine, is partially due to binding and/or reaction of EPS components to/with those agents, which provides protection to the bacteria within the biofilm (reviewed by Costerton et al., 1999; Mah and O'Toole, 2001; Stewart, 2002). A recent study comparing the toxicity of heavy metals to biofilm and planktonic cells of *P. aeruginosa* concluded that biofilm cells were up to 600 times more resistant to copper than planktonic cells (Teitzel and Parsek, 2003). The authors attributed this behavior to sequestration and/or complexation of the metal by EPS and cells at the biofilm/bulk liquid interface, which led to a protection mechanism of the cells at the lower levels of the biofilm, near the substratum. This is consistent with our data from the octanol and cadmium experiments.

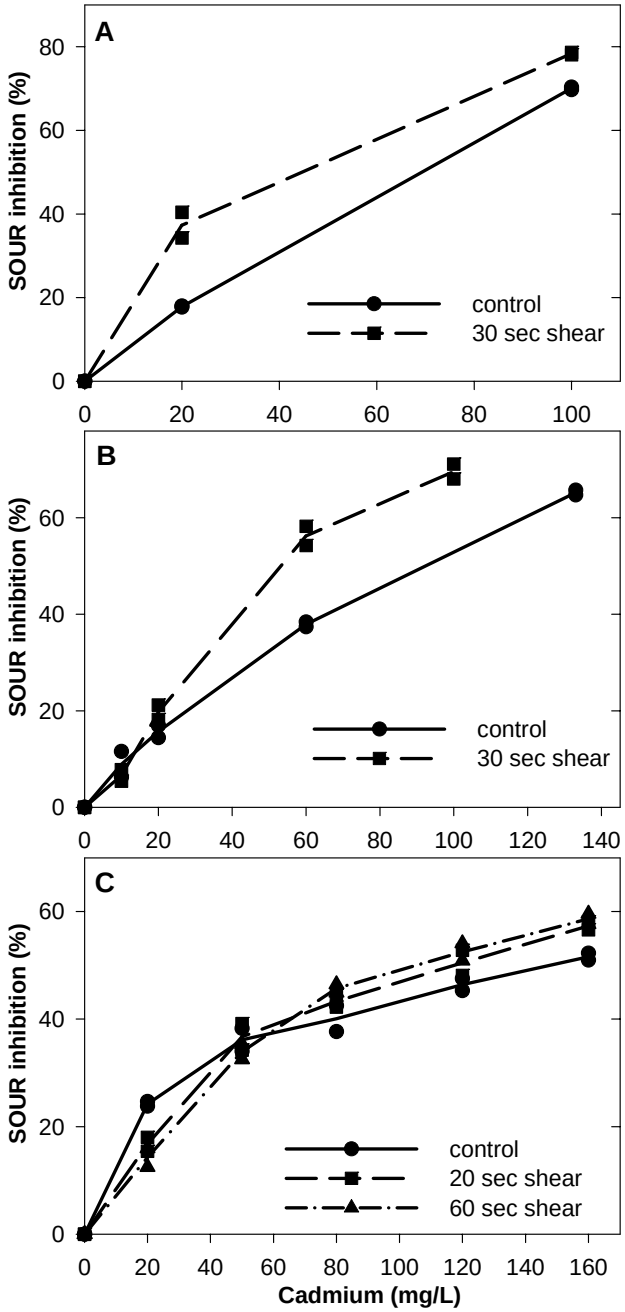

Figure 5 – Respiration inhibition of unsheared (control) and sheared mixed liquor by cadmium. Times of shearing are indicated. A and B – set A. C – set B. Data points represent actual SOUR values and lines represent the average of the SOUR duplicates (% inhibition relative to the control in both cases).

Interestingly, the protective effect of EPS is apparently not only associated with the quantity of EPS within the system, but also with the location of that matrix, since the presence of EPS in solution versus EPS in the floc matrix did not prevent the increased toxicity of the tested chemicals for the sheared sludge. Therefore, the protection mechanism is not only related to the

binding capacity of a system as a whole, but to the availability of binding sites in a location that protects the bacteria from being the target of the toxin. We hypothesize that this phenomenon may be related to the fact that floc size is another important factor dictating the net toxicity response. We have previously suggested that floc size plays a role in the differences in sensitivity to cadmium and DNP of membrane bioreactor mixed liquor and conventional activated sludge mixed liquor (Henriques et al., 2005).

SOUR inhibition was identical between sheared and unsheared mixed liquor for soluble, hydrophilic chemicals

The NEM and cyanide experiments (Figures 6 and 7) yielded results that are consistent with the hypothesis that floc structure is not an important factor controlling the toxicity response for chemicals that do not establish interactions with EPS. The difference in respiration inhibition produced by NEM and cyanide on the sheared biomasses compared to the unsheared mixed liquor was never greater than 7% (Figures 6 and 7). Both NEM and cyanide are highly soluble and hydrophilic compounds. Therefore, it is likely that they can easily diffuse through the floc without establishing interactions with the EPS matrix, making the existence of an EPS matrix "irrelevant" in terms of toxicity reaching the bacterial cells.

We also tested DNP as an additional toxin (Figure 8). DNP is not as hydrophobic as octanol (log K_{ow} = 1.54, from ATSDR, 2006a) and it has never been shown to establish interactions with the EPS matrix. In fact, we have evidence that DNP does not tend to sorb significantly to activated sludge flocs, from previous experiments in which we monitored the effects of DNP shock loads on activated sludge maintained in sequencing batch reactors (Love et al., 2005). However, DNP is an uncoupler of oxidative phosphorylation, which means that it has the ability to carry protons across biological membranes and, therefore, it can penetrate the hydrophobic core of the lipid bilayer and does have affinity for hydrophobic materials. In addition, we wanted to test a chemical with hydrophilic/hydrophobic characteristics that would be intermediate between octanol, and cyanide/NEM (which have much lower log K_{ow}, log K_{ow} (NaCN) = 0.44, from ATSDR, 2006b and log K_{ow} (NEM) = 0.58, from USNLM, 2004).

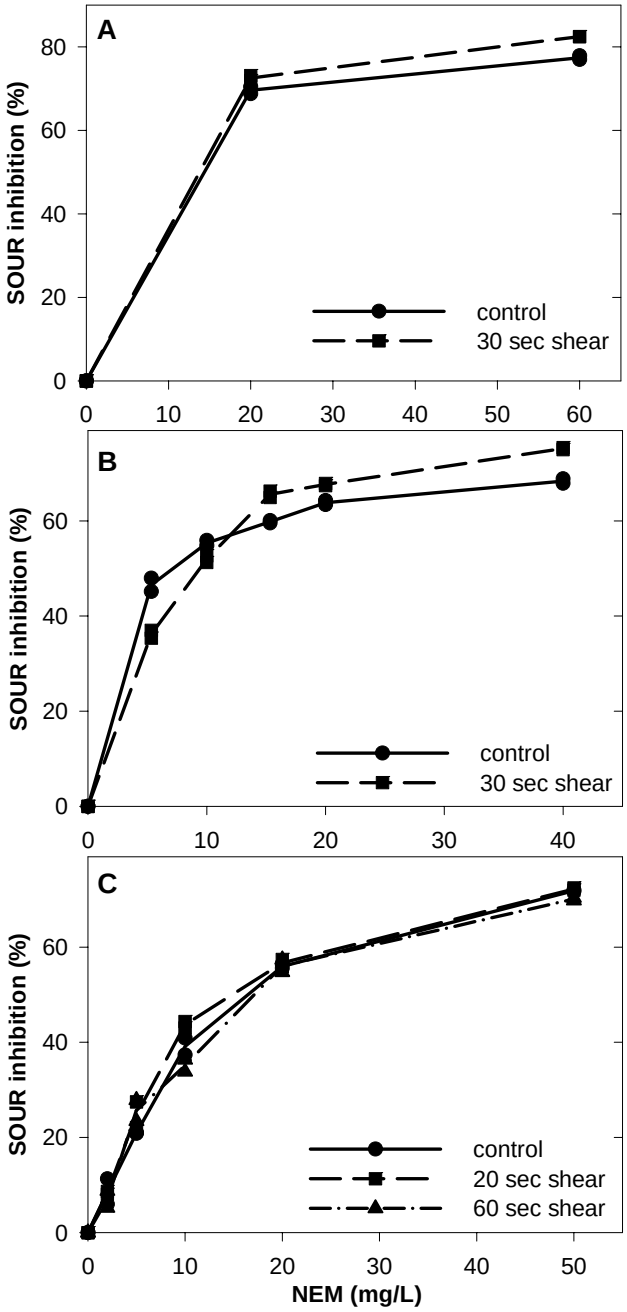

Figure 6 – Respiration inhibition of unsheared (control) and sheared mixed liquor by NEM. Times of shearing are indicated. A and B – set A. C – set B. Data points represent actual SOUR values and lines represent the average of the SOUR duplicates (% inhibition relative to the control in both cases).

The results with DNP were similar to those obtained with the cadmium experiments, except that the effect of increased toxicity of the chemical in sheared sludge was much more subtle. While for the first experiment (Figure 8A) there was a slight increase in the sensitivity of

sheared activated sludge compared to the unsheared biomass (up to 9% increase), when we repeated the experiment there was virtually no difference in respiration inhibition for the different biomasses tested (Figure 8B). Since DNP possesses intermediate properties regarding the potential to interact with the EPS matrix, these results corroborate our hypothesis that EPS may function as a barrier to chemicals that interact with the polymer matrix (octanol and cadmium), but not to chemicals that can freely diffuse through that matrix (NEM and cyanide).

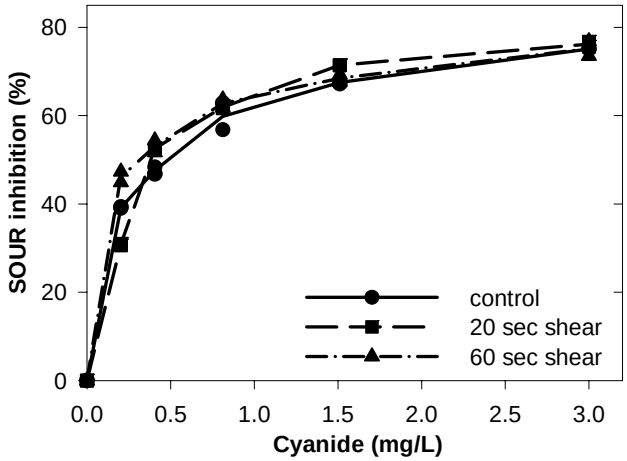

Figure 7 – Respiration inhibition of unsheared (control) and sheared mixed liquor by cyanide (set B). Times of shearing are indicated. Data points represent actual SOUR values and lines represent the average of the SOUR duplicates (% inhibition relative to the control in both cases).

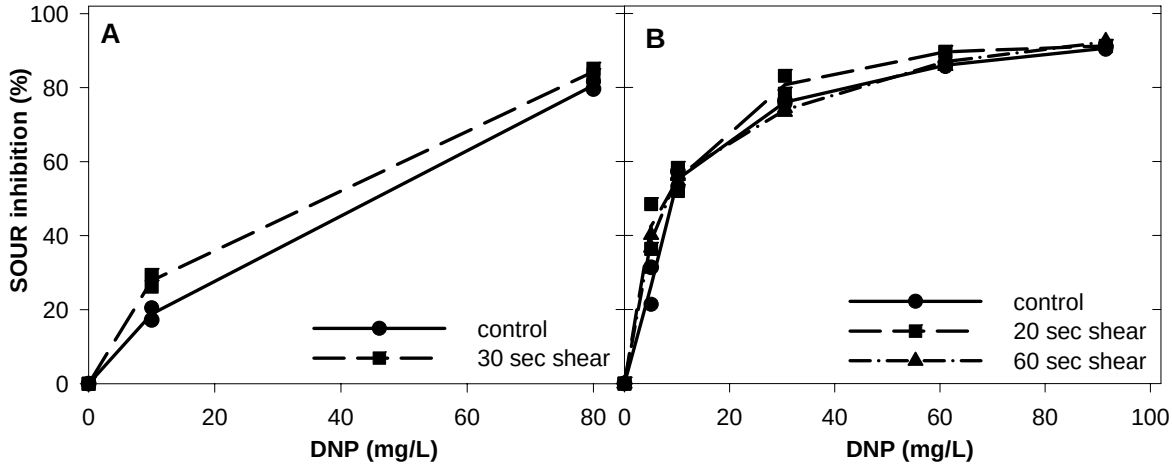

Figure 8 – Respiration inhibition of unsheared (control) and sheared mixed liquor by DNP. Times of shearing are indicated. A – set A. B – set B. Data points represent actual SOUR values and lines represent the average of the SOUR duplicates (% inhibition relative to the control in both cases).

Environmental significance

Taken together, the results obtained from the shear studies with all the toxins provide insight into the role of floc structure in determining the toxicity response of activated sludge to different chemicals. We suggest that both the EPS matrix and floc size are factors that contribute to that response. The cadmium experiments indicate floc size as an important factor determining the SOUR inhibition response. Also, the fact that EPS was maintained in the supernatant of the flocs in the sheared sludge, and that differences in toxicity were still seen between sheared and unsheared sludges for octanol and cadmium, corroborates the idea that floc size plays a role in defining the sensitivity of activated sludge cultures to toxic chemicals. However, because with some chemicals the sensitivity of activated sludge increased when the flocs were sheared and with other toxins that did not occur, it appears that floc size is not the only factor that affects the respiration inhibition response. If that was the case, then a similar effect of increased SOUR inhibition should be seen for all the chemicals tested, since the floc size was reduced in all the experiments due to shear. Rather, the characteristics of the toxin, such as solubility, hydrophobicity/hydrophilicity, tendency to become floc-associated and mode of action seem to influence the inhibitory response and the effects at the floc level. Furthermore, these characteristics directly affect the interactions that are established between the toxin and the EPS matrix, and since the EPS matrix was also significantly affected by mechanical shearing, we believe that the presence of the EPS matrix also contributes to reduce the toxicity of some chemicals to the bacterial cells within the flocs.

The results reported in this study contribute to a better understanding of the factors that control the toxicity response of activated sludge to a wide range of chemical toxins. We believe that a better understanding of the toxicity mechanisms occurring within activated sludge systems and the factors that affect those mechanisms may contribute to the development of more efficient operational practices to both create robust wastewater treatment systems that can better sustain the impacts of shock loads of chemical toxins, and provide operators with tools to minimize the effects of such shock loads on the treatment process.

Conclusions

Based on the results obtained in this study, the main conclusions from the research work presented here are as follows:

- EPS in activated sludge flocs protect the bacterial community against chemicals that establish interactions with the polymer matrix, by impeding access of the chemical to the bacterial cells. This effect was seen with both cadmium and octanol, through a decrease in the respiration rate of sheared biomass versus unsheared biomass.
- Floc size is an important parameter when evaluating the toxicity of specific chemicals to activated sludge bacteria, but does not explain *per se* the toxicity responses observed for sheared and unsheared mixed liquors to cadmium, octanol, cyanide, NEM and DNP.
- Floc structure and size do not play a role in the toxicity response of activated sludge to hydrophilic, soluble toxins, such as cyanide and NEM.

Acknowledgments

Primary funding for this project was provided by the Water Environment Research Foundation, project 01-CTS-2. I. D. S. Henriques received a PhD fellowship (SFRH/BD/4689/2001) from the FCT (Fundação para a Ciência e a Tecnologia), Portugal. We would like to acknowledge the staff and undergraduate assistants at Virginia Tech for their help in completing the experiments presented here, and the staff at the Blacksburg-Virginia Tech Sanitation Authority Wastewater Treatment Plant for allowing us to access the plant and to get mixed liquor samples.

References

Agency for Toxic Substances and Disease Registry. (2006a) *Toxicological Profile for Dinitrophenols*. http://www.atsdr.cdc.gov/toxprofiles/tp64.html. Accessed 04-09-06.

Agency for Toxic Substances and Disease Registry. (2006b) *Toxicological Profile for Cyanide*. http://www.atsdr.cdc.gov/toxprofiles/tp8.html. Accessed 04-09-06.

American Public Health Association, American Water Works Association, Water Environment Federation (1998) *Standard Methods for the Examination of Water and Wastewater*, 20th ed. Washington, DC.

Andreadakis, A.D. (1993) Physical and Chemical Properties of Activated Sludge Floc. *Water Res.* **27:** 1707-1714.

Bearden, A.P., Sinks, G.D., Vaes, W.H.J., Ramos, E.U., Hermens, J.L.M., and Schultz, T.W. (1999) Bioavailability, Biodegradation, and Acclimation of *Tetrahymena pyriformis* to 1-Octanol. *Ecotox. Environ. Safe.* **44:** 86-91.

Biggs, C., Lant, P., and Hounslow, M. (2003) Modeling the Effect of Shear History on Activated Sludge Flocculation. *Water Sci. Technol.* **47:** 251-257.

Biggs, C.A. and Lant, P.A. (2000) Activated Sludge Flocculation: On-Line Determination of Floc Size and the Effect of Shear. *Water Res.* **34:** 2542-2550.

Brunk, C.F., Jones, K.C., and James, T.W. (1979) Assay for Nanogram Quantities of DNA in Cellular Homogenates. *Anal. Biochem.* **92:** 497-500.

Chaignon, V., Lartiges, B.S., El Samrani, A., and Mustin, C. (2002) Evolution of Size Distribution and Transfer of Mineral Particles Between Flocs in Activated Sludges: An Insight Into Floc Exchange Dynamics. *Water Res.* **36:** 676-684.

Costerton, J.W., Lewandowski, Z., Caldwell, D.E., Korber, D.R., and Lappinscott, H.M. (1995) Microbial Biofilms. *Annu. Rev. Microbiol.* **49:** 711-745.

Costerton, J.W., Stewart, P.S., and Greenberg, E.P. (1999) Bacterial Biofilms: A Common Cause of Persistent Infections. *Science* **284:** 1318-1322.

Dignac, M.F., Urbain, V., Rybacki, D., Bruchet, A., Snidaro, D., and Scribe, P. (1998) Chemical Description of Extracellular Polymers: Implication on Activated Sludge Floc Structure. *Water Sci. Technol.* **38:** 45-53.

Dubois, M., Gilles, K.A., Hamilton, J.K., Rebers, P.A., and Smith, F. (1956) Colorimetric Method for Determination of Sugars and Related Substances. *Anal. Chem.* **28:** 350-357.

Farrell, A. and Quilty, B. (2002) Substrate-Dependent Autoaggregation of *Pseudomonas putida* CP1 During the Degradation of Mono-Chlorophenols and Phenol. *J. Ind. Microbiol. Biot.* **28:** 316-324.

Finlayson, J.C., Liao, B., Droppo, I.G., Leppard, G.G., and Liss, S.N. (1998) The Relationship Between the Structure of Activated Sludge Flocs and the Sorption of Hydrophobic Pollutants. *Water Sci. Technol.* **37:** 353-357.

Frølund, B., Griebe, T., and Nielsen, P.H. (1995) Enzymatic Activity in the Activated Sludge Floc Matrix. *Appl. Microbiol. Biot.* **43:** 755-761.

Frølund, B., Palmgren, R., Keiding, K., and Nielsen, P.H. (1996) Extraction of Extracellular Polymers From Activated Sludge Using a Cation Exchange Resin. *Water Res.* **30:** 1749-1758.

Guibaud, G., Comte, S., Bordas, F., Dupuy, S., and Baudu, M. (2005) Comparison of the Complexation Potential of Extracellular Polymeric Substances (EPS) Extracted from Activated Sludges and Produced by Pure Bacteria Strains, for Cadmium, Lead and Nickel. *Chemosphere* **59:** 629-638.

Henriques, I.D.S., Kelly, R.T., Dauphinais, J.L., and Love, N.G. (in review) Activated Sludge Inhibition by Chemical Stressors: A Comprehensive Study. *Water Environ. Res.*

Henriques, I.D.S., Kelly, R.T., and Love, N.G. (in review) Short-Term versus Long-Term Respiration Inhibition in Nitrifying and Non-Nitrifying Activated Sludge Exposed to Chemical Toxins. *Water Environ. Res.*

Henriques, I.D.S., Holbrook, R.D., Kelly, R.T., and Love, N.G. (2005) The Impact of Floc Size on Respiration Inhibition by Soluble Toxicants – A Comparative Investigation. *Water Res.* **39:** 2559-2568.

Higgins, M.J. and Novak, J.T. (1997a) The Effect of Cations on the Settling and Dewatering of Activated Sludges: Laboratory Results. *Water Environ. Res.* **69:** 215-224.

Higgins, M.J. and Novak, J.T. (1997b) Characterization of Exocellular Protein and Its Role in Bioflocculation. *J. Environ. Eng.-ASCE* **123:** 479-485.

Jang, A., Kim, S.M., Kim, S.Y., Lee, S.G., and Kim, I.S. (2001) Effect of Heavy metals (Cu, Pb, and Ni) on the Compositions of EPS in Biofilms. *Water Sci. Technol.* **43:** 41-48.

Jorand, F., Boue-Bigne, F., Block, J.C., and Urbain, V. (1998) Hydrophobic/Hydrophilic Properties of Activated Sludge Exopolymeric Substances. *Water Sci.Technol.* **37:** 307-315.

Jorand, F., Guicherd, P., Urbain, V., Manem, J., and Block, J.C. (1994) Hydrophobicity of Activated Sludge Flocs and Laboratory-Grown Bacteria. *Water Sci. Technol.* **30:** 211-218.

Jorand, F., Zartarian, F., Thomas, F., Block, J.C., Bottero, J.Y., Villemin, G., Urbain, V., and Manem, J. (1995) Chemical and Structural (2D) Linkage Between Bacteria Within Activated Sludge Flocs. *Water Res.* **29:** 1639-1647.

Leriche, V., Briandet, R., and Carpentier, B. (2003) Ecology of Mixed Biofilms Subjected Daily to a Chlorinated Alkaline Solution: Spatial Distribution of Bacterial Species Suggests a Protective Effect of One Species to Another. *Environ. Microbiol.* **5:** 64-71.

Liao, B.Q., Allen, D.G., Droppo, I.G., Leppard, G.G., and Liss, S.N. (2001) Surface Properties of Sludge and Their Role in Bioflocculation and Settleability. *Water Res.* **35:** 339-350.

Liss, S.N., Liao, B.Q., Droppo, I.G., Allen, D.G., and Leppard, G.G. (2002) Effect of Solids Retention Time on Floc Structure. *Water Sci. Technol.***46:** 431-438.

Liu, Y., Lam, M.C., and Fang, H.H.P. (2001) Adsorption of Heavy Metals by EPS of Activated Sludge. *Water Sci. Technol.* **43:** 59-66.

Love, N.G., Henriques, I.D.S., and Kelly, R.T. (2005) *Upset Early Warning Systems for Biological Treatment Processes - Source and Effect Relationships*. Report No. 01-CTS-2. Water Environment Research Foundation. Alexandria, VA.

Lowry, O.H., Rosebrough, N.J., Farr, A.L., and Randall, R.J. (1951) Protein Measurement with the Folin Phenol Reagent. *J. Biol. Chem.* **193:** 265-275.

Mah, T.F.C. and O'Toole, G.A. (2001) Mechanisms of Biofilm Resistance to Antimicrobial Agents. *Trends Microbiol.* **9:** 34-39.

Morgan-Sagastume, F. and Allen, D.G. (2005) Activated Sludge Deflocculation under Temperature Upshifts from 30 to 45 Degrees C. *Water Res.* **39:** 1061-1074.

Muller, C.D. (2001) High-Intensity Shear as a Wet Sludge Disintegration Technology and a Mechanism for Floc Structure Analysis. M.S. Thesis. Virginia Polytechnic Institute and State University. Blacksburg, VA.

Scuras, S., Daigger, G.T., and Grady, C.P.L. (1998) Modeling the Activated Sludge Floc Microenvironment. *Water Sci. Technol.* **37:** 243-250.

Sikkema, J., Debont, J.A.M., and Poolman, B. (1995) Mechanisms of Membrane Toxicity of Hydrocarbons. *Microbiol. Rev.* **59:** 201-222.

Snidaro, D., Zartarian, F., Jorand, F., Bottero, J.Y., Block, J.C., and Manem, J. (1997) Characterization of Activated Sludge Flocs Structure. *Water Sci. Technol.* **36:** 313-320.

Stewart, P.S. (2002) Mechanisms of Antibiotic Resistance in Bacterial Biofilms. *Int. J. Med. Microbiol.* **292:** 107-113.

Teitzel, G.M. and Parsek, M.R. (2003) Heavy Metal Resistance of Biofilm and Planktonic *Pseudomonas aeruginosa*. *Appl. Environ. Microbiol.* **69:** 2313-2320.

U.S. National Library of Medicine, Specialized Information Services, ChemIDplus Advanced. (2004) *ChemIDplus Advanced Record, NAME*: *ETHYLMALEIMIDE*. http://chem.sis.nlm.nih.gov/chemidplus/chemidheavy.jsp. Accessed 04-09-06.

Wilen, B.M., Jin, B., and Lant, P. (2003) Relationship Between Flocculation of Activated Sludge and Composition of Extracellular Polymeric Substances. *Water Sci. Technol.* **47:** 95-103.

Wilen, B.M., Keiding, K., and Nielsen, P.H. (2000a) Anaerobic Deflocculation and Aerobic Reflocculation of Activated Sludge. *Water Res.* **34:** 3933-3942.

Wilen, B.M., Nielsen, J.L., Keiding, K., and Nielsen, P.H. (2000b) Influence of Microbial Activity on the Stability of Activated Sludge Flocs. *Colloid. Surface. B* **18:** 145-156.

Zartarian, F., Mustin, C., Bottero, J.Y., Villemin, G., Thomas, F., Ailleres, L., Champenois, M., Grulois, P., and Manem, J. (1994) Spatial Arrangement of the Components of Activated Sludge Flocs. *Water Sci. Technol.* **30:** 243-250.

Zita, A. and Hermansson, M. (1997) Effects of Bacterial Cell Surface Structures and Hydrophobicity on Attachment to Activated Sludge Flocs. *Appl. Environ. Microbiol.* **63:** 1168-1170.

Chapter 5. Metabolic Footprinting: A New Approach to Identify Physiological Changes in Complex Microbial Communities upon Exposure to Toxic Chemicals

Inês D. Henriques [1], Diana S. Aga [2], Pedro Mendes [3], and Nancy G. Love [1,4]*

[1] Department of Civil and Environmental Engineering, Virginia Tech, [2] Department of Chemistry, State University of New York at Buffalo, [3] Virginia Bioinformatics Institute, Virginia Tech, and [4] Department of Biological Sciences, Virginia Tech

* Corresponding Author Contact Information: Address – Department of Civil and Environmental Engineering, Virginia Tech, 418 Durham Hall, Blacksburg, VA 24060, E-mail – nlove@vt.edu, Phone – (540)231-3980, Fax – (540)231-7916

Abstract

The impact of cadmium, 2,4-dinitrophenol (DNP) and N-ethyl-maleimide (NEM) shock loads on the composition of the soluble fraction of activated sludge mixed liquor was analyzed by liquid chromatography-mass spectrometry (LC-MS). Fresh mixed liquor was divided in four different batches and subjected to different conditions: no addition of chemical (control) and spike additions of cadmium, DNP or NEM. The results indicate that there was a significant release of biomolecules (proteins, carbohydrates and humic acids) from the floc structure into the bulk liquid due to chemical stress. Discriminant function analysis with genetic algorithm variable selection (GA-DFA) was able to differentiate the samples from the different reactors, thereby indicating that the footprints of the soluble phase generated by LC-MS were different for the four conditions tested and, therefore, toxin-specific. These footprints, thus, contain information about specific biomolecular differences between the samples, and we found that only a limited amount of m/z (mass to charge) ratios from the mass spectra data (which originally contained information for 1609 m/z ratios) was needed to differentiate between the control and each chemical toxin-derived samples. The discriminant m/z ratios were also toxin-specific. In addition, since the experiments were conducted with mixed liquor from four distinct wastewater treatment plants, the discriminating m/z ratios may potentially be used as universal stress biomarkers in activated sludge systems. These results are promising and indicate that LC-MS may be used for the discovery of activated sludge stress biomarkers to allow the development of new toxin detection technologies for upset early warning.

Introduction

Biological wastewater treatment systems rely on a complex microbial consortium structurally organized in biological flocs to carry out the degradation of soluble and insoluble components present in raw sewage. These systems are susceptible to toxic shock loads of industrial chemicals, which can impact the treatment efficiency severely (Love and Bott, 2000). When challenged with a toxin, activated sludge communities may undergo different physiological and structural modifications that can result in macroscopic effects such as floc disintegration or deflocculation (Neufeld, 1976; Bott and Love, 2001; Bott and Love, 2002), increase in effluent soluble chemical oxygen demand (COD) (Henriques et al., in review) and inhibition of nitrification (Khin et al., 2002; Kelly et al., 2004; Kim et al., 2006). Experiments conducted in our laboratory showed that exposure of mixed liquor to different chemical toxins resulted in an increase of the soluble concentration of COD in the effluent of toxin-exposed reactors (Henriques et al., in review; Love et al., 2005). Although we were not certain about the origin of the increased soluble COD, we hypothesized that it resulted from the release of biofloc-associated compounds due to specific mechanisms occurring upon exposure of the bioflocs to the chemical toxins. Furthermore, we hypothesized that the materials released from activated sludge biological flocs during chemical stress events were toxin-specific, as the mechanisms responsible for the release effect were likely dependent on: 1) the type of physical/chemical interactions established between the toxin and the floc extracellular polymeric substances (EPS) in which the bacteria are embedded, and 2) the mode of action of the toxin and stress responses elicited by the bacterial populations within the flocs. The analysis of the soluble materials in the supernatant of chemically stressed mixed liquor could, therefore, reveal important physiological and structural changes induced by the stress condition.

Metabolic footprinting consists of analyzing and comparing the "exome", "exometabolome" or extracellular matrix (spent culture medium in the case of bacterial cultures) produced under different conditions (Dunn and Ellis, 2005; Kell et al., 2005; Villas-Boas et al., 2005). The application of metabolic footprinting to activated sludge communities and other complex microbial communities has several advantages over analyzing the intracellular materials (metabolic fingerprinting), as it does not require complex extraction and quenching/preservation methods and allows analysis and comparison of samples taken under different environmental conditions. In addition, analyzing aggregate biomolecules released upon exposure to stress, such

as total protein and total carbohydrate, can yield important information (Henriques and Love, in preparation), but a more detailed analysis of these biomolecules can provide a "footprint" of the different compounds that are released under stress conditions, which can potentially provide much more information, both quantitative and qualitative. For example, distinct footprint patterns can relate to the nature of the chemical causing the stress and the extent to which selected bands in the footprint are expressed may reveal dose:response relationships. In addition, specific compounds within the footprints can be identified and used as bacterial stress biomarkers, which can potentially lead to the development of sensing technologies for upset early warning. Furthermore, using an aggregate footprinting method allows one to use the method on indigenous activated sludge cultures, and does not rely upon knowing specifics about the composition of the community.

Metabolic footprinting has been used to differentiate between different physiological states of wild type yeast and different yeast single-gene deletion mutants (Allen et al., 2003), to discriminate between different *Escherichia coli* tryptophan mutants (Kaderbhai et al., 2003) and to distinguish between modes of action of several antifungal substances on yeast cells (Allen et al., 2004). Similarly, we believe that the application of metabolic footprinting to compare changes in extracellular metabolite patterns in response to toxin exposure can be a powerful technique to detect physiological changes in activated sludge populations that correlate with specific modes of process deterioration.

A literature search revealed that metabolic footprinting has not yet been applied to compare complex environmentally-relevant microbial communities exposed to different environmental conditions. The few examples found in the literature refer to studies that use a broader definition of the term metabolic fingerprinting, which includes carbon utilization profiles by bacteria as metabolic fingerprints (Ahmed et al., 2005; Baudoin et al., 2001). One study of activated sludge EPS used size exclusion chromatography and Fourier transform infrared spectroscopy (FT-IR) to characterize and compare EPS from different wastewater treatment plants and different operational conditions (Garnier et al., 2005). EPS fingerprints were fairly stable with time when normal operation occurred, but changed dramatically when upset events causing deflocculation of the biomass took place, shifting to smaller molecules (Garnier et al., 2005). This study shows that alterations at the level of EPS composition occur in response to stress events in activated sludge communities, and that those alterations may be identified

through fingerprints generated through a spectroscopic technique. However, the soluble phase of the mixed liquor (supernatant) was not analyzed during the study.

The objective of this study was to generate metabolic footprints of activated sludge mixed liquor subjected to cadmium, N-ethyl-maleimide (NEM) and 2,4-dinitrophenol (DNP) shock loads and compare them to control conditions, using liquid chromatography – mass spectrometry (LC-MS) techniques. Cadmium and NEM are electrophilic (thiol-reactive) chemicals, which have been shown to cause strong deflocculation events of activated sludge (Bott and Love, 2002; Henriques et al., in review), while DNP is an uncoupler of oxidative phosphorylation, that we found to produce moderate to low increases in effluent total suspended solids (TSS) and soluble COD (Henriques et al., in review) in the effluent of sequencing batch reactors (SBRs). In this study, we identify m/z (mass to charge) ratios for soluble materials that are released from activated sludge flocs during an upset event, and determine those ratios that occur most often in similarly-shocked mixed liquors from four wastewater treatment plants. Ultimate identification of these compounds may lead to the development of methods that allow fast and reliable identification of toxins that cause upset events, and the development of early warning tools that can minimize or eliminate the impact of toxins in biological treatment systems.

Materials and Methods

Batch experiments with activated sludge mixed liquor. A batch experiment was designed in order to generate samples for metabolic footprinting of activated sludge mixed liquor under chemical stress conditions. Mixed liquor from full-scale activated sludge facilities was obtained fresh and immediately transported to the laboratory. To stabilize the growth state of the biomass, the mixed liquor was aerated and fed synthetic wastewater composed of acetate, glycerol, nitrogen (as NH_4Cl) and phosphorous (as Na_2HPO_4) for a period of at least three hours before the start of an experiment. The synthetic wastewater simulated the organic load of the primary effluent of the plant from which the mixed liquor had been retrieved; acetate and glycerol were chosen as the carbon sources because they are readily biodegradable and do not interfere with protein, humic acid and polysaccharide analyses. Nitrogen and phosphorous concentrations in the feed were determined based on the amounts stoichiometrically required for biomass growth given the organic load, an assumed growth yield of 0.6 mg biomass COD formed/mg COD

removed, and a theoretical biomass composition given by $C_{60}H_{87}O_{23}N_{12}P$ (Grady et al., 1999). The synthetic wastewater concentration was high so that the total volume of feed applied was negligible (less than 5%) relative to the volume of mixed liquor. After the stabilization period, four 1.5 L aliquots of the source mixed liquor were measured into separate containers. These four reactors were aerated and fed independently through the use of a syringe pump. The synthetic wastewater used to feed the reactors was prepared in the same manner as the feed used during the stabilization period, in order to maintain the same load of nutrients to the biomass during the entire experimental period. At time zero, three of the reactors were spiked with pre-selected amounts of cadmium (100 mg/L Cd added as $CdCl_2$), DNP (20 mg/L) and NEM (15 mg/L). The fourth reactor was a control, to which no toxin was added. Sampling from all the reactors occurred within 5 minutes of toxin addition (< 5 minutes), 45 minutes, 3 hours and 5 hours after the chemical shock. For replication purposes, this batch experiment was conducted twice, with two different batches of mixed liquor from the same plant collected on different days (48 hours apart). Four different mixed liquors were tested from four different wastewater treatment plants, resulting in a total of eight experiments.

Sample preparation for metabolic footprinting. Samples for the analysis of the components in the soluble fraction were obtained by centrifuging mixed liquor for 15 minutes at 4°C and 12,000xg, and filtering the centrate through 0.45 μm nitrocellulose filters. The samples were frozen (-20°C) immediately after sample preparation and later freeze dried.

LC-MS methodology for metabolic footprinting. The freeze dried samples were reconstituted in 1 mL of a 90% H_2O/10% methanol (v/v) mixture and centrifuged for 10 minutes at 3500xg (room temperature) to separate the clear supernatant from the remaining precipitate. The reconstituted samples were transferred into 2 mL vials and loaded in the LC autosampler, which was maintained at 4°C during the analysis. The samples were analyzed using an LCQ Advantage™ ion trap mass spectrometer connected to a Surveyor LC system (Thermo Finnigan, San Jose, CA, USA). The separation was performed starting with a mobile phase of 100% water (with 0.3% formic acid, held for 3 minutes), and was changed with a linear gradient to a final composition of 95% acetonitrile and 5% water (with 0.3% formic acid) over 25 minutes. This composition was maintained for an additional 2 minutes before the mobile phase was returned to the initial conditions. The column used was a Thermo Hypersil-Keystone (Bellefonte, PA, USA) BetaBasic C18 column (100 x 2.1 mm internal diameter with 3 μm particle size). The flow rate

was 200 μL per minute, the column temperature was 30°C, and the injection volume was 20 μL. The ion trap mass spectrometer was equipped with electrospray ionization and was operated in positive ion mode. The capillary temperature was 225°C, capillary voltage was 10 V and the spray voltage was 5.0 kV for all applications. Nitrogen was used as a sheath gas at a flow rate of 30 arbitrary units, and the auxiliary gas was injected at a flow rate of 15 arbitrary units. These parameters were optimized for maximum signal of two reference standards: a low molecular weight standard, caffeine ($[M+H]^+$ of 195), and a higher molecular weight standard, C^{13} labeled Acetyl Co-A ($[M+H]^+$ of 812). Blanks consisting of nanopure water were also analyzed to detect potential carry over or instrument contamination. The mass spectrometer was setup to detect m/z ratios in the range 150-2000. The LCQ automatic gain control was used to determine ion injection time in the trap, with a maximum limit at 300 ms. In order to avoid systematic errors related to cross-contamination or sample carry-over, the order in which the samples were analyzed was randomized among different treatment plants, times of sampling, and types of chemical shock.

Chemical analyses. Mixed liquor suspended solids (MLSS) and mixed liquor volatile suspended solids (MLVSS) analyses were conducted in triplicate at time < 5 minutes, 3 hours and 5 hours after the shock, for all the reactors, using the method outlined in Standard Methods (APHA et al., 1998). Proteins, polysaccharides and humic acids in the soluble phase were analyzed in triplicate on samples stored at -20^{o}C, which were previously prepared as the samples for metabolic footprinting. Polysaccharides were analyzed by the Dubois method (Dubois et al., 1956), while protein and humic substances were analyzed by the Lowry method (Lowry et al., 1951) with the modifications proposed by Frølund et al. (1995).

Alkaline phosphatase (AP) assays. AP is a periplasmic enzyme that has been used as a sensitive indicator of cytoplasmic membrane damage in activated sludge biomass (Bott and Love, 2002). Cell lysis due to chemical shock was evaluated through AP assays following the method by Bott and Love (2002). The assays were conducted on the soluble fraction and mixed liquor solids (mixed liquor cell-free extracts, positive control), at 45 minutes, 3 hours and 5 hours after toxin addition, for all the reactors. AP assays were conducted for at least one of the experiments with mixed liquor from a specific treatment plant, a total of five times out of eight experiments. Statistical analysis was conducted for chemical analyses and AP assays data using

Student's t-Tests with two-tailed distributions. The significance level used to evaluate statistical significance was $\alpha = 0.05$.

Pre-processing of MS data. Given the complexity and vast amounts of data produced by the LC-MS analysis, multivariate statistical methods had to be applied in order to convert the data into useful information, and to show trends that could be imperceptible otherwise. Since only the mass spectral data were used in the statistical analysis, there was no need for chromatographic alignment of data. Prior to the application of the statistical methods, the data were processed in the following manner: 1) for each sample, only the m/z data observed within the time interval 4-21 minutes were used to eliminate unretained matrix in the void volume and discard the highly hydrophobic matrix that comes out after column wash; 2) after analyzing the data from the nanopure water blanks, low molecular weight compounds (m/z range of 150-350) were excluded from the samples' data set due to high signal-to-noise (S/N) ratios; in addition, m/z ratios in the nanopure water blanks with an intensity greater than 3x the noise level in those blanks (m/z range 350-2000) were also excluded from the samples' data set, a total of 42 m/z ratios; 3) following previously reported methodologies (Allen et al., 2003; Kaderbhai et al., 2003), each LC-MS array was reduced into a single MS vector by summing the intensities of a given m/z ratio over the entire run period (4-21 minutes); additionally, each MS vector was simplified by reducing the intensity data to the nearest integer m/z ratio; this resulted in a single vector with 1609 values, with m/z range 350-2000, for each sample; the reduction of the data to a single MS vector and integer m/z ratios was performed automatically by the LC-MS software Excalibur™, Home Page version 1.3 (Thermo Finnigan, San Jose, CA, USA); 4) finally, prior to statistical analysis, each MS vector was normalized to the total intensity for that vector, so that different spectra could be compared quantitatively (Allen et al., 2003; Kaderbhai et al., 2003).

Statistical analysis of MS data. The mass spectra of the soluble phase of all reactors contained several hundreds of peaks, which made visual interpretation of the data virtually impossible. In order to detect the main differences between the shocked and control samples, we applied multivariate statistical analysis methods to the pre-processed data generated through LC-MS. Specifically, we used a multivariate statistical method called discriminant function analysis (DFA), coupled with genetic algorithm (GA) variable selection (GA-DFA). DFA is a supervised statistical clustering method (Manly, 1994). This means that the class to which a specific sample belongs to is known *a priori* and the method uses that information to generate a model that tries

to pair the input information with the target group that the sample belongs to, thus providing better clustering of the data (Goodacre et al., 2004). This *a priori* information is, therefore, used to minimize within-group variance and maximize between-group variance. According to Jarvis and Goodacre (2005), unlike other multivariate methods such as principal component analysis (PCA), GA-DFA can be used to select a limited number of variables (m/z ratios) from a full data set, with the goal of formulating robust models that give an indication of those variables that are most important to discriminate among the different classes of samples being analyzed. These models are expressed as a combination of distinct discriminant functions (DFs), which are linear combinations of the variables that serve as the input to the analysis. In the case of the GA-DFA applied in this study, these variables (m/z ratios) are selected by the GA component, which reduces the initial 1609 m/z ratios to a limited number optimized prior to analysis (less than 50 in our study). The optimization is made by finding the minimum number of variables that results in a DFA model with 100% sample classification accuracy. The number of DFs generated by DFA is the number of classes minus one. Because genetic algorithms generate a solution to a problem that has many possible solutions, and do this through a stochastic approach, there is a need for running GA-DFA multiple times in order to identify the variables that are most often selected and, therefore, that are of biological importance. This Monte Carlo approach then ranks each of the variables (m/z ratios) according to the number of times they were used in a single classification (a single run of the GA-DFA algorithm). In this study, we ran GA-DFA at least 10,000 times for each comparison that was performed. The software used in the analysis was Ometer v. 0.55 (http://mendes.vbi.vt.edu/tiki-index.php?page=ometer).

Results and Discussion

Biomass growth state was stable during the experiments. Overall, MLSS and MLVSS levels in the reactors did not vary significantly during the experimental period of 5 hours (data not shown), indicating that the biomass growth state was kept stable during the independent batch experiments. The MLSS and MLVSS concentrations differed among different mixed liquors, which was expected given that they were retrieved from different treatment plants. The concentrations varied approximately between 1700 – 3000 mg/L and 1400 – 2400 mg/L, for MLSS and MLVSS respectively. In most cases (28 reactors out of 32), the variation between the solids concentration at time < 5 minutes and 5 hours after the beginning of the experiments was

less than 9% of the initial value, and the average variation for MLVSS was -1.5 ± 4.1% (n = 28). There was one experiment out of the eight that were conducted in which the MLVSS levels in all four reactors dropped by approximately 17-20% during the experimental period of 5 hours. Although we are not sure about what caused this behavior, we believe that the impact of this drop on the overall data analysis is not important, as the same behavior was observed for all the reactors and the data analysis is performed on a comparative basis (control to chemical-stressed mixed liquors).

Chemical shock resulted in release of proteins, carbohydrates and humic substances from activated sludge flocs. We measured the concentration of proteins, carbohydrates and humic substances in the soluble phase of the reactors over time and found that these biomolecules increased significantly in comparison to the unshocked control, especially in the cadmium and NEM-shocked reactors. Since the feed used to stabilize the growth of the microbial community over the experimental period did not contain any of these materials, we conclude that significant release of these biomolecules occurred from the activated sludge flocs in response to chemical stress. An example of this release is shown in Figure 1 for one of the experiments. In this example, we saw a clear increase in the concentration of proteins, carbohydrates and humic acids in the supernatant of the mixed liquor shocked with cadmium and NEM, which reached a maximum 5 hours after the shock. The DNP-shocked reactor did not show such a marked effect in this experiment, although a minor increase in both the protein and carbohydrate concentrations could still be observed.

Overall, we found statistically significant differences between the control and shocked reactors in the variation of the soluble phase concentration of these biomolecules over time (paired two-tailed distribution t-Tests, $p < 0.045$, actual p values in Table 1). The only exception to this was for the variation of the humic acids' concentration in the reactors shocked with DNP, which was not statistically different from the variation in the control reactors (paired two-tailed distribution t-Test, $p = 0.31$). Immediately after the chemical shock (time < 5 minutes), the different biomolecule concentrations in all the reactors were similar, as the difference (mg/L) between the concentration in the shocked reactors versus the concentration in the control at that time point varied between 0.00-1.3 mg/L (0.01 ± 0.48 mg/L, n = 24), 0.02-0.62 mg/L (0.04 ± 0.25 mg/L, n = 24) and 0.00-1.8 mg/L (0.40 ± 0.76 mg/L, n = 24), respectively for carbohydrates, proteins and humic acids. Although some variation was observed among

different experiments, which was expected due to the mixed liquor differences, the concentration of proteins in the shocked reactors increased with time and, in most cases, reached a maximum at the last sampling point (5 hours after the chemical shock, Table 1). The release of proteins from the activated sludge flocs was most clear in the cadmium and NEM-shocked mixed liquors (average increase of more than 3 mg/L proteins in the soluble phase), while DNP caused a more modest but still significant release effect (0.8 mg/L average increase). Similarly, cadmium and NEM shocks also resulted in a more substantial release of carbohydrates (above 2.5 mg/L on average) from the activated sludge flocs than DNP (0.8 mg/L average increase).

The data pertaining to the release of biomolecules from activated sludge flocs under different chemical stress conditions is a first indication that the mechanism through which such release takes place is toxin-specific, corroborating our initial hypothesis. Toxin specificity seems to be both quantitative and qualitative; for the same mixed liquor, NEM led to a more intense release of humic substances than cadmium (paired two-tailed distribution t-Test, $p = 0.0026$) or DNP (paired two-tailed distribution t-Test, $p = 0.0001$), and DNP resulted in a significantly more modest release of carbohydrates and proteins than cadmium or NEM (paired two-tailed distribution t-Tests, $p < 0.03$ for all the comparisons). This conclusion is important to take into consideration when trying to understand the mechanism through which the release of these substances occurs. In addition, the results were relatively consistent between the different biomasses used, indicating that they represent a general trend for activated sludge systems.

Other types of stress have been reported to result in the release of biomolecules from activated sludge mixed liquor. For example, anaerobic conditions together with shear stress (Wilen et al., 2000a; Wilen et al., 2000b) and shear stress alone (Henriques and Love, in preparation) have been shown to result in an increase in the mixed liquor supernatant concentrations of protein, humic substances and carbohydrates. Similarly, Morgan-Sagastume and Allen (2005) have shown that temperature upshifts lead to release of proteins, carbohydrates, DNA and humic substances from the floc structure into the bulk liquid. More importantly, the release of biomolecules from activated sludge flocs under stress conditions has been linked to EPS solubilization mechanisms in the studies indicated above, and a link between microbial activity and floc integrity has also been established (Wilen et al., 2000b). This means that conditions that result in disturbance of the microbial activity within activated sludge flocs, such as chemical stress, may result in altered floc structure leading to the release of soluble

components from the floc into the surrounding medium. This idea is consistent with the results presented here.

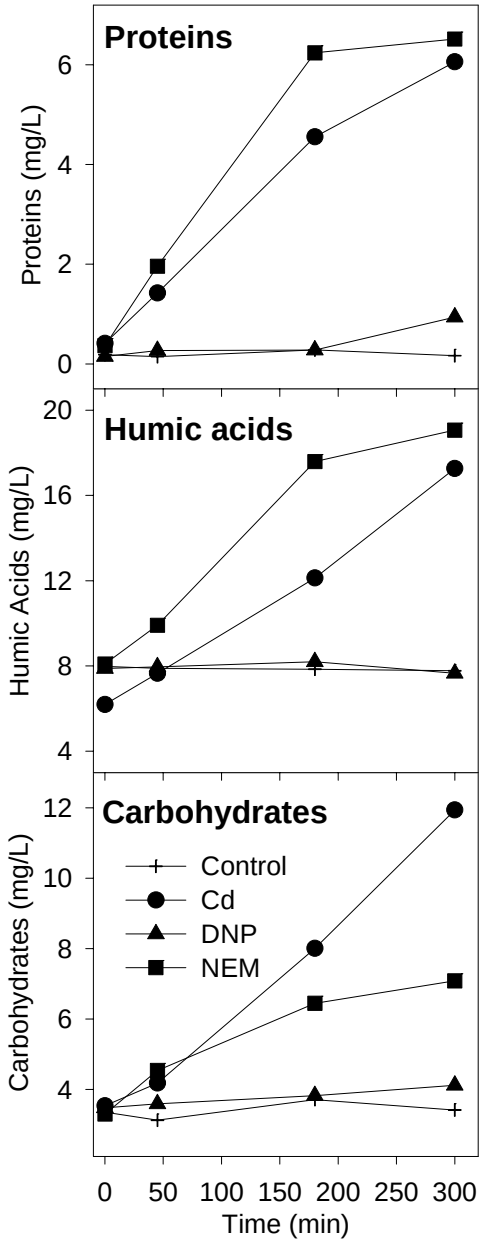

Figure 1 – Example of the variation of proteins, humic acids and carbohydrates with time in the mixed liquor supernatant (soluble phase) of the shocked reactors (Cadmium-Cd, DNP and NEM) versus the control (experiment 1). Data points represent average of at least triplicate measurements. Standard deviations for multiple absorbance (or transmittance) measurements for each analysis were less than 5% of the average value and are not shown. Data points at time zero represent samples taken within the first 5 minutes after the chemical shock.

Table 1 – Difference (mg/L) between the soluble concentrations of carbohydrates, proteins and humic acids at the beginning (time < 5 minutes) and end (5 hours, unless otherwise indicated) of the experimental period. Difference = $[biomolecule]_{5hrs} - [biomolecule]_{<5min}$. Standard deviations for multiple absorbance (or transmittance) measurements for each analysis were less than 10% of the average value and are not shown.

Experiment	Carbohydrates				Proteins				Humic acids			
	Control	Cd	DNP	NEM	Control	Cd	DNP	NEM	Control	Cd	DNP	NEM
1	0.06	8.40	0.65	3.79	-0.02	5.65	0.79	6.15	-0.21	11.07	0.31 [a]	10.97
2	0.06	7.90	0.52	3.48	0.04	6.09	0.11 [a]	5.31 [a]	0.06	8.71	0.55	11.35
3	0.80	3.16	1.41	2.56	-0.01	3.91	-0.07	0.46 [a]	0.28	3.42	0.07 [b]	5.34
4	-0.19	1.89	1.07	0.86	-0.77	4.16	0.13 [a]	0.46 [a]	2.79	5.58	1.82	6.11
5	0.30	1.46	1.41	2.85	-0.15	3.60	1.93	5.40	1.72	6.31	1.53	9.96
6	0.32	2.41	1.37	2.55	-1.38	0.41 [b]	0.99	2.78	1.68	6.89	5.05	10.63
7	-1.36	2.21 [a]	0.00	1.98	0.35	3.44	0.37	2.13 [a]	-1.00	2.11	-0.67	5.35
8	1.32	2.95	0.26	3.80	0.19	0.43 [b]	2.26 [b]	3.26 [b]	-0.08	2.39	0.51	6.05
average	0.16	3.80	0.84	2.73	-0.22	3.46	0.82	3.24	0.66	5.81	1.15	8.22
std. dev. [c]	0.78	2.74	0.56	1.00	0.57	2.10	0.87	2.22	1.27	3.13	1.76	2.72
p value [d]		0.0085	0.044	0.0001		0.0011	0.023	0.0026		0.0026	0.31	0.0001

[a] difference was determined between time < 5 minutes and 3 hours, as this was the sampling point at which maximum values of the respective biomolecule concentration occurred in solution; in all other cases, the maximum concentration was observed at 5 hours.

[b] difference was determined between time < 5 minutes and 45 minutes, as this was the sampling point at which maximum values of the respective biomolecule concentration occurred in solution; in all other cases, the maximum concentration was observed at 5 hours.

[c] standard deviation.

[d] p value for paired two-tailed distribution t-Test for comparison between the variation in the control and in the shocked reactors.

No significant cell lysis was observed in response to chemical shock. AP assays were conducted, in order to investigate if cell lysis was a significant source of the materials released from the flocs. The results obtained at the concentrations of toxins tested show that the toxicity effects were not severe enough to cause major cell lysis of the bacteria embedded in the mixed liquor flocs. The average enzyme activity (measured in units of AP activity per g MLVSS) in the mixed liquor bulk liquid (soluble samples) was 0.0012 ± 0.0014 (n = 15), 0.0019 ± 0.0016 (n = 14), 0.0033 ± 0.0018 (n = 15), and 0.0027 ± 0.0015 (n = 15), for the control, cadmium, DNP and NEM reactors, respectively. Although some increase was noted in the supernatant of the shocked reactors versus the control, the enzyme activity in the mixed liquor cell-free extracts, which represents the floc-associated activity, was at least 10.5x , 5.5x, 9x and 11x higher than in the soluble samples for the control, cadmium, DNP and NEM reactors, respectively. This indicates that most of the enzyme activity remained associated with the floc structure in all the reactors. The results from the cell-free extracts also indicate that neither DNP nor NEM affected enzyme activity, as the difference in the total floc-associated activity of the enzyme between the control and the DNP or NEM-shocked reactors was not statistically significant (data not shown). NEM had been previously found not to interfere with AP activity up to a concentration of 2,000 mg/L (Bott and Love, 2002). Cadmium, however, seemed to affect enzyme activity slightly because the AP activity measured in the cadmium-exposed mixed liquor samples was, on average, 2.2x lower than that in the control samples. However, this should not impact the trends obtained with cadmium significantly, as the enzyme activity in the cell-free extracts of the cadmium-containing samples were still quantifiable and the enzyme inhibition in the soluble samples was likely much lower than in the mixed liquor cell-free extracts. Cadmium strongly binds to activated sludge flocs, leading to a partition of the metal between the solid and soluble phases. We previously found that approximately 90% of the cadmium spiked into mixed liquor sorbed onto activated sludge flocs, leading to a soluble concentration that was only 10% of the initial spike (Love et al., 2005). Therefore, given that the concentration of cadmium in the soluble phase was much lower than in the floc-associated fraction, the inhibition of AP activity in the soluble phase is considered negligible, which validates the results that we obtained for cadmium.

Metabolic footprints from shocked reactors were different from the control and toxin-specific. When we visually analyzed the chromatograms generated through LC-MS, we noticed that there were clear differences between the control and shocked reactor samples, especially for the later sampling times during the experimental period (3 hours and 5 hours, data not shown). In general, the control chromatograms had fewer and less intense peaks than the chromatograms for the samples derived from the stressed mixed liquors. However, the complexity of the chromatograms did not allow us to determine general trends from the data, as differences could also be seen among samples belonging to the same type of reactor for different experiments. We, therefore, used GA-DFA to distinguish between the mass spectra of soluble samples from the control and shocked reactors. GA-DFA resulted in a clear discrimination between the four classes of samples (control, cadmium, DNP and NEM) tested (example in Figure 2). This main finding indicates that the metabolic footprints of the soluble samples retrieved from the control and shocked reactors contain sufficient information to allow the samples to be correctly classified based on the metabolic footprints alone. This also corroborates our hypothesis that the substances released under chemical stress from activated sludge flocs are toxin-specific. Discrimination between the four classes was possible even when the samples from all the different biomasses were included in the analysis, suggesting that at least some of the peaks in the mass spectra are not mixed liquor-specific and can potentially be used as universal activated sludge toxin-specific biomarkers.

When GA-DFA was run with all the samples obtained during this study (including the samples taken for the different time points), 30 variables (of the initial 1609 m/z ratios) were used to formulate a model with three DFs (Figure 2). In the example of one GA-DFA run in Figure 2, all three DFs were necessary to distinguish between the classes: DF1 provided a separation between the cadmium and control samples, DF2 distinguished between NEM and control samples and DF3 between DNP and control samples. The DFs also allowed differentiation between the samples from the different chemical shocks. Although not shown, DNP samples projected on the DF1 versus DF2 plot appeared in the same area as the control samples. Therefore, DF1 also distinguished between cadmium and DNP samples, and cadmium and NEM samples, while DF2 could separate the NEM and DNP samples. Overall, GA-DFA allowed differentiation between any two classes within the matrix when all the samples were included.

Given the complexity of the analysis matrix when all four classes of samples were included, there were many possible combinations of 30 different m/z ratios that resulted in good discrimination between the groups. This was observed when we conducted GA-DFA multiple times to find if there were some m/z ratios that were most likely to be selected (and, therefore, most discriminant) among the 1609 variables, to separate the four classes of samples together (Figure 3). Figure 3 shows that a considerable amount of different m/z ratios were selected more than 2% of the time and that the maximum selection frequency that occurred (891 times in 10,000 runs for m/z 1683) was less than 10% (or 1,000 of 10,000 runs). Overall, the complexity of the frequency plot (large number of m/z selected and relatively low frequency levels) is a result of the original complexity of the environmental matrix being analyzed, which leads to many possible different solutions for the discrimination problem. This could be alleviated, in part, by increasing the number of replicate experiments, as more replicates would provide more constraints to the solution space.

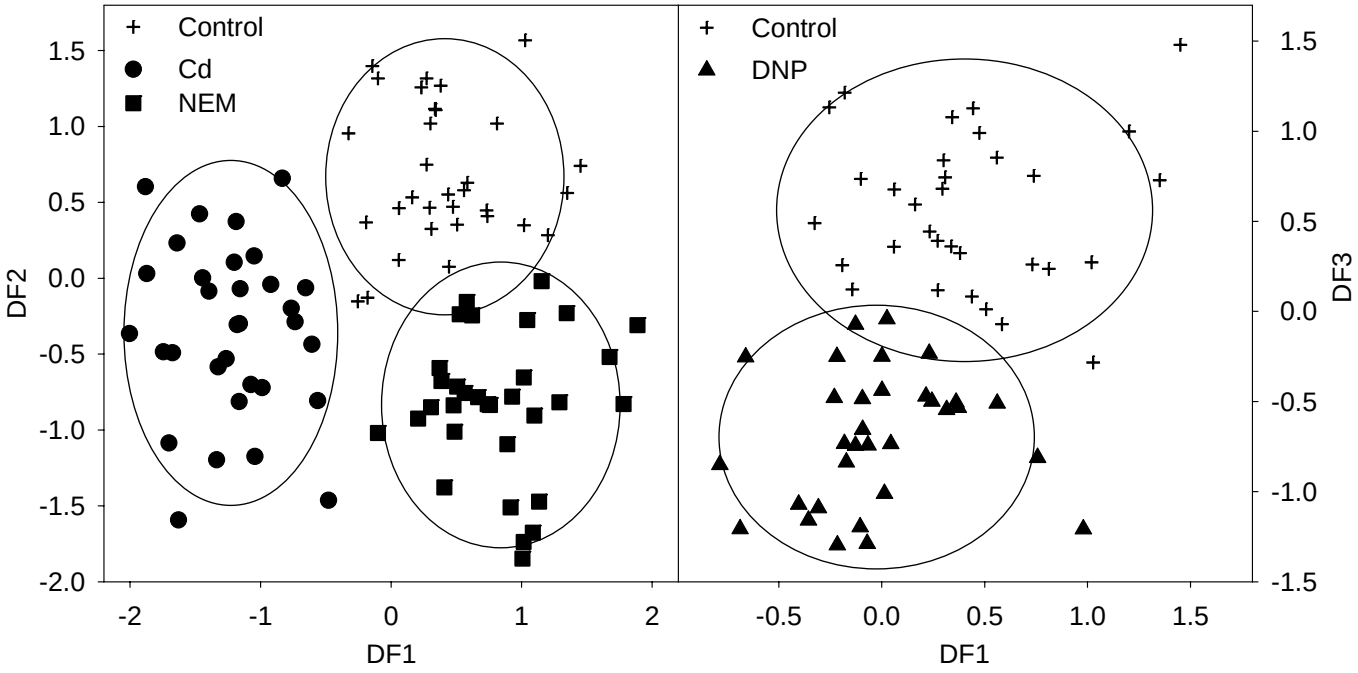

Figure 2 – Results from one GA-DFA run to compare between the mass spectra data of the soluble samples obtained during experiments with activated sludge subjected to shock loads of cadmium (Cd), DNP and NEM. GA-DFA was applied to the four classes of samples together. 30 m/z ratios were used to distinguish between the classes. All the samples collected during the experiments were incorporated in this statistical analysis, including samples from the different mixed liquors tested and different time points. The ellipses represent the (mean ± 2 standard deviations) along each of the DFs for each class.

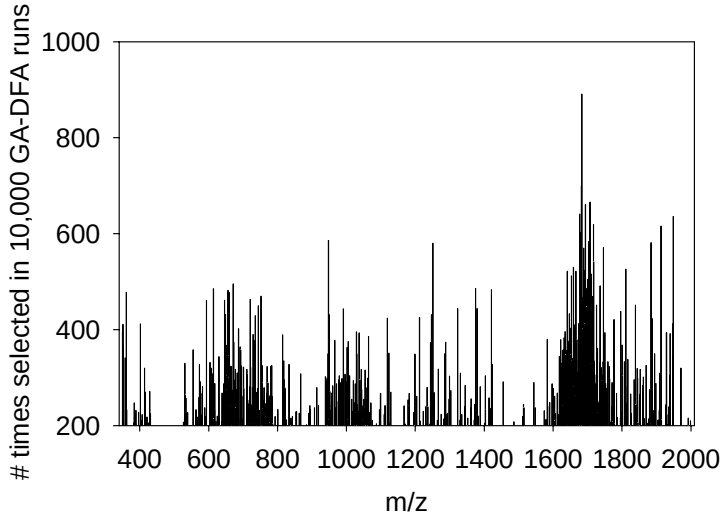

Figure 3 – Results of 10,000 GA-DFA runs applied to the mass spectra data of the four classes of soluble samples (control, cadmium, DNP and NEM) together. This graph only shows the m/z ratios that were selected the most (more than 200 times) by the GA to distinguish between the four classes. In each GA-DFA run, 30 m/z ratios were selected to distinguish between the classes. All the samples collected during the experiments were incorporated in this statistical analysis, including samples from the different mixed liquors tested and different time points.

When GA-DFA was run between two classes of samples only (control versus each chemical shock), the total number and selection frequency of the discriminant m/z ratios improved significantly relative to the analysis of all four classes together (Figure 4 versus Figures 2 and 3). We were able to observe good discrimination between the control samples and the samples obtained from the cultures subjected to each chemical stress (Figures 4 A, B and C). Figures 4 A, B and C give a representative example of the discrimination between control and shocked reactor samples based on a DF formulated with only four different m/z ratios. The four m/z ratios used in each comparison (highlighted in Figures 4 D, E and F and in Table 2) were, each, selected more than 20% of the time by the GA, indicating that these m/z ratios alone contain enough information to allow a clear differentiation between the control and chemical stress-derived samples. In addition, we obtained a selection frequency for the top m/z ratio above 50% (selected more than 10,000 times in 20,000) for each comparison. Given that different mixed liquors were used in this analysis, the fact that we had such high frequency for some of the discriminant m/z ratios reveals that these biomolecules are likely universal stress biomarkers for activated sludge communities subjected to cadmium, DNP or NEM shock loads.

The m/z ratios with a selection frequency of more than 10% for each case are presented in Table 2, while frequency plots are shown in Figures 4 D, E and F. An interesting trend that

can be observed from these data is that cadmium shock resulted in the release of biomolecules with characteristic m/z values above 1200 in most cases, while discriminant m/z ratios associated with DNP shock were mostly below 1000 and NEM-associated m/z ratios were spread through the analytical range that was analyzed (350-2000). For cadmium and NEM, the higher discriminant m/z ratios are likely high molecular weight biopolymers (proteins and carbohydrates) for which we observed a significant increase in the soluble phase concentrations. However, the lower m/z ratios that seemed to be selected as the most important to distinguish between DNP and control samples may correspond to biomolecules belonging to other classes of compounds, which is consistent with the weak release effect of proteins and carbohydrates observed in response to DNP shock. Overall, these results are consistent with the release patterns for proteins, carbohydrates and humic substances observed from each chemical shock source and they provide additional evidence of the toxin-specific nature of the chemical shock-induced release of biomolecules from activated sludge flocs.

As a methodological approach, metabolic footprinting is not designed to identify the molecules responsible for the discrimination between the groups of samples, but rather to allow sample classification and pattern recognition among vast amounts of data (Dunn and Ellis, 2005; Kell et al., 2005; Villas-Boas et al., 2005). However, we have found that the classification of the samples between control and each shocked-reactor class required only a minimal number of variables (four m/z ratios) from the 1609 original variables in the data set. Identifying a small number of m/z ratios that can be used to discriminate between control samples and samples that have been exposed to a specific chemical stress may be the first step to identify important biomolecules released under stress. Identification of such molecules can target future experiments towards developing a better understanding of the mechanisms behind the release of materials from activated sludge flocs into the bulk liquid upon exposure to toxic chemicals and, overall, the stress responses of activated sludge bacteria.

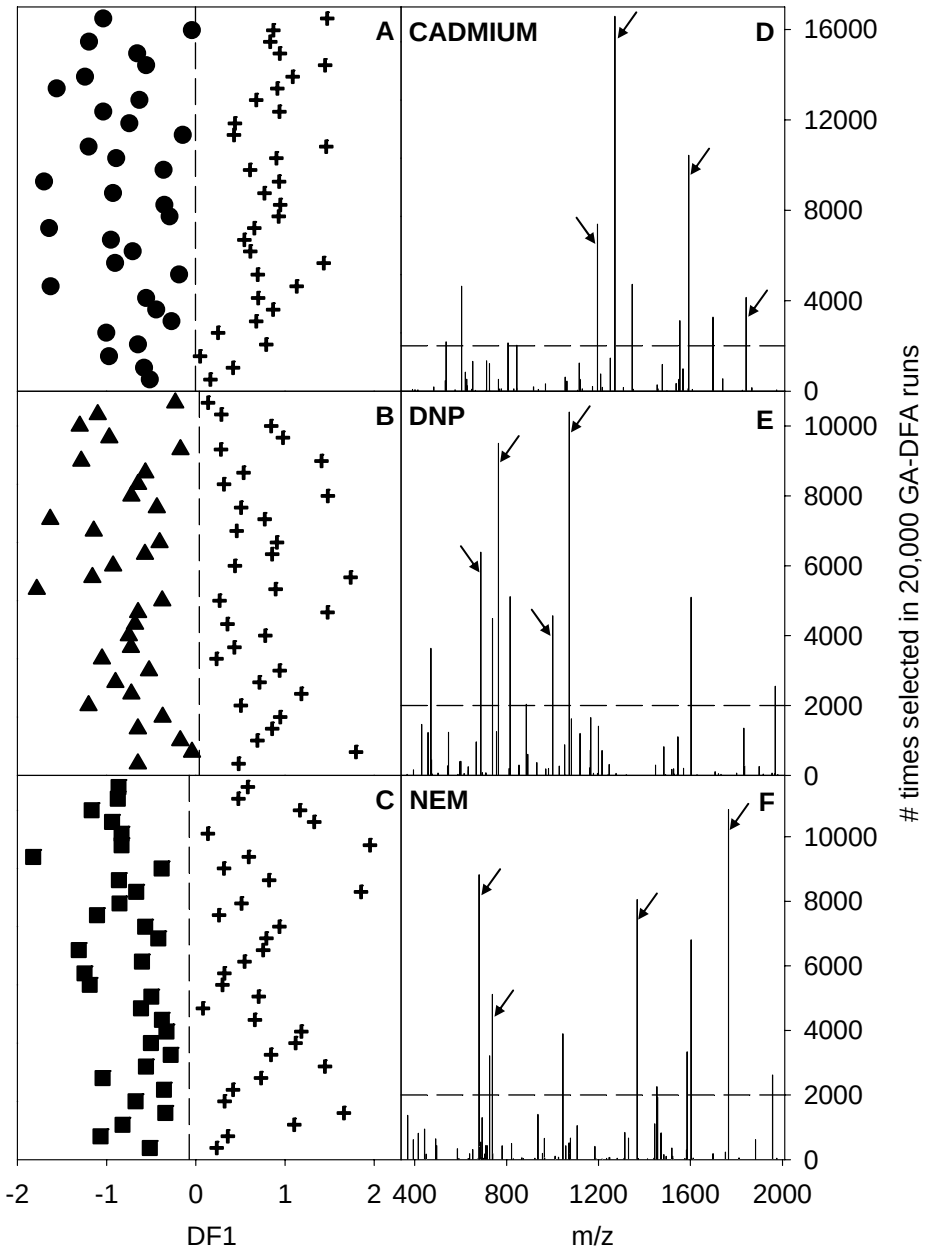

Figure 4 – GA-DFA of mass spectra data for the soluble samples obtained over time (all time points included) during experiments with activated sludge subjected to shock loads of cadmium, DNP and NEM. GA-DFA was applied to two classes of samples at a time (A and D – comparison of control and cadmium samples; B and E – comparison of control and DNP samples; C and F – comparison of control and NEM samples). Four m/z ratios were used to distinguish between the two classes. A, B and C represent results for one GA-DFA run (Control - +, cadmium - ●, DNP - ▲ and NEM - ■). The m/z ratios selected to determine the values of DF1 (DF1 is a linear combination of the intensity observed for each of these m/z) are highlighted in D, E and F through arrows and are given in Table 2. D, E and F represent the results of 20,000 GA-DFA runs (m/z ratios selected the most to distinguish between the two classes). m/z ratios with frequencies above the dashed line, were selected more than 10% of the time.

Table 2 – m/z ratios selected more than 2,000 times (in 20,000 GA-DFA runs), to distinguish between the control reactor and each shocked reactor samples. GA-DFA was run 20,000 times, and four m/z ratios were selected in each run. GA-DFA was applied to two classes of samples at a time.

Cadmium vs. Control		DNP vs. Control		NEM vs. Control	
m/z	# times selected in 20,000 GA-DFA runs	m/z	# times selected in 20,000 GA-DFA runs	m/z	# times selected in 20,000 GA-DFA runs
1271*	16,589	1072*	10,403	1765*	10,842
1592*	10,435	764*	9,508	680*	8,827
1195*	7,395	687*	6,396	1368*	8,058
1346	4,728	815	5,119	1602	6,809
604	4,649	1602	5,103	737*	5,122
1842*	4,150	1000*	4,567	1045	3,901
1698	3,278	738	4,489	1585	3,339
1554	3,120	470	3,639	726	3,217
536	2,185	1969	2,555	1957	2,619
806	2,134	885	2,036	1454	2,261
844	2,038				

***** variables (m/z ratios) selected by the GA to define the values of DF1, shown in Figures 4 A, B and C.

Conceptually, there are four possible origins for the materials released from activated sludge flocs under chemical stress conditions: 1) release of intracellular materials into the bulk liquid due to major cell lysis caused by intense toxicity, 2) release of intracellular compounds actively secreted due to specific bacterial stress response mechanisms, 3) solubilization of EPS components due to physical-chemical interactions that take place between the chemical and the EPS matrix, that lead to a rearrangement of the EPS molecular network, and 4) release of EPS components as a secondary consequence of bacterial stress response mechanisms. We found that cell lysis was not a major contribution to the release of biomolecules that we measured. We, therefore, conclude that the release of these materials is linked with the other three mechanisms proposed above. We believe that the overall response is likely a combination of all the mechanisms and that they are interdependent, in the sense that a certain bacterial stress response may lead to alterations in the EPS matrix. This is certainly the case with NEM and cadmium, which are both eletrophilic chemicals.

NEM has been shown to cause intense potassium efflux from the cytoplasm of bacterial cells into the surrounding environment in activated sludge cultures (Bott and Love, 2002; Bott

and Love, 2004). This potassium efflux, which results from a bacterial stress response to electrophilic chemicals called glutathione-gated potassium efflux (GGKE), ultimately leads to weakening of the EPS molecular network and floc disintegration due to imbalances in the cationic content within the EPS matrix based on theories proposed by Higgins and Novak (1997). The same stress response and coupled EPS structural modification mechanisms may also explain the cadmium-induced release of biomolecules observed in this study. In the case of cadmium, however, the charged nature of the metal also likely contributes to the overall effects at the level of EPS matrix alterations and EPS release, which could explain the differences between cadmium and NEM-induced release of biomolecules into the soluble phase and their different footprints. Contrary to NEM, an uncharged hydrophilic chemical, cadmium binds to EPS very strongly (Guibaud et al., 2005; Jang et al., 2001; Liu et al., 2001) and certain EPS components may have a greater affinity for the metal than others, influencing what EPS materials are released and what remain within the floc matrix.

As an uncoupler of oxidative phosphorylation, DNP has the ability to carry protons across biological membranes and, therefore, the mode of action of this chemical on bacterial cells is primarily linked to disruption of the proton motive force (PMF) and of the metabolic processes linked to energy production and maintenance. This mode of action is very different from that of NEM and cadmium, and most likely results in different bacterial stress responses. Work conducted with *E. coli* exposed to DNP showed that 53 proteins were synthesized due to DNP exposure (Gage and Neidhardt, 1993). Among the 53 induced proteins were heat shock proteins, carbon, nitrogen and phosphorus starvation proteins, and 24 unknown proteins unique to DNP stress. In addition, due to its semi-hydrophobic nature, DNP has the potential to interact with the EPS matrix.

Given the differences between the modes of action and chemical structure of the toxins tested in this study, the toxin-specific nature of the footprints generated for the different conditions is logical. Overall, the metabolic footprinting data indicates that specific chemical toxins induce specific responses from activated sludge cultures, which corresponds well with the idea that both the physical-chemical interactions between the EPS matrix and the toxin, and the bacterial stress responses elicited upon exposure to the toxin, are different for each toxic agent.

Metabolic footprints from shocked reactors varied with time, as compared to the control reactor footprints. We compared the samples from the control and each shocked reactor, for each sampling time point to understand if there were differences in the compounds being released from the activated sludge flocs over time. From the chromatograms generated through LC-MS, we could visually observe that, in general, the intensity of the peaks in the samples from the shocked reactors increased over time (data not shown), but qualitative trends were difficult to determine due to the variability and complexity of the data. GA-DFA analysis showed that only two m/z ratios were necessary to discriminate between the two classes compared for each time point (Table 3). In most cases, the top two m/z ratios selected among multiple GA-DFA runs were selected in more than 70% of the runs and the total number of m/z ratios selected for all the runs together represented less than 2.5% of the total available number of 1609, showing high specificity for the selected m/z ratios. Interestingly, for different sampling time points, different m/z ratios were responsible for the separation between the control and a specific chemical shock, showing that the metabolic footprint of a shocked reactor changed qualitatively over time.

Differences between the composition of the soluble phase of the control reactor and the reactors shocked with each of the chemicals for the first sampling time point (within 5 minutes of chemical addition), which could not be observed visually, were observed through GA-DFA analysis. This suggests that at least some of the mechanisms responsible for the release of materials from the floc structure into the bulk liquid occur within minutes of toxin exposure in activated sludge systems, which is consistent with previous observations showing that stress responses in activated sludge systems occur very rapidly (Bott and Love, 2001; Bott and Love, 2002). This observation can be important for future developments of this work, as biomarkers that are released shortly after exposure of bacterial cells to chemical toxins are preferred as targets for developing sensing and monitoring technologies.

Table 3 – Top two m/z ratios selected during multiple GA-DFA runs (15,000 to 30,000 runs), to distinguish between the control reactor and each shocked reactor samples at each sampling time point. Two m/z were selected in each GA-DFA run. GA-DFA was applied to two classes of samples at a time.

Time	Cadmium vs. Control		DNP vs. Control		NEM vs. Control	
	m/z	frequency (%)*	m/z	frequency (%)*	m/z	frequency (%)*
< 5 min	717	99	1593	89	488	47
	1461	98	1368	88	1417	47
45 min	604	100	1712	92	351	100
	1010	100	1015	92	1431	100
3 hrs	1175	97	556	99	948	86
	1738	87	1933	80	1438	75
5 hrs	1703	95	414	71	817	100
	1593	79	447	71	769	99

***** frequency (%) = (# times selected / total # GA-DFA runs) x 100

Environmental significance. Environmentally-relevant bacterial populations are frequently exposed to toxic pollutants in their native habitats. These populations occur both in natural and engineered systems, such as wastewater treatment plants. We have shown that the activation of specific responses by activated sludge cultures due to exposure to toxic chemicals results in detectable changes in the chemical composition of the mixed liquor's soluble phase, and that these changes are common to different activated sludge populations. Furthermore, we have shown that it is possible to "measure" and "expose" those changes through the utilization of mass spectrometry analytical techniques combined with multivariate statistical methods. To our knowledge, this study reflects the first attempt to use metabolomics-derived techniques to a complex and environmentally-relevant microbial population.

We believe that the development of environmental metabolomics will result in new technologies for environmental monitoring. The identification of new bacterial stress biomarkers may contribute to the development of biosensors. For example, antibodies can be created against a high number of bacterial stress biomarkers to be applied on antibody microarrays, which can be utilized to detect a number of different toxic substances simultaneously. In addition, the utilization of mini mass spectrometers for real time field monitoring is another technology in which the information from metabolic footprinting studies can potentially be used. Integrated with GIS and database management systems, biosensor and portable mass spectrometry

technologies promise great developments in the fields of environmental and public health monitoring, and can potentially be applied to a range of natural and engineered systems.

Acknowledgments

This work was funded by the Water Environment Research Foundation project no. 01-CTS-2. I. D. S. Henriques received a fellowship (SFRH/BD/4689/2001) from the Fundação para a Ciência e a Tecnologia, Portugal. We would like to acknowledge the important assistance of Seamus O'Connor, Dr. Charles Bott, Angela Batt, Mark Garland, Kevin Grove and Maeva Tureau during this work. We would especially like to thank the staff at the wastewater treatment plants that were used as the source of mixed liquor in these studies, for giving us access to the plants and allowing us to get samples.

References

Ahmed, W., Neller, R., and Katouli, M. (2005) Host Species-Specific Metabolic Fingerprint Database for Enterococci and *Escherichia coli* and its Application to Identify Sources of Fecal Contamination in Surface Waters. *Appl. Environ. Microbiol.* **71:** 4461-4468.

Allen, J., Davey, H.M., Broadhurst, D., Heald, J.K., Rowland, J.J., Oliver, S.G., and Kell, D.B. (2003) High-Throughput Classification of Yeast Mutants for Functional Genomics Using Metabolic Footprinting. *Nat. Biotechnol.* **21:** 692-696.

Allen, J., Davey, H.M., Broadhurst, D., Rowland, J.J., Oliver, S.G., and Kell, D.B. (2004) Discrimination of Modes of Action of Antifungal Substances by Use of Metabolic Footprinting. *Appl. Environ. Microbiol.* **70:** 6157-6165.

American Public Health Association, American Water Works Association, Water Environment Federation. (1998) *Standard Methods for the Examination of Water and Wastewater*, 20th ed. Washington, DC.

Baudoin, E., Benizri, E., and Guckert, A. (2001) Metabolic Fingerprint of Microbial Communities from Distinct Maize Rhizosphere Compartments. *Eur. J. Soil Biol.* **37:** 85-93.

Bott, C.B. and Love, N.G. (2001) The Immunochemical Detection of Stress Proteins in Activated Sludge Exposed to Toxic Chemicals. *Water Res.* **35:** 91-100.

Bott, C.B. and Love, N.G. (2002) Investigating a Mechanistic Cause for Activated Sludge Deflocculation in Response to Shock Loads of Toxic Electrophilic Chemicals. *Water Environ. Res.* **74:** 306-315.

Bott, C.B. and Love, N.G. (2004) Implicating the Glutathione-Gated Potassium Efflux System as a Cause of Electrophile-Induced Activated Sludge Deflocculation. *Appl. Environ. Microbiol.* **70:** 5569-5578.

Dubois, M., Gilles, K.A., Hamilton, J.K., Rebers, P.A., and Smith, F. (1956) Colorimetric Method for Determination of Sugars and Related Substances. *Anal. Chem.* **28:** 350-357.

Dunn, W.B. and Ellis, D.I. (2005) Metabolomics: Current Analytical Platforms and Methodologies. *Trac-Trend. Anal. Chem.* **24:** 285-294.

Frølund, B., Griebe, T., and Nielsen, P.H. (1995) Enzymatic Activity in the Activated Sludge Floc Matrix. *Appl. Microbiol. Biot.* **43:** 755-761.

Gage, D.J. and Neidhardt, F.C. (1993) Adaptation of *Escherichia coli* to the Uncoupler of Oxidative Phosphorylation 2,4-Dinitrophenol. *J. Bacteriol.* **175:** 7105-8.

Garnier, C., Gorner, T., Lartiges, B.S., Abdelouhab, S., and de Donato, P. (2005) Characterization of Activated Sludge Exopolymers from Various Origins: A Combined Size-Exclusion Chromatography and Infrared Microscopy Study. *Water Res.* **39:** 3044-3054.

Goodacre, R., Vaidyanathan, S., Dunn, W.B., Harrigan, G.G., and Kell, D.B. (2004) Metabolomics by Numbers: Acquiring and Understanding Global Metabolite Data. *Trends Biotechnol.* **22:** 245-252.

Grady, C.P.L., Daigger, G.T., and Lim, H.C. (1999) *Biological Wastewater Treatment*, 2nd ed. Marcel Dekker, Inc. New York, NY.

Guibaud, G., Comte, S., Bordas, F., Dupuy, S., and Baudu, M. (2005) Comparison of the Complexation Potential of Extracellular Polymeric Substances (EPS) Extracted from Activated Sludges and Produced by Pure Bacteria Strains, for Cadmium, Lead and Nickel. *Chemosphere* **59:** 629-638.

Henriques, I.D.S., Kelly, R.T., Dauphinais, J.L., and Love, N.G. (in review) Activated Sludge Inhibition by Chemical Stressors: A Comprehensive Study. *Water Environ. Res.*

Henriques, I.D.S. and Love, N.G. (in preparation) Floc Structure and Floc Size Play a Role in the Toxicity Response of Activated Sludge Bacteria to Chemical Toxins. *Water Res.*

Higgins, M.J. and Novak, J.T. (1997) The Effect of Cations on the Settling and Dewatering of Activated Sludges: Laboratory Results. *Water Environ. Res.* **69:** 215-224.

Jang, A., Kim, S.M., Kim, S.Y., Lee, S.G., and Kim, I.S. (2001) Effect of Heavy Metals (Cu, Pb, and Ni) on the Compositions of EPS in Biofilms. *Water Sci. Technol.* **43:** 41-48.

Jarvis, R.M. and Goodacre, R. (2005) Genetic Algorithm Optimization for Pre-Processing and Variable Selection of Spectroscopic Data. *Bioinformatics* **21:** 860-868.

Kaderbhai, N.N., Broadhurst, D.I., Ellis, D.I., Goodacre, R., and Kell, D.B. (2003) Functional Genomics via Metabolic Footprinting: Monitoring Metabolite Secretion by *Escherichia coli*

Tryptophan Metabolism Mutants Using FT-IR and Direct Injection Electrospray Mass Spectrometry. *Compar. Funct. Genom.* **4:** 376-391.

Kell, D.B., Brown, M., Davey, H.M., Dunn, W.B., Spasic, I., and Oliver, S.G. (2005) Metabolic Footprinting and Systems Biology: The Medium is the Message. *Nat. Rev. Microbiol.* **3:** 557-565.

Kelly, R.T., Henriques, I.D.S., and Love, N.G. (2004) Chemical Inhibition of Nitrification in Activated Sludge. *Biotechnol. Bioeng.* **85:** 683-694.

Khin, T., Gheewala, S. H., and Annachhatre, A. P. (2002) Modeling of Nitrification Inhibition With Aniline in Suspended-Growth Processes. *Water Environ. Res.* **74:** 531-540.

Kim, K. T., Kim, I. S., Hwang, S. H., and Kim, S. D. (2006) Estimating the Combined Effects of Copper and Phenol to Nitrifying Bacteria in Wastewater Treatment Plants. *Water Res.* **40:** 561-568.

Liu, Y., Lam, M.C., and Fang, H.H.P. (2001) Adsorption of Heavy Metals by EPS of Activated Sludge. *Water Sci. Technol.* **43:** 59-66.

Love, N.G. and Bott, C.B. (2000) *A Review and Needs Survey of Upset Early Warning Devices*. Project 99-WWF-2. Water Environment Research Foundation. Alexandria, VA.

Love, N.G., Henriques, I.D.S., and Kelly, R.T. (2005) *Upset Early Warning Systems for Biological Treatment Processes - Source and Effect Relationships*. Report No. 01-CTS-2. Water Environment Research Foundation. Alexandria, VA.

Lowry, O.H., Rosebrough, N.J., Farr, A.L., and Randall, R.J. (1951) Protein Measurement with the Folin Phenol Reagent. *J. Biol. Chem.* **193:** 265-275.

Manly, B.F.J. (1994) *Multivariate Statistical Methods: A Primer*, 2nd ed. Chapman & Hall/CRC. New York, NY.

Morgan-Sagastume, F. and Allen, D.G. (2005) Activated Sludge Deflocculation under Temperature Upshifts from 30 to 45 Degrees C. *Water Res.* **39:** 1061-1074.

Neufeld, R. D. (1976) Heavy Metals-Induced Deflocculation of Activated Sludge. *J. Water Pollut. Control Fed.*, **48** (8), 1940.

Villas-Boas, S.G., Mas, S., Akesson, M., Smedsgaard, J., and Nielsen, J. (2005) Mass Spectrometry in Metabolome Analysis. *Mass Spectrom. Rev.* **24:** 613-646.

Wilen, B.M., Keiding, K., and Nielsen, P.H. (2000a) Anaerobic Deflocculation and Aerobic Reflocculation of Activated Sludge. *Water Res.* **34:** 3933-3942.

Wilen, B.M., Nielsen, J.L., Keiding, K., and Nielsen, P.H. (2000b) Influence of Microbial Activity on the Stability of Activated Sludge Flocs. *Colloid. Surface. B* **18:** 145-156.

Appendix A – Data for Chapter 3

Table 1 - Data for Figure 1 in Chapter 3: effluent soluble COD (mg/L) in cadmium-shocked reactors versus the control.

Cadmium (2 day SRT)					Cadmium (10 day SRT)				
cycle	control	IC_{15}	IC_{25}	IC_{50}	cycle	control	IC_{15}	IC_{25}	IC_{50}
1	44	72	132	154	1	30	46	48	60
2	66	178	244	318	2	26	60	70	88
3	36	190	300	360	3	38	60	84	110
4	32	192	306	418	4	26	44	62	78
6	42	68	264		5	22	52	50	82
8	10	22	146	216	7	36	46	53	74
10	46	62	112	176	9	24	34	46	60
12	40	48	58	68	11	22	-	38	42
14	40	50	58	62	15	30	38	48	46
16	60	76	76	102	19	-	-	46	42
20	38	62	64	74	23	32	40	28	22
24	40	66	86	96					

Table 2 - Data for Figure 1 in Chapter 3: effluent soluble COD (mg/L) in CDNB-shocked reactors versus the control.

CDNB (2 day SRT)			CDNB (10 day SRT)		
cycle	control	IC_{50}	cycle	control	IC_{50}
1	88	280	1	36	69
2	98	422	2	42	112
3	98	330	3	32	82
4	104	172	4	54	67
6	82	116	6	30	63
8	70	82	8	34	56
10	78	72	10	36	64
12	72	60	12	32	70
14	78	72	16	38	61
		66	20	24	55
		66	24	24	31
		64	28	38	51
			32	20	34
			36	24	23

Table 3 - Data for Figure 1 in Chapter 3: effluent soluble COD (mg/L) in pH 11-shocked reactors versus the control.

pH 11 (2 day SRT)			pH 11 (10 day SRT)		
cycle	control	pH 11	cycle	control	pH 11
1	42	476	1	50	382
2	40	608	2	50	358
3	34	544	3	52	160
4	48	398	4	46	110
5	38	98	6	52	94
7	56	-	8	54	82
9	44	64	10	50	68
11	38	70	12	62	92
13	40	78	16	32	60
15	50	86	20	26	44
19	26	60	24	38	56
23	40	74			

Table 4 - Data for Figure 1 in Chapter 3: effluent soluble COD (mg/L) in DNP-shocked reactors versus the control.

DNP (10 day SRT)		
cycle	control	IC_{50}
1	32	30
2	24	47
3	30	42
4	15	34
6	18	27
8	14	20
10	18	20
12	10	15
16	20	18

Table 5 - Data for Figure 2 in Chapter 3: effluent TSS (mg/L) in cadmium-shocked reactors versus the control.

Cadmium (2 day SRT)					Cadmium (10 day SRT)				
cycle	control	IC_{15}	IC_{25}	IC_{50}	cycle	control	IC_{15}	IC_{25}	IC_{50}
1	84	180	149	149	1	50	71	152	116
2	99	231	223	224	2	36	105	113	150
3	85	207	205	207	3	26	99	110	137
4	69	169	173	173	4	47	106	94	127
6	80	232	133	124	5	40	89	113	127
8	61	60	60	104	7	36	72	86	78
10	91	97	121	125	9	31	68	84	86
12	75	91	125	135	11	30	-	70	62
14	51	67	180	124	15	40	63	75	70
16	79	91	107	137	19	-	-	66	66
20	51	97	97	132	23	30	62	98	99
24	53	101	68	101	27	26	50	74	69
1	84	180	149	149	31	24	41	30	30
2	99	231	223	224	35	47	53	80	63
					43	29	43	52	65
					51	25	30	40	60
					59	17	29	31	23
					67	14	37	33	46
					75	15	25	33	33
					83	28	18	23	24
					1	50	71	152	116
					2	36	105	113	150

Table 6 - Data for Figure 2 in Chapter 3: effluent TSS (mg/L) in CDNB-shocked reactors versus the control.

CDNB (2 day SRT)			CDNB (10 day SRT)		
cycle	control	IC_{50}	cycle	control	IC_{50}
1	143	162	1	37	37
2	119	130	2	3	8
3	111	134	3	13	20
4	99	114	4	17	14
6	101	144	6	16	19
8	72	116	8	5	12
			10	18	20
			12	26	22
			16	-	16
			20	-	20
			24	18	19
			28	18	18

Table 7 - Data for Figure 2 in Chapter 3: effluent TSS (mg/L) in pH 11-shocked reactors versus the control.

pH 11 (2 day SRT)			pH 11 (10 day SRT)		
cycle	control	pH 11	cycle	control	pH 11
1	192	484	1	141	317
2	169	350	2	53	329
3	183	343	3	67	168
4	218	228	4	78	195
5	197	210	6	67	111
7	212	187	8	43	100
9	177	113	10	56	80
11	137	48	12	35	57
13	123	57	16	-	-
15	130	29	20	56	32
19	78	39	24	133	103
23	96	103			

Table 8 - Data for Figure 2 in Chapter 3: effluent TSS (mg/L) in DNP-shocked reactors versus the control.

DNP (10 day SRT)		
cycle	control	IC_{50}
1	20	40
2	31	55
3	34	54
4	26	48
6	10	37
8	27	34
10	5	8
12	13	20
16	14	18
20	9	22
24	21	17

Table 9 - Data for Figure 3 in Chapter 3: MLVSS (mg/L) in cadmium-shocked reactors versus the control.

Cadmium (2 day SRT)					Cadmium (10 day SRT)				
cycle	control	IC_{15}	IC_{25}	IC_{50}	cycle	control	IC_{15}	IC_{25}	IC_{50}
2	777	733	677	793	1	973	1009	1133	944
5	870	663	527	537	3	1007	1000	871	773
9	910	743	563	533	5	964	978	913	767
13	897	723	637	613	9	989	940	789	764
17	947	780	557	597	11	1053	1016	962	953
21	907	690	513	547	15	1031	1013	936	762
25	937	723	630	487	20	998	991	1111	949
					23	867	787	873	756
					29	898	916	864	978

Table 10 - Data for Figure 3 in Chapter 3: MLVSS (mg/L) in pH 11-shocked reactors versus the control.

pH 11 (2 day SRT)			pH 11 (10 day SRT)		
cycle	control	pH 11	cycle	control	pH 11
1	1357	920	2	1202	887
3	1370	820	5	1219	982
5	1240	825	9	1147	887
8	713	543	13	1093	947
12	533	350	17	992	747
16	743	390	21	1337	1220
20	747	530	25	1116	1084
24	813	530	29	1300	1260
			33	1482	1537

Table 11 - Data for Figure 3 in Chapter 3: MLVSS (mg/L) in DNP-shocked reactors versus the control.

DNP (10 day SRT)				
cycle	control	IC_{15}	IC_{25}	IC_{50}
2	2116	2053	2016	1997
3	2104	1922	1956	1877
5	2124	1884	1891	1887
7	2224	1878	1856	1733
9	2253	1836	1838	1773
11	2269	1798	1824	1703
13	2224	1704	1780	1643
17	2020	1700	1687	1607
21	1900	1609	1667	1610
25	1851	1613	1678	1613
29	1749	1520	1560	1577
33	1487	1416	1438	1490

Table 12 - Data for Figure 4 in Chapter 3: SOUR (mg O_2/g MLVSS-hr) in cadmium-shocked reactors versus the control.

Cadmium (2 day SRT)					Cadmium (10 day SRT)				
cycle	control	IC_{15}	IC_{25}	IC_{50}	cycle	control	IC_{15}	IC_{25}	IC_{50}
2	119	9	5	2	1	34	9	6	3
5	106	25	16	5	3	36	18	10	3
9	117	77	92	100	5	40	23	22	14
13	120	101	79	98	9	32	24	25	23
17	128	132	112	109	15	27	27	32	31
25	142	145	118	113					

Table 13 - Data for Figure 4 in Chapter 3: SOUR (mg O_2/g MLVSS-hr) in CDNB-shocked reactors versus the control.

CDNB (2 day SRT)					CDNB (10 day SRT)				
cycle	control	IC_{15}	IC_{25}	IC_{50}	cycle	control	IC_{15}	IC_{25}	IC_{50}
2	88	76	71	15	2	77	48	27	9
5	92	89	88	67	5	66	72	47	42
9	112	114	112	106	9	68	64	74	70
13	95	101	101	102	13	85	84	93	79
17	119	121	119	107	21	97	82	85	98
25	123	115	118	113					

Table 14 - Data for Figure 4 in Chapter 3: SOUR (mg O_2/g MLVSS-hr) in DNP-shocked reactors versus the control.

DNP (2 day SRT)					DNP (10 day SRT)				
cycle	control	IC_{15}	IC_{25}	IC_{50}	cycle	control	IC_{15}	IC_{25}	IC_{50}
2	114	87	77	66	2	60	57	48	29
5	104	92	76	75	3	73	72	57	31
9	128	107	111	113	5	64	67	61	40
13	144	123	131	124	7	75	77	75	62
17	121	117	112	119	9	67	83	76	68
25	132	106	105	105	11	78	99	97	86
					13	85	102	98	101
					17	90	111	110	115
					21	94	112	117	121
					29	91	115	120	128
					37	90	120	127	136

Table 15 - Data for Figure 5 in Chapter 3: SOUR (mg O_2/g MLVSS-hr) in Zn-CN-shocked reactors versus the control.

Zn-CN (2 day SRT)					Zn-CN (10 day SRT)				
cycle	control	IC_{15}	IC_{25}	IC_{50}	cycle	control	IC_{15}	IC_{25}	IC_{50}
2	80	91	83	17	2	28	29	20	10
5	103	106	101	65	5	42	41	34	23
9	129	125	134	112	9	46	54	47	40
13	158	135	148	137	13	72	70	66	57
17	128	34	28	28	21	89	76	68	59
25	152	125	167	155	29	77	85	83	74

Table 16 - Data for Figure 5 in Chapter 3: SOUR (mg O_2/g MLVSS-hr) in pH 11-shocked reactors versus the control.

pH 11(2 day SRT)		
cycle	control	pH 11
2	93	1
4	109	37
8	101	130
11	164	149
15	211	137
24	143	155

Table 17 - Data for Figure 5 in Chapter 3: SOUR (mg O_2/g MLVSS-hr) in ammonia-shocked reactors versus the control.

NH_3 (2 day SRT)				
cycle	control	3X	9X	18X
2	117	114	81	60
5	93	90	81	50
9	104	102	96	100
13	141	165	149	51
17	113	122	119	129
25	137	135	133	137

Appendix B – Data for Chapter 4

Table 1 - Data for Table 1 in Chapter 4: concentration of DNA (mg/L) in the soluble phase of unshocked mixed liquor.

Experiment	Condition*		Average	Std. Dev.
DNP	control	beg	0.74	0.00
		end	0.66	0.07
	20 sec	beg	3.68	0.07
		end	1.29	0.07
	60 sec	beg	4.99	0.00
		end	1.52	0.07
Cyanide	control	beg	0.74	0.00
		end	0.74	0.00
	20 sec	beg	1.21	0.00
		end	0.86	0.00
	60 sec	beg	3.15	0.07
		end	1.09	0.00
NEM	control	beg	0.78	0.07
		end	0.74	0.00
	20 sec	beg	0.86	0.00
		end	0.98	0.00
	60 sec	beg	2.26	0.00
		end	1.09	0.00
Cadmium	control	beg	0.66	0.07
		end	0.74	0.00
	20 sec	beg	1.17	0.07
		end	0.90	0.07
	60 sec	beg	2.38	0.00
		end	1.09	0.00
Octanol	control	beg	1.09	0.00
		end	1.05	0.07
	20 sec	beg	2.05	0.04
		end	1.60	0.07
	60 sec	beg	2.76	0.07
		end	2.03	0.00

* control – unsheared mixed liquor
20 sec – 20 sec sheared mixed liquor
60 sec – 60 sec sheared mixed liquor
beg – beginning of SOUR run period
end – end of SOUR run period

Table 2 - Data for Table 1 in Chapter 4: concentration of carbohydrates (mg/L) in the soluble phase of unshocked mixed liquor.

Condition*		Replicate #		Average	Std. Dev.
DNP experiment					
control	beg	1	2.42		
		2	2.42		
		3	2.13	2.32	0.16
	end	1	2.42		
		2	2.27		
		3	2.13	2.27	0.14
20 sec	beg	1	8.52		
		2	8.89		
		3	10.03	9.15	0.79
	end	1	6.08		
		2	5.11		
		3	5.43	5.54	0.50
60 sec	beg	1	11.86		
		2	12.07		
		3	12.07	12.00	0.12
	end	1	7.10		
		2	6.93		
		3	7.10	7.04	0.10
Cyanide experiment					
control	beg	1	2.99		
		2	2.70		
		3	3.28	2.99	0.29
	end	1	2.99		
		2	2.99		
		3	3.58	3.18	0.34
20 sec	beg	1	5.11		
		2	4.80		
		3	4.64	4.85	0.24
	end	1	4.03		
		2	3.88		
		3	3.28	3.73	0.39
60 sec	beg	1	8.16		
		2	7.80		
		3	9.08	8.34	0.66
	end	1	5.11		
		2	5.76		
		3	4.95	5.27	0.42

Condition		Replicate #		Average	Std. Dev.
NEM experiment					
control	beg	1	2.42		
		2	2.99		
		3	1.99	2.47	0.50
	end	1	1.99		
		2	2.13		
		3	2.13	2.09	0.08
20 sec	beg	1	3.88		
		2	3.58		
		3	3.58	3.68	0.17
	end	1	2.70		
		2	3.13		
		3	2.84	2.89	0.22
60 sec	beg	1	8.16		
		2	7.27		
		3	8.52	7.98	0.64
	end	1	4.18		
		2	3.88		
		3	3.88	3.98	0.18
Cadmium experiment					
control	beg	1	2.42		
		2	2.70		
		3	2.42	2.51	0.16
	end	1	2.56		
		2	2.56		
		3	2.13	2.42	0.24
20 sec	beg	1	3.88		
		2	4.18		
		3	3.88	3.98	0.18
	end	1	2.84		
		2	2.84		
		3	2.84	2.84	0.00
60 sec	beg	1	7.98		
		2	9.84		
		3	10.03	9.28	1.14
	end	1	5.59		
		2	3.88		
		3	3.88	4.45	0.99

Condition		Replicate #		Average	Std. Dev.
Octanol experiment					
control	beg	1	3.12		
		2	3.12		
		3	4.26		
		4	4.46	3.74	0.72
	end	1	4.26		
		2	4.46		
		3	3.49		
		4	4.07	4.07	0.42
20 sec	beg	1	6.06		
		2	6.68		
		3	7.10		
		4	7.74	6.90	0.71
	end	1	4.46		
		2	4.66		
		3	5.45		
		4	5.05	4.90	0.44
60 sec	beg	1	11.86		
		2	13.10		
		3	11.62	12.19	0.79
	end	1	10.20		
		2	8.18		
		3	8.40		
		4	8.40	8.79	0.94

* control – unsheared mixed liquor
20 sec – 20 sec sheared mixed liquor
60 sec – 60 sec sheared mixed liquor
beg – beginning of SOUR run period
end – end of SOUR run period

Table 3 - Data for Table 1 in Chapter 4: absorbance measurements for the determination of the concentration of proteins and humic acids in the soluble phase of unshocked mixed liquor (triplicates of two independent samples).

Condition**	Replicate #	With $CuSO_4$				Without $CuSO_4$			
		Absorbance	Avg. Abs.	Std. Dev. Abs.	Corrected Avg. Abs.*	Absorbance	Avg. Abs.	Std. Dev. Abs.	Corrected Avg. Abs.*
DNP experiment									
control beg	1	0.059				0.032			
	2	0.058				0.031			
	3	0.059				0.032			
	4	0.058				0.032			
	5	0.058				0.032			
	6	0.058	0.058	0.000	0.031	0.032	0.032	0.000	0.024
control end	1	0.059				0.033			
	2	0.059				0.033			
	3	0.059				0.033			
	4	0.058				0.033			
	5	0.059				0.033			
	6	0.060	0.059	0.001	0.032	0.033	0.033	0.000	0.025
20 sec beg	1	0.204				0.081			
	2	0.202				0.081			
	3	0.195				0.081			
	4	0.193				0.081			
	5	0.188				0.081			
	6	0.189	0.195	0.007	0.168	0.081	0.081	0.000	0.073
20 sec end	1	0.107				0.042			
	2	0.107				0.042			
	3	0.104				0.042			
	4	0.104				0.042			
	5	0.102				0.042			
	6	0.102	0.104	0.002	0.077	0.042	0.042	0.000	0.034
60 sec beg	1	0.283				0.119			
	2	0.282				0.118			
	3	0.279				0.120			
	4	0.278				0.120			
	5	0.276				0.124			

Condition**	Replicate #	With $CuSO_4$				Without $CuSO_4$			
		Absorbance	Avg. Abs.	Std. Dev. Abs.	Corrected Avg. Abs.*	Absorbance	Avg. Abs.	Std. Dev. Abs.	Corrected Avg. Abs.*
DNP experiment (cont.)									
	6	0.275	0.279	0.003	0.251	0.123	0.121	0.002	0.113
60 sec end	1	0.124				0.047			
	2	0.124				0.047			
	3	0.124				0.047			
	4	0.124				0.047			
	5	0.128				0.048			
	6	0.128	0.126	0.002	0.098	0.047	0.047	0.000	0.039
Cyanide experiment									
control beg	1	0.064				0.036			
	2	0.064				0.036			
	3	0.063				0.037			
	4	0.064				0.037			
	5	0.064				0.037			
	6	0.063	0.064	0.001	0.033	0.037	0.037	0.000	0.029
control end	1	0.064				0.037			
	2	0.064				0.037			
	3	0.065				0.037			
	4	0.064				0.037			
	5	0.065				0.038			
	6	0.067	0.065	0.001	0.035	0.038	0.037	0.000	0.030
20 sec beg	1	0.092				0.045			
	2	0.090				0.045			
	3	0.093				0.045			
	4	0.095				0.045			
	5	0.095				0.045			
	6	0.093	0.093	0.002	0.063	0.045	0.045	0.000	0.037
20 sec end	1	0.074				0.039			
	2	0.074				0.039			
	3	0.075				0.039			
	4	0.074				0.039			
	5	0.074				0.039			
	6	0.074	0.074	0.000	0.044	0.039	0.039	0.000	0.031

Condition**	Replicate #	With $CuSO_4$				Without $CuSO_4$			
		Absorbance	Avg. Abs.	Std. Dev. Abs.	Corrected Avg. Abs.*	Absorbance	Avg. Abs.	Std. Dev. Abs.	Corrected Avg. Abs.*
Cyanide experiment (cont.)									
60 sec beg	1	0.167				0.072			
	2	0.167				0.072			
	3	0.168				0.072			
	4	0.165				0.072			
	5	0.164				0.073			
	6	0.163	0.166	0.002	0.136	0.073	0.073	0.000	0.065
60 sec end	1	0.085				0.042			
	2	0.085				0.042			
	3	0.084				0.042			
	4	0.083				0.042			
	5	0.085				0.045			
	6	0.086	0.085	0.001	0.054	0.046	0.043	0.002	0.035
NEM experiment									
control beg	1	0.062				0.038			
	2	0.061				0.038			
	3	0.062				0.038			
	4	0.062				0.038			
	5	0.063				0.038			
	6	0.062	0.062	0.001	0.032	0.039	0.038	0.000	0.030
control end	1	0.065				0.043			
	2	0.063				0.043			
	3	0.066				0.042			
	4	0.066				0.042			
	5	0.066				0.041			
	6	0.065	0.065	0.001	0.035	0.041	0.042	0.001	0.034
20 sec beg	1	0.084				0.042			
	2	0.084				0.042			
	3	0.082				0.041			
	4	0.082				0.041			
	5	0.084				0.041			
	6	0.084	0.083	0.001	0.053	0.041	0.041	0.000	0.033
20 sec end	1	0.071				0.038			

Condition**	Replicate #	With $CuSO_4$				Without $CuSO_4$			
		Absorbance	Avg. Abs.	Std. Dev. Abs.	Corrected Avg. Abs.*	Absorbance	Avg. Abs.	Std. Dev. Abs.	Corrected Avg. Abs.*
NEM experiment (cont.)									
	2	0.071				0.038			
	3	0.071				0.038			
	4	0.071				0.038			
	5	0.071				0.039			
	6	0.073	0.072	0.001	0.041	0.039	0.038	0.000	0.031
60 sec beg	1	0.150				0.061			
	2	0.150				0.061			
	3	0.151				0.061			
	4	0.151				0.061			
	5	0.150				0.062			
	6	0.149	0.150	0.001	0.123	0.062	0.061	0.000	0.054
60 sec end	1	0.087				0.042			
	2	0.087				0.042			
	3	0.086				0.043			
	4	0.086				0.043			
	5	0.085				0.043			
	6	0.085	0.086	0.001	0.059	0.043	0.042	0.000	0.035
Cadmium experiment									
control beg	1	0.063				0.037			
	2	0.063				0.037			
	3	0.062				0.037			
	4	0.062				0.037			
	5	0.062				0.038			
	6	0.062	0.062	0.000	0.035	0.038	0.037	0.001	0.029
control end	1	0.064				0.037			
	2	0.063				0.037			
	3	0.063				0.037			
	4	0.063				0.037			
	5	0.063				0.037			
	6	0.063	0.063	0.000	0.036	0.037	0.037	0.000	0.029
20 sec beg	1	0.090				0.042			
	2	0.089				0.042			

Condition**	Replicate #	With $CuSO_4$ Absorbance	Avg. Abs.	Std. Dev. Abs.	Corrected Avg. Abs.*	Without $CuSO_4$ Absorbance	Avg. Abs.	Std. Dev. Abs.	Corrected Avg. Abs.*
Cadmium experiment (cont.)									
	3	0.089				0.043			
	4	0.088				0.043			
	5	0.088				0.043			
	6	0.088	0.089	0.001	0.061	0.043	0.043	0.000	0.035
20 sec end	1	0.070				0.038			
	2	0.069				0.038			
	3	0.068				0.038			
	4	0.069				0.038			
	5	0.068				0.038			
	6	0.068	0.069	0.001	0.041	0.038	0.038	0.000	0.030
60 sec beg	1	0.161				0.068			
	2	0.161				0.068			
	3	0.158				0.069			
	4	0.158				0.069			
	5	0.155				0.070			
	6	0.155	0.158	0.003	0.130	0.070	0.069	0.001	0.061
60 sec end	1	0.090				0.044			
	2	0.090				0.044			
	3	0.089				0.044			
	4	0.089				0.044			
	5	0.088				0.044			
	6	0.088	0.089	0.001	0.061	0.044	0.044	0.000	0.036
Octanol experiment									
control beg	1	0.077				0.045			
	2	0.077				0.044			
	3	0.076				0.044			
	4	0.076				0.044			
	5	0.076				0.045			
	6	0.075	0.076	0.001	0.046	0.045	0.044	0.000	0.037
control end	1	0.077				0.044			
	2	0.077				0.044			
	3	0.077				0.044			

Condition**	Replicate #	With $CuSO_4$ Absorbance	Avg. Abs.	Std. Dev. Abs.	Corrected Avg. Abs.*	Without $CuSO_4$ Absorbance	Avg. Abs.	Std. Dev. Abs.	Corrected Avg. Abs.*
Octanol experiment (cont.)									
	4	0.077				0.044			
	5	0.078				0.044			
	6	0.077	0.077	0.000	0.047	0.044	0.044	0.000	0.036
20 sec beg	1	0.136				0.056			
	2	0.136				0.057			
	3	0.135				0.056			
	4	0.134				0.056			
	5	0.135				0.057			
	6	0.135	0.135	0.001	0.105	0.057	0.056	0.000	0.049
20 sec end	1	0.106				0.051			
	2	0.106				0.051			
	3	0.107				0.053			
	4	0.106				0.053			
	5	0.107				0.052			
	6	0.107	0.106	0.001	0.076	0.052	0.052	0.001	0.044
60 sec beg	1	0.192				0.069			
	2	0.192				0.069			
	3	0.194				0.069			
	4	0.193				0.069			
	5	0.192				0.069			
	6	0.192	0.192	0.001	0.162	0.069	0.069	0.000	0.061
60 sec end	1	0.142				0.056			
	2	0.143				0.056			
	3	0.138				0.056			
	4	0.138				0.055			
	5	0.142				0.056			
	6	0.142	0.141	0.002	0.111	0.056	0.056	0.000	0.048

* Corrected Average Absorbance = Average Absorbance – Average Absorbance Blank (nanopure water + reagents)
** control – unsheared mixed liquor, 20 sec – 20 sec sheared mixed liquor, 60 sec – 60 sec sheared mixed liquor, beg – beginning of SOUR run period, end – end of SOUR run period

Table 4 - Data for Table 1 in Chapter 4: concentration of proteins and humic acids in the soluble phase of unshocked mixed liquor.

Condition*	Abs. with $CuSO_4$	Abs. without $CuSO_4$	Abs. proteins**	Abs. humic acids**	Proteins (mg/L)	Humic Acids (mg/L)
DNP experiment						
control beg	0.0308	0.0239	0.0087	0.0222	0.6	5.2
control end	0.0315	0.0251	0.0081	0.0235	0.5	5.6
20 sec beg	0.1677	0.0730	0.1184	0.0493	12.1	12.5
20 sec end	0.0767	0.0342	0.0531	0.0236	5.0	5.6
60 sec beg	0.2514	0.1129	0.1731	0.0782	18.5	20.6
60 sec end	0.0981	0.0393	0.0734	0.0247	7.2	5.9
Cyanide experiment						
control beg	0.0334	0.0290	0.0056	0.0278	0.5	6.4
control end	0.0347	0.0296	0.0064	0.0283	0.6	6.5
20 sec beg	0.0628	0.0369	0.0324	0.0304	3.0	7.1
20 sec end	0.0438	0.0310	0.0160	0.0278	1.5	6.4
60 sec beg	0.1356	0.0648	0.0885	0.0471	8.8	11.0
60 sec end	0.0544	0.0354	0.0238	0.0306	2.2	7.1
NEM experiment						
control beg	0.0319	0.0300	0.0023	0.0296	0.2	6.8
control end	0.0350	0.0340	0.0012	0.0337	0.1	7.8
20 sec beg	0.0530	0.0335	0.0244	0.0286	2.3	6.6
20 sec end	0.0414	0.0305	0.0135	0.0278	1.3	6.4
60 sec beg	0.1228	0.0536	0.0865	0.0363	8.6	9.0
60 sec end	0.0586	0.0346	0.0300	0.0286	2.7	6.9
Cadmium experiment						
control beg	0.0347	0.0295	0.0065	0.0282	0.4	6.8
control end	0.0357	0.0294	0.0079	0.0278	0.5	6.7
20 sec beg	0.0611	0.0347	0.0329	0.0281	3.0	6.8
20 sec end	0.0412	0.0297	0.0144	0.0268	1.1	6.5
60 sec beg	0.1304	0.0609	0.0869	0.0436	8.6	11.0
60 sec end	0.0615	0.0361	0.0317	0.0298	2.9	7.3
Octanol experiment						
control beg	0.0460	0.0366	0.0117	0.0343	1.1	8.0
control end	0.0471	0.0359	0.0139	0.0331	1.3	7.7
20 sec beg	0.1050	0.0486	0.0705	0.0345	6.9	8.0
20 sec end	0.0762	0.0441	0.0401	0.0361	3.8	8.4
60 sec beg	0.1623	0.0612	0.1263	0.0360	13.1	8.4
60 sec end	0.1106	0.0479	0.0783	0.0323	7.7	7.5

* control – unsheared mixed liquor
20 sec – 20 sec sheared mixed liquor
60 sec – 60 sec sheared mixed liquor
beg – beginning of SOUR run period
end – end of SOUR run period

** Abs. proteins = 1.25 x (Abs. with $CuSO_4$ – Abs. without $CuSO_4$)
Abs. humic acids = 1.25 x Abs. without $CuSO_4$ – 0.25 x Abs. with $CuSO_4$

Table 5 - Data for Figure 2 in Chapter 4: median floc diameters measured during the DNP shear experiment (triplicates of two independent samples).

	unsheared	60 sec sheared	
	beginning	beginning	end
1A	61.6	27.5	40.6
1B	73.4	30.5	41.4
1C	66.5	24.7	39.7
2A	68.2	33.0	42.1
2B	66.1	30.9	42.0
2C	67.3	32.0	41.4
average	67.2	29.8	41.2
standard deviation	3.8	3.1	0.9

Table 6 - Data for Figure 2 in Chapter 4: median floc diameters measured during the cyanide shear experiment (triplicates of two independent samples).

	unsheared		20 sec sheared		60 sec sheared	
	beginning	end	beginning	end	beginning	end
1A	68.6	68.6	36.9	43.0	23.5	39.8
1B	69.1	69.0	37.7	43.1	25.7	40.3
1C	68.4	67.0	38.2	42.2	26.4	39.5
2A	68.1	68.5	37.7	41.5	25.8	39.5
2B	68.8	67.6	36.7	41.4	23.8	39.8
2C	69.1	68.4	35.1	40.1	27.2	40.4
average	68.7	68.2	37.0	41.9	25.4	39.9
standard deviation	0.4	0.7	1.1	1.1	1.5	0.4

Table 7 - Data for Figure 2 in Chapter 4: median floc diameters measured during the NEM shear experiment (triplicates of two independent samples).

	unsheared		20 sec sheared		60 sec sheared	
	beginning	end	beginning	end	beginning	end
1A	66.3	68.5	33.2	45.8	26.3	37.5
1B	68.2	68.1	32.6	45.8	27.5	37.4
1C	67.1	68.1	33.4	45.4	27.1	36.0
2A	68.2	67.8	33.1	45.8	27.3	37.4
2B	67.1	68.8	33.4	46.9	28.2	38.8
2C	67.8	67.4	34.0	46.1	27.2	38.9
average	67.5	68.1	33.3	45.9	27.3	37.7
standard deviation	0.7	0.5	0.5	0.5	0.6	1.1

Table 8 - Data for Figure 2 in Chapter 4: median floc diameters measured during the cadmium shear experiment (triplicates of two independent samples).

	unsheared		20 sec sheared		60 sec sheared	
	beginning	end	beginning	end	beginning	end
1A	67.8	69.1	33.0	45.0	26.5	36.7
1B	69.1	68.9	32.5	44.3	27.6	37.1
1C	67.5	70.1	33.7	43.2	26.6	37.1
2A	68.5	67.5	32.2	46.9	27.1	38.6
2B	69.7	69.1	32.3	45.8	27.9	38.2
2C	69.3	66.7	32.9	44.9	28.2	36.5
average	68.7	68.5	32.8	45.0	27.3	37.4
standard deviation	0.9	1.2	0.6	1.3	0.7	0.9

Table 9 - Data for Figure 2 in Chapter 4: median floc diameters measured during the octanol shear experiment (triplicates of two independent samples).

	unsheared		20 sec sheared		60 sec sheared	
	beginning	end	beginning	end	beginning	end
1A	66.2	66.8	32.7	39.1	26.4	36.4
1B	66.5	66.0	30.8	40.2	29.2	37.3
1C	65.8	66.9	35.3	39.4	29.4	37.0
2A	67.5	66.6	35.3	39.0	29.3	37.3
2B	66.7	67.5	35.2	38.9	29.9	36.1
2C		66.7	35.7	39.2	28.8	36.8
average	66.5	66.8	34.1	39.3	28.8	36.8
standard deviation	0.6	0.5	2.0	0.5	1.3	0.5

Table 10 - Data for Figure 3 in Chapter 4: example of PSD of unsheared mixed liquor.

Particle size	% particles		
(μm)	A1	A2	B
262.40	0.7	0.4	0.2
229.10	2.2	1.0	0.4
200.00	5.7	2.3	0.8
174.60	11.2	4.4	1.7
152.40	17.5	7.4	3.3
133.10	16.2	8.6	4.9
116.20	14.1	10.2	7.6
101.40	9.8	10.3	9.9
88.58	6.3	9.4	11.2
77.34	3.8	8.1	11.3
67.52	2.3	6.7	10.3
58.95	1.5	5.4	8.6
51.47	1.0	4.3	6.7
44.94	0.7	3.4	5.0
39.23	0.6	2.7	3.6
34.25	0.5	2.2	2.6
29.91	0.4	1.8	1.9
26.11	0.4	1.5	1.4
22.80	0.4	1.3	1.2
19.90	0.4	1.1	0.9
17.38	0.4	1.0	0.8
15.17	0.4	1.0	0.8
13.25	0.5	0.9	0.8
11.56	0.5	0.9	0.7
10.10	0.5	0.8	0.7
8.82	0.5	0.8	0.7
7.70	0.4	0.7	0.6
6.72	0.3	0.5	0.4
5.87	0.2	0.3	0.3
5.12	0.2	0.2	0.2
4.47	0.1	0.2	0.1
3.90	0.1	0.1	0.1
3.41	0.1	0.1	0.1

Table 11 - Data for Figure 3 in Chapter 4: example of PSD of unsheared and sheared mixed liquor from the cyanide shear experiment.

Particle size (μm)	% particles					
	unsheared		20 sec sheared		60 sec sheared	
	beginning	end	beginning	end	beginning	end
262.40	0.2	0.2	0.0	0.1	0.0	0.0
229.10	0.4	0.4	0.2	0.2	0.0	0.1
200.00	0.8	0.8	0.3	0.3	0.0	0.3
174.60	1.7	1.7	0.4	0.5	0.1	0.5
152.40	3.3	3.3	0.8	0.9	0.2	0.8
133.10	4.9	4.9	1.1	1.4	0.4	1.2
116.20	7.6	7.6	1.7	2.2	0.6	1.8
101.40	9.9	9.8	2.5	3.4	0.9	2.8
88.58	11.2	11.1	3.4	4.7	1.4	4.0
77.34	11.3	11.2	4.6	6.2	2.0	5.3
67.52	10.3	10.3	6.0	7.7	2.8	6.9
58.95	8.6	8.6	7.3	8.8	3.9	8.3
51.47	6.7	6.7	8.6	9.4	5.2	9.4
44.94	5.0	5.1	9.1	9.1	6.5	9.6
39.23	3.6	3.7	8.9	8.2	7.6	8.9
34.25	2.6	2.7	8.2	7.0	8.5	7.8
29.91	1.9	2.0	7.1	5.7	8.9	6.4
26.11	1.4	1.5	5.8	4.5	8.4	5.0
22.80	1.2	1.2	4.7	3.6	7.7	3.9
19.90	0.9	0.9	3.6	2.7	6.4	3.0
17.38	0.8	0.8	2.8	2.2	5.3	2.3
15.17	0.8	0.8	2.4	1.9	4.5	2.0
13.25	0.8	0.8	2.1	1.7	3.7	1.8
11.56	0.7	0.7	1.8	1.5	3.1	1.5
10.10	0.7	0.7	1.6	1.4	2.7	1.4
8.82	0.7	0.7	1.5	1.3	2.4	1.3
7.70	0.6	0.6	1.2	1.1	1.9	1.1
6.72	0.4	0.4	0.8	0.8	1.3	0.8
5.87	0.3	0.3	0.6	0.5	1.0	0.6
5.12	0.2	0.2	0.4	0.4	0.8	0.4
4.47	0.1	0.2	0.3	0.3	0.6	0.3
3.90	0.1	0.1	0.2	0.2	0.5	0.2
3.41	0.1	0.1	0.2	0.2	0.4	0.2
2.98	0.0	0.0	0.1	0.1	0.3	0.1
2.60	0.0	0.0	0.0	0.0	0.1	0.0
2.27	0.0	0.0	0.0	0.0	0.0	0.0
1.98	0.0	0.0	0.0	0.0	0.0	0.0

Table 12 - Data for Figure 4 in Chapter 4: OUR, SOUR and % inhibition SOUR for unsheared mixed liquor.

Octanol (mg/L)	OUR (mg O_2/L-min)		R^2		SOUR (mg O_2/g VSS-hr)			% inhibition		
	1	2	1	2	1	2	Average	1	2	Average
0	0.27	0.30	1.00	1.00	11.20	12.20	11.70	Control beginning		
0	0.24	0.25	1.00	1.00	10.93	11.00	10.96	Control end		
100	0.25	0.25	1.00	1.00	10.48	10.61	10.54	5.4	4.2	4.8
151	0.21	0.22	1.00	1.00	8.92	9.54	9.23	21.2	15.7	18.5
201	0.19	0.20	1.00	1.00	8.07	8.42	8.24	29.5	26.4	28.0
277	0.09	0.12	0.99	1.00	4.03	5.28	4.65	65.1	54.4	59.8
352	0.06	0.06	0.99	0.99	2.50	2.35	2.42	77.7	79.0	78.3

Table 13 - Data for Figure 4 in Chapter 4: OUR, SOUR and % inhibition SOUR for 20 sec sheared mixed liquor.

Octanol (mg/L)	OUR (mg O_2/L-min)		R^2		SOUR (mg O_2/g VSS-hr)			% inhibition		
	1	2	1	2	1	2	Average	1	2	Average
0	0.33	0.34	1.00	1.00	13.52	13.72	13.62	Control beginning		
0	0.32	0.33	0.99	0.99	13.67	13.91	13.79	Control end		
100	0.28	0.28	1.00	1.00	11.62	11.54	11.58	15.6	16.2	15.9
151	0.22	0.24	1.00	1.00	9.22	9.98	9.60	32.6	27.1	29.8
201	-	-	-	-	-	-	-	-	-	-
277	0.12	0.13	1.00	1.00	4.84	5.30	5.07	64.5	61.2	62.9
352	0.06	0.06	0.99	0.99	2.68	2.54	2.61	80.5	81.5	81.0

Table 14 - Data for Figure 4 in Chapter 4: OUR, SOUR and % inhibition SOUR for 60 sec sheared mixed liquor.

Octanol (mg/L)	OUR (mg O_2/L-min)		R^2		SOUR (mg O_2/g VSS-hr)			% inhibition		
	1	2	1	2	1	2	Average	1	2	Average
0	0.29	0.30	1.00	1.00	11.00	11.40	11.20	Control beginning		
0	0.45	0.47	0.99	0.99	18.74	19.58	19.16	Control end		
100	0.29	0.29	1.00	1.00	11.26	11.41	11.33	19.2	18.1	18.6
151	0.25	0.25	1.00	1.00	9.77	10.01	9.89	36.8	35.3	36.1
201	0.22	0.23	1.00	1.00	8.72	9.20	8.96	48.3	45.5	46.9
277	0.12	0.16	1.00	1.00	4.67	6.18	5.43	74.5	66.3	70.4
352	0.07	0.06	0.99	1.00	2.65	2.33	2.49	79.3	81.8	80.5

Table 15 - Data for Figure 5A in Chapter 4: OUR, SOUR and % inhibition SOUR.

Cadmium (mg/L)	OUR (mg O_2/L-min)		R^2		SOUR (mg O_2/g VSS-hr)			% inhibition		
	1	2	1	2	1	2	Average	1	2	Average
unsheared										
0	0.71	0.72	1.00	1.00	34.38	34.77	34.57	Control beginning		
0	0.69	0.77	1.00	1.00	30.55	34.27	32.41	Control end		
20	0.59	0.59	1.00	1.00	27.48	27.56	27.52	18.0	17.7	17.8
100	0.21	0.20	0.99	0.99	10.15	9.95	10.05	69.7	70.3	70.0
30 sec sheared										
0	0.81	0.88	1.00	1.00	37.72	40.97	39.34	Control beginning*		
0	0.60	0.61	1.00	1.00	25.75	25.94	25.84	Control end*		
20	0.52	0.58	1.00	1.00	23.46	25.86	24.66	40.4	34.3	37.3
100	0.18	0.18	0.99	0.99	8.41	8.64	8.53	78.6	78.0	78.3

* Only the control SOUR measured at the beginning of the experiment was used for the determination of the % inhibition SOUR. This was done because the value of the control SOUR taken at the end of the experimental period was too low, presumably due to contamination of the mixed liquor sample.

Table 16 - Data for Figure 5B in Chapter 4: OUR, SOUR and % inhibition SOUR.

Cadmium (mg/L)	OUR (mg O_2/L-min)		R^2		SOUR (mg O_2/g VSS-hr)			% inhibition		
	1	2	1	2	1	2	Average	1	2	Average
unsheared										
0	0.70	0.61	1.00	1.00	26.77	23.06	24.92	Control beginning		
0	0.84	0.87	1.00	1.00	31.55	32.87	32.21	Control end		
10	0.66	0.70	1.00	1.00	25.26	26.78	26.02	11.6	6.2	8.9
20	0.62	0.64	1.00	1.00	23.73	24.45	24.09	16.9	14.4	15.7
60	0.45	0.46	0.99	0.99	17.60	17.88	17.74	38.4	37.4	37.9
133	0.24	0.25	0.99	0.99	9.80	10.08	9.94	65.7	64.7	65.2
30 sec sheared										
0	0.97	0.99	1.00	1.00	33.83	34.72	34.28	Control beginning		
0	0.82	0.85	1.00	1.00	28.93	30.02	29.48	Control end		
10	0.43	0.47	0.99	0.99	15.33	16.79	16.06	7.8	5.4	6.6
20	0.32	0.29	0.99	0.99	11.73	10.60	11.17	21.2	18.2	19.7
60	0.97	0.99	1.00	1.00	33.83	34.72	34.28	58.2	54.2	56.2
100	0.82	0.85	1.00	1.00	28.93	30.02	29.48	68.0	71.1	69.6

Table 17 - Data for Figure 5C in Chapter 4: OUR, SOUR and % inhibition SOUR for unsheared mixed liquor.

Cadmium (mg/L)	OUR (mg O_2/L-min)		R^2		SOUR (mg O_2/g VSS-hr)			% inhibition		
	1	2	1	2	1	2	Average	1	2	Average
0	0.31	0.32	1.00	1.00	12.08	12.55	12.32	Control beginning		
0	0.37	0.39	0.99	0.99	14.42	15.30	14.86	Control end		
20	0.26	0.26	1.00	1.00	10.24	10.36	10.30	24.7	23.8	24.2
50	0.21	0.22	1.00	1.00	8.39	8.97	8.68	38.3	34.0	36.1
80	0.19	0.21	1.00	1.00	7.82	8.47	8.14	42.5	37.7	40.1
120	0.17	0.18	1.00	1.00	7.13	7.43	7.28	47.5	45.3	46.4
160	0.16	0.15	1.00	1.00	6.67	6.49	6.58	50.9	52.3	51.6

Table 18 - Data for Figure 5C in Chapter 4: OUR, SOUR and % inhibition SOUR for 20 sec sheared mixed liquor.

Cadmium (mg/L)	OUR (mg O_2/L-min)		R^2		SOUR (mg O_2/g VSS-hr)			% inhibition		
	1	2	1	2	1	2	Average	1	2	Average
0	0.38	0.39	1.00	1.00	14.92	15.21	15.07	Control beginning		
0	0.36	0.40	1.00	1.00	14.23	15.71	14.97	Control end		
20	0.31	0.32	1.00	1.00	12.31	12.70	12.51	18.0	15.4	16.7
50	0.23	0.24	1.00	1.00	9.14	9.88	9.51	39.2	34.2	36.7
80	0.20	0.21	1.00	1.00	8.36	8.68	8.52	44.3	42.2	43.3
120	0.17	0.19	1.00	1.00	7.09	7.79	7.44	52.8	48.1	50.4
160	0.15	0.15	1.00	1.00	6.30	6.52	6.41	58.1	56.6	57.3

Table 19 - Data for Figure 5C in Chapter 4: OUR, SOUR and % inhibition SOUR for 60 sec sheared mixed liquor.

Cadmium (mg/L)	OUR (mg O_2/L-min)		R^2		SOUR (mg O_2/g VSS-hr)			% inhibition		
	1	2	1	2	1	2	Average	1	2	Average
0	0.40	0.41	1.00	1.00	15.91	16.34	16.13	Control beginning		
0	0.29	0.30	1.00	1.00	11.50	11.97	11.73	Control end		
20	0.29	0.30	1.00	1.00	11.70	12.19	11.95	16.0	12.5	14.2
50	0.22	0.23	1.00	1.00	9.01	9.40	9.20	35.3	32.5	33.9
80	0.18	0.18	1.00	1.00	7.46	7.68	7.57	46.5	44.9	45.7
120	0.15	0.16	1.00	1.00	6.39	6.84	6.62	54.1	50.9	52.5
160	0.13	0.14	1.00	1.00	5.63	5.90	5.76	59.6	57.7	58.6

Table 20 - Data for Figure 6A in Chapter 4: OUR, SOUR and % inhibition SOUR.

NEM (mg/L)	OUR (mg O_2/L-min)		R^2		SOUR (mg O_2/g VSS-hr)			% inhibition		
	1	2	1	2	1	2	Average	1	2	Average
unsheared										
0	0.71	0.72	1.00	1.00	34.38	34.77	34.57	Control beginning		
0	0.69	0.77	1.00	1.00	30.55	34.27	32.41	Control end		
20	0.21	0.22	0.99	0.99	9.92	10.47	10.19	70.4	68.7	69.6
60	0.16	0.16	0.99	0.99	7.43	7.72	7.58	77.8	76.9	77.4
30 sec sheared										
0	0.81	0.88	1.00	1.00	37.72	40.97	39.34	Control beginning*		
0	0.60	0.61	1.00	1.00	25.75	25.94	25.84	Control end*		
20	0.24	0.25	0.99	0.99	10.58	11.05	10.81	73.1	71.9	72.5
60	0.15	0.15	0.99	0.99	6.90	6.92	6.91	82.5	82.4	82.4

* Only the control SOUR measured at the beginning of the experiment was used for the determination of the % inhibition SOUR. This was done because the value of the control SOUR taken at the end of the experimental period was too low, presumably due to contamination of the mixed liquor sample.

Table 21 - Data for Figure 6B in Chapter 4: OUR, SOUR and % inhibition SOUR.

NEM (mg/L)	OUR (mg O_2/L-min)		R^2		SOUR (mg O_2/g VSS-hr)			% inhibition		
	1	2	1	2	1	2	Average	1	2	Average
unsheared										
0	0.53	0.55	1.00	1.00	22.91	23.79	23.35	Control beginning		
0	0.64	0.66	1.00	1.00	26.57	27.69	27.13	Control end		
5	0.31	0.32	1.00	1.00	13.14	13.84	13.49	47.9	45.1	46.5
10	0.26	0.27	0.99	0.99	11.13	11.41	11.27	55.9	54.8	55.3
15	0.24	0.24	0.99	0.99	10.08	10.21	10.15	60.1	59.5	59.8
20	0.21	0.22	0.99	0.99	9.02	9.24	9.13	64.3	63.4	63.8
40	0.18	0.19	0.99	0.99	7.87	8.11	7.99	68.8	67.9	68.4
30 sec sheared										
0	0.78	0.79	1.00	1.00	32.38	32.77	32.57	Control beginning		
0	0.76	0.74	1.00	1.00	31.48	30.39	30.94	Control end		
5	0.48	0.50	1.00	1.00	20.01	20.54	20.27	37.0	35.3	36.2
10	0.36	0.37	0.99	0.99	15.03	15.49	15.26	52.7	51.2	51.9
15	0.26	0.27	0.99	0.99	10.72	11.15	10.94	66.2	64.9	65.6
20	0.24	0.25	0.99	0.99	10.21	10.35	10.28	67.9	67.4	67.6
40	0.19	0.19	0.99	0.99	7.81	7.94	7.87	75.4	75.0	75.2

Table 22 - Data for Figure 6C in Chapter 4: OUR, SOUR and % inhibition SOUR for unsheared mixed liquor.

NEM (mg/L)	OUR (mg O_2/L-min)		R^2		SOUR (mg O_2/g VSS-hr)			% inhibition		
	1	2	1	2	1	2	Average	1	2	Average
0	0.37	0.34	1.00	1.00	14.92	13.44	14.18	Control beginning		
0	0.35	0.32	0.99	0.99	14.19	13.18	13.68	Control end		
2	0.32	0.30	1.00	1.00	13.10	12.36	12.73	6.0	11.3	8.6
5	0.27	0.27	1.00	1.00	11.03	11.00	11.02	20.8	21.0	20.9
10	0.21	0.20	1.00	1.00	8.73	8.24	8.48	37.3	40.9	39.1
20	0.15	0.15	1.00	1.00	6.19	6.08	6.14	55.5	56.4	56.0
50	0.09	0.09	0.98	0.98	3.94	3.90	3.92	71.7	72.0	71.9

Table 23 - Data for Figure 6C in Chapter 4: OUR, SOUR and % inhibition SOUR for 20 sec sheared mixed liquor.

NEM (mg/L)	OUR (mg O_2/L-min)		R^2		SOUR (mg O_2/g VSS-hr)			% inhibition		
	1	2	1	2	1	2	Average	1	2	Average
0	0.38	0.36	1.00	1.00	16.00	15.19	15.59	Control beginning		
0	0.36	0.33	1.00	1.00	14.82	13.79	14.31	Control end		
2	0.33	0.33	0.99	0.99	13.75	13.66	13.70	8.1	8.7	8.4
5	0.28	0.26	1.00	1.00	11.65	10.84	11.25	22.1	27.5	24.8
10	0.20	0.20	1.00	1.00	8.52	8.32	8.42	43.0	44.4	43.7
20	0.15	0.15	1.00	1.00	6.59	6.36	6.48	55.9	57.4	56.7
50	0.10	0.09	0.99	0.99	4.19	4.12	4.15	72.0	72.4	72.2

Table 24 - Data for Figure 6C in Chapter 4: OUR, SOUR and % inhibition SOUR for 60 sec sheared mixed liquor.

NEM (mg/L)	OUR (mg O_2/L-min)		R^2		SOUR (mg O_2/g VSS-hr)			% inhibition		
	1	2	1	2	1	2	Average	1	2	Average
0	0.36	0.32	1.00	1.00	15.34	13.62	14.48	Control beginning		
0	0.35	0.32	0.99	0.99	14.48	13.45	13.97	Control end		
2	0.32	0.31	1.00	1.00	13.48	12.98	13.23	5.2	8.8	7.0
5	0.26	0.24	1.00	1.00	10.89	10.26	10.58	23.4	27.8	25.6
10	0.22	0.21	1.00	1.00	9.41	9.05	9.23	33.8	36.4	35.1
20	0.15	0.14	1.00	1.00	6.44	6.06	6.25	54.8	57.4	56.1
50	0.10	0.10	0.99	0.99	4.30	4.21	4.25	69.8	70.4	70.1

Table 25 - Data for Figure 7 in Chapter 4: OUR, SOUR and % inhibition SOUR for unsheared mixed liquor.

Cyanide (mg/L)	OUR (mg O_2/L-min)		R^2		SOUR (mg O_2/g VSS-hr)			% inhibition		
	1	2	1	2	1	2	Average	1	2	Average
0	0.24	0.25	1.00	1.00	10.10	10.23	10.16	Control beginning		
0	0.27	0.27	1.00	1.00	11.29	11.31	11.30	Control end		
0.2	0.16	0.16	1.00	1.00	6.55	6.51	6.53	39.0	39.3	39.2
0.4	0.13	0.14	1.00	1.00	5.54	5.71	5.63	48.3	46.8	47.6
0.8	0.11	0.09	1.00	1.00	4.64	3.99	4.31	56.8	62.8	59.8
1.5	0.08	0.08	1.00	1.00	3.45	3.52	3.49	67.8	67.2	67.5
3.0	0.06	0.06	1.00	1.00	2.68	2.67	2.67	75.0	75.1	75.1

Table 26 - Data for Figure 7 in Chapter 4: OUR, SOUR and % inhibition SOUR for 20 sec sheared mixed liquor.

Cyanide (mg/L)	OUR (mg O_2/L-min)		R^2		SOUR (mg O_2/g VSS-hr)			% inhibition		
	1	2	1	2	1	2	Average	1	2	Average
0	0.26	0.27	1.00	1.00	10.80	11.34	11.07	Control beginning		
0	0.26	0.26	1.00	1.00	11.36	11.13	11.24	Control end		
0.2	0.18	0.18	1.00	1.00	7.74	7.70	7.72	30.6	31.0	30.8
0.4	0.12	0.12	1.00	1.00	5.29	5.29	5.29	52.6	52.5	52.5
0.8	0.10	0.10	1.00	1.00	4.28	4.22	4.25	61.7	62.2	61.9
1.5	0.07	0.07	1.00	1.00	3.19	3.18	3.19	71.4	71.5	71.4
3.0	0.06	0.06	1.00	1.00	2.72	2.60	2.66	75.6	76.7	76.2

Table 27 - Data for Figure 7 in Chapter 4: OUR, SOUR and % inhibition SOUR for 60 sec sheared mixed liquor.

Cyanide (mg/L)	OUR (mg O_2/L-min)		R^2		SOUR (mg O_2/g VSS-hr)			% inhibition		
	1	2	1	2	1	2	Average	1	2	Average
0	0.23	0.23	1.00	1.00	10.49	10.18	10.34	Control beginning		
0	0.20	0.18	1.00	1.00	8.82	8.09	8.46	Control end		
0.2	0.11	0.12	1.00	1.00	4.95	5.18	5.06	47.3	44.9	46.1
0.4	0.10	0.10	0.99	1.00	4.29	4.54	4.41	54.4	51.7	53.0
0.8	0.08	0.08	1.00	1.00	3.41	3.59	3.50	63.7	61.8	62.8
1.5	0.07	0.06	1.00	1.00	3.04	2.88	2.96	67.6	69.3	68.5
3.0	0.05	0.05	0.99	1.00	2.18	2.49	2.33	76.8	73.5	75.2

Table 28 - Data for Figure 8A in Chapter 4: OUR, SOUR and % inhibition SOUR.

DNP (mg/L)	OUR (mg O_2/L-min)		R^2		SOUR (mg O_2/g VSS-hr)			% inhibition		
	1	2	1	2	1	2	Average	1	2	Average
unsheared										
0	0.71	0.72	1.00	1.00	34.38	34.77	34.57	Control beginning		
0	0.69	0.77	1.00	1.00	30.55	34.27	32.41	Control end		
10	0.57	0.59	1.00	1.00	26.64	27.72	27.18	20.5	17.2	18.8
80	0.12	0.14	1.00	1.00	6.16	6.84	6.50	81.6	79.6	80.6
30 sec sheared										
0	0.81	0.88	1.00	1.00	37.72	40.97	39.34	Control beginning*		
0	0.60	0.61	1.00	1.00	25.75	25.94	25.84	Control end*		
10	0.62	0.65	1.00	1.00	27.77	29.03	28.40	29.4	26.2	27.8
80	0.12	0.13	1.00	1.00	5.86	6.52	6.19	85.1	83.4	84.3

* Only the control SOUR measured at the beginning of the experiment was used for the determination of the % inhibition SOUR. This was done because the value of the control SOUR taken at the end of the experimental period was too low, presumably due to contamination of the mixed liquor sample.

Table 29 - Data for Figure 8B in Chapter 4: OUR, SOUR and % inhibition SOUR for unsheared mixed liquor.

DNP (mg/L)	OUR (mg O_2/L-min)		R^2		SOUR (mg O_2/g VSS-hr)			% inhibition		
	1	2	1	2	1	2	Average	1	2	Average
0	0.62	0.59	1.00	1.00	24.45	23.02	23.73	Control beginning		
0	0.61	0.59	1.00	1.00	23.60	22.76	23.18	Control end		
5	0.47	0.41	1.00	1.00	18.44	16.11	17.27	21.4	31.3	26.4
10	0.28	0.25	1.00	1.00	10.96	10.02	10.49	53.3	57.3	55.3
31	0.14	0.14	1.00	1.00	5.72	5.53	5.62	75.6	76.4	76.0
61	0.08	0.08	1.00	1.00	3.37	3.18	3.28	85.6	86.5	86.0
92	0.05	0.05	1.00	1.00	2.27	2.13	2.20	90.3	90.9	90.6

Table 30 - Data for Figure 8B in Chapter 4: OUR, SOUR and % inhibition SOUR for 20 sec sheared mixed liquor.

DNP (mg/L)	OUR (mg O_2/L-min)		R^2		SOUR (mg O_2/g VSS-hr)			% inhibition		
	1	2	1	2	1	2	Average	1	2	Average
0	0.72	0.65	0.99	0.98	29.57	26.83	28.20	Control beginning		
0	0.55	0.51	0.99	0.99	22.78	21.16	21.97	Control end		
5	0.38	0.31	1.00	1.00	15.96	12.93	14.44	36.4	48.5	42.4
10	0.29	0.25	1.00	1.00	12.04	10.47	11.25	52.0	58.3	55.1
31	0.13	0.10	1.00	1.00	5.44	4.24	4.84	78.3	83.1	80.7
61	0.06	0.06	1.00	1.00	2.60	2.62	2.61	89.6	89.5	89.6
92	0.05	0.05	1.00	0.97	2.22	2.20	2.21	91.1	91.2	91.2

Table 31 - Data for Figure 8B in Chapter 4: OUR, SOUR and % inhibition SOUR for 60 sec sheared mixed liquor.

DNP (mg/L)	OUR (mg O_2/L-min)		R^2		SOUR (mg O_2/g VSS-hr)			% inhibition		
	1	2	1	2	1	2	Average	1	2	Average
0	0.52	0.51	1.00	1.00	22.25	21.84	22.05	Control beginning		
0	0.49	0.45	0.99	0.99	20.62	18.86	19.74	Control end		
5	0.31	0.29	1.00	1.00	13.23	12.51	12.87	36.7	40.1	38.4
10	0.21	0.21	1.00	1.00	9.18	9.09	9.14	56.0	56.5	56.3
31	0.13	0.12	1.00	1.00	5.56	5.34	5.45	73.4	74.4	73.9
61	0.07	0.06	1.00	1.00	2.97	2.49	2.73	85.8	88.1	86.9
92	0.04	0.03	0.99	1.00	1.67	1.55	1.61	92.0	92.6	92.3

Appendix C – Data for Chapter 5

Table 1 - Data for Table 1 in Chapter 5: concentration of carbohydrates (mg/L) in the soluble phase of the control and shocked reactors over time.

Sampling Time	Reactor	Replicate #		Average	Std. Dev.
Experiment 1					
< 5 minutes	Control	1	3.36		
		2	3.36		
		3	3.36	3.36	0.00
	Cadmium	1	4.42		
		2	3.19		
		3	3.01	3.54	0.77
	DNP	1	3.36		
		2	3.36		
		3	3.71	3.48	0.20
	NEM	1	3.36		
		2	3.19		
		3	3.36	3.30	0.10
45 minutes	Control	1	3.19		
		2	3.01		
		3	3.19	3.13	0.10
	Cadmium	1	4.42		
		2	4.06		
		3	4.06	4.18	0.21
	DNP	1	3.36		
		2	3.88		
		3	3.53	3.59	0.27
	NEM	1	5.14		
		2	4.24		
		3	4.24	4.54	0.52
3 hours	Control	1	4.06		
		2	3.71		
		3	3.36	3.71	0.35
	Cadmium	1	8.20		
		2	8.00		
		3	7.80	8.00	0.20
	DNP	1	3.71		
		2	4.06		
		3	3.71	3.83	0.20
	NEM	1	6.26		
		2	6.26		
		3	6.83	6.45	0.33
5 hours	Control	1	3.53		
		2	3.36		
		3	3.36	3.42	0.10

Sampling Time	Reactor	Replicate #		Average	Std. Dev.
Experiment 1 (cont.)					
	Cadmium	1	11.79		
		2	12.01		
		3	12.01	11.93	0.13
	DNP	1	4.06		
		2	4.06		
		3	4.24	4.12	0.10
	NEM	1	7.22		
		2	7.02		
		3	7.02	7.09	0.11
Experiment 2					
< 5 minutes	Control	1	3.53		
		2	3.53		
		3	3.19	3.42	0.20
	Cadmium	1	3.01		
		2	3.01		
		3	3.01	3.01	0.00
	DNP	1	3.36		
		2	3.19		
		3	3.36	3.30	0.10
	NEM	1	3.36		
		2	3.36		
		3	3.71	3.48	0.20
45 minutes	Control	1	3.53		
		2	3.36		
		3	3.36	3.42	0.10
	Cadmium	1	4.06		
		2	3.88		
		3	4.06	4.00	0.10
	DNP	1	3.71		
		2	3.53		
		3	3.36	3.53	0.17
	NEM	1	4.42		
		2	4.42		
		3	4.42	4.42	0.00
3 hours	Control	1	3.36		
		2	3.71		
		3	3.36	3.48	0.20
	Cadmium	1	8.00		
		2	8.00		
		3	7.80	7.94	0.11
	DNP	1	3.71		
		2	3.88		
		3	4.06	3.88	0.18
	NEM	1	6.45		
		2	6.26		
		3	6.26	6.32	0.11
5 hours	Control	1	3.36		
		2	3.53		

Sampling Time	Reactor	Replicate #		Average	Std. Dev.
Experiment 2 (cont.)					
		3	3.53	3.48	0.10
	Cadmium	1	11.13		
		2	11.13		
		3	10.48	10.91	0.37
	DNP	1	3.71		
		2	3.71		
		3	4.06	3.83	0.20
	NEM	1	6.83		
		2	7.02		
		3	7.02	6.96	0.11
Experiment 3					
< 5 minutes	Control	1	5.61		
		2	5.06		
		3	4.70	5.12	0.46
	Cadmium	1	5.06		
		2	5.06		
		3	4.88	5.00	0.10
	DNP	1	5.43		
		2	5.80		
		3	5.80	5.68	0.21
	NEM	1	5.24		
		2	6.56		
		3	5.80	5.87	0.66
45 minutes	Control	1	5.99		
		2	5.43		
		3	5.80	5.74	0.29
	Cadmium	1	5.06		
		2	4.88		
		3	4.88	4.94	0.10
	DNP	1	6.18		
		2	6.18		
		3	5.80	6.05	0.22
	NEM	1	6.37		
		2	5.99		
		3	7.34	6.57	0.70
3 hours	Control	1	5.80		
		2	5.43		
		3	5.61	5.61	0.19
	Cadmium	1	6.56		
		2	6.75		
		3	6.95	6.75	0.19
	DNP	1	6.18		
		2	5.80		
		3	5.80	5.93	0.22
	NEM	1	7.75		
		2	7.54		
		3	7.75	7.68	0.12
5 hours	Control	1	6.18		

Sampling Time	Reactor	Replicate #		Average	Std. Dev.
Experiment 3 (cont.)					
		2	5.80		
		3	5.80	5.93	0.22
	Cadmium	1	8.36		
		2	8.36		
		3	7.75	8.16	0.35
	DNP	1	7.34		
		2	7.34		
		3	6.56	7.08	0.45
	NEM	1	8.15		
		2	8.57		
		3	8.57	8.43	0.24
Experiment 4					
< 5 minutes	Control	1	5.71		
		2	5.53		
		3	5.53	5.59	0.11
	Cadmium	1	4.79		
		2	4.97		
		3	5.16	4.97	0.18
	DNP	1	5.71		
		2	5.34		
		3	5.16	5.40	0.28
	NEM	1	6.67		
		2	7.66		
		3	6.28	6.87	0.71
45 minutes	Control	1	5.90		
		2	5.53		
		3	6.09	5.84	0.29
	Cadmium	1	5.34		
		2	5.34		
		3	5.34	5.34	0.00
	DNP	1	5.71		
		2	5.71		
		3	5.90	5.78	0.11
	NEM	1	6.09		
		2	5.90		
		3	6.09	6.03	0.11
3 hours	Control	1	5.34		
		2	5.34		
		3	5.71	5.46	0.22
	Cadmium	1	6.87		
		2	6.09		
		3	6.09	6.35	0.45
	DNP	1	6.09		
		2	6.09		
		3	5.90	6.03	0.11
	NEM	1	7.26		
		2	7.66		
		3	5.34	6.75	1.24

Sampling Time	Reactor	Replicate #		Average	Std. Dev.
Experiment 4 (cont.)					
5 hours	Control	1	5.34		
		2	5.53		
		3	5.34	5.40	0.11
	Cadmium	1	6.87		
		2	6.87		
		3	6.87	6.87	0.00
	DNP	1	6.28		
		2	6.67		
		3	6.48	6.48	0.19
	NEM	1	7.66		
		2	7.66		
		3	7.86	7.73	0.12
			5.71		
Experiment 5					
< 5 minutes	Control	1	4.48		
		2	4.48		
		3	4.12	4.36	0.21
	Cadmium	1	3.76		
		2	3.76		
		3	4.12	3.88	0.21
	DNP	1	4.12		
		2	4.12		
		3	4.12	4.12	0.00
	NEM	1	4.48		
		2	4.12		
		3	4.30	4.30	0.18
45 minutes	Control	1	4.48		
		2	4.12		
		3	4.12	4.24	0.21
	Cadmium	1	4.12		
		2	4.12		
		3	4.30	4.18	0.10
	DNP	1	4.48		
		2	4.48		
		3	4.48	4.48	0.00
	NEM	1	4.85		
		2	4.85		
		3	4.85	4.85	0.00
3 hours	Control	1	4.48		
		2	4.48		
		3	4.30	4.42	0.10
	Cadmium	1	4.85		
		2	4.85		
		3	4.85	4.85	0.00
	DNP	1	5.03		
		2	4.85		
		3	5.03	4.97	0.11
	NEM	1	5.98		

Sampling Time	Reactor	Replicate #		Average	Std. Dev.
Experiment 5 (cont.)					
		2	5.98		
		3	6.17	6.04	0.11
5 hours	Control	1	4.48		
		2	4.66		
		3	4.85	4.66	0.18
	Cadmium	1	5.22		
		2	5.41		
		3	5.41	5.34	0.11
	DNP	1	5.59		
		2	5.59		
		3	5.41	5.53	0.11
	NEM	1	7.15		
		2	7.15		
		3	7.15	7.15	0.00
Experiment 6					
< 5 minutes	Control	1	4.44		
		2	4.05		
		3	4.05	4.18	0.22
	Cadmium	1	3.67		
		2	3.67		
		3	3.67	3.67	0.00
	DNP	1	4.24		
		2	4.24		
		3	4.05	4.18	0.11
	NEM	1	4.44		
		2	4.63		
		3	4.44	4.50	0.11
45 minutes	Control	1	3.67		
		2	4.05		
		3	3.86	3.86	0.19
	Cadmium	1	4.44		
		2	4.44		
		3	4.05	4.31	0.22
	DNP	1	4.05		
		2	4.05		
		3	4.24	4.12	0.11
	NEM	1	4.44		
		2	4.63		
		3	4.63	4.57	0.11
3 hours	Control	1	4.24		
		2	4.05		
		3	4.05	4.12	0.11
	Cadmium	1	5.42		
		2	5.61		
		3	5.22	5.42	0.20
	DNP	1	4.63		
		2	4.63		
		3	4.82	4.69	0.11

Sampling Time	Reactor	Replicate #		Average	Std. Dev.
Experiment 6 (cont.)					
	NEM	1	6.02		
		2	6.02		
		3	6.02	6.02	0.00
5 hours	Control	1	4.63		
		2	4.44		
		3	4.44	4.50	0.11
	Cadmium	1	6.02		
		2	6.02		
		3	6.22	6.09	0.12
	DNP	1	5.42		
		2	5.61		
		3	5.61	5.55	0.12
	NEM	1	6.84		
		2	6.63		
		3	7.68	7.05	0.56
Experiment 7					
< 5 minutes	Control	1	7.77		
		2	6.12		
		3	7.77	7.22	0.95
	Cadmium	1	6.12		
		2	5.32		
		3	7.77	6.40	1.25
	DNP	1	6.94		
		2	7.77		
		3	6.12	6.94	0.82
	NEM	1	6.94		
		2	7.77		
		3	7.77	7.49	0.48
45 minutes	Control	1	6.12		
		2	7.77		
		3	6.94	6.94	0.82
	Cadmium	1	6.94		
		2	6.12		
		3	7.77	6.94	0.82
	DNP	1	6.94		
		2	6.94		
		3	6.94	6.94	0.00
	NEM	1	8.61		
		2	7.77		
		3	7.77	8.05	0.49
3 hours	Control	1	6.94		
		2	6.94		
		3	7.77	7.21	0.48
	Cadmium	1	8.61		
		2	9.46		
		3	7.77	8.61	0.85
	DNP	1	6.94		
		2	7.77		

Sampling Time	Reactor	Replicate #		Average	Std. Dev.
Experiment 7 (cont.)					
		3	6.12	6.94	0.82
	NEM	1	9.46		
		2	7.77		
		3	9.46	8.90	0.98
5 hours	Control	1	6.12		
		2	5.32		
		3	6.12	5.86	0.46
	Cadmium	1	7.77		
		2	9.46		
		3	7.77	8.33	0.98
	DNP	1	6.12		
		2	6.12		
		3	6.94	6.39	0.47
	NEM	1	9.46		
		2	8.61		
		3	10.33	9.47	0.86
Experiment 8					
< 5 minutes	Control	1	4.53		
		2	4.53		
		3	4.53	4.53	0.00
	Cadmium	1	3.75		
		2	4.53		
		3	4.53	4.27	0.45
	DNP	1	6.12		
		2	5.32		
		3	4.53	5.32	0.80
	NEM	1	4.53		
		2	4.53		
		3	4.53	4.53	0.00
45 minutes	Control	1	4.53		
		2	4.53		
		3	4.53	4.53	0.00
	Cadmium	1	4.53		
		2	6.12		
		3	4.53	5.06	0.92
	DNP	1	4.53		
		2	4.53		
		3	5.32	4.79	0.46
	NEM	1	6.12		
		2	6.12		
		3	6.12	6.12	0.00
3 hours	Control	1	5.32		
		2	6.12		
		3	6.12	5.86	0.46
	Cadmium	1	5.32		
		2	6.12		
		3	6.12	5.86	0.46
	DNP	1	4.53		

Sampling Time	Reactor	Replicate #		Average	Std. Dev.
Experiment 8 (cont.)					
		2	4.53		
		3	5.32	4.79	0.46
	NEM	1	7.77		
		2	7.77		
		3	7.77	7.77	0.00
5 hours	Control	1	6.12		
		2	5.32		
		3	6.12	5.86	0.46
	Cadmium	1	7.77		
		2	7.77		
		3	6.12	7.22	0.95
	DNP	1	5.32		
		2	5.32		
		3	6.12	5.59	0.46
	NEM	1	8.61		
		2	7.77		
		3	8.61	8.33	0.49

Table 2 - Data for Table 1 in Chapter 5: absorbance measurements for the determination of the concentration of proteins and humic acids in the soluble phase of the control and shocked reactors (triplicates of two independent samples).

Sampling Time and Reactor		Replicate #	With $CuSO_4$				Without $CuSO_4$			
			Absorbance	Avg. Abs.	Std. Dev. Abs.	Corrected Avg. Abs.*	Absorbance	Avg. Abs.	Std. Dev. Abs.	Corrected Avg. Abs.*
Experiment 1										
< 5 minutes	Control	1	0.054				0.031			
		2	0.054				0.031			
		3	0.054				0.031			
		4	0.054				0.031			
		5	0.054				0.032			
		6	0.054	0.054	0.000	0.026	0.031	0.031	0.000	0.023
	Cadmium	1	0.055				0.027			
		2	0.052				0.026			
		3	0.050				0.028			
		4	0.048				0.027			
		5	0.051				0.027			
		6	0.049	0.051	0.002	0.023	0.027	0.027	0.001	0.019
	DNP	1	0.054				0.031			
		2	0.053				0.031			
		3	0.054				0.031			
		4	0.053				0.031			
		5	0.054				0.031			
		6	0.053	0.053	0.000	0.026	0.031	0.031	0.000	0.023
	NEM	1	0.056				0.032			
		2	0.056				0.032			
		3	0.055				0.032			
		4	0.055				0.032			
		5	0.055				0.032			
		6	0.055	0.055	0.000	0.028	0.031	0.032	0.000	0.024
45 minutes	Control	1	0.054				0.031			
		2	0.053				0.031			
		3	0.053				0.031			
		4	0.053				0.031			
		5	0.053				0.031			
		6	0.053	0.053	0.000	0.026	0.031	0.031	0.000	0.023

Sampling Time and Reactor		Replicate #	With $CuSO_4$				Without $CuSO_4$			
			Absorbance	Avg. Abs.	Std. Dev. Abs.	Corrected Avg. Abs.*	Absorbance	Avg. Abs.	Std. Dev. Abs.	Corrected Avg. Abs.*
Experiment 1 (cont.)										
	Cadmium	1	0.062				0.032			
		2	0.062				0.032			
		3	0.062				0.033			
		4	0.061				0.032			
		5	0.061				0.032			
		6	0.061	0.062	0.001	0.034	0.032	0.032	0.000	0.024
	DNP	1	0.055				0.031			
		2	0.055				0.031			
		3	0.055				0.031			
		4	0.054				0.031			
		5	0.054				0.031			
		6	0.054	0.054	0.000	0.027	0.031	0.031	0.000	0.023
	NEM	1	0.071				0.039			
		2	0.071				0.038			
		3	0.071				0.038			
		4	0.071				0.038			
		5	0.071				0.038			
		6	0.070	0.071	0.000	0.043	0.038	0.038	0.000	0.031
3 hours	Control	1	0.054				0.031			
		2	0.054				0.031			
		3	0.054				0.031			
		4	0.054				0.031			
		5	0.054				0.031			
		6	0.054	0.054	0.000	0.027	0.031	0.031	0.000	0.023
	Cadmium	1	0.094				0.047			
		2	0.093				0.047			
		3	0.095				0.047			
		4	0.093				0.047			
		5	0.094				0.048			
		6	0.094	0.094	0.001	0.066	0.048	0.047	0.000	0.040
	DNP	1	0.055				0.032			
		2	0.055				0.032			
		3	0.055				0.032			

Sampling Time and Reactor		Replicate #	With $CuSO_4$				Without $CuSO_4$			
			Absorbance	Avg. Abs.	Std. Dev. Abs.	Corrected Avg. Abs.*	Absorbance	Avg. Abs.	Std. Dev. Abs.	Corrected Avg. Abs.*
Experiment 1 (cont.)										
		4	0.055				0.032			
		5	0.055				0.032			
		6	0.055	0.055	0.000	0.028	0.032	0.032	0.000	0.024
	NEM	1	0.118				0.063			
		2	0.118				0.063			
		3	0.119				0.063			
		4	0.118				0.063			
		5	0.119				0.063			
		6	0.119	0.118	0.001	0.091	0.063	0.063	0.000	0.055
5 hours	Control	1	0.053				0.030			
		2	0.053				0.031			
		3	0.053				0.031			
		4	0.053				0.031			
		5	0.053				0.031			
		6	0.053	0.053	0.000	0.026	0.031	0.031	0.000	0.023
	Cadmium	1	0.117				0.062			
		2	0.115				0.061			
		3	0.117				0.062			
		4	0.117				0.062			
		5	0.116				0.063			
		6	0.116	0.116	0.001	0.089	0.062	0.062	0.000	0.054
	DNP	1	0.057				0.032			
		2	0.057				0.032			
		3	0.057				0.032			
		4	0.056				0.032			
		5	0.057				0.033			
		6	0.056	0.057	0.001	0.029	0.032	0.032	0.000	0.024
	NEM	1	0.130				0.072			
		2	0.129				0.072			
		3	0.131				0.073			
		4	0.130				0.073			
		5	0.131				0.073			
		6	0.131	0.130	0.001	0.103	0.072	0.072	0.000	0.064

Sampling Time and Reactor		Replicate #	With $CuSO_4$				Without $CuSO_4$			
			Absorbance	Avg. Abs.	Std. Dev. Abs.	Corrected Avg. Abs.*	Absorbance	Avg. Abs.	Std. Dev. Abs.	Corrected Avg. Abs.*
Experiment 2										
< 5 minutes	Control	1	0.056				0.030			
		2	0.056				0.030			
		3	0.056				0.030			
		4	0.056				0.030			
		5	0.055				0.030			
		6	0.055	0.056	0.000	0.028	0.030	0.030	0.000	0.022
	Cadmium	1	0.049				0.026			
		2	0.049				0.025			
		3	0.052				0.026			
		4	0.047				0.025			
		5	0.049				0.028			
		6	0.048	0.049	0.002	0.021	0.026	0.026	0.001	0.018
	DNP	1	0.057				0.030			
		2	0.056				0.030			
		3	0.056				0.030			
		4	0.055				0.031			
		5	0.056				0.030			
		6	0.055	0.056	0.001	0.029	0.030	0.030	0.000	0.022
	NEM	1	0.058				0.031			
		2	0.057				0.031			
		3	0.059				0.031			
		4	0.058				0.031			
		5	0.058				0.031			
		6	0.058	0.058	0.001	0.031	0.031	0.031	0.000	0.023
45 minutes	Control	1	0.057				0.030			
		2	0.056				0.030			
		3	0.057				0.030			
		4	0.056				0.030			
		5	0.057				0.031			
		6	0.055	0.056	0.001	0.029	0.031	0.030	0.000	0.022
	Cadmium	1	0.060				0.031			
		2	0.059				0.031			
		3	0.063				0.031			

Sampling Time and Reactor		Replicate #	With $CuSO_4$				Without $CuSO_4$			
			Absorbance	Avg. Abs.	Std. Dev. Abs.	Corrected Avg. Abs.*	Absorbance	Avg. Abs.	Std. Dev. Abs.	Corrected Avg. Abs.*
Experiment 2 (cont.)										
		4	0.060				0.030			
		5	0.063				0.031			
		6	0.060	0.061	0.002	0.033	0.030	0.031	0.000	0.022
	DNP	1	0.056				0.030			
		2	0.056				0.030			
		3	0.056				0.030			
		4	0.056				0.030			
		5	0.057				0.031			
		6	0.055	0.056	0.001	0.028	0.031	0.030	0.000	0.022
	NEM	1	0.072				0.038			
		2	0.073				0.038			
		3	0.073				0.038			
		4	0.073				0.038			
		5	0.073				0.038			
		6	0.073	0.073	0.000	0.045	0.038	0.038	0.000	0.030
3 hours	Control	1	0.057				0.030			
		2	0.056				0.030			
		3	0.057				0.030			
		4	0.056				0.030			
		5	0.058				0.030			
		6	0.058	0.057	0.001	0.030	0.030	0.030	0.000	0.022
	Cadmium	1	0.098				0.046			
		2	0.097				0.046			
		3	0.098				0.046			
		4	0.096				0.046			
		5	0.097				0.046			
		6	0.096	0.097	0.001	0.069	0.046	0.046	0.000	0.037
	DNP	1	0.058				0.031			
		2	0.056				0.031			
		3	0.058				0.031			
		4	0.058				0.031			
		5	0.058				0.031			
		6	0.057	0.058	0.001	0.030	0.031	0.031	0.000	0.023

Sampling Time and Reactor		Replicate #	With $CuSO_4$				Without $CuSO_4$			
			Absorbance	Avg. Abs.	Std. Dev. Abs.	Corrected Avg. Abs.*	Absorbance	Avg. Abs.	Std. Dev. Abs.	Corrected Avg. Abs.*
Experiment 2 (cont.)										
	NEM	1	0.124				0.064			
		2	0.123				0.064			
		3	0.122				0.063			
		4	0.122				0.063			
		5	0.122				0.064			
		6	0.123	0.123	0.001	0.095	0.064	0.064	0.000	0.055
5 hours	Control	1	0.056				0.030			
		2	0.057				0.030			
		3	0.056				0.030			
		4	0.055				0.030			
		5	0.057				0.030			
		6	0.056	0.056	0.001	0.029	0.030	0.030	0.000	0.022
	Cadmium	1	0.120				0.060			
		2	0.119				0.060			
		3	0.120				0.060			
		4	0.121				0.060			
		5	0.119				0.061			
		6	0.119	0.119	0.001	0.092	0.060	0.060	0.000	0.051
	DNP	1	0.058				0.032			
		2	0.058				0.032			
		3	0.058				0.032			
		4	0.057				0.032			
		5	0.058				0.032			
		6	0.058	0.058	0.000	0.030	0.032	0.032	0.000	0.023
	NEM	1	0.128				0.070			
		2	0.127				0.070			
		3	0.128				0.070			
		4	0.127				0.070			
		5	0.128				0.070			
		6	0.129	0.128	0.001	0.100	0.070	0.070	0.000	0.062
Experiment 3										
< 5 minutes	Control	1	0.086				0.061			
		2	0.085				0.061			

Sampling Time and Reactor		Replicate #	With $CuSO_4$				Without $CuSO_4$			
			Absorbance	Avg. Abs.	Std. Dev. Abs.	Corrected Avg. Abs.*	Absorbance	Avg. Abs.	Std. Dev. Abs.	Corrected Avg. Abs.*
Experiment 3 (cont.)										
		3	0.085				0.061			
		4	0.085				0.061			
		5	0.085				0.061			
		6	0.084	0.085	0.000	0.052	0.061	0.061	0.000	0.049
	Cadmium	1	0.078				0.053			
		2	0.073				0.052			
		3	0.076				0.054			
		4	0.073				0.052			
		5	0.077				0.053			
		6	0.073	0.075	0.002	0.042	0.052	0.053	0.001	0.041
	DNP	1	0.086				0.061			
		2	0.085				0.061			
		3	0.085				0.061			
		4	0.085				0.061			
		5	0.087				0.063			
		6	0.086	0.086	0.001	0.053	0.061	0.061	0.001	0.049
	NEM	1	0.090				0.063			
		2	0.093				0.063			
		3	0.090				0.065			
		4	0.090				0.064			
		5	0.091				0.066			
		6	0.091	0.091	0.001	0.058	0.066	0.065	0.002	0.053
45 minutes	Control	1	0.086				0.062			
		2	0.086				0.062			
		3	0.087				0.063			
		4	0.087				0.063			
		5	0.088				0.062			
		6	0.089	0.087	0.001	0.054	0.062	0.062	0.000	0.050
	Cadmium	1	0.091				0.057			
		2	0.087				0.056			
		3	0.090				0.058			
		4	0.087				0.057			
		5	0.091				0.059			

Sampling Time and Reactor		Replicate #	With $CuSO_4$				Without $CuSO_4$			
			Absorbance	Avg. Abs.	Std. Dev. Abs.	Corrected Avg. Abs.*	Absorbance	Avg. Abs.	Std. Dev. Abs.	Corrected Avg. Abs.*
Experiment 3 (cont.)										
		6	0.089	0.089	0.002	0.056	0.060	0.058	0.002	0.046
	DNP	1	0.084				0.060			
		2	0.084				0.060			
		3	0.084				0.060			
		4	0.084				0.062			
		5	0.086				0.060			
		6	0.086	0.085	0.001	0.052	0.066	0.061	0.003	0.049
	NEM	1	0.095				0.066			
		2	0.095				0.067			
		3	0.095				0.065			
		4	0.095				0.067			
		5	0.096				0.067			
		6	0.096	0.095	0.000	0.063	-	0.066	0.001	0.054
3 hours	Control	1	0.085				0.061			
		2	0.085				0.061			
		3	0.085				0.061			
		4	0.085				0.061			
		5	0.086				0.061			
		6	0.086	0.085	0.001	0.053	0.061	0.061	0.000	0.049
	Cadmium	1	0.117				0.069			
		2	0.113				0.068			
		3	0.120				0.068			
		4	0.114				0.068			
		5	0.118				0.068			
		6	0.117	0.117	0.002	0.084	0.067	0.068	0.001	0.056
	DNP	1	0.083				0.059			
		2	0.083				0.059			
		3	0.084				0.059			
		4	0.084				0.059			
		5	0.083				0.060			
		6	0.083	0.083	0.000	0.050	0.060	0.059	0.000	0.047
	NEM	1	0.112				0.081			
		2	0.113				0.081			

Sampling Time and Reactor		Replicate #	With $CuSO_4$				Without $CuSO_4$			
			Absorbance	Avg. Abs.	Std. Dev. Abs.	Corrected Avg. Abs.*	Absorbance	Avg. Abs.	Std. Dev. Abs.	Corrected Avg. Abs.*
Experiment 3 (cont.)										
		3	0.111				0.081			
		4	0.111				0.081			
		5	0.111				0.081			
		6	0.111	0.112	0.001	0.079	0.081	0.081	0.000	0.069
5 hours	Control	1	0.086				0.062			
		2	0.084				0.062			
		3	0.088				0.062			
		4	0.086				0.062			
		5	0.087				0.062			
		6	0.085	0.086	0.001	0.053	0.062	0.062	0.000	0.050
	Cadmium	1	0.134				0.078			
		2	0.133				0.077			
		3	0.136				0.078			
		4	0.139				0.076			
		5	0.137				0.077			
		6	0.134	0.135	0.002	0.103	0.077	0.077	0.001	0.065
	DNP	1	0.079				-			
		2	0.080				-			
		3	0.079				-			
		4	0.078				-			
		5	0.079				-			
		6	0.079	0.079	0.001	0.046	-			
	NEM	1	0.108				-	-	-	-
		2	0.107				-			
		3	0.108				0.087			
		4	0.107				0.087			
		5	0.108				-			
		6	0.108	0.108	0.001	0.075	-	0.087	0.000	0.075
Experiment 4										
< 5 minutes	Control	1	0.080				0.058			
		2	0.080				0.058			
		3	0.081				0.058			
		4	0.080				0.058			

Sampling Time and Reactor		Replicate #	With $CuSO_4$				Without $CuSO_4$			
			Absorbance	Avg. Abs.	Std. Dev. Abs.	Corrected Avg. Abs.*	Absorbance	Avg. Abs.	Std. Dev. Abs.	Corrected Avg. Abs.*
Experiment 4 (cont.)										
		5	0.081				0.058			
		6	0.081	0.081	0.000	0.048	0.058	0.058	0.000	0.046
	Cadmium	1	0.068				0.050			
		2	0.070				0.049			
		3	0.071				0.050			
		4	0.065				0.049			
		5	0.070				0.050			
		6	0.065	0.068	0.003	0.035	0.049	0.049	0.001	0.038
	DNP	1	0.081				0.058			
		2	0.080				0.058			
		3	0.081				0.058			
		4	0.080				0.058			
		5	0.080				0.058			
		6	0.079	0.080	0.000	0.047	0.058	0.058	0.000	0.046
	NEM	1	0.082				0.058			
		2	0.082				0.058			
		3	0.082				0.059			
		4	0.081				0.059			
		5	0.081				0.058			
		6	0.081	0.082	0.001	0.049	0.058	0.059	0.000	0.047
45 minutes	Control	1	0.082				0.059			
		2	0.081				0.059			
		3	0.082				0.059			
		4	0.082				0.059			
		5	0.083				0.059			
		6	0.081	0.082	0.001	0.049	0.058	0.059	0.000	0.047
	Cadmium	1	0.084				0.054			
		2	0.086				0.053			
		3	0.086				0.054			
		4	0.081				0.053			
		5	0.087				0.054			
		6	0.082	0.084	0.002	0.052	0.053	0.054	0.001	0.042
	DNP	1	0.080				0.057			

Sampling Time and Reactor		Replicate #	With $CuSO_4$				Without $CuSO_4$			
			Absorbance	Avg. Abs.	Std. Dev. Abs.	Corrected Avg. Abs.*	Absorbance	Avg. Abs.	Std. Dev. Abs.	Corrected Avg. Abs.*
Experiment 4 (cont.)										
		2	0.080				0.057			
		3	0.080				0.058			
		4	0.080				0.057			
		5	0.081				0.057			
		6	0.080	0.080	0.000	0.047	0.057	0.057	0.000	0.045
	NEM	1	0.090				0.062			
		2	0.090				0.062			
		3	0.089				0.062			
		4	0.088				0.062			
		5	0.089				0.062			
		6	0.089	0.089	0.001	0.056	0.062	0.062	0.000	0.050
3 hours	Control	1	0.081				0.058			
		2	0.080				0.057			
		3	0.084				0.058			
		4	0.084				0.057			
		5	0.081				0.057			
		6	0.080	0.082	0.002	0.049	0.057	0.057	0.000	0.045
	Cadmium	1	0.115				0.064			
		2	0.113				0.064			
		3	0.114				0.064			
		4	0.111				0.064			
		5	0.116				0.065			
		6	0.111	0.113	0.002	0.081	0.064	0.064	0.000	0.052
	DNP	1	0.081				0.057			
		2	0.081				0.056			
		3	0.080				0.057			
		4	0.079				0.057			
		5	0.080				-			
		6	0.080	0.080	0.001	0.047	-	0.057	0.000	0.045
	NEM	1	0.101				0.073			
		2	0.101				0.073			
		3	0.101				0.074			
		4	0.101				0.074			

Sampling Time and Reactor		Replicate #	With $CuSO_4$				Without $CuSO_4$			
			Absorbance	Avg. Abs.	Std. Dev. Abs.	Corrected Avg. Abs.*	Absorbance	Avg. Abs.	Std. Dev. Abs.	Corrected Avg. Abs.*
Experiment 4 (cont.)										
		5	0.102				0.074			
		6	0.101	0.101	0.000	0.068	0.074	0.074	0.000	0.062
5 hours	Control	1	0.101				0.079			
		2	0.100				0.078			
		3	0.091				0.079			
		4	0.091				0.079			
		5	0.096				0.078			
		6	0.095	0.096	0.004	0.051	0.079	0.079	0.001	0.051
	Cadmium	1	0.146				0.095			
		2	0.146				0.092			
		3	0.151				0.093			
		4	0.151				0.090			
		5	0.152				0.093			
		6	0.150	0.149	0.003	0.105	0.091	0.092	0.002	0.064
	DNP	1	0.087				0.074			
		2	0.087				0.075			
		3	0.091				0.074			
		4	0.091				0.075			
		5	0.089				0.074			
		6	0.089	0.089	0.001	0.044	0.074	0.074	0.000	0.046
	NEM	1	0.109				0.093			
		2	0.109				0.093			
		3	0.113				0.092			
		4	0.113				0.091			
		5	0.122				0.091			
		6	0.122	0.115	0.006	0.070	0.091	0.092	0.001	0.064
Experiment 5										
< 5 minutes	Control	1	0.058				0.039			
		2	0.057				0.041			
		3	0.058				0.037			
		4	0.057				0.038			
		5	0.058				0.037			
		6	0.057	0.057	0.001	0.037	0.036	0.038	0.002	0.033

Sampling Time and Reactor		Replicate #	With $CuSO_4$				Without $CuSO_4$			
			Absorbance	Avg. Abs.	Std. Dev. Abs.	Corrected Avg. Abs.*	Absorbance	Avg. Abs.	Std. Dev. Abs.	Corrected Avg. Abs.*
Experiment 5 (cont.)										
	Cadmium	1	0.059				0.037			
		2	0.057				0.037			
		3	0.061				0.038			
		4	0.058				0.036			
		5	0.058				0.037			
		6	0.056	0.058	0.002	0.038	0.036	0.037	0.001	0.032
	DNP	1	0.058				0.040			
		2	0.057				0.045			
		3	0.059				0.038			
		4	0.057				0.044			
		5	0.060				0.037			
		6	0.061	0.059	0.002	0.039	0.038	0.040	0.003	0.035
	NEM	1	0.060				0.037			
		2	0.058				0.038			
		3	0.059				0.039			
		4	0.059				0.045			
		5	0.060				0.037			
		6	0.058	0.059	0.001	0.039	0.037	0.039	0.003	0.034
45 minutes	Control	1	0.059				0.040			
		2	0.058				-			
		3	0.059				0.037			
		4	0.058				0.037			
		5	0.058				0.038			
		6	0.058	0.059	0.001	0.039	0.038	0.038	0.001	0.033
	Cadmium	1	0.068				0.040			
		2	0.069				-			
		3	0.068				0.040			
		4	0.067				0.039			
		5	0.068				0.040			
		6	0.066	0.068	0.001	0.048	0.040	0.040	0.000	0.035
	DNP	1	0.060				0.041			
		2	0.058				0.049			
		3	0.061				0.039			

Sampling Time and Reactor		Replicate #	With $CuSO_4$				Without $CuSO_4$			
			Absorbance	Avg. Abs.	Std. Dev. Abs.	Corrected Avg. Abs.*	Absorbance	Avg. Abs.	Std. Dev. Abs.	Corrected Avg. Abs.*
Experiment 5 (cont.)										
		4	0.058				0.041			
		5	0.060				0.040			
		6	0.060	0.060	0.001	0.040	0.044	0.042	0.004	0.037
	NEM	1	0.073				-			
		2	0.071				-			
		3	0.073				0.045			
		4	0.073				0.044			
		5	0.074				0.045			
		6	0.073	0.073	0.001	0.053	0.045	0.045	0.000	0.040
3 hours	Control	1	0.062				0.041			
		2	0.059				0.050			
		3	0.060				0.041			
		4	0.059				0.041			
		5	0.059				0.039			
		6	0.058	0.060	0.001	0.040	0.041	0.042	0.004	0.037
	Cadmium	1	0.101				0.056			
		2	0.087				0.053			
		3	0.103				0.056			
		4	0.092				0.051			
		5	0.101				0.055			
		6	0.089	0.095	0.007	0.076	0.053	0.054	0.002	0.049
	DNP	1	0.059				0.042			
		2	0.059				0.046			
		3	0.059				0.038			
		4	0.059				0.040			
		5	0.060				0.038			
		6	0.058	0.059	0.000	0.039	0.040	0.041	0.003	0.036
	NEM	1	0.119				-			
		2	0.115				-			
		3	0.119				0.070			
		4	0.111				0.073			
		5	0.119				0.071			
		6	0.114	0.116	0.004	0.096	0.072	0.071	0.001	0.066

Sampling Time and Reactor		Replicate #	With $CuSO_4$				Without $CuSO_4$			
			Absorbance	Avg. Abs.	Std. Dev. Abs.	Corrected Avg. Abs.*	Absorbance	Avg. Abs.	Std. Dev. Abs.	Corrected Avg. Abs.*
Experiment 5 (cont.)										
5 hours	Control	1	0.063				0.043			
		2	0.061				0.046			
		3	0.062				0.044			
		4	0.062				0.045			
		5	0.063				0.042			
		6	0.062	0.062	0.001	0.042	0.044	0.044	0.001	0.039
	Cadmium	1	0.118				0.067			
		2	0.103				0.065			
		3	0.114				0.066			
		4	0.111				0.066			
		5	0.129				0.067			
		6	0.106	0.113	0.009	0.093	0.065	0.066	0.001	0.061
	DNP	1	0.083				0.050			
		2	0.082				0.052			
		3	0.084				0.048			
		4	0.080				0.049			
		5	0.084				0.049			
		6	0.081	0.082	0.001	0.062	0.048	0.049	0.002	0.044
	NEM	1	0.146				0.084			
		2	0.145				0.084			
		3	0.144				0.084			
		4	0.137				0.082			
		5	0.145				0.084			
		6	0.136	0.142	0.004	0.122	0.081	0.083	0.001	0.078
Experiment 6										
< 5 minutes	Control	1	0.114				0.080			
		2	0.114				0.078			
		3	0.103				0.079			
		4	0.103				0.079			
		5	0.107				0.080			
		6	0.106	0.108	0.005	0.063	0.080	0.079	0.001	0.051
	Cadmium	1	0.097				0.076			
		2	0.095				0.075			

Sampling Time and Reactor		Replicate #	With $CuSO_4$				Without $CuSO_4$			
			Absorbance	Avg. Abs.	Std. Dev. Abs.	Corrected Avg. Abs.*	Absorbance	Avg. Abs.	Std. Dev. Abs.	Corrected Avg. Abs.*
Experiment 6 (cont.)										
		3	0.099				0.076			
		4	0.094				0.074			
		5	0.105				0.077			
		6	0.104	0.099	0.004	0.054	0.071	0.075	0.002	0.047
	DNP	1	0.104				0.080			
		2	0.104				0.080			
		3	0.114				0.081			
		4	0.114				0.080			
		5	0.109				0.080			
		6	0.109	0.109	0.004	0.064	0.080	0.080	0.000	0.052
	NEM	1	0.113				0.080			
		2	0.113				0.081			
		3	0.118				0.079			
		4	0.118				0.079			
		5	0.109				0.079			
		6	0.109	0.113	0.004	0.069	0.078	0.079	0.001	0.051
45 minutes	Control	1	0.102				0.079			
		2	0.102				0.078			
		3	0.108				0.080			
		4	0.108				0.080			
		5	0.109				0.080			
		6	0.109	0.106	0.003	0.062	0.079	0.079	0.001	0.051
	Cadmium	1	0.111				0.079			
		2	0.111				0.077			
		3	0.105				0.081			
		4	0.103				0.072			
		5	0.101				0.079			
		6	0.100	0.105	0.005	0.060	0.075	0.077	0.003	0.049
	DNP	1	0.109				0.082			
		2	0.109				0.078			
		3	0.105				0.081			
		4	0.106				0.081			
		5	0.111				0.082			

Sampling Time and Reactor		Replicate #	With $CuSO_4$				Without $CuSO_4$			
			Absorbance	Avg. Abs.	Std. Dev. Abs.	Corrected Avg. Abs.*	Absorbance	Avg. Abs.	Std. Dev. Abs.	Corrected Avg. Abs.*
Experiment 6 (cont.)										
		6	0.111	0.109	0.003	0.064	0.081	0.081	0.001	0.053
	NEM	1	0.115				0.085			
		2	0.115				0.085			
		3	0.115				0.086			
		4	0.114				0.085			
		5	0.116				0.086			
		6	0.117	0.116	0.001	0.071	0.085	0.085	0.001	0.057
3 hours	Control	1	0.099				0.081			
		2	0.099				0.079			
		3	0.099				0.082			
		4	0.098				0.080			
		5	0.099				0.081			
		6	0.095	0.098	0.001	0.053	0.078	0.080	0.001	0.052
	Cadmium	1	0.114				0.089			
		2	0.109				0.092			
		3	0.120				0.090			
		4	0.105				0.082			
		5	0.118				0.091			
		6	0.097	0.111	0.009	0.066	0.086	0.088	0.004	0.060
	DNP	1	0.106				0.081			
		2	0.103				0.078			
		3	0.106				0.082			
		4	0.101				0.077			
		5	0.106				0.081			
		6	0.106	0.105	0.002	0.060	0.079	0.080	0.002	0.052
	NEM	1	0.153				0.108			
		2	0.149				0.107			
		3	0.153				0.108			
		4	0.150				0.106			
		5	0.153				0.107			
		6	0.153	0.152	0.002	0.107	0.106	0.107	0.001	0.079
5 hours	Control	1	0.099				0.082			
		2	0.096				0.082			

Sampling Time and Reactor		Replicate #	With $CuSO_4$				Without $CuSO_4$			
			Absorbance	Avg. Abs.	Std. Dev. Abs.	Corrected Avg. Abs.*	Absorbance	Avg. Abs.	Std. Dev. Abs.	Corrected Avg. Abs.*
Experiment 6 (cont.)										
		3	0.099				0.083			
		4	0.099				0.082			
		5	0.097				0.083			
		6	0.097	0.098	0.001	0.053	0.080	0.082	0.001	0.054
	Cadmium	1	0.129				0.100			
		2	0.118				0.100			
		3	0.128				0.100			
		4	0.121				0.099			
		5	0.128				0.100			
		6	0.120	0.124	0.005	0.079	0.095	0.099	0.002	0.071
	DNP	1	0.138				0.101			
		2	0.129				0.098			
		3	0.140				0.101			
		4	0.140				0.099			
		5	0.141				0.101			
		6	0.139	0.138	0.005	0.093	0.100	0.100	0.001	0.072
	NEM	1	0.182				0.123			
		2	0.181				0.117			
		3	0.180				0.124			
		4	0.175				0.123			
		5	0.179				0.124			
		6	0.179	0.180	0.002	0.135	0.122	0.122	0.003	0.094
Experiment 7										
< 5 minutes	Control	1	0.084				0.066			
		2	0.082				0.065			
		3	0.086				0.066			
		4	0.080				0.065			
		5	0.085				0.067			
		6	0.081	0.083	0.002	0.038	0.066	0.066	0.001	0.038
	Cadmium	1	0.083				0.062			
		2	0.077				0.058			
		3	0.083				0.060			
		4	0.078				0.060			

Sampling Time and Reactor		Replicate #	With $CuSO_4$				Without $CuSO_4$			
			Absorbance	Avg. Abs.	Std. Dev. Abs.	Corrected Avg. Abs.*	Absorbance	Avg. Abs.	Std. Dev. Abs.	Corrected Avg. Abs.*
Experiment 7 (cont.)										
		5	0.082				0.061			
		6	0.079	0.080	0.003	0.036	0.059	0.060	0.001	0.032
	DNP	1	0.085				0.066			
		2	0.082				0.065			
		3	0.086				0.066			
		4	0.081				0.064			
		5	0.085				0.065			
		6	0.081	0.083	0.002	0.039	0.065	0.065	0.001	0.037
	NEM	1	0.084				0.064			
		2	0.081				0.063			
		3	0.084				0.063			
		4	0.082				0.062			
		5	0.084				0.065			
		6	0.083	0.083	0.001	0.038	0.063	0.063	0.001	0.035
45 minutes	Control	1	0.084				0.065			
		2	0.081				0.065			
		3	0.084				0.068			
		4	0.081				0.068			
		5	0.085				0.065			
		6	0.081	0.083	0.002	0.038	0.064	0.066	0.002	0.038
	Cadmium	1	0.088				0.062			
		2	0.084				0.062			
		3	0.088				0.062			
		4	0.083				0.061			
		5	0.088				0.062			
		6	0.086	0.086	0.002	0.042	0.062	0.062	0.000	0.034
	DNP	1	0.084				0.065			
		2	0.083				0.063			
		3	0.084				0.064			
		4	0.084				0.063			
		5	0.085				0.065			
		6	0.081	0.083	0.001	0.039	0.064	0.064	0.001	0.036
	NEM	1	0.090				0.068			

Sampling Time and Reactor		Replicate #	With $CuSO_4$				Without $CuSO_4$			
			Absorbance	Avg. Abs.	Std. Dev. Abs.	Corrected Avg. Abs.*	Absorbance	Avg. Abs.	Std. Dev. Abs.	Corrected Avg. Abs.*
Experiment 7 (cont.)										
		2	0.090				0.066			
		3	0.090				0.068			
		4	0.088				0.067			
		5	0.091				0.069			
		6	0.089	0.090	0.001	0.045	0.067	0.068	0.001	0.040
3 hours	Control	1	0.059				0.042			
		2	0.058				0.042			
		3	0.060				0.041			
		4	0.059				0.041			
		5	0.061				0.042			
		6	0.060	0.059	0.001	0.038	0.042	0.042	0.000	0.033
	Cadmium	1	0.078				0.045			
		2	0.078				0.045			
		3	0.079				0.045			
		4	0.079				0.045			
		5	0.079				0.045			
		6	0.078	0.079	0.000	0.057	0.045	0.045	0.000	0.037
	DNP	1	0.058				0.040			
		2	0.058				0.040			
		3	0.058				0.042			
		4	0.057				0.040			
		5	0.058				0.040			
		6	0.058	0.058	0.000	0.036	0.040	0.040	0.001	0.032
	NEM	1	0.090				0.058			
		2	0.089				0.058			
		3	0.090				0.059			
		4	0.090				0.058			
		5	0.090				0.059			
		6	0.089	0.090	0.000	0.068	0.059	0.059	0.000	0.050
5 hours	Control	1	0.057				0.043			
		2	0.057				-			
		3	0.057				0.039			
		4	0.057				0.039			

Sampling Time and Reactor		Replicate #	With $CuSO_4$				Without $CuSO_4$			
			Absorbance	Avg. Abs.	Std. Dev. Abs.	Corrected Avg. Abs.*	Absorbance	Avg. Abs.	Std. Dev. Abs.	Corrected Avg. Abs.*
Experiment 7 (cont.)										
		5	0.057				0.039			
		6	0.056	0.057	0.000	0.035	0.040	0.040	0.002	0.032
	Cadmium	1	0.096				0.051			
		2	0.090				0.051			
		3	0.091				0.050			
		4	0.090				0.050			
		5	0.090				0.051			
		6	0.089	0.091	0.003	0.069	0.051	0.051	0.000	0.042
	DNP	1	0.059				0.040			
		2	0.058				0.040			
		3	0.058				0.041			
		4	0.058				0.041			
		5	0.058				0.041			
		6	0.058	0.058	0.000	0.036	0.041	0.041	0.000	0.033
	NEM	1	0.091				0.062			
		2	0.090				0.062			
		3	0.091				0.062			
		4	0.091				0.062			
		5	0.091				0.063			
		6	0.090	0.091	0.000	0.069	0.063	0.062	0.000	0.054
Experiment 8										
< 5 minutes	Control	1	0.058				0.040			
		2	0.057				0.040			
		3	0.058				0.040			
		4	0.058				0.040			
		5	0.057				0.040			
		6	0.057	0.058	0.000	0.036	0.040	0.040	0.000	0.032
	Cadmium	1	0.054				0.038			
		2	0.052				0.035			
		3	0.055				0.039			
		4	0.055				0.037			
		5	0.058				0.037			
		6	0.055	0.055	0.002	0.033	0.037	0.037	0.001	0.029

Sampling Time and Reactor		Replicate #	With $CuSO_4$				Without $CuSO_4$			
			Absorbance	Avg. Abs.	Std. Dev. Abs.	Corrected Avg. Abs.*	Absorbance	Avg. Abs.	Std. Dev. Abs.	Corrected Avg. Abs.*
Experiment 8 (cont.)										
	DNP	1	0.058				0.040			
		2	0.058				0.040			
		3	0.058				0.040			
		4	0.057				0.040			
		5	0.058				0.040			
		6	0.057	0.058	0.000	0.036	0.040	0.040	0.000	0.032
	NEM	1	0.059				0.039			
		2	0.058				0.039			
		3	0.058				0.040			
		4	0.058				0.039			
		5	0.059				0.040			
		6	0.059	0.059	0.000	0.037	0.040	0.040	0.000	0.032
45 minutes	Control	1	0.058				0.040			
		2	0.057				0.040			
		3	0.058				0.040			
		4	0.058				0.040			
		5	0.058				0.040			
		6	0.060	0.058	0.001	0.036	0.040	0.040	0.000	0.032
	Cadmium	1	0.061				0.037			
		2	0.060				0.037			
		3	0.059				0.038			
		4	0.058				0.038			
		5	0.058				0.038			
		6	0.057	0.059	0.001	0.037	0.038	0.038	0.001	0.030
	DNP	1	0.059				0.041			
		2	0.058				0.041			
		3	0.058				0.041			
		4	0.059				0.041			
		5	0.059				0.041			
		6	0.059	0.059	0.000	0.037	0.041	0.041	0.000	0.032
	NEM	1	0.065				0.044			
		2	0.064				0.044			
		3	0.064				0.045			

Sampling Time and Reactor		Replicate #	With $CuSO_4$				Without $CuSO_4$			
			Absorbance	Avg. Abs.	Std. Dev. Abs.	Corrected Avg. Abs.*	Absorbance	Avg. Abs.	Std. Dev. Abs.	Corrected Avg. Abs.*
Experiment 8 (cont.)										
		4	0.064				0.044			
		5	0.064				0.044			
		6	0.064	0.064	0.000	0.042	0.044	0.044	0.000	0.036
3 hours	Control	1	0.059				0.040			
		2	0.058				0.040			
		3	0.058				0.040			
		4	0.057				0.040			
		5	0.060				0.040			
		6	0.059	0.058	0.001	0.037	0.040	0.040	0.000	0.032
	Cadmium	1	0.079				0.045			
		2	0.079				0.045			
		3	0.079				0.045			
		4	0.078				0.045			
		5	0.080				0.045			
		6	0.079	0.079	0.001	0.057	0.045	0.045	0.000	0.037
	DNP	1	0.058				0.040			
		2	0.058				0.041			
		3	0.058				0.041			
		4	0.058				0.041			
		5	0.059				0.041			
		6	0.057	0.058	0.000	0.036	0.041	0.041	0.000	0.032
	NEM	1	0.089				0.057			
		2	0.089				0.057			
		3	0.089				0.057			
		4	0.089				0.057			
		5	0.089				0.057			
		6	0.089	0.089	0.000	0.067	0.057	0.057	0.000	0.049
5 hours	Control	1	0.057				0.040			
		2	0.057				0.040			
		3	0.057				0.039			
		4	0.057				0.040			
		5	0.057				0.039			
		6	0.057	0.057	0.000	0.035	0.040	0.040	0.000	0.032

Sampling Time and Reactor	Replicate #	With $CuSO_4$				Without $CuSO_4$			
		Absorbance	Avg. Abs.	Std. Dev. Abs.	Corrected Avg. Abs.*	Absorbance	Avg. Abs.	Std. Dev. Abs.	Corrected Avg. Abs.*
Experiment 8 (cont.)									
Cadmium	1	0.092				0.051			
	2	0.091				0.051			
	3	0.092				0.051			
	4	0.091				0.052			
	5	0.091				0.051			
	6	0.090	0.091	0.001	0.069	0.051	0.051	0.000	0.043
DNP	1	0.059				0.042			
	2	0.058				0.042			
	3	0.059				0.042			
	4	0.058				0.042			
	5	0.059				0.042			
	6	0.058	0.058	0.001	0.036	0.042	0.042	0.000	0.034
NEM	1	0.092				0.063			
	2	0.091				0.063			
	3	0.092				0.064			
	4	0.091				0.064			
	5	0.092				0.064			
	6	0.091	0.091	0.001	0.070	0.064	0.064	0.000	0.055

* Corrected Average Absorbance = Average Absorbance – Average Absorbance Blank (nanopure water + reagents)

Table 3 - Data for Table 1 in Chapter 5: concentration of proteins and humic acids in the soluble phase of the control and shocked reactors over time.

Sampling Time and Reactor		Abs. with $CuSO_4$	Abs. without $CuSO_4$	Abs. proteins*	Abs. humic acids*	Proteins (mg/L)	Humic Acids (mg/L)
Experiment 1							
< 5 minutes	Control	0.026	0.023	0.004	0.023	0.18	7.99
	Cadmium	0.023	0.019	0.005	0.018	0.41	6.19
	DNP	0.026	0.023	0.004	0.022	0.15	7.88
	NEM	0.028	0.024	0.005	0.023	0.37	8.09
45 minutes	Control	0.026	0.023	0.004	0.022	0.14	7.89
	Cadmium	0.034	0.024	0.012	0.022	1.42	7.65
	DNP	0.027	0.023	0.004	0.022	0.27	7.96
	NEM	0.043	0.031	0.016	0.027	1.96	9.90
3 hours	Control	0.027	0.023	0.005	0.022	0.28	7.85
	Cadmium	0.066	0.040	0.033	0.033	4.55	12.12
	DNP	0.028	0.024	0.005	0.023	0.28	8.20
	NEM	0.091	0.055	0.045	0.046	6.24	17.59
5 hours	Control	0.026	0.023	0.004	0.022	0.16	7.77
	Cadmium	0.089	0.054	0.043	0.046	6.06	17.26
	DNP	0.029	0.024	0.007	0.023	0.94	7.65
	NEM	0.103	0.064	0.049	0.054	6.52	19.06
Experiment 2							
< 5 minutes	Control	0.028	0.022	0.008	0.020	1.15	6.69
	Cadmium	0.021	0.018	0.005	0.017	0.70	5.59
	DNP	0.029	0.022	0.009	0.020	1.17	6.74
	NEM	0.031	0.023	0.010	0.021	1.36	6.99
45 minutes	Control	0.029	0.022	0.009	0.020	1.21	6.80
	Cadmium	0.033	0.022	0.014	0.019	1.88	6.52
	DNP	0.028	0.022	0.008	0.020	1.10	6.89
	NEM	0.045	0.030	0.019	0.026	2.57	8.80
3 hours	Control	0.030	0.022	0.010	0.020	1.36	6.62
	Cadmium	0.069	0.037	0.040	0.029	5.30	10.04
	DNP	0.030	0.023	0.009	0.021	1.29	6.97
	NEM	0.095	0.055	0.050	0.045	6.67	15.77
5 hours	Control	0.029	0.022	0.009	0.020	1.19	6.75
	Cadmium	0.092	0.051	0.051	0.041	6.79	14.30
	DNP	0.030	0.023	0.009	0.022	1.19	7.30
	NEM	0.100	0.062	0.048	0.052	6.40	18.34
Experiment 3							
< 5 minutes	Control	0.052	0.049	0.004	0.048	0.22	9.96
	Cadmium	0.042	0.041	0.002	0.041	0.03	8.34
	DNP	0.053	0.049	0.005	0.048	0.26	10.02
	NEM	0.058	0.053	0.007	0.051	0.44	10.67
45 minutes	Control	0.054	0.050	0.005	0.049	0.30	10.27
	Cadmium	0.056	0.046	0.013	0.043	0.99	8.91
	DNP	0.052	0.049	0.003	0.049	0.15	10.09
	NEM	0.063	0.054	0.010	0.052	0.74	10.92
3 hours	Control	0.053	0.049	0.004	0.048	0.23	10.03
	Cadmium	0.084	0.056	0.035	0.049	2.88	10.21

Sampling Time and Reactor		Abs. with $CuSO_4$	Abs. without $CuSO_4$	Abs. proteins*	Abs. humic acids*	Proteins (mg/L)	Humic Acids (mg/L)
Experiment 3 (cont.)							
	DNP	0.050	0.047	0.004	0.047	0.19	9.68
	NEM	0.079	0.069	0.012	0.067	0.90	14.07
5 hours	Control	0.053	0.050	0.004	0.049	0.21	10.24
	Cadmium	0.103	0.065	0.046	0.056	3.93	11.76
	DNP	-	-	-	-	-	-
	NEM	0.075	0.075	0.000	0.075	-0.17	16.01
Experiment 4							
< 5 minutes	Control	0.048	0.046	0.002	0.046	0.03	9.52
	Cadmium	0.035	0.038	-0.003	0.038	-0.37	7.82
	DNP	0.047	0.046	0.002	0.046	0.01	9.44
	NEM	0.049	0.047	0.003	0.046	0.11	9.54
45 minutes	Control	0.049	0.047	0.003	0.046	0.09	9.58
	Cadmium	0.052	0.042	0.012	0.039	0.94	8.03
	DNP	0.047	0.045	0.002	0.045	0.06	9.32
	NEM	0.056	0.050	0.007	0.049	0.51	10.14
3 hours	Control	0.049	0.045	0.004	0.045	0.24	9.22
	Cadmium	0.081	0.052	0.035	0.045	2.95	9.35
	DNP	0.047	0.045	0.003	0.044	0.14	9.11
	NEM	0.068	0.062	0.008	0.060	0.56	12.62
5 hours	Control	0.051	0.051	0.000	0.051	-0.73	12.31
	Cadmium	0.105	0.064	0.050	0.054	3.80	13.40
	DNP	0.044	0.046	-0.002	0.047	-0.97	11.27
	NEM	0.070	0.064	0.008	0.062	-0.11	15.65
Experiment 5							
< 5 minutes	Control	0.037	0.033	0.006	0.032	0.32	8.79
	Cadmium	0.038	0.032	0.008	0.031	0.55	8.43
	DNP	0.039	0.035	0.004	0.034	0.19	9.51
	NEM	0.039	0.034	0.006	0.033	0.40	9.01
45 minutes	Control	0.039	0.033	0.007	0.032	0.44	8.77
	Cadmium	0.048	0.035	0.016	0.032	1.40	8.79
	DNP	0.040	0.037	0.003	0.037	0.03	10.16
	NEM	0.053	0.040	0.016	0.037	1.42	10.14
3 hours	Control	0.040	0.037	0.003	0.037	0.04	10.15
	Cadmium	0.076	0.049	0.033	0.042	3.30	11.74
	DNP	0.039	0.036	0.004	0.035	0.15	9.61
	NEM	0.096	0.066	0.037	0.059	3.76	16.54
5 hours	Control	0.042	0.039	0.004	0.038	0.17	10.52
	Cadmium	0.093	0.061	0.041	0.053	4.14	14.74
	DNP	0.062	0.044	0.023	0.040	2.12	11.04
	NEM	0.122	0.078	0.055	0.067	5.80	18.98
Experiment 6							
< 5 minutes	Control	0.063	0.051	0.015	0.048	0.50	11.71
	Cadmium	0.054	0.047	0.009	0.045	0.03	10.72
	DNP	0.064	0.052	0.015	0.049	0.56	11.87
	NEM	0.069	0.051	0.022	0.047	1.12	11.34
45 minutes	Control	0.062	0.051	0.013	0.049	0.37	11.76
	Cadmium	0.060	0.049	0.014	0.046	0.44	11.11

Sampling Time and Reactor		Abs. with $CuSO_4$	Abs. without $CuSO_4$	Abs. proteins*	Abs. humic acids*	Proteins (mg/L)	Humic Acids (mg/L)
Experiment 6 (cont.)							
	DNP	0.064	0.053	0.014	0.050	0.42	12.14
	NEM	0.071	0.057	0.017	0.054	0.69	13.28
3 hours	Control	0.053	0.052	0.001	0.052	-0.67	12.72
	Cadmium	0.066	0.060	0.007	0.059	-0.16	14.62
	DNP	0.060	0.052	0.010	0.050	0.13	12.01
	NEM	0.107	0.079	0.035	0.072	2.36	18.50
5 hours	Control	0.053	0.054	-0.001	0.054	-0.88	13.39
	Cadmium	0.079	0.071	0.010	0.069	0.12	17.61
	DNP	0.093	0.072	0.026	0.067	1.55	16.91
	NEM	0.135	0.094	0.051	0.084	3.90	21.97
Experiment 7							
< 5 minutes	Control	0.038	0.038	0.001	0.038	-0.72	8.72
	Cadmium	0.036	0.032	0.005	0.031	-0.38	6.92
	DNP	0.039	0.037	0.001	0.037	-0.65	8.57
	NEM	0.038	0.035	0.004	0.035	-0.46	7.90
45 minutes	Control	0.038	0.038	0.000	0.038	-0.75	8.74
	Cadmium	0.042	0.034	0.009	0.032	0.03	7.21
	DNP	0.039	0.036	0.003	0.035	-0.49	8.11
	NEM	0.045	0.040	0.007	0.038	-0.19	8.88
3 hours	Control	0.038	0.033	0.005	0.032	-0.23	8.11
	Cadmium	0.057	0.037	0.025	0.032	2.03	7.94
	DNP	0.036	0.032	0.004	0.031	-0.32	7.84
	NEM	0.068	0.050	0.022	0.046	1.67	11.91
5 hours	Control	0.035	0.032	0.004	0.031	-0.37	7.72
	Cadmium	0.069	0.042	0.034	0.036	3.05	9.03
	DNP	0.036	0.033	0.005	0.032	-0.28	7.90
	NEM	0.069	0.054	0.018	0.051	1.22	13.25
Experiment 8							
< 5 minutes	Control	0.036	0.032	0.005	0.031	-0.29	7.71
	Cadmium	0.033	0.029	0.005	0.028	-0.27	6.90
	DNP	0.036	0.032	0.005	0.031	-0.28	7.72
	NEM	0.037	0.032	0.006	0.030	-0.10	7.53
45 minutes	Control	0.036	0.032	0.005	0.031	-0.21	7.68
	Cadmium	0.037	0.030	0.009	0.028	0.21	6.89
	DNP	0.037	0.032	0.005	0.031	-0.22	7.84
	NEM	0.042	0.036	0.008	0.034	0.07	8.66
3 hours	Control	0.037	0.032	0.006	0.031	-0.19	7.71
	Cadmium	0.057	0.037	0.025	0.032	2.08	7.99
	DNP	0.036	0.032	0.005	0.032	-0.31	7.89
	NEM	0.067	0.049	0.023	0.044	1.77	11.49
5 hours	Control	0.035	0.032	0.005	0.031	-0.31	7.63
	Cadmium	0.069	0.043	0.033	0.037	2.94	9.29
	DNP	0.036	0.034	0.004	0.033	-0.41	8.22
	NEM	0.070	0.055	0.018	0.052	1.18	13.58

* Abs. proteins = 1.25 x (Abs. with $CuSO_4$ – Abs. without $CuSO_4$)
Abs. humic acids = 1.25 x Abs. without $CuSO_4$ – 0.25 x Abs. with $CuSO_4$

Table 4 - Data for Figure 2 in Chapter 5: values of DF1, DF2 and DF3 for each sample (resulting from one GA-DFA run).

Sample	DF1	DF2	DF3
Cadmium			
Cd 11-3 3h Sol	-0.834	0.659	-0.238
Cd 11-3 45m Sol	-1.883	0.603	-0.273
Cd 11-3 5h Sol	-0.987	-0.721	-0.048
Cd 11-3 T0 Sol	-1.628	-1.594	-1.288
Cd 11-5 3h Sol	-1.337	-1.197	-0.144
Cd 11-5 45m Sol	-1.164	-0.814	0.766
Cd 11-5 5h Sol	-1.703	-1.086	-0.306
Cd 11-5 T0 Sol	-1.075	-0.701	-0.145
Cd 6-14 3h Sol	-1.049	0.147	-0.841
Cd 6-14 45m Sol	-1.396	-0.086	-0.041
Cd 6-14 5h Sol	-1.179	-0.306	1.500
Cd 6-14 T0 Sol	-1.188	0.373	1.281
Cd 6-16 3h Sol	-1.162	-0.300	0.167
Cd 6-16 45m Sol	-0.563	-0.807	-0.408
Cd 6-16 5h Sol	-1.044	-1.175	1.081
Cd 6-16 T0 Sol	-1.873	0.030	-0.017
Cd 6-27 3h Sol	-2.004	-0.366	0.929
Cd 6-27 45m Sol	-1.674	-0.493	0.785
Cd 6-27 5h Sol	-1.325	-0.585	0.010
Cd 6-27 T0 Sol	-0.921	-0.041	0.052
Cd 6-29 3h Sol	-0.479	-1.463	0.117
Cd 6-29 45m Sol	-1.745	-0.486	-0.599
Cd 6-29 5h Sol	-0.606	-0.437	-0.360
Cd 6-29 T0 Sol	-0.765	-0.199	-0.100
Cd 9-5 3h Sol	-0.735	-0.287	-0.145
Cd 9-5 45m Sol	-1.468	0.424	0.740
Cd 9-5 5h Sol	-1.202	0.105	0.533
Cd 9-5 T0 Sol	-1.264	-0.532	-0.513
Cd 9-7 3h Sol	-1.641	0.232	-0.201
Cd 9-7 45m Sol	-1.157	-0.070	1.176
Cd 9-7 5h Sol	-1.445	0.002	1.812
Cd 9-7 T0 Sol	-0.656	-0.063	0.291
Control			
Ctrl 11-3 3h Sol	0.233	1.257	0.443
Ctrl 11-3 45m Sol	1.202	0.283	0.999
Ctrl 11-3 5h Sol	-0.255	-0.152	1.132
Ctrl 11-3 T0 Sol	0.732	0.447	0.260
Ctrl 11-5 3h Sol	-0.101	1.317	0.736
Ctrl 11-5 45m Sol	0.342	1.107	1.078
Ctrl 11-5 5h Sol	0.061	0.462	0.676
Ctrl 11-5 T0 Sol	0.584	0.629	-0.071
Ctrl 6-14 3h Sol	0.337	1.117	0.361
Ctrl 6-14 45m Sol	1.451	0.741	1.480
Ctrl 6-14 5h Sol	1.027	1.568	-0.284

Sample	DF1	DF2	DF3
Control (cont.)			
Ctrl 6-14 T0 Sol	0.438	0.551	0.082
Ctrl 6-16 3h Sol	0.272	1.316	0.392
Ctrl 6-16 45m Sol	0.308	0.325	0.743
Ctrl 6-16 5h Sol	1.019	0.349	0.273
Ctrl 6-16 T0 Sol	-0.192	0.368	0.256
Ctrl 6-27 3h Sol	0.475	0.471	0.990
Ctrl 6-27 45m Sol	0.444	0.076	1.127
Ctrl 6-27 5h Sol	0.301	1.019	0.839
Ctrl 6-27 T0 Sol	1.350	0.562	0.728
Ctrl 6-29 3h Sol	-0.180	-0.128	1.214
Ctrl 6-29 3h Sol2	0.162	0.532	0.593
Ctrl 6-29 45m Sol	0.272	0.748	0.117
Ctrl 6-29 5h Sol	0.559	0.580	0.854
Ctrl 9-5 3h Sol	0.060	0.120	0.359
Ctrl 9-5 45m Sol	0.295	0.464	0.681
Ctrl 9-5 5h Sol	-0.326	0.955	0.490
Ctrl 9-5 T0 Sol	0.381	1.269	0.324
Ctrl 9-7 3h Sol	0.739	0.409	0.753
Ctrl 9-7 45m Sol	0.812	1.019	0.236
Ctrl 9-7 5h Sol	0.507	0.353	0.012
Ctrl 9-7 T0 Sol	-0.143	1.397	0.122
DNP			
DNP 11-3 3h Sol	-0.661	1.205	-0.254
DNP 11-3 45m Sol	0.757	0.666	-0.812
DNP 11-3 5h Sol	0.361	0.716	-0.504
DNP 11-3 T0 Sol	-0.172	0.844	-0.837
DNP 11-5 3h Sol	0.001	0.534	-0.250
DNP 11-5 45m Sol	-0.216	0.532	-1.297
DNP 11-5 5h Sol	-0.181	-0.203	-0.733
DNP 11-5 T0 Sol	-0.071	1.425	-1.288
DNP 6-14 3h Sol	-0.356	0.591	-1.160
DNP 6-14 45m Sol	0.979	0.865	-1.209
DNP 6-14 5h Sol	0.244	0.322	-0.499
DNP 6-14 T0 Sol	-0.688	0.761	-1.208
DNP 6-16 3h Sol	-0.093	0.436	-0.656
DNP 6-16 45m Sol	0.001	0.674	-0.439
DNP 6-16 5h Sol	0.025	0.513	-0.043
DNP 6-16 T0 Sol	-0.218	0.643	-0.251
DNP 6-27 3h Sol	0.315	0.741	-0.546
DNP 6-27 45m Sol	-0.787	0.432	-0.851
DNP 6-27 5h Sol	-0.094	0.972	-0.485
DNP 6-27 T0 Sol	-0.067	0.772	-0.743
DNP 6-29 3h Sol	-0.105	-0.720	-1.197
DNP 6-29 45m Sol	0.231	0.520	-0.233
DNP 6-29 5h Sol	-0.404	0.464	-1.071
DNP 6-29 T0 Sol	-0.127	0.872	-0.072
DNP 9-5 3h Sol	0.372	0.423	-0.534
DNP 9-5 45m Sol	-0.231	1.066	-0.479

Sample	DF1	DF2	DF3
DNP (cont.)			
DNP 9-5 T0 Sol	0.214	-0.044	-0.471
DNP 9-7 3h Sol	0.013	0.269	-1.011
DNP 9-7 45m Sol	-0.127	-0.522	-0.744
DNP 9-7 45m Sol2	0.561	0.751	-0.510
DNP 9-7 5h Sol	-0.308	-0.203	-1.091
DNP 9-7 T0 Sol	0.043	-0.078	-0.735
NEM			
NEM 11-3 3h Sol	0.479	-0.837	-0.663
NEM 11-3 45m Sol	0.564	-0.756	0.549
NEM 11-3 5h Sol	1.016	-1.739	0.731
NEM 11-3 T0 Sol	1.017	-0.654	0.154
NEM 11-5 3h Sol	0.386	-0.677	0.018
NEM 11-5 45m Sol	0.408	-1.379	-0.956
NEM 11-5 5h Sol	0.891	-1.093	0.269
NEM 11-5 T0 Sol	0.667	-0.783	-0.919
NEM 6-14 3h Sol	0.507	-0.714	-0.417
NEM 6-14 45m Sol	-0.101	-1.021	0.135
NEM 6-14 5h Sol	0.927	-0.781	0.018
NEM 6-14 T0 Sol	0.740	-0.830	-0.338
NEM 6-16 3h Sol	1.154	-0.019	0.300
NEM 6-16 45m Sol	0.916	-1.511	0.144
NEM 6-16 5h Sol	0.581	-0.157	0.374
NEM 6-16 T0 Sol	0.371	-0.592	-0.243
NEM 6-27 3h Sol	1.346	-0.229	0.423
NEM 6-27 45m Sol	1.044	-0.276	-0.464
NEM 6-27 5h Sol	1.888	-0.310	-1.092
NEM 6-27 T0 Sol	1.781	-0.829	-0.286
NEM 6-29 3h Sol	1.007	-1.848	0.539
NEM 6-29 45m Sol	1.087	-1.676	-0.403
NEM 6-29 5h Sol	1.290	-0.817	0.002
NEM 6-29 T0 Sol	0.621	-0.245	-0.146
NEM 9-5 3h Sol	1.135	-1.472	0.370
NEM 9-5 45m Sol	0.758	-0.835	-0.229
NEM 9-5 5h Sol	0.207	-0.925	0.565
NEM 9-5 T0 Sol	0.306	-0.851	-0.053
NEM 9-7 3h Sol	1.097	-0.906	0.436
NEM 9-7 45m Sol	1.675	-0.518	0.102
NEM 9-7 5h Sol	0.487	-1.012	0.122
NEM 9-7 T0 Sol	0.526	-0.238	-0.394

Table 5 - Data for Figure 2 in Chapter 5: output from GA-DFA run.

ometer results for d0/V-002

Multiple Discriminant Analysis with Variable Selection - GA-DFA

128 samples in 4 classes.

Class distributions	
class	**samples**
c	32
cd	32
d	32
n	32

Attributes used in the classification:

- 562
- 1948
- 1354
- 1390
- 628
- 578
- 700
- 692
- 662
- 1174
- 494
- 701
- 1234
- 1189
- 1296
- 1170
- 1437
- 531
- 1377
- 830
- 630
- 843
- 1199
- 950
- 744
- 736

- 774
- 826
- 671
- 618

Overall accuracy: 99.2188 %.

Wilke's lambda: 0.24021

Sum of inverse of eigenvalues: 5.117

Misclassified samples		
sample	**real class**	**predicted class**
Ctrl 9-7 T0 Sol.txt	c	d

Confusion matrix					
	c	cd	d	n	False Negative
c	**31**	0	1	0	3.13 %
cd	0	**32**	0	0	0.00 %
d	0	0	**32**	0	0.00 %
n	0	0	0	**32**	0.00 %
False Positive	0.00 %	0.00 %	3.03 %	0.00 %	

generated with ometer version 0.54 on Tue Mar 21 15:50:02 2006 with
```
ometer -m=ga-dfa --ga-genes=30 --ga-population=50 --ga-generations=600 -o
d0/V-002 sol4classesallplants.dat
```

Table 6 - Data for Figure 3 in Chapter 5: results from 10,000 GA-DFA runs (m/z ratios arranged from highest to lowest selection frequency).

m/z ratio	# times selected	Selection frequency (%)
1683	891	8.9
1682	700	7.0
1707	666	6.7
1694	661	6.6
1677	641	6.4
1949	636	6.4
1717	619	6.2
1913	616	6.2
1680	604	6.0
948	586	5.9
1703	583	5.8
1884	581	5.8
1251	580	5.8
1746	571	5.7
1689	570	5.7
1718	541	5.4
1659	530	5.3
1811	526	5.3
1690	524	5.2
1641	522	5.2
1666	522	5.2
1711	516	5.2
1653	512	5.1
1701	505	5.1
671	495	5.0
1736	491	4.9
1375	486	4.9
1696	486	4.9
614	485	4.9
1421	483	4.8
656	482	4.8
361	478	4.8
660	477	4.8
752	470	4.7
1684	469	4.7
1715	469	4.7
721	463	4.6
594	461	4.6
646	461	4.6
1704	453	4.5
1726	451	4.5
1839	451	4.5
744	450	4.5
1702	450	4.5

m/z ratio	# times selected	Selection frequency (%)
1685	449	4.5
1698	447	4.5
1323	444	4.4
1379	444	4.4
991	443	4.4
1679	442	4.4
1796	438	4.4
1647	433	4.3
649	432	4.3
950	431	4.3
1247	431	4.3
735	429	4.3
1212	425	4.3
1119	424	4.2
1887	423	4.2
1714	422	4.2
1777	421	4.2
1688	415	4.2
1675	413	4.1
1948	413	4.1
402	412	4.1
1692	412	4.1
351	411	4.1
1662	410	4.1
1649	403	4.0
687	402	4.0
1686	402	4.0
1691	401	4.0
1676	399	4.0
350	396	4.0
1635	396	4.0
1029	395	4.0
1750	394	3.9
1929	394	3.9
1037	393	3.9
1940	392	3.9
729	390	3.9
815	389	3.9
1687	389	3.9
1064	386	3.9
1632	383	3.8
1583	380	3.8
1622	379	3.8
1669	379	3.8
966	378	3.8
732	377	3.8
1645	376	3.8
1005	375	3.8
673	374	3.7

m/z ratio	# times selected	Selection frequency (%)
1288	374	3.7
1712	374	3.7
736	373	3.7
1244	373	3.7
1642	369	3.7
352	368	3.7
1800	368	3.7
651	367	3.7
691	364	3.6
1699	364	3.6
1002	363	3.6
1729	361	3.6
1631	359	3.6
555	358	3.6
693	358	3.6
1627	357	3.6
1640	357	3.6
850	355	3.6
1123	351	3.5
947	350	3.5
1286	350	3.5
1895	350	3.5
1030	349	3.5
1199	349	3.5
1636	347	3.5
1650	347	3.5
648	346	3.5
657	345	3.5
1947	345	3.5
630	344	3.4
1618	344	3.4
1287	342	3.4
358	341	3.4
355	340	3.4
1657	340	3.4
733	338	3.4
1817	338	3.4
1633	337	3.4
1673	337	3.4
610	335	3.4
818	335	3.4
1654	335	3.4
1705	335	3.4
1719	335	3.4
391	334	3.3
427	334	3.3
1644	333	3.3
1745	333	3.3
1759	333	3.3

m/z ratio	# times selected	Selection frequency (%)
1807	333	3.3
604	332	3.3
1697	332	3.3
1735	331	3.3
531	330	3.3
1625	330	3.3
1710	330	3.3
833	328	3.3
1424	328	3.3
1651	328	3.3
573	327	3.3
694	325	3.3
755	325	3.3
783	325	3.3
1870	325	3.3
663	324	3.2
781	324	3.2
667	323	3.2
770	323	3.2
1763	323	3.2
701	322	3.2
722	321	3.2
1739	321	3.2
414	320	3.2
607	320	3.2
1971	320	3.2
1695	319	3.2
1844	319	3.2
1267	318	3.2
678	317	3.2
711	317	3.2
1043	317	3.2
1853	317	3.2
1054	316	3.2
1667	315	3.2
1671	314	3.1
1681	313	3.1
1747	311	3.1
683	310	3.1
1331	309	3.1
1909	309	3.1
612	308	3.1
712	308	3.1
867	308	3.1
996	307	3.1
1725	306	3.1
1744	305	3.1
1938	305	3.1
652	304	3.0

m/z ratio	# times selected	Selection frequency (%)
979	304	3.0
1009	304	3.0
1403	304	3.0
1801	304	3.0
1299	303	3.0
939	302	3.0
1862	301	3.0
659	300	3.0
1743	300	3.0
944	299	3.0
1062	299	3.0
1638	299	3.0
1845	299	3.0
987	298	3.0
990	298	3.0
1764	298	3.0
676	296	3.0
819	296	3.0
1835	296	3.0
978	295	3.0
1039	295	3.0
1664	295	3.0
611	294	2.9
650	294	2.9
943	294	2.9
1020	294	2.9
1623	294	2.9
1655	294	2.9
1656	294	2.9
1740	293	2.9
575	292	2.9
999	291	2.9
1455	291	2.9
1544	290	2.9
1771	290	2.9
756	289	2.9
772	289	2.9
983	289	2.9
618	288	2.9
1752	288	2.9
1898	288	2.9
644	287	2.9
971	287	2.9
1026	287	2.9
1597	287	2.9
1722	287	2.9
1724	286	2.9
1648	285	2.9
1713	285	2.9

m/z ratio	# times selected	Selection frequency (%)
1038	284	2.8
1345	284	2.8
1693	284	2.8
1860	284	2.8
960	283	2.8
1815	282	2.8
582	281	2.8
719	281	2.8
965	281	2.8
1388	281	2.8
1660	281	2.8
727	280	2.8
1234	280	2.8
1709	280	2.8
761	279	2.8
821	279	2.8
914	279	2.8
1060	279	2.8
1600	278	2.8
1755	278	2.8
702	277	2.8
742	277	2.8
822	277	2.8
576	276	2.8
1652	276	2.8
653	275	2.8
681	275	2.8
1044	275	2.8
1880	275	2.8
669	274	2.7
1303	273	2.7
429	271	2.7
952	271	2.7
1720	271	2.7
416	270	2.7
1129	270	2.7
739	269	2.7
1040	269	2.7
1042	269	2.7
1254	269	2.7
1661	269	2.7
581	268	2.7
639	268	2.7
957	268	2.7
1612	268	2.7
769	267	2.7
1099	267	2.7
1182	267	2.7
1784	267	2.7

m/z ratio	# times selected	Selection frequency (%)
665	266	2.7
1825	266	2.7
1852	266	2.7
696	265	2.7
532	264	2.6
762	263	2.6
1700	263	2.6
1751	263	2.6
776	262	2.6
1663	262	2.6
700	261	2.6
728	261	2.6
784	261	2.6
816	261	2.6
1204	261	2.6
1604	261	2.6
1629	261	2.6
1716	260	2.6
572	259	2.6
710	259	2.6
1203	258	2.6
1414	258	2.6
534	257	2.6
658	257	2.6
1626	257	2.6
1362	256	2.6
720	255	2.6
1015	255	2.6
1051	255	2.6
1059	255	2.6
1298	255	2.6
1179	254	2.5
1668	254	2.5
1708	254	2.5
718	253	2.5
773	253	2.5
988	253	2.5
409	252	2.5
759	252	2.5
1734	252	2.5
1851	252	2.5
972	251	2.5
1380	251	2.5
985	250	2.5
1023	248	2.5
1590	248	2.5
1814	248	2.5
384	247	2.5
1071	247	2.5

m/z ratio	# times selected	Selection frequency (%)
1731	247	2.5
764	246	2.5
1776	246	2.5
715	245	2.5
726	244	2.4
1032	244	2.4
1372	244	2.4
1514	244	2.4
951	243	2.4
1840	243	2.4
1927	243	2.4
613	242	2.4
894	242	2.4
919	242	2.4
1112	242	2.4
664	241	2.4
1047	241	2.4
1167	241	2.4
1181	241	2.4
1628	241	2.4
640	240	2.4
1343	240	2.4
1584	240	2.4
1230	239	2.4
1236	239	2.4
1770	239	2.4
1936	239	2.4
968	238	2.4
589	237	2.4
679	237	2.4
907	237	2.4
1052	237	2.4
1361	237	2.4
1515	237	2.4
1548	237	2.4
1812	237	2.4
684	236	2.4
716	236	2.4
1417	236	2.4
1741	236	2.4
757	235	2.4
895	235	2.4
1728	235	2.4
1809	235	2.4
801	234	2.3
1045	234	2.3
362	233	2.3
563	233	2.3
1096	233	2.3

m/z ratio	# times selected	Selection frequency (%)
1404	233	2.3
1603	233	2.3
389	232	2.3
747	232	2.3
953	232	2.3
1908	232	2.3
617	231	2.3
1415	231	2.3
1574	231	2.3
1624	231	2.3
1891	231	2.3
380	230	2.3
647	230	2.3
1018	230	2.3
1034	230	2.3
1223	230	2.3
1674	230	2.3
1738	230	2.3
1894	230	2.3
436	229	2.3
854	229	2.3
855	229	2.3
397	228	2.3
562	228	2.3
670	228	2.3
1000	228	2.3
1067	228	2.3
1799	228	2.3
539	227	2.3
1027	227	2.3
1063	227	2.3
1195	227	2.3
1730	227	2.3
535	226	2.3
863	226	2.3
891	226	2.3
982	226	2.3
1293	226	2.3
1607	226	2.3
1827	226	2.3
1911	226	2.3
431	225	2.3
771	224	2.2
1275	224	2.2
1292	224	2.2
1615	224	2.2
407	223	2.2
566	223	2.2
746	223	2.2

m/z ratio	# times selected	Selection frequency (%)
763	223	2.2
1110	223	2.2
1335	223	2.2
1619	223	2.2
1665	223	2.2
1930	223	2.2
580	222	2.2
1025	222	2.2
1753	222	2.2
1810	222	2.2
1843	222	2.2
625	220	2.2
1248	220	2.2
1383	220	2.2
1614	220	2.2
590	219	2.2
743	219	2.2
766	219	2.2
793	219	2.2
843	219	2.2
1512	219	2.2
1896	219	2.2
421	218	2.2
567	218	2.2
1658	218	2.2
1897	218	2.2
980	217	2.2
984	217	2.2
1786	217	2.2
631	216	2.2
754	216	2.2
839	216	2.2
1352	216	2.2
1678	216	2.2
1795	216	2.2
1992	216	2.2
404	215	2.2
692	215	2.2
1008	215	2.2
1864	215	2.2
615	214	2.1
698	214	2.1
1283	214	2.1
1723	214	2.1
1877	214	2.1
1035	213	2.1
1579	213	2.1
1670	213	2.1
1797	213	2.1

m/z ratio	# times selected	Selection frequency (%)
826	212	2.1
949	212	2.1
1003	212	2.1
1330	212	2.1
1371	212	2.1
1904	212	2.1
1915	212	2.1
403	211	2.1
406	211	2.1
765	211	2.1
1016	211	2.1
1048	211	2.1
1075	211	2.1
1255	211	2.1
1264	211	2.1
836	210	2.1
1605	210	2.1
1999	210	2.1
359	209	2.1
621	209	2.1
638	209	2.1
823	209	2.1
959	209	2.1
1214	209	2.1
1634	209	2.1
1706	209	2.1
1906	209	2.1
956	208	2.1
1486	208	2.1
1766	208	2.1
1773	208	2.1
527	207	2.1
774	207	2.1
383	206	2.1
424	206	2.1
758	206	2.1
777	206	2.1
842	206	2.1
1846	206	2.1
723	205	2.1
1124	205	2.1
1284	205	2.1
1401	205	2.1
1873	205	2.1
730	204	2.0
786	204	2.0
1087	204	2.0
1233	204	2.0
1778	204	2.0

m/z ratio	# times selected	Selection frequency (%)
1879	204	2.0
1171	203	2.0
1242	203	2.0
1420	203	2.0
1774	203	2.0
1931	203	2.0
530	202	2.0
571	202	2.0
884	202	2.0
376	201	2.0
797	201	2.0
1790	201	2.0
394	200	2.0
974	200	2.0
1144	200	2.0
1630	200	2.0
1858	200	2.0

Table 7 - Data for Figure 4A in Chapter 5: value of DF1 for each sample (resulting from one GA-DFA run conducted with control and cadmium samples).

Control Sample	DF1	Cadmium Sample	DF1
Ctrl 11-3 3h Sol	0.164	Cd 11-3 3h Sol	-0.515
Ctrl 11-3 45m Sol	0.417	Cd 11-3 45m Sol	-0.580
Ctrl 11-3 5h Sol	0.049	Cd 11-3 5h Sol	-0.974
Ctrl 11-3 T0 Sol	0.789	Cd 11-3 T0 Sol	-0.648
Ctrl 11-5 3h Sol	0.251	Cd 11-5 3h Sol	-1.004
Ctrl 11-5 45m Sol	0.677	Cd 11-5 45m Sol	-0.272
Ctrl 11-5 5h Sol	0.867	Cd 11-5 5h Sol	-0.445
Ctrl 11-5 T0 Sol	0.700	Cd 11-5 T0 Sol	-0.557
Ctrl 6-14 3h Sol	1.131	Cd 6-14 3h Sol	-1.628
Ctrl 6-14 45m Sol	0.695	Cd 6-14 45m Sol	-0.187
Ctrl 6-14 5h Sol	1.435	Cd 6-14 5h Sol	-0.905
Ctrl 6-14 T0 Sol	0.612	Cd 6-14 T0 Sol	-0.707
Ctrl 6-16 3h Sol	0.546	Cd 6-16 3h Sol	-0.952
Ctrl 6-16 45m Sol	0.657	Cd 6-16 45m Sol	-1.645
Ctrl 6-16 5h Sol	0.929	Cd 6-16 5h Sol	-0.294
Ctrl 6-16 T0 Sol	0.947	Cd 6-16 T0 Sol	-0.351
Ctrl 6-27 3h Sol	0.771	Cd 6-27 3h Sol	-0.928
Ctrl 6-27 45m Sol	0.934	Cd 6-27 45m Sol	-1.700
Ctrl 6-27 5h Sol	0.609	Cd 6-27 5h Sol	-0.361
Ctrl 6-27 T0 Sol	0.904	Cd 6-27 T0 Sol	-0.892
Ctrl 6-29 3h Sol	1.463	Cd 6-29 3h Sol	-1.201
Ctrl 6-29 3h Sol2	0.429	Cd 6-29 45m Sol	-0.145
Ctrl 6-29 45m Sol	0.438	Cd 6-29 5h Sol	-0.745
Ctrl 6-29 5h Sol	0.938	Cd 6-29 T0 Sol	-1.037
Ctrl 9-5 3h Sol	0.679	Cd 9-5 3h Sol	-0.631
Ctrl 9-5 45m Sol	0.915	Cd 9-5 45m Sol	-1.559
Ctrl 9-5 5h Sol	1.087	Cd 9-5 5h Sol	-1.243
Ctrl 9-5 T0 Sol	1.450	Cd 9-5 T0 Sol	-0.556
Ctrl 9-7 3h Sol	0.942	Cd 9-7 3h Sol	-0.657
Ctrl 9-7 45m Sol	0.835	Cd 9-7 45m Sol	-1.198
Ctrl 9-7 5h Sol	0.870	Cd 9-7 5h Sol	-0.044
Ctrl 9-7 T0 Sol	1.473	Cd 9-7 T0 Sol	-1.037

Table 8 - Data for Figure 4A in Chapter 5: output from GA-DFA run.

ometer results for d0/V-041

Multiple Discriminant Analysis with Variable Selection - GA-DFA

64 samples in 2 classes.

Class distributions	
class	**samples**
c	32
cd	32

Attributes used in the classification:

- 1592
- 1842
- 1195
- 1271

Overall accuracy: 100.0000 %.

Wilke's lambda: 0.55558

Sum of inverse of eigenvalues: 1.2501

Confusion matrix			
	c	cd	False Negative
c	**32**	0	0.00 %
cd	0	**32**	0.00 %
False Positive	0.00 %	0.00 %	

generated with ometer version 0.54 on Thu Mar 23 15:43:58 2006 with
`ometer -m=ga-dfa --ga-genes=4 --ga-population=50 --ga-generations=200 -o d0/V-041 solccdallplants.dat`

Table 9 - Data for Figure 4B in Chapter 5: value of DF1 for each sample (resulting from one GA-DFA run conducted with control and DNP samples).

Control Sample	DF1	DNP Sample	DF1
Ctrl 11-3 3h Sol	0.479	DNP 11-3 3h Sol	-0.649
Ctrl 11-3 45m Sol	1.795	DNP 11-3 45m Sol	-0.043
Ctrl 11-3 5h Sol	0.690	DNP 11-3 5h Sol	-0.174
Ctrl 11-3 T0 Sol	0.856	DNP 11-3 T0 Sol	-0.650
Ctrl 11-5 3h Sol	0.946	DNP 11-5 3h Sol	-0.372
Ctrl 11-5 45m Sol	0.505	DNP 11-5 45m Sol	-1.200
Ctrl 11-5 5h Sol	1.182	DNP 11-5 5h Sol	-0.723
Ctrl 11-5 T0 Sol	0.713	DNP 11-5 T0 Sol	-0.901
Ctrl 6-14 3h Sol	0.940	DNP 6-14 3h Sol	-0.524
Ctrl 6-14 45m Sol	0.233	DNP 6-14 45m Sol	-1.051
Ctrl 6-14 5h Sol	0.434	DNP 6-14 5h Sol	-0.726
Ctrl 6-14 T0 Sol	0.779	DNP 6-14 T0 Sol	-0.751
Ctrl 6-16 3h Sol	0.355	DNP 6-16 3h Sol	-0.682
Ctrl 6-16 45m Sol	1.477	DNP 6-16 45m Sol	-0.647
Ctrl 6-16 5h Sol	0.268	DNP 6-16 5h Sol	-0.375
Ctrl 6-16 T0 Sol	0.895	DNP 6-16 T0 Sol	-1.781
Ctrl 6-27 3h Sol	1.736	DNP 6-27 3h Sol	-1.158
Ctrl 6-27 45m Sol	0.439	DNP 6-27 45m Sol	-0.926
Ctrl 6-27 5h Sol	0.857	DNP 6-27 5h Sol	-0.569
Ctrl 6-27 T0 Sol	0.911	DNP 6-27 T0 Sol	-0.405
Ctrl 6-29 3h Sol	0.459	DNP 6-29 3h Sol	-1.143
Ctrl 6-29 3h Sol2	0.771	DNP 6-29 45m Sol	-1.631
Ctrl 6-29 45m Sol	0.508	DNP 6-29 5h Sol	-0.437
Ctrl 6-29 5h Sol	1.480	DNP 6-29 T0 Sol	-0.721
Ctrl 9-5 3h Sol	0.317	DNP 9-5 3h Sol	-0.646
Ctrl 9-5 45m Sol	0.535	DNP 9-5 45m Sol	-0.565
Ctrl 9-5 5h Sol	1.409	DNP 9-5 T0 Sol	-1.283
Ctrl 9-5 T0 Sol	0.282	DNP 9-7 3h Sol	-0.170
Ctrl 9-7 3h Sol	0.978	DNP 9-7 45m Sol	-0.969
Ctrl 9-7 45m Sol	0.845	DNP 9-7 45m Sol2	-1.300
Ctrl 9-7 5h Sol	0.287	DNP 9-7 5h Sol	-1.098
Ctrl 9-7 T0 Sol	0.138	DNP 9-7 T0 Sol	-0.230

Table 10 - Data for Figure 4B in Chapter 5: output from GA-DFA run.

ometer results for d0/V-022

Multiple Discriminant Analysis with Variable Selection - GA-DFA

64 samples in 2 classes.

Class distributions	
class	**samples**
c	32
d	32

Attributes used in the classification:

- 1072
- 687
- 764
- 1000

Overall accuracy: 100.0000 %.

Wilke's lambda: 0.56638

Sum of inverse of eigenvalues: 1.3062

Confusion matrix			
	c	d	False Negative
c	**32**	0	0.00 %
d	0	**32**	0.00 %
False Positive	0.00 %	0.00 %	

generated with ometer version 0.54 on Thu Mar 23 15:43:01 2006 with
`ometer -m=ga-dfa --ga-genes=4 --ga-population=50 --ga-generations=300 -o d0/V-022 solcdnpallplants.dat`

Table 11 - Data for Figure 4C in Chapter 5: value of DF1 for each sample (resulting from one GA-DFA run conducted with control and NEM samples).

Control Sample	DF1	NEM Sample	DF1
Ctrl 11-3 3h Sol	0.235	NEM 11-3 3h Sol	-0.515
Ctrl 11-3 45m Sol	0.359	NEM 11-3 45m Sol	-1.069
Ctrl 11-3 5h Sol	1.104	NEM 11-3 5h Sol	-0.821
Ctrl 11-3 T0 Sol	1.659	NEM 11-3 T0 Sol	-0.341
Ctrl 11-5 3h Sol	0.323	NEM 11-5 3h Sol	-0.674
Ctrl 11-5 45m Sol	0.419	NEM 11-5 45m Sol	-0.357
Ctrl 11-5 5h Sol	0.731	NEM 11-5 5h Sol	-1.045
Ctrl 11-5 T0 Sol	1.448	NEM 11-5 T0 Sol	-0.559
Ctrl 6-14 3h Sol	0.844	NEM 6-14 3h Sol	-0.281
Ctrl 6-14 45m Sol	1.119	NEM 6-14 45m Sol	-0.503
Ctrl 6-14 5h Sol	1.183	NEM 6-14 5h Sol	-0.329
Ctrl 6-14 T0 Sol	0.663	NEM 6-14 T0 Sol	-0.380
Ctrl 6-16 3h Sol	0.080	NEM 6-16 3h Sol	-0.615
Ctrl 6-16 45m Sol	0.705	NEM 6-16 45m Sol	-0.499
Ctrl 6-16 5h Sol	0.300	NEM 6-16 5h Sol	-1.189
Ctrl 6-16 T0 Sol	0.320	NEM 6-16 T0 Sol	-1.246
Ctrl 6-27 3h Sol	0.548	NEM 6-27 3h Sol	-0.603
Ctrl 6-27 45m Sol	0.756	NEM 6-27 45m Sol	-1.311
Ctrl 6-27 5h Sol	0.792	NEM 6-27 5h Sol	-0.421
Ctrl 6-27 T0 Sol	0.938	NEM 6-27 T0 Sol	-0.566
Ctrl 6-29 3h Sol	0.262	NEM 6-29 3h Sol	-1.108
Ctrl 6-29 3h Sol2	0.512	NEM 6-29 45m Sol	-0.854
Ctrl 6-29 45m Sol	1.852	NEM 6-29 5h Sol	-0.667
Ctrl 6-29 5h Sol	0.822	NEM 6-29 T0 Sol	-0.862
Ctrl 9-5 3h Sol	0.317	NEM 9-5 3h Sol	-0.381
Ctrl 9-5 45m Sol	0.593	NEM 9-5 45m Sol	-1.823
Ctrl 9-5 5h Sol	1.954	NEM 9-5 5h Sol	-0.831
Ctrl 9-5 T0 Sol	0.136	NEM 9-5 T0 Sol	-0.831
Ctrl 9-7 3h Sol	1.327	NEM 9-7 3h Sol	-0.940
Ctrl 9-7 45m Sol	1.167	NEM 9-7 45m Sol	-1.166
Ctrl 9-7 5h Sol	0.479	NEM 9-7 5h Sol	-0.873
Ctrl 9-7 T0 Sol	0.582	NEM 9-7 T0 Sol	-0.867

Table 12 - Data for Figure 4C in Chapter 5: output from GA-DFA run.

ometer results for d0/V-020

Multiple Discriminant Analysis with Variable Selection - GA-DFA

64 samples in 2 classes.

Class distributions	
class	**samples**
c	32
n	32

Attributes used in the classification:

- 737
- 1765
- 1368
- 680

Overall accuracy: 100.0000 %.

Wilke's lambda: 0.5661

Sum of inverse of eigenvalues: 1.3047

Confusion matrix			
	c	n	False Negative
c	**32**	0	0.00 %
n	0	**32**	0.00 %
False Positive	0.00 %	0.00 %	

generated with ometer version 0.54 on Thu Mar 23 15:42:50 2006 with
`ometer -m=ga-dfa --ga-genes=4 --ga-population=50 --ga-generations=200 -o d0/V-020 solcnemallplants.dat`

Table 13 - Data for Figure 4D in Chapter 5: results from 20,000 GA-DFA runs (control versus cadmium samples; m/z ratios arranged from highest to lowest selection frequency).

m/z ratio	# times selected	selection frequency (%)
1271	16589	82.9
1592	10435	52.2
1195	7395	37.0
1346	4728	23.6
604	4649	23.2
1842	4150	20.8
1698	3278	16.4
1554	3120	15.6
536	2185	10.9
806	2134	10.7
844	2038	10.2
1251	1463	7.3
712	1349	6.7
652	1322	6.6
1116	1248	6.2
725	1224	6.1
1477	1187	5.9
1567	990	5.0
620	849	4.2
1209	771	3.9
1055	622	3.1
1740	561	2.8
626	534	2.7
1119	526	2.6
764	526	2.6
1550	524	2.6
533	468	2.3
1062	445	2.2
1537	345	1.7
969	328	1.6
1455	288	1.4
856	279	1.4
628	253	1.3
1173	208	1.0
483	191	1.0
917	188	0.9
1216	176	0.9
1308	167	0.8
1867	158	0.8
843	139	0.7
1590	112	0.6
1129	110	0.6
1458	109	0.5
831	108	0.5

m/z ratio	# times selected	selection frequency (%)
777	104	0.5
769	94	0.5
1351	93	0.5
648	88	0.4
390	83	0.4
1608	80	0.4
938	78	0.4
575	66	0.3
401	63	0.3
413	54	0.3
1975	52	0.3
1825	51	0.3
1109	43	0.2
710	37	0.2
726	37	0.2
664	36	0.2
1060	34	0.2
1497	32	0.2
1465	23	0.1
1509	23	0.1
767	23	0.1
520	21	0.1
719	20	0.1
1087	18	0.1
607	17	0.1
1850	12	0.1
910	12	0.1
933	12	0.1
967	12	0.1
1807	10	0.1
529	10	0.1
1038	9	0.0
462	9	0.0
421	8	0.0
955	8	0.0
1182	7	0.0
495	7	0.0
707	7	0.0
1561	6	0.0
1739	6	0.0
1864	6	0.0
514	6	0.0
715	6	0.0
1765	4	0.0
1816	4	0.0
497	4	0.0
532	4	0.0
1047	3	0.0
1070	3	0.0

m/z ratio	# times selected	selection frequency (%)
1081	3	0.0
1237	3	0.0
1360	3	0.0
1429	3	0.0
1854	3	0.0
1895	3	0.0
1916	3	0.0
449	3	0.0
1107	2	0.0
1224	2	0.0
1363	2	0.0
1474	2	0.0
1475	2	0.0
1553	2	0.0
1557	2	0.0
1606	2	0.0
490	2	0.0
790	2	0.0
838	2	0.0
859	2	0.0
965	2	0.0
995	2	0.0
1048	1	0.0
1113	1	0.0
1145	1	0.0
1164	1	0.0
1169	1	0.0
1184	1	0.0
1194	1	0.0
1210	1	0.0
1253	1	0.0
1348	1	0.0
1394	1	0.0
1445	1	0.0
1468	1	0.0
1513	1	0.0
1663	1	0.0
1665	1	0.0
1724	1	0.0
1730	1	0.0
1827	1	0.0
1859	1	0.0
1957	1	0.0
446	1	0.0
447	1	0.0
476	1	0.0
582	1	0.0
662	1	0.0
711	1	0.0

m/z ratio	# times selected	selection frequency (%)
758	1	0.0
768	1	0.0
851	1	0.0
867	1	0.0
870	1	0.0
924	1	0.0
962	1	0.0

Table 14 - Data for Figure 4E in Chapter 5: results from 20,000 GA-DFA runs (control versus DNP samples; m/z ratios arranged from highest to lowest selection frequency).

m/z ratio	# times selected	selection frequency (%)
1072	10403	52.0
764	9508	47.5
687	6396	32.0
815	5119	25.6
1602	5103	25.5
1000	4567	22.8
738	4489	22.4
470	3639	18.2
1969	2555	12.8
885	2036	10.2
1166	1657	8.3
1081	1621	8.1
430	1461	7.3
1199	1409	7.0
1832	1354	6.8
756	1251	6.3
547	1234	6.2
458	1232	6.2
1119	1203	6.0
1546	1107	5.5
667	959	4.8
1052	878	4.4
1484	824	4.1
1164	724	3.6
1215	714	3.6
892	604	3.0
473	452	2.3
812	440	2.2
600	404	2.0
596	401	2.0
931	370	1.9
492	340	1.7
1246	318	1.6
1448	294	1.5
853	294	1.5
543	274	1.4
1835	271	1.4
1029	267	1.3
1899	254	1.3
632	249	1.2
1162	224	1.1
1570	208	1.0
811	200	1.0
982	199	1.0

m/z ratio	# times selected	selection frequency (%)
1526	189	0.9
970	187	0.9
1525	174	0.9
1518	171	0.9
394	156	0.8
633	145	0.7
1707	106	0.5
694	79	0.4
710	75	0.4
1955	70	0.4
1801	69	0.3
501	67	0.3
1177	66	0.3
1276	60	0.3
1967	59	0.3
1195	58	0.3
615	54	0.3
1722	45	0.2
1530	43	0.2
1916	42	0.2
476	40	0.2
1542	38	0.2
588	33	0.2
1733	31	0.2
367	29	0.1
930	28	0.1
1980	27	0.1
1055	21	0.1
1628	19	0.1
1320	18	0.1
1241	17	0.1
1491	17	0.1
1194	16	0.1
1319	16	0.1
1331	14	0.1
1952	13	0.1
1549	10	0.1
1775	10	0.1
1779	9	0.0
1191	8	0.0
1253	8	0.0
1045	7	0.0
1071	6	0.0
358	6	0.0
901	6	0.0
1471	5	0.0
472	5	0.0
597	5	0.0
618	5	0.0

m/z ratio	# times selected	selection frequency (%)
844	5	0.0
1073	4	0.0
1340	4	0.0
1454	4	0.0
1519	4	0.0
863	4	0.0
1138	3	0.0
1497	3	0.0
1522	3	0.0
1593	3	0.0
1647	3	0.0
1985	3	0.0
414	3	0.0
463	3	0.0
799	3	0.0
1238	2	0.0
1460	2	0.0
1566	2	0.0
1739	2	0.0
1954	2	0.0
1973	2	0.0
391	2	0.0
443	2	0.0
636	2	0.0
685	2	0.0
751	2	0.0
925	2	0.0
966	2	0.0
1046	1	0.0
1074	1	0.0
1084	1	0.0
1207	1	0.0
1211	1	0.0
1243	1	0.0
1342	1	0.0
1436	1	0.0
1438	1	0.0
1529	1	0.0
1550	1	0.0
1555	1	0.0
1560	1	0.0
1562	1	0.0
1586	1	0.0
1681	1	0.0
1711	1	0.0
1839	1	0.0
1848	1	0.0
1996	1	0.0
351	1	0.0

m/z ratio	# times selected	selection frequency (%)
404	1	0.0
406	1	0.0
449	1	0.0
510	1	0.0
539	1	0.0
550	1	0.0
572	1	0.0
590	1	0.0
709	1	0.0
819	1	0.0
933	1	0.0
938	1	0.0
978	1	0.0

Table 15 - Data for Figure 4F in Chapter 5: results from 20,000 GA-DFA runs (control versus NEM samples; m/z ratios arranged from highest to lowest selection frequency).

m/z ratio	# times selected	selection frequency (%)
1765	10842	54.2
680	8827	44.1
1368	8058	40.3
1602	6809	34.0
737	5122	25.6
1045	3901	19.5
1585	3339	16.7
726	3217	16.1
1957	2619	13.1
1454	2261	11.3
1457	1929	9.6
936	1400	7.0
369	1370	6.9
693	1308	6.5
1445	1112	5.6
1106	1059	5.3
443	952	4.8
1314	842	4.2
1471	833	4.2
415	819	4.1
1077	670	3.4
1330	668	3.3
964	657	3.3
491	648	3.2
393	623	3.1
1883	621	3.1
687	546	2.7
1071	523	2.6
821	500	2.5
710	441	2.2
715	436	2.2
495	435	2.2
1057	434	2.2
780	430	2.2
1184	414	2.1
683	396	2.0
1519	359	1.8
585	337	1.7
652	313	1.6
1582	301	1.5
1752	234	1.2
955	192	1.0
1075	190	1.0
1698	190	1.0

m/z ratio	# times selected	selection frequency (%)
739	188	0.9
639	184	0.9
706	182	0.9
449	176	0.9
1484	157	0.8
1010	112	0.6
1522	112	0.6
1494	103	0.5
690	84	0.4
1025	72	0.4
1246	69	0.3
865	68	0.3
1248	60	0.3
965	58	0.3
1073	56	0.3
866	54	0.3
1612	53	0.3
1812	51	0.3
1810	50	0.3
1441	47	0.2
923	45	0.2
1976	43	0.2
1281	42	0.2
698	42	0.2
1235	38	0.2
1311	37	0.2
592	35	0.2
1374	33	0.2
632	32	0.2
1576	31	0.2
872	31	0.2
1413	27	0.1
828	25	0.1
494	22	0.1
1525	21	0.1
1190	20	0.1
1215	20	0.1
673	18	0.1
1733	16	0.1
1835	16	0.1
531	15	0.1
1656	13	0.1
916	13	0.1
1205	12	0.1
371	12	0.1
547	11	0.1
1087	10	0.1
1535	10	0.1
1973	10	0.1

m/z ratio	# times selected	selection frequency (%)
1100	9	0.0
1877	9	0.0
703	9	0.0
1665	8	0.0
1439	7	0.0
1753	7	0.0
1779	7	0.0
849	7	0.0
579	6	0.0
742	6	0.0
1011	5	0.0
1438	5	0.0
1503	5	0.0
1603	5	0.0
1969	5	0.0
367	5	0.0
1023	4	0.0
1604	4	0.0
534	4	0.0
956	4	0.0
1199	3	0.0
1223	3	0.0
1668	3	0.0
1778	3	0.0
1822	3	0.0
1838	3	0.0
488	3	0.0
1084	2	0.0
1157	2	0.0
1222	2	0.0
1480	2	0.0
1530	2	0.0
1906	2	0.0
1919	2	0.0
450	2	0.0
481	2	0.0
786	2	0.0
819	2	0.0
1005	1	0.0
1039	1	0.0
1128	1	0.0
1331	1	0.0
1443	1	0.0
1464	1	0.0
1589	1	0.0
1659	1	0.0
1791	1	0.0
1845	1	0.0
1889	1	0.0

m/z ratio	# times selected	selection frequency (%)
391	1	0.0
418	1	0.0
446	1	0.0
477	1	0.0
505	1	0.0
544	1	0.0
562	1	0.0
571	1	0.0
732	1	0.0
735	1	0.0
738	1	0.0
952	1	0.0

Table 16 - Data for Table 3 in Chapter 5: results from 15,000 GA-DFA runs (control versus cadmium samples; m/z ratios arranged from highest to lowest selection frequency).

time < 5 minutes		45 minutes		3 hours		5 hours	
m/z ratio	# times selected	m/z ratio	# times selected	m/z ratio	# times selected	m/z ratio	# times selected
717	14862	604	15000	1175	14614	1703	14320
1461	14768	1010	14998	1738	13017	1593	11777
553	56	1551	2	428	1849	1993	1541
1063	54			1364	252	1353	694
1407	48			397	102	1033	680
1290	39			1927	102	1035	678
951	34			1604	32	1897	308
1630	24			818	32	649	2
711	18						
1590	17						
1902	17						
1129	17						
682	11						
1438	10						
1567	7						
1838	5						
1701	5						
1822	4						
718	2						
547	2						

Table 17 - Data for Table 3 in Chapter 5: results from 30,000 GA-DFA runs (control versus DNP samples; m/z ratios arranged from highest to lowest selection frequency).

time < 5 minutes		45 minutes		3 hours		5 hours	
m/z ratio	# times selected	m/z ratio	# times selected	m/z ratio	# times selected	m/z ratio	# times selected
1593	26762	1712	27532	556	29849	414	21435
1368	26293	1015	27532	1933	24107	447	21393
1158	3707	1357	2189	420	5803	1839	6458
1188	3238	708	2187	693	54	585	6431
		1969	279	401	54	1284	2034
		539	279	1644	44	713	2033
		842	2	1780	14	1073	54
				1116	11	1964	15
				1101	8	818	13
				1304	8	578	13
				436	7	1493	13
				486	7	1170	13
				1099	4	1269	11
				1202	3	864	10
				707	3	1574	9
				914	3	768	9
				1221	3	1898	6
				1999	3	1894	6
				540	3	1414	6
				1251	3	1440	5
				485	3	524	4
				1679	2	1854	4
				1831	1	1698	3
				683	1	1274	3
				1966	1	705	3
				1869	1	1434	2
						1659	2
						764	2
						1959	2
						629	2
						880	1
						804	1
						1407	1
						387	1
						1622	1
						698	1

Table 18 - Data for Table 3 in Chapter 5: results from 20,000 GA-DFA runs (control versus NEM samples; m/z ratios arranged from highest to lowest selection frequency).

time < 5 minutes		45 minutes		3 hours		5 hours	
m/z ratio	# times selected	m/z ratio	# times selected	m/z ratio	# times selected	m/z ratio	# times selected
488	9305	351	19996	948	17100	817	19985
1417	9303	1431	19980	1438	15029	769	19797
524	6138	1095	12	1560	2821	513	185
1814	6137	1434	4	439	2147	1665	12
1671	2031	648	4	1152	1943	1761	11
1072	1334	1543	2	1798	819	897	4
1997	1312	1575	2	1200	39	1025	2
1116	1251			1905	39	1153	1
1559	827			1492	25	1492	1
815	826			795	19	1910	1
1731	719			1099	15	1969	1
1005	268			1093	2		
997	268			986	2		
1566	90						
700	90						
831	78						
1176	4						
1289	4						
1362	3						
1378	3						
614	3						
1158	2						
996	2						
1544	1						
772	1						